2016

CENOZOIC TERRESTRIAL PALAEOENVIRONEMTAL CHANGE: AN INVESTIGATION OF THE PETROCKSTOWE AND BOVEY BASINS, SOUTH WEST UNITED KINGDOM

CHAANDA, MOHAMMED SULEIMAN

http://hdl.handle.net/10026.1/5347

http://dx.doi.org/10.24382/4943
Plymouth University

CENOZOIC TERRESTRIAL PALAEOENVIRONEMTAL CHANGE: AN INVESTIGATION OF THE PETROCKSTOWE AND BOVEY BASINS, SOUTH WEST UNITED KINGDOM

by

MOHAMMED SULEIMAN CHAANDA

A thesis submitted to Plymouth University for the partial fulfilment for the degree of

DOCTOR OF PHILOSOPHY

School of Geography, Earth and Environmental Sciences

Faculty of Science and Technology

May 2016

Signed: 

Date: 25-05-2016

CENOZOIC TERRESTRIAL PALAEOENVIRONMENTAL CHANGE: AN INVESTIGATION OF THE BOVEY AND PETROCKSTOWE BASINS, SOUTH WEST UNITED KINGDOM, Mohammed S. Chaanda

The Petrockstowe and Bovey basins are two similar pull apart (strike slip) basins located on the Sticklepath – Lustleigh Fault Zone (SLFZ) in Devon, SW England. The SLFZ is one of the several faults on the Cornubian Peninsula and may be linked to Variscan structures rejuvenated in Palaeogene times. The bulk of the basins' fill consists of clays, silts, lignites and sands of Palaeogene age, comparable to the Lough Neagh Basin (Northern Ireland), which is also thought to be part of the SLFZ. In this study a multiproxy approach involving sedimentary facies analysis, palynological analysis, stable carbon isotope ($\delta^{13}C$) analysis and organic carbon palaeothermometer analyses were applied in an attempt to understand the depositional environment in both basins. A negative carbon isotope excursion (CIE) with a magnitude of 2‰ was recorded at ~ 580 m in the siltstone, silty clay to clay lithofacies in the lower part of Petrockstowe Basin, with minimum $\delta^{13}C_{TOC}$ values of -28.6‰. The CIE spans a depth of 7 m. Palynological characteristics of this excursion are correlated with the Cogham Lignite in the southern UK, which is the only established PETM section in the UK, and other continental sections to test whether the palynology associated with this CIE can be used to date it. The age model proposed herein correlates the CIE to the Eocene Thermal Maximum -2 (ETM2; ~ 52.5Ma) event. Key pollen and spore assemblages found in the lower Petrockstowe Basin are *Monocolpopollenites*, *Inaperturopollenites*, *Laevigatisporites*, Bisaccate conifer pollen and *Tricolporopollenites*, which suggest an Eocene age, while those occurring in the upper part of the Petrockstowe and Bovey basins are *Arecipites*, *Inaperturopollenites*, *Monocolpopollenites*, *Tricolporopollenites*, *Sequoiapollenites*, and *Pompeckjodaepollenites*, which have suggested botanical affinities to modern tropical to sub-tropical genera signifying a climate that was frost-free at the time of sediment deposition. This assemblage further suggests that these sediments are Oligocene to middle Oligocene in age. In the upper part of the Petrockstowe Basin, reconstructed mean annual air temperatures (MAT) demonstrate a clear departure from the mean temperature of 24.5^{o}C at 10 m to 19.5^{o}C towards the top of the core, indicating a steady continuous decline similar to the temperature departures seen in the Solent Group in the Hampshire Basin, Isle of Wight, UK which has an establsihed Eocene – Oligocene succession.

CONTENTS

LIST OF FIGURES

LIST OF PLATES

LIST OF TABLES

ACKNOWLEDGEMENTS

In the name of Allah, the most gracious, the most merciful, whom praise goes to, I wish to register my gratitude for giving me life, sound health and strength to undertake this project and making it possible to deliver it within the stipulated time.

Because there is a long list of names of those who have in one way or the other contributed to the success of this research, it is not possible to list all the names. First and foremost, I would like to express my sincere appreciation and gratitude to my Director of Studies, Dr Stephen T. Grimes, for unending supervision, support, encouragement and relentless efforts from the conception of this project to the end, which has made it possible to achive the aims. Steve has given me open door access to him at any point in time through-out the course of the research and that has made things easy for me. I find Steve to be a very good source of inspiration to me more especially when he finds that I am in a tight corner; he always approaches things in a tactfull and, diplomatic way. To this end, Steve is not only a supervisor but a friend.

Secondly, special thanks are given to other members of my Supervisory Team in the persons of Prof. Gregory D. Price, Dr Mark Anderson and Dr Rhodri Jerrett for the enormous wealth of knowledge that I tapped and enjoyed from them, not only by brainstorming at frequent meetings, but by showing personal interest in the project especially when it was getting difficult to get access to the field section of the Bovey Basin and the core repository at the British Geological Survey, Keyworth, Nottingham.

I would like to acknowledge Mr Scott Renshaw, and Mrs Tracey, all of the BGS core store for not only making the cores accessible to me but giving me all the necessary support and comfort while logging and sampling the Petrockstowe cores.

Also Mr Martin and Ms Clover of the Sibelco UK, who were always ready to show me the outcrops at the South John Acres Lane Quarry, Kingstenton during my field seasons.

I would not forget to register the training I received from Prof Melanie Leng of the National Isotope Geoscience Laboratory, Keyworth, for granting me access to their facilities to carry out the stable isotope analyses even at short notice.

I would like to say a massive thank you to Dr Paul Sutton who has been very patient with me, supportive and encouraging in the course of the lipid extraction. He has never relented in his efforts to help me.

A huge thank you goes to Prof. Richard D. Pancost for accepting to run the GDGTs analyses in his laboratory, also to his team, specially Dr Kyle Kwyor, and Gordon Inglis, my very own good friend/colleague at the Urbino 2012 summer school.

Also, while not strickly a supervisor, I would like to give a huge thank you to Dr Meriel Fitzpatrick for her ideas on palynology, which has helped me. Also worth acknowledging are Dr Guy Harrington, and Prof. Justin Hans for their help with palynological identification, and Mrs Jane Flint for preparing the palynological samples.

Special thanks goes to Dr Hayley Manners who is not just a collegaue but a friend, who has supported me especially with the geochemical aspect of the analyses.

My appreciation goes to Dr Helen Hughes, Dr Jodie Fishe, Dr Katie Head for placing all orders of comsuables and giving all the support I needed in the laboratory, and to the all CRES research group members.

My PhD research was funded by the Tertiary Education Trust Fund (TETFund) Abuja, via the intervention of academic staff training and development programme to the Federal University of Petroleum Resources, Effurun, Nigeria, and as such I would like to thank the Univeristy for nominating me.

I owe a huge thank you to my family and friends who have tolerated and bestowed confidence in what I am doing. Firstly, I would like to say a special thank you to my Mum Maimuna and my late Dad Baba Suleiman who passed on towards the end of the research, and he had wished to see my

return, but God did not allow him to witness my return, may Allah grant his soul Rahama. I would like to express my sincere appreciation to my Uncle, Dr D. F. Jatau who has been solidly behind me. The list of family and friends is too long to be contain here, but to mention few: Y. S. Bibinu, G. Birma, B. Arabi, F. Zara, Hajia Kande, Dr. A. Yushau, Aisha Abba. I say thank you to all of you out there.

I would not forget to mention my collegues/friends in the office who have made the journey together; Dr Waleed Hamed, Dr Saleh El-enezi, Israel Etobro, Dr Emiko Kent, Alex Dawson, Hazel Gibson, Dr Chinwendu, Dr Ahmed Omer, Dr Will Forster, Dr Matthew Mayer, Dr Deborah Wall-Palmer and Dr Andy Leighton. Others are Giulia Alessandrini and Madeleine Vickers

Finally, but not the least, a BIG THANK YOU to my dearest wife Maryam, daughters Fatima, Maymunah (Goggo), and the latest boy of the house Sulayman (Sultan) who have patiently beared my late coming home at the expense of their play time; with-out your understanding, love, prayers and support, I would not have made it to this stage. May Allah (SWA) bless you all!

AUTHOR'S DECLARATION

At no time during the registration for the degree of Doctor of Philosophy has the author been registered for any other University award without prior agreement of the Graduate Committee.

Work submitted for this research degree at the Plymouth University has not formed part of any other degree either at Plymouth University or at another establishment.

This study was financed with the aid of a studentship from the Tertiary Education Trust Fund (TetFund) as an intervention to the Federal University of Petroleum Resources, Effurun, Nigeria.

A programme of advance study was undertaken, which included Quaternary Palynology Training, Greifswald University, Germany; Past Global Change Reconstruction and Modelling Techniques, Urbino Summer School, University of Urbino, Italy; and Pollen and Spore Masters Course, University of Utrecht, Netherlands.

Relevant scientific seminars and conferences were regularly attended during the course of my studentship and findings were presented in the form of oral and poster presentation; external institutions were visited for consultation purposes. Two abstracts have been published.

In the course of this research, travel grants were awarded by the Higher Eduaction Academy (HEA) travel grant scholarship to attend conference "Postgraduate who teach Geography, Earth and Environmental Sceinces" at the Geographical Society London, in March 2012; the Doctoral Training Centre for Earth and Environmental Science, University of Plymouth; the International Association of Sedimentologist for travel to attend the European Geosciences Union (EGU) General Assembly in 2014 and the Micropalaeontoligical Society (TMS) travel busaries to attend the Micropalaeontological Society (TMS) 2015 AGM, Liverpool.

Presentation and Conferences Attended:

1. Centre for Research in Earth Sciences (CRES) Postgraduate Conference; **oral presentation** titled: "Terrestrial climate reconstruction through the Palaeogene greenhouse and icehouse climate events". 16th November, 2011.
2. Urbino Summer School; **poster presentation** titled: "Terrestrial Reconstructions across the Cenozoic Greenhouse and Icehouse climate events". 11th July – 29th July, 2012.
3. EGU General Assembly 2014 **Poster Presentation** titled: "An Integrated geochemical and facies analysis of Palaeogene fluvio-lacustrine sediments in the Petrockstowe and Bovey Basin, UK". 27th April – 2nd May, 2014.

Word count of main body of thesis: **41, 175**

Signed: 

Date: 25-05-2016

CHAPTER 1- INTRODUCTION

1.0 INTRODUCTION

The Earth is currently experiencing a period of climatic instability, with ca. 0.5^{o}C/yr temperature change since the Last Glacial Maximum (LGM), accelerating to 0.5 – 0.8^{o}C/yr in the last century due to the anthropogenic release of greenhouse gases such as CO_2 (Luterbacher *et al.* 2000). In the geological past, global temperature change has been linked to changes in the concentration of atmospheric CO_2, with major perturbations to biota and the hydrological cycle (Bowen *et al.* 2006, Pagani *et al.* 2006, Sluijs *et al.* 2007b, Pearson *et al.* 2009). Hence the consequences for society of the present day are potentially significant.

Numerous means of predicting future climate change and its consequences are being pursued. These include computer based modelling studies of long-term ocean-atmosphere carbon cycling (LOSCAR), three dimensional oceans and atmospheric circulation modelling (GENIE-1), integrated assessment models (IAMs) and General Circulation Models (GCMs) (Liu *et al.* 2009, Ridgwell & Schmidt 2010, Huber & Caballero 2011, Lunt *et al.* 2011). Another approach has been to interrogate the geological past for potentially analogous time periods. A commonly cited analogue for modern day CO_2 release and subsequent warming are so called hyperthermal events in the Palaeogene (Coxall *et al.* 2005, Zachos *et al.* 2005, Ridgwell & Schmidt 2010, Pearson *et al.* 2009, Zeebe *et al.* 2009, McInerney & Wing 2011).

The early Palaeogene was characterised by a series of short-lived hyperthermals, or transient episodes of oceanic and atmospheric warming. The largest of these, the Palaeocene-Eocene Thermal Maximum (PETM; ca. ~55.5 Ma ago) was typified by 5^{o}C − 8^{o}C temperature increase, a 3 – 5‰ negative carbon isotope excursion (CIE), and profound shifts in biotic communities (Röhl *et al.* 2005, Murphy *et al.* 2010a, McInerney & Wing 2011). The increase in temperature was associated with the release of a large mass (>10^8 gt) of isotopically depleted CO_2 or CH_4 into the ocean – atmosphere system (Zachos *et al.* 2005,

Panchuk *et al.* 2008, DeConto *et al.* 2012), warm high latitudes, warm surface-and- deep oceans, and intensified hydrological cycles (Pagani *et al.* 2005, Pearson *et al.* 2007) comparable to, within a factor of two, that observed from anthropogenic emissions (Dickens *et al.* 1995, Dickens *et al.* 1997, Raven *et al.* 2005). A recent finding by Bowen *et al*. (2014) suggests that the PETM had one or more reservoirs capable of repeated, catastrophic carbon release. Significantly these carbon release rates were similar to those associated with modern anthropogenic emissions (Ciais *et al.* 2013) compared to earlier reports (Cui *et al.* 2011, Wright & Schaller 2013). In contrast to the warmth of the early Eocene, the late Eocene is marked by an icehouse event, termed the first Oligocene glaciation event, or Oi-1 (33.9 Myr), during which there was a significant expansion of ice on Antarctica (Zachos *et al.* 2001). The Oi-1 event was typified by a temperature decrease of $3 - 4^{o}C$ of deep sea waters over ~ 300 kyr, associated with a decrease in CO_2 concentration from 450 p.p.m.v. to ~1500 p.pp.m.v. and a central mean of ~ 760 p.p.m.v. (Pearson *et al.* 2009).

1.1 RATIONALE

The Earth climate during the early Palaeogene abruptly warmed by $5 – 8\ ^{o}C$ associated with massive release of several thousands of pentagrams of carbon as methane and/or carbon dioxide into the ocean-atmosphere system within ~10kyr, on the basis of a carbon isotope excursion, widespread dissolution of deep sea carbonate, biotic extinction and global warming (Zachos *et al.* 2001, Zachos *et al.* 2008). Also, it is the period of most prominent Earth's climatic evolution in the transition from extreme global warmth in the early Eocene greenhouse climate ~55 Ma to the present glaciated state. The appearance of large ice sheets on the Antarctica ~ 34 Ma was linked to decreasing atmospheric CO_2 (Zachos *et al.* 1996, Tripati *et al.* 2005). How the Earth's temperature changed during this climate transition remains poorly understood, and the impact of these hyperthermal events are mostly documented on a regional basis mainly from marine sections. A better understanding of the dynamics of Earth's climate system can be achieved by the use of different climate models

and different palaeoclimate proxies for their reconstruction. Therefore, multi-proxy methods like sedimentary facies analysis, palynological analysis, stable carbon isotope ($\delta^{13}C_{TOC}$), Methylation of Branched Tetraethers and Cyclisation of Branched Tetraethers (MBT'/CBT) index are frequently applied in studying sedimentary records of the Palaeocene-Eocene Thermal Maximum (PETM), Eocene Thermal Maximum (ETM -2), and the Eocene-Oligocene transition for a better understanding of how the Earth system responds to such climate uncertainties. This study adopts this well established approach.

1.2 PALAEOCENE-EOCENE CLIMATE

The early Palaeogene was characterized by a series of dynamic climatic re-organization both on long - ($> 10^6$ years) and short – ($<10^4$ years) time scales (Kennett & Stott 1991, Dickens *et al.* 1997, Zachos *et al.* 2003, Tripati & Elderfield 2005, Sluijs *et al.* 2006, Norris *et al.* 2013, Littler *et al.* 2014). It is on record that the Earth's surface experienced a long term warming condition as far back as Late Palaeocene (~ 58Ma) to early Eocene (~50 Ma) which resulted in a temperature rise by at least 5^{o}C in the deep ocean temperature and an extended period of extreme warmth, referred to as the Early Eocene Climatic Optimum (EECO, ~50 – 52 Ma) (Zachos *et al.* 2001, Lourens *et al.* 2005, Zachos *et al.* 2008, Bijl *et al.* 2010, Friedrich *et al.* 2012).

In order to appreciate the mechanisms and the principles responsible for the hyperthermal events in the Palaeogene, a brief explanation of its background, impact and causes are enumerated in sections 1.4.1 – 1.4.3.

1.2.1 Background to the PETM

The first breakthrough in understanding the PETM came from the works of Kennett and Stott (1991) who gave an account of rapid shifts in stable carbon and oxygen isotope ratios observed in species-specific foraminiferal carbonate from Ocean Drilling Program (ODP) Site 690B, off the coast of Antarctica. They presented the key features of the event as a rapid

onset (which they estimated to be ~ 6 ka), a decrease in oxygen isotope ratios (indicating warming of 3 – 4°C in surface water and ~ 6°C in deep water), a negative shift in the $\delta^{13}C$ of benthic (~2‰) and planktic (~4‰) foraminifera, an influx of diverse surface water microfossil assemblage with subtropical affinities, an increase in kaolinites, and an elimination, or even reversal, of depth gradients in both $\delta^{13}C$ and $\delta^{18}O$. All these were synchronous with a previously documented extinction of benthic foraminifera (Thomas 1989).

After the recognition of the PETM by Kenneth & Stott (1991), a negative carbon isotope excursion (CIE) was recognised in pedogenic carbonate and mammalian tooth enamel derived from continental rocks (Koch *et al.* 1992). It was recognised that the CIE coincided with the largest mammalian faunal turnover of the Cenozoic. The work of Koch et al. (1992) established the PETM as a global event that could be detected in the continental realm and showed how the CIE could be used to correlate marine and continental sections. Aubry (2000) also resolved the problem of formalising a Palaeocene - Eocene boundary that could be used in both terrestrial and marine section. The CIE became a global chemostratigraphic marker, enabling the precise correlation of biotic and climatic events worldwide (Dupuis *et al.* 2003). The CIE is so important for precisely correlating marine and continental strata that the Palaeocene – Eocene boundary is now defined by the onset of the CIE (Dupuis *et al.* 2003).

The methods used in the estimation of the duration of the PETM are astronomical cyclostratigraphy (Röhl *et al.* 2005) and extra-terrestrial ^{3}He fluxes e.g. (Murphy *et al.* 2010), where orbital timescales suggest a duration of between120 – 220 ka (Farley & Eltgroth 2003). The onset of the CIE has been estimated to have occurred in < 10 ka (Zachos *et al.* 2005), but the dissolution of the uppermost Palaeocene and the lowermost Eocene carbonate associated within the CIE in many deep marine sections makes it difficult to estimate the duration of the onset (Murphy *et al.* 2010). The onset of the CIE in continental

sections (e.g. Bighorn Basin), which are not affected by carbonate dissolution, occupies 4 – 7 m of section, equivalent to 8 – 23 ka based on calculated sedimentation rates (Bowen *et al.* 2001, Magioncalda *et al.* 2004, Aziz *et al.* 2008).

The Palaeocene– Eocene boundary was earlier defined by the placement of a Global Boundary Stratotype Section and Point (GSSP) in the Dababiya Quarry section of Egypt and is most commonly recognised by the base of the CIE (Gradstein *et al.* 2004).

1.2.2 Impact

The PETM is characterised by a global temperature rise, initially inferred from a >1‰ negative excursion in $\delta^{18}O$ of benthic foraminifera, indicating a deep-sea temperature increase of ~ 6°C (Kennett & Stott 1991, Thomas & Shackleton 1996, Zachos *et al.* 2001). A similar magnitude of temperature increase has also been inferred from Mg/Ca ratios in planktic foraminifera (Zachos *et al.* 2003, Tripati & Elderfield 2005). Planktic foraminiferal $\delta^{18}O$ and Mg/Ca ratios are also generally consistent with ~5°C of warming, although estimates reach up to 8°C of warming using data from Ocean Drilling Program (ODP) Site 690, Maud Rise (Kennett & Stott 1991) and Wilson Lake, New Jersey (Zachos *et al.* 2006). There is much variation in the extent of warming associated with the PETM. It is important to highlight that the temperature increase in the Arctic (Lomonosov Ridge) determined from biomarker palaeothermometers (Tetra Ether Index (TEX_{86}) and Glycerol Dialkyl Glycerol Tetraether lipids (GDGTs)) are between ~ 5 – 8°C (Sluijs *et al.* 2006, Weijers *et al.* 2007). The absence of greater warming at polar latitudes during the PETM implies an absence of the ice albedo feedback loop that would have amplified warming at high latitudes if sea or land ice had been present in the Palaeocene (Sluijs *et al.* 2006).

Previous estimates of continental warming during the PETM range from ~5°C using leaf - margin analyses of palaeofloras (Wing *et al.* 2000), to ca. 2 – 7°C using oxygen isotopes in mammalian tooth enamel (Fricke *et al.* 1998) ($\delta^{18}O$) or soil carbonates (Koch *et al.* 2003).

These estimates averaged a large interval of late Palaeocene time, however, and with the exception of the soil carbonate, lacked the resolution to detect a change in climate directly below the CIE. The input of carbon is evidenced by prominent negative CIEs in carbonate and organic matter, as well as dissolution of carbonate in deep-sea sediments (Zachos *et al.* 2005, Pagani *et al.* 2006). The global record of the PETM CIE (lasting ~ 220 ka) (Farley & Eltgroth 2003) observed in stable isotope records of oceanic carbonates, will therefore, be recorded in sedimentary archives, and consequently in terrestrial organic matter.

The PETM is also associated with a relocation of the sources of oceanic deep waters (Thomas 1998), a decrease in the thermal gradients between pole/equator and surface water (Zachos *et al.* 2005), an acidification of sea water that gave rise to a mass extinction of benthic foraminifera (Kennett & Stott 1991) and a change in the palaeoflora (Wing *et al.* 2005, Nunes & Norris 2006).

During the PETM, there was a salient increase in the abundance and geographic range of the hetetrophic dinoflagellate *Apectidinum* (Crouch *et al.* 2001, Sluijs *et al.* 2007a). This lineage, which had been largely restricted to low latitudes in the Palaeocene, expanded to polar latitudes in both hemispheres during the PETM which suggest warmer climates globally, attaining abundance of >40% dinocysts in many samples (Sluijs *et al.* 2007a).

A turnover of terrestrial mammal faunas (commonly referred to as the Mammalian Dispersal Event (MDE)) also took place, including the first appearance of some of the modern orders (artiodactyls, perissodactyls, carnivores and primates), at the Palaeocene – Eocene boundary (Clarkfordian-Wasatchian boundary in North America; (Gingerich 2001); at the Gashatan-Bumbanian boundary in Asia (Ting *et al.* 2003) and the Cernaysian-Neusian boundary in Europe (Smith 2000, Smith *et al.* 2006).

Wing & Harrington (2001) in their palaeobotanical studies of the Fort Union and Willwood formations from the Bighorn Basin of north Wyoming, analysed 60 fossil pollen samples from a 900 m section spanning ~ 3 million years of the Palaeocene and early Eocene, found little change across the Palaeocene − Eocene transition, though there was a lack of samples from the PETM. Once megafloras were found within the CIE at the Bighorn Basin of north west Wyoming they proved to be radically different in composition from those immediately before and after (Wing *et al.* 2005). Pre- and post-PETM megafloras are a mix of deciduous and evergreen broad leaved lineages as well as conifers in the cypress family (Wing *et al.* 1995). Though the PETM had a dramatic effect on megafloral composition, palynofloral change in the same section was subtle, with the bald cypress, birch, and walnut families abundant throughout the Palaeocene – Eocene interval (Harrington 2001, Wing *et al.* 2005). PETM palynofloras differed from those immediately before and after only in rare occurrences of pollen types from the Gulf Coastal plain, which otherwise do not occur so far north (Wing *et al.* 2005).

Harrington & Jaramillo (2007) observed the declining terrestrial palynomorphs diversity across the Palaeocene Eocene boundary in the Gulf Coastal Plain of Mississippi, and suggested the possibility of elevated extinction among paratropical plants during the PETM.

1.2.3 Possible Mechanisms

The Palaeocene-Eocene CIE provides crucial constraints for understanding the mechanisms behind the PETM. There are many hypotheses that have been proposed as the cause of the PETM (Dickens *et al.* 1995, Dickens *et al.* 1997, Kurtz *et al.* 2003, Svensen *et al.* 2004, Cramer & Kent 2005, Maclennan & Jones 2006, Zachos *et al.* 2008, Dickens 2011). The widely accepted source appears to be the sudden release of substantial quantities of isotopically-light methane from the dissociation of sea floor clathrate deposits (Dickens *et al.* 1995, Dickens *et al.* 1997, Dickens 2011). The mechanism for the release of the clathrate

deposits include changes in ocean circulation patterns (Nunes & Norris 2006), or by decreasing pressure resulting from slope failure (Katz *et al.* 2001).

The release of methane by thermal dissociation of gas hydrate on the continental slopes

According to Dickens *et al*. (1997) methane hydrates are mainly located around North America and Greenland. The change in oceanic circulation is considered to be the potential cause of the switched over in deep water formation from the Southern Hemisphere to the Northern Hemisphere (Nunes & Norris 2006) assuming that the location of the reservoirs of PETM methane hydrate were similar to those of the methane hydrate found today, might have cause the rise in temperature to destabilise and release the methane hydrate (Thomas *et al.* 2002). The increase in ocean temperature or the decrease in pole to equator sea surface temperature gradients or the changes in continental fresh water run-off is considered as the possible cause for the change in ocean circulation (Thomas *et al.* 2002, Nunes & Norris 2006).

Therefore, additional sources have been postulated which included thermogenic methane generated via emplacement of sills (Svensen *et al.* 2004) into organically rich sediments leading to the release of enormous quantities of thermogenic methane into the ocean/atmosphere system (Bowen *et al.* 2004). Such a mechanism fails to explain other likely Paleogene carbon injection events, or why these might be paced by changes in Earth's orbital parameters (Dickens 2011) (see below). A link between North Atlantic volcanism and the PETM has long been suspected (e.g. Dickens *et al.* 1995, Thomas and Shackleton, 1996).

The release of carbon from permafrost soils at high latitudes as feed back

The PETM has been linked to high-latitude orbital forcing through the carbon cycle feedbacks involving permafrost soil carbon. This has been demonstrated by the use of astronomically calibrated cyclostratigraphic records from central Italy (Galeotti *et al.* 2010) to highlight that early Eocene hyperthermals took place during orbital forcing which is the primary trigger for these smaller rhythmic climatic and sedimentological patterns and a combination of high eccentricity and high obliquity. The result indicated the possibility that high latitude climate forcing triggered the release of massive amounts of terrestrial carbon, which subsequently generated global warming. Deconto *et al*. (2012) suggested that the high elevation of the circum-Arctic and Antarctica could be favourable locations for the storage of massive carbon in the late Palaeocene and early Eocene times. By implication, these environments achieved threshold climatically during long-term warming, which gave rise to thawing of permafrost and the sudden release of stored soil carbon that might have been triggered during maximum long eccentricity and obliquity orbital cycles (Schaefer *et al*. 2011). This hypothesis seems to present a reasonable explanation for both onset and termination of the hyperthermal event, but the termination may need to be supported by yet another mechanism.

In the same way, Littler *et al*. (2014) also documented negative CIEs and $\delta^{18}O$ events to coincide with maximum eccentricity, with changes in $\delta^{18}O$ leading changes in $\delta^{13}C$ by ~6 (±5) kyr in the 405 kyr band and by ~3(±1) kyr in the 100 kyr band on average in the South Atlantic, during the late Palaeocene − early Eocene. Littler *et al*. (2014) observed that shoaling of the lysocline and accompanied changes in the global exogenic carbon cycle could have been responsible for the increase carbonate dissolution. Though most of these mechanisms have been proposed to be independent to one another, it is probable that a combination of these different mechanisms may have been responsible for the onset of the CIE (Zachos *et al.* 2008).

Lunt *et al*. (2011) suggested a climatological trigger for carbon injection, for instance via enhancement of seasonal extremes which caused changes in ocean circulation and in turn led to dissociation of submarine methane hydrates. Accordingly, most records tends to suggest that some of the warming took place before the injection of $\delta^{13}C$ depleted carbon, which may have catalysed the injection of carbon over tens of thousands of years (Sluijs *et al.* 2007b, Kender *et al.* 2012). In the same vein, analyses of a ~ 70 m thick palaeosol succession, yielded changes in temperatures obtained from $\delta^{18}O$ values on tooth enamel from a mammal Corphodon in the Bighorn Basin, Wyoming (Kraus *et al.* 2013). Their findings shows that there was shift to drier soils prior to the PETM, consistent with earlier studies in documenting warming prior to the onset of the negative CIE related to the PETM.

In a related study, Bowen *et al*. (2014) obtained a high resolution carbon isotope record from terrestrial deposits of Bighorn Basin spanning the PETM. Using a carbon cycle model of the ocean-atmosphere-biosphere in making deduction, results revealed that the initiation of the PETM was characterised by two distinct carbon releases rather than one event, which is separated by a significant recovery to background values. They reported that one or more carbon reservoirs were responsible for the PETM CIE, and that they were capable of repeated, catastrophic carbon release, and the rate of this release during the PETM could be compared to modern anthropogenic emission, not as earlier suggested by Cui *et al*. (2011) and Wright & Schaller (2013).

Similarly, Foreman (2014) using a sedimentological proxy noted a thick boundary sandstone in north-west Wyoming hosted the main body of the PETM, representing ~ 113 kyr of time when global pCO_2 levels and temperature were high. The resultant effect was an evidence of short-term climate perturbations that might have manifested within large-scale depositional patterns likely due to tectonics.

Analysis of the stable carbon isotope composition of higher plant leaf waxes (n-alkanes) from terrestrial and lagoonal sediments at Vesterival section in Normandy, France by Garel *et al*. (2013), reveal a CIE of -4.5‰, which extended through the Sparnacian of the Palaeocene − Eocene. Similarly, palynofacies records show an abrupt shift from a closed, quiescent marsh pond to an open eutrophic swamp, dominated by algal blooms, consistent with the CIE onset and drier episodes just before the PETM, which may help to understand the triggering of this hyperthermal event and moister climate associated with a stronger seasonality during the early PETM (Garel *et al.* 2013).

Elderett *et al*. (2014) observed a change in terrestrial vegetation prior to the CIE, concomitant with anomalous marine ecological change, which is comparable to the occurrence of *Apectodinum augustum*, which could have triggered extreme carbon injection. A clear reduction in boreal conifers and an increase in mesothermal to megathermal taxa, justify the shift of the taxa towards wetter and warmer climate (Eldrett *et al.* 2014). Moreover, Hollis *et al*. (2015) recorded a gradual decrease in $\delta^{13}C$ of 2‰ lighter than uppermost Palaeocene value in the Southern Pacific ocean (DSDP site 277, Campell Plateau). This was likely a result of diagenetic alteration, where $\delta^{18}O$ and Mg/Ca value from foraminiferal tests used in the determination revealed intermediate and surface water were warmed by ~6^{o} at the onset of the PETM before the $\delta^{13}C$ excursion got fully developed. Consequently, it showed that the initial carbon perturbation in this region had a pronounced effect on Southern Pacific Ocean circulation resulting in expansion of warm surface waters poleward.

Bowen and Zachos (2010) observed that the rate of recovery is an order of magnitude more rapid than that expected for carbon drawdown by silicate weathering alone. This signifies that 2000 Pg of carbon were sequestrated as organic carbon over 30, 000 – 40, 000 yrs at the end of the PETM. Hence, sequestration of carbon could be the result to be regrowth of carbon reservoirs in the biosphere or shallow lithosphere. To sum up, regardless of any one

of the proposed sources of carbon, none are likely to be solely responsible for the injection of carbon that caused the hyperthermal event. More likely, a combination of two or more, were involved. Proxies, models and mass balance calculations and subsequent records of PETM may help to determine the magnitude of the CIE associated to the PETM and would give an enhanced possible source of the carbon (see Figure 1.1).

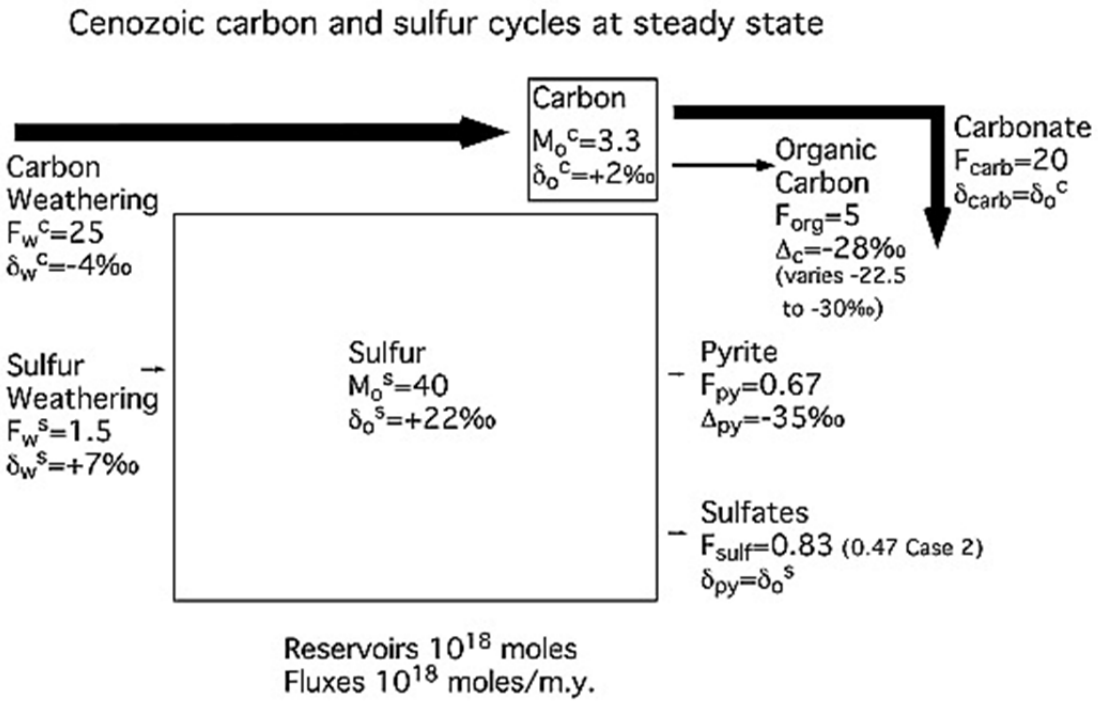

Figure 1.1: Model diagram showing the carbon and sulfur cycles which comprises of a small reservoir with large input and output fluxes while the sulfur cycle is a large reservoir with very small fluxes. Arrows denotes the magnitude of the fluxes. This model also shows how cabon and sulfur cycles are used to calculate burial histories of C_{org} and S_{py} in both terrestrial and marine environments, adopted from (Kurtz *et al*. 2003).

1.3 EOCENE THERMAL MAXIMUM 2 (ETM2)

After the PETM, other less pronounced transient warming events occurred. These include the Eocene Thermal Maximum-2 (ETM-2; ~53.6Ma), also referred to "Elmo", and the hyperthermal event referred to as Eocene Thermal Maximum-3 (ETM-3; ~52.5Ma). Both

are among the short-lived, extreme global warming events that characterised the early Cenozoic following the PETM (~55.5 Ma) (Kennett & Stott 1991, Thomas & Zachos 2000, Lourens *et al.* 2005, Röhl *et al.* 2005, Agnini *et al.* 2009). However, the impacts of many of these events are only documented locally (Nicolo *et al.* 2007, Stap *et al.* 2010). The common features of these hyperthermals are carbonate dissolution horizons and negative carbon isotope excursions similar to those observed during the PETM, but less severe (Thomas 1999, Lourens *et al.* 2005, Zachos *et al.* 2005, Agnini *et al.* 2009, McInerney & Wing 2011, Komar *et al.* 2013). Other similar events with smaller magnitudes have been documented from the Palaeocene (the early Palaeocene event (ELPE)); and at Walvis Ridge, ETM-2 is identified by a CIE of -1.4‰ (Cramer *et al.* 2003) in relation to a 3^{o}C deep-sea warming in comparison to PETM that is characterised with a gradual CIE (Stap *et al.* 2010, Lauretano *et al.* 2015). There was also a marked turn over in mammalian fossil assemblages in Biohorizone B across the Wastachian 4 to Wastachian 5 biozone boundary (Gingerich 1980, Chew 2009) where it has been speculated that the ETM-2 is located (Clyde *et al.* 2007, Chew 2009). It is important to highlight that the biohorizon B extinction during ETM-2 is similar to the turnover during the PETM with the peak of the first and last appearance of mammal taxa that caused an increased in diversity. The extinction of *Hoplomylus* and *Ectocion* that originated before the PETM, and the initial appearance of *Bunophorus* that first appeared during the PETM, are the main criteria used biostratigraphically to identify Biohorizon B (Chew 2009, Abels *et al.* 2012). This is a justification that supported the macro-evolutionary dynamics which depends on the interaction between species and ecology (Abels *et al.* 2012). The mechanism responsible for these isotopic shifts can only be explained through the process of rapid introduction of a large mass of isotopically depleted carbon, probably on the scale of in thousands of petagrams, to the ocean/atmospheric system (Dickens *et al.* 1997, Zeebe *et al.* 2009, Dickens 2011). Although the mechanisms that lead to the initial release of the methane is still been debated (Sluijs *et al.* 2007b) several triggers have been suggested as earlier discussed in section 1.3.4. (Figure 1.2) showing the relationship between marine, atmospheric and continental carbon reservoirs. In a similar

study, Galeotti *et al*. (2010) reported their results from the orbital chronology of early Eocene hyperthermals from central Italy that ETM-2 occurs in 1 short-eccentricity cycle before the Chron C24r/C24n3n boundary while ETM-3 falls within 1.5 eccentricity cycles above the base of C24n1n. They concluded both events corresponded to isolation maxima within a very long modulation period of eccentricity of about 1.2 Myr which might had triggered the role of orbital control in ETM-2 and ETM-3.

Furthermore, Gibbs *et al*. (2012) has shown that high covariance values are associated with the PETM and a linear trend of decline with decreasing size of CIE for ETM-2, I1 and H2 suggests a scaling of biotic response which is in agreement with the evidence for scale temperature change in CIE's (Stap *et al.* 2010). A preliminary study from Dababiya section, Egypt has also shown evidence for ETM-2 in a shelf sequence, which reveals anomalous sedimentological features that corresponded to changes in benthic and planktic foraminifera as well as ostracods (Stassen *et al.* 2012).

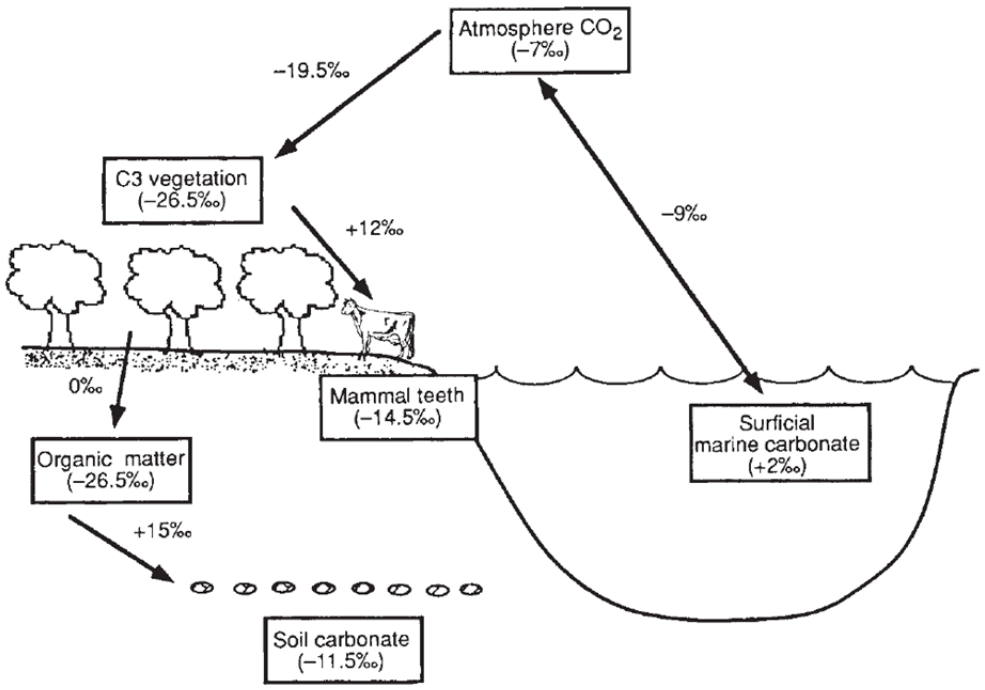

Figure 1.2: A model showing coupling between marine, atmospheric and continental carbon reservoirs, (assuming that Palaeocene-Eocene floras had only C3 plants, with the fractionation characteristic of the plants used was -19.5‰) (Mook 1986, O'Leary 1988, Koch *et al*. 1992).

1.4 EARLY EOCENE CLIMATIC OPTIMUM (EECO) AND EOCENE CLIMATIC OPTIMUM (MECO)

The highest temperature of the Cenozoic was reached in the early Eocene (Early Eocene Climatic Optimum, or EECO; ~52 – 50 Ma) (Bohaty & Zachos 2003, Bohaty *et al.* 2009). This event was then followed by long term high-latitude and deep-sea cooling, which continued through the middle and late Eocene (Zachos *et al.* 2001, Zachos *et al.* 2008, Bijl *et al.* 2009) (Figure 1.3). As the cooling proceeded, the Earth was in a state of what is referred to as doubthouse climate state, which was a state between the greenhouse (high temperatures and atmospheric pCO_2 levels) and the icehouse state (low temperature and pCO_2 levels), before the development of the Antarctic continental ice sheet in the early Oligocene (Zachos *et al.* 1996, Coxall *et al.* 2005, Lear *et al.* 2008).

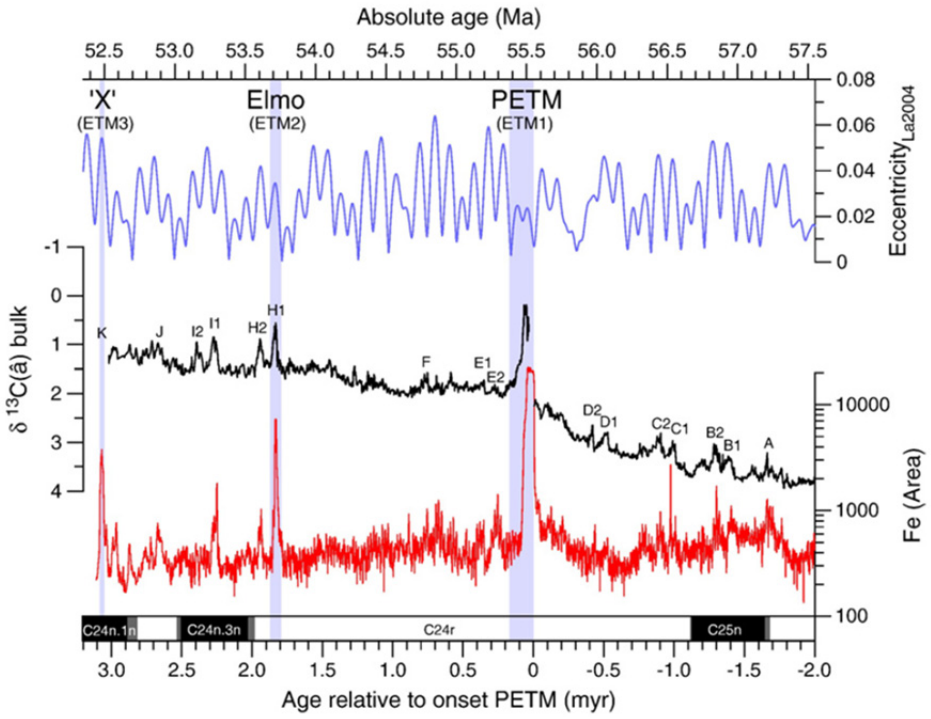

Figure 1.3: Global climate hyperthermal events over the past 58 Ma based on data generated from Site 1262 bulk sediments δ13C isotope and Fe records plotted as ±millions of years relative to the base of PETM (0.0 Myr) on the lower axis (from Zachos *et al*. 2010 with data generated from (Cramer *et al*. 2003, Lasker *et al*. 2004, Westerhold *et al*. 2008).

Following the EECO, the long term cooling was repeatedly interrupted by transient warming events (Tripati *et al.* 2005, Edgar *et al.* 2007). The most prolonged and intense event was the Middle Eocene Climatic Optimum (MECO) (Bohaty & Zachos 2003, Sluijs *et al.* 2013). Bohaty & Zachos (2003) recorded a distinct shift in the values of $\delta^{18}O$ in the Indian and Atlantic sectors of the southern ocean at 41.5 Ma (MECO). The shift in the $\delta^{18}O$ signal was thought to have affected both surface waters and middle bathyal deep waters (Bohaty & Zachos 2003).

Bohaty & Zachos (2003) suggested the MECO was not caused by methane hydrate dissociation but rather by a transient rise in atmospheric $_{P}CO_2$ levels. Although, the Palaeogene period has experienced extreme warming events that affected the biota, like the PETM (Sluijs *et al.* 2007a), there are only a few research papers related to the biotic response to the MECO in marine sedimentary sections. One example is the work of Witkowski *et al*. (2012) which centered on siliceous plankton in South Indian Ocean. The section experienced rapid assemblage changes in association with autotrophic and heterophic siliceous microfossil taxa (Galazzo *et al.* 2013). One of the major distinctions between the MECO and the PETM is that the MECO carbon isotope records vary geographically (Spofforth *et al.* 2010). Also, oceanic $\delta^{13}C$ records show considerable geologic variability, but have generally rising $\delta^{13}C$ values across MECO, with a brief, ~ 0.5‰ negative CIE during the peak warming phase of MECO, which clearly postdates the early, gradual warming (Bohaty *et al.* 2009). The MECO is well expressed in the Italian sections of the pelagic carbonates in Scaglia Rossa and Scaglia Variegata formations, representing deposition in the western Tethys Ocean (Jovane *et al.* 2007), and in the Alano section, Italy (Galazzo *et al.* 2013).

1.5 EOCENE – OLIGOCENE TRANSITION

A change in the state of the Earth's ocean and climate system occurred at the end of the Eocene (~ 34 Ma), when the greenhouse climate that had been sustained since the Cretaceous period evolved to the icehouse conditions characterising the Oligocene epoch through to the present time (Miller *et al.* 1987, Lear *et al.* 2000, Zachos *et al.* 2001). The most significant climate event in the long-term cooling trend of the Cenozoic era appears to be the Oi-1 cooling event at ca. 33.5 Ma (Miller *et al.* 1991), as seen in oxygen isotope records which climaxed during the late Eocene. As shown in Figure 1.4, this event was part of an abrupt increase in $\delta^{18}O$, reflecting a combination of global cooling and ice growth in Antarctica (Shackleton & Kennett 1975, Zachos *et al.* 2001, Lear *et al.* 2004, Coxall *et al.* 2005, Lear *et al.* 2008).

High-resolution reconstructions of seawater $\delta^{18}O$ show a ~ +1‰ shift that is interpreted as recording a sudden and massive expansion of ice volume, along with the occurrence of ice-rafted debris in the Southern Ocean and a change in clay and mineralogy consistent with increased glacial erosion on Antarctica (Lear *et al.* 2000, Coxall *et al.* 2005).

The Eocene – Oligocene Global Stratotype Section and Point (GSSP) is located in an abandoned quarry, along the provincial road of the Conero Regional Natural Park called Massingnano, Italy. The section spans the geological interval from the latest Eocene to the early Oligocene (Premoli Silva *et al.* 1988, Lanci & Lowrie 1997) which is a thick greenish-grey marl bed of the lower part of the Scaglia Cinerea Formation (Premoli Silva *et al.* 1988, Premoli Silva & Jenkins 1993). In this section both the planktonic foraminifera *Hankenina* and *Cribrohantkenina*, Eocene genera of the *Hantkenidae*, become extinct, this extinction marks the E – O boundary (Coccioni *et al.* 1988, Nocchi *et al.* 1988, Premoli Silva & Jenkins 1993, Berggren & Pearson 2005).

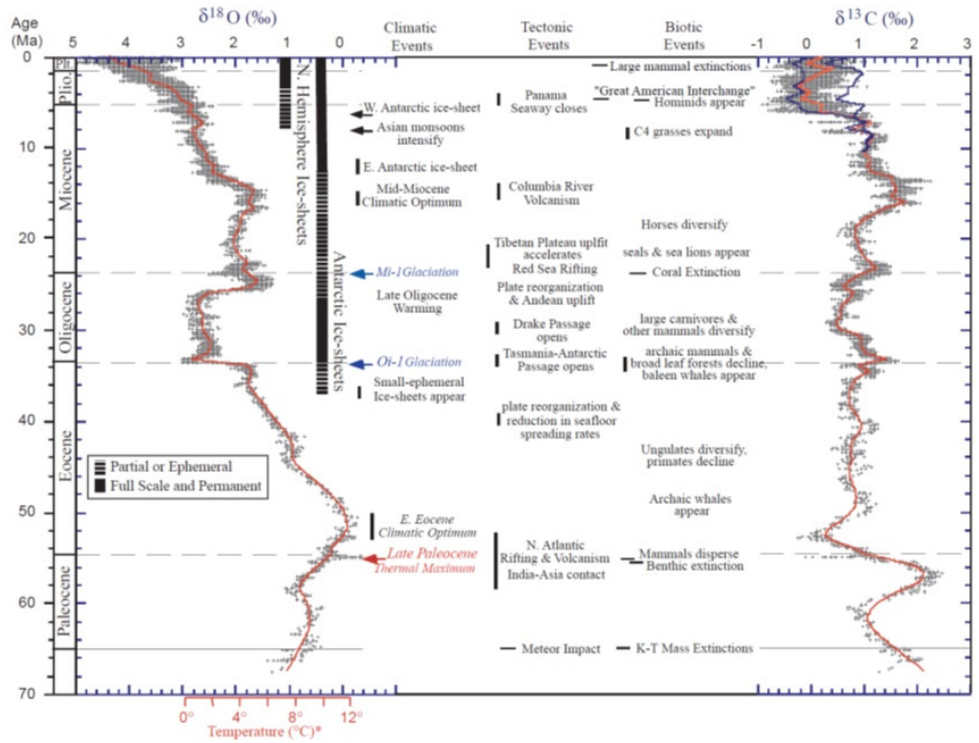

Figure 1. 4: Global deep-sea and carbon isotope records based on data compiled from more than 40 Deep Sea Drilling Project (DSDP) sites (from Zachos *et al*. 2001).

1.5.1 Possible Mechanisms

The Oi-1 is thought to mark the initiation of a permanent Cenozoic ice sheet on the Antarctic continent but the casual mechanisms remain widely debated. There are two major hypothesis postulated to explain the transition from greenhouse to icehouse world (Oi-1 glaciation):

1. The tectonic opening of the Southern Ocean gateways, which enabled the formation of the Antarctic Circumpolar Current (ACC) and the subsequent thermal isolation of the Antarctic continent (Kennett & Shackleton 1976, Robert & Kennett 1997). The initial growth of the East Antarctic ice sheet near the time of Eocene/Oligocene boundary has been attributed to the tectonic opening of the ocean gateways between Antarctica and Australia (Tasmanian Passage), and Antarctic and South America (Drake Passage), which lead to the initiation of the ACC (Kennett 1977, Exon 2000). This idea is supported by ocean general circulation model simulations, showing that the opening of the Drake Passage and the organisation of an ACC

reduces southward oceanic heat transport and cools Southern Ocean sea surface temperatures by ~ 3°C (Nong *et al.* 2000, Toggweiler & Samuels 1998).

2. A threshold in long-term Cenozoic decline in atmospheric CO_2 concentration is crossed, initiating ice-sheet height/mass-balance feedbacks that cause the ice caps to expand rapidly with large orbital variations, eventually coalescing into a continental scale East Antarctic Ice Sheet (DeConto & Pollard 2003). The cooling due to declining CO_2 would have gradually lowered annual snowline elevations until they intersected extensive regions of high Antarctic topography. It is worthy to note that immediately before a threshold was reached, feedbacks related to snow/ice-albedo and ice-sheet height/mass balance (Birchfield *et al.* 1982, Abe-Ouchi & Blatter 1993) could have initiated rapid ice-sheet growth during orbital periods favourable for the accumulation of glacial ice.
3. A corollary component to this global climatic transition has been proposed by Jovane *et al*. (2007) based on Eocene data from the Neotethys Sector. The hypothesis is known as the Subtropical Eocene Neotethys (STENT) current hypothesis. This suggests that the closing of the Neotethys gateway, which occurred as a result of local and regional tectonics, in combination with local, regional, or global sea-level changes, could represent the trigger or one of the causes that drove the cooling across the E/O boundary.

1.5.2 Impact

The Eocene/Oligocene transition was associated with a dramatic oceanographic reorganisation and the largest cooling episode of the Cenozoic (Kennett 1977, Exon 2000, DeConto & Pollard 2003, Coxall *et al.* 2005, Scher *et al.* 2011). There was a major increase in ocean productivity (Berger 2007), a very large drop in the calcite compensation depth (CCD) (Van Andel *et al.* 1975, Rea & Lyle 2005), pulses of strongly erosive Antarctic bottom water (Kennett & Shackleton 1976, Wright & Miller 1996) and Northern component

water (Miller 1992). A decrease in temperature and ocean acidity led to a drop in the calcite compensation depth (CCD), which in turn led to an increase in $CaCO_3$ preservation (Pagani *et al.* 2005). The CO_2 threshold below which glaciation occurs in the Antarctica is 750 p.p.m.v. based on boron isotope pH proxy on exceptionally well preserved microfossils (Pearson *et al.* 2009). For the Northern Hemisphere the glaciation must drop to 280 p.p.m.v (Pearson *et al.* 2009). This was not achieved until ~25 Ma based on isotope–capable global climate/ice-sheet model which accommodated both long term decline of Cenozoic atmospheric CO_2 levels and the effects of orbital forcing (Pearson & Palmer 2000, Pagani *et al.* 2005, DeConto *et al.* 2008, Pearson *et al.* 2009). Terrestrial cooling is indicated by pollen changes (Owen *et al.* 1998) and a mammalian turnover (Hooker *et al.* 2004). For example, Meng and McKenna (1998) reported that there is a distinct pattern of faunal turnovers in the Mongolian Palaeogene climate/mammalian-evolution link, where perissodactyl-dominated faunas of the Eocene were abruptly replaced by rodent/Lagomorph dominant faunas of the Oligocene. Meng and Mckenna (1998) interpreted the turnovers to be the result of global climatic reorganisation around the Eocene − Oligocene boundary. The event reflects a change in the environment from a warm, humid Eocene, to a cool, arid Oligocene. Although, the rise in Oligocene fauna is coincident with late Eocene cooling, an absence of significant correlation between both Palaeocene fauna and the number of general fauna with the late Eocene $\delta^{18}O$ isotopic values suggesting that the climatic change was not the sole factor (Figueirido *et al.* 2012).

1.5.3 Temperature versus ice volume change

The Oi-1 began gradually with benthic foraminiferal $\delta^{18}O$ values increasing by 0.6 ‰ over 300 kyr and culminated with values increasing by an additional 0.8 ‰ in 50 kyr (Zachos *et al.* 1996). Approximately 0.5 ‰ of this increase can be attributed to increased ice volume, while the remaining portion must reflect a 3 ^{o}C – 4 ^{o}C decline in deep sea temperature (Zachos *et al.* 1996).

Coxall *et al*. (2005) greatly improved our understanding of the Oi-1 by showing that a transition from a relatively deglaciated climate state in the latest Eocene to a climate state with well-developed ice sheets on Antarctica in earliest Oligocene time, was completed within 300 kyr and was composed of two 40 kyr steps (Coxall *et al.* 2005, Scher *et al.* 2011). At the height of the Oi-1 glacial maximum, deep water temperatures were slightly warmer than present and an ice cap with a volume at least 50% of that of the present day existed on the east Antarctica (Scher *et al.* 2011) (Figure 1.5).

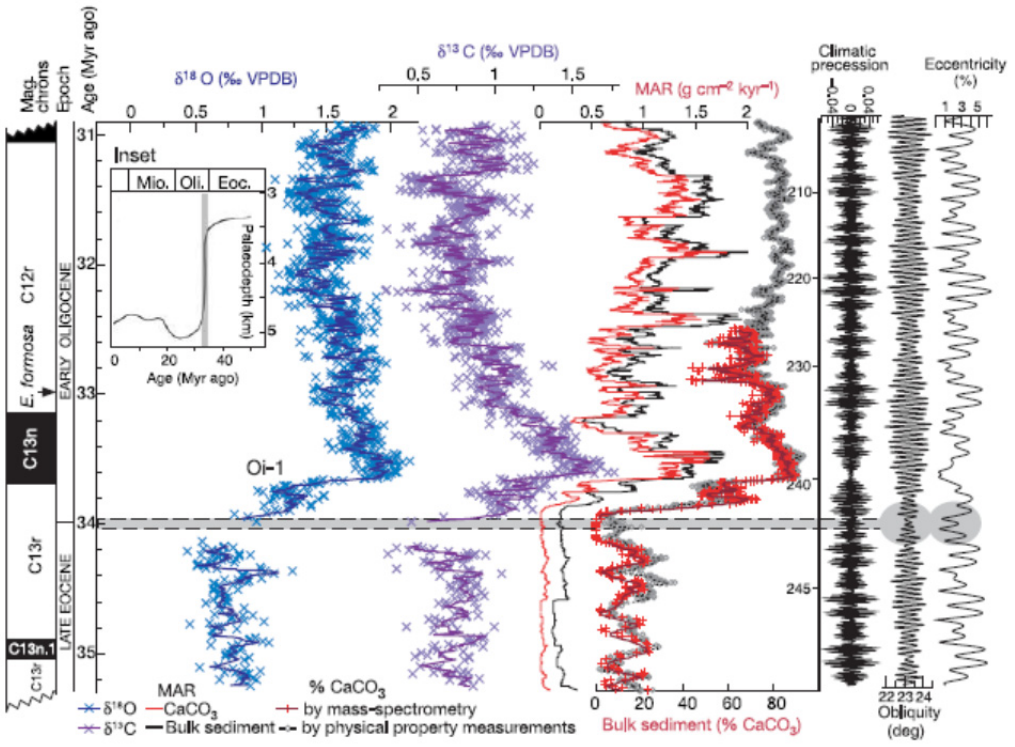

Figure 1.5: Palaeoceanographic records showing changes in global climate and ocean chemistry for the Eocene/Oligocene transition. The insert shows published CCD for the Equatorial Pacific Ocean 50 myrs ago (from Coxall *et al*. 2005).

In the terrestrial realm for instance oxygen isotope derived summer palaeotemperature for the continental fresh-water in the Northern Hemisphere, Isles of Wight, UK (Grimes *et al.* 2005), reconstructed palaeoprecipitation from palaeosols in Oregon and Nebraska, US (Sheldon & Retallack 2004) show that terrestrial data is sparse and contradictory for this time period. For example Grimes *et al*. (2005) show virtually no climatic change and only

weak faunal responses (Prothero & Heaton 1996) during the EOT; whereas Zanazzi *et al*. (2007) imply increased aridity and Elderrett *et al*. (2009) demonstrated increased seasonality and or aridity from key Ocean Drilling Projects (ODP) sites 913, 645 and 985, Norwegian Greenland Sea in the high-northern latitudes for the Eocene – Oligocene interval. Elderrett *et al*. (2009) on the basis of bioclimatic analysis of terrestrially derived spore and pollen assemblages preserved in marine sediments showed that a cooling of ~ 5^{o}C in cold-month (winter) with mean temperature to 0 – 2 ^{o}C, and a progressive increased seasonality before the Oi-1 glaciation event.

In another multiproxy study, Wade *et al*. (2012) suggested that cooling during the Eocene Oligocene transition was particularly associated with increased seasonality, with the majority of the cooling during the winter months. New data obtained recently using $\delta^{18}O$ in aragonite shells of freshwater gastropods *Viviparus lentus* from the Solent Group, Hampshire Basin, United Kingdom, shows a decrease in growing-season surface water temperatures (~10^{o}C) during the Eocene – Oligocene transition, which is similar to an average decrease in mean annual air temperature of 4 – 6^{o}C from late Eocene to early Oligocene (Hren *et al.* 2013). Lastly, Mosbrugger *et al*. (2005) and Hren *et al*. (2013) suggested a strong linkage between atmospheric CO_2 concentration, the temperature of the Northern Hemisphere, and the extent of the ice sheet in Antarctica.

In a related study Kotthoff *et al*. (2014) have shown that hinterland vegetation of the New Jersey Shelf was characterised by oak-hickory forest towards the lowlands and was conifer dominated in the highlands, during the Oligocene to the middle Miocene. Kotthoff *et al*. (2014) emphasised that there were several expansions of the conifer forest during the Oligocene period, which they related to cooling events. Their results signified an increase in annual temperatures from ~11.5^{o}C to > 16^{o}C during the Oligocene, based on pollen-based climate data.

1.6 LOCATION OF THE STUDY AREA

1.6.1 General Location

The Palaeogene Petrockstow and Bovey basins are located in Devon, Southwest England (Figure 1.6) and are related to the Sticklepath-Lustleigh fault zone. The Bovey Basin lies to the southeast of Dartmoor while the Petrockstow Basin is to the northwest (Figure 1.7).

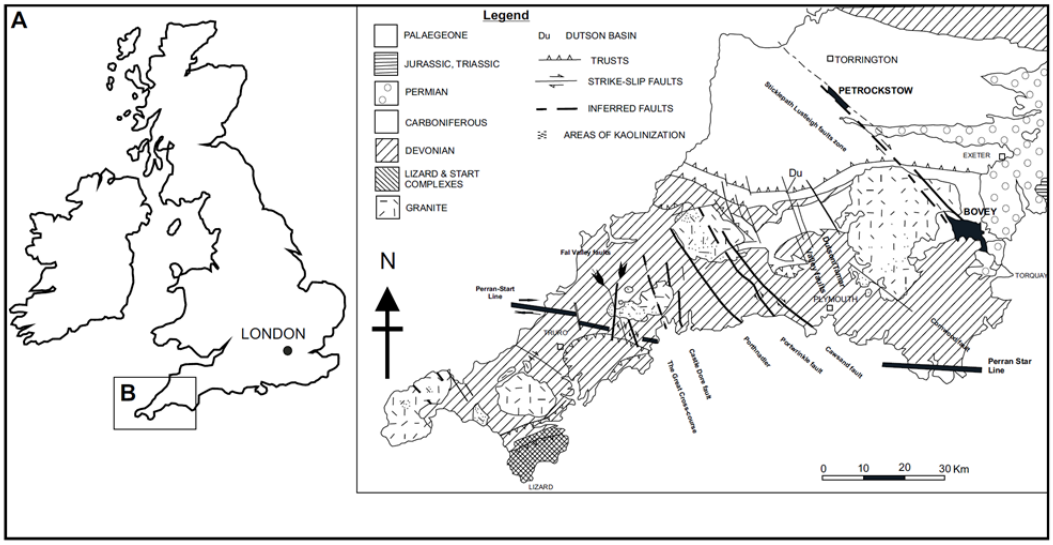

Figure 1.6: General geological map of the southwest UK showing Petrockstowe and Bovey basins (Bristow & Robson 1994).

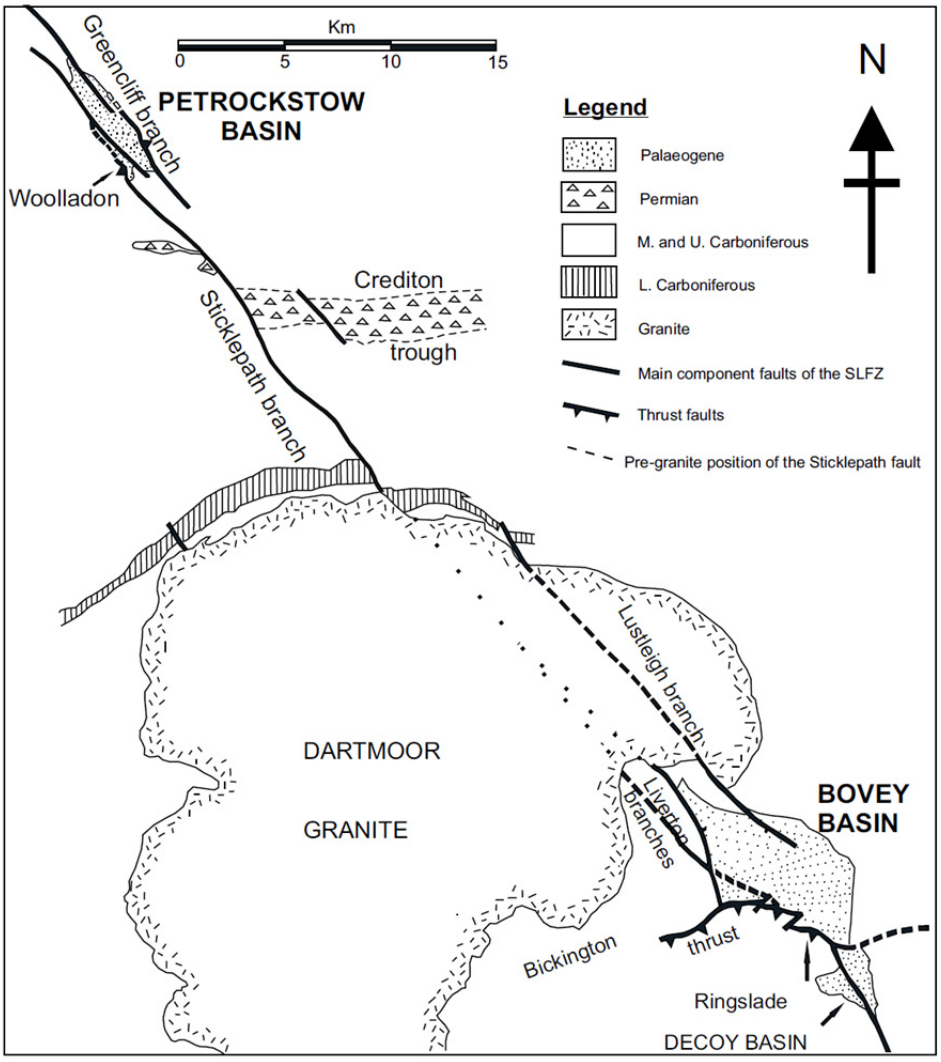

Figure 1.7: Map showing the location of Petrockstowe and Bovey basins (Bristow & Robson 1994).

1.6.2 Structural control and sedimentary fill of the Petrockstowe and Bovey basins

The Petrockstowe and Bovey basins lie on the line of the Sticklepath - Lustleigh Fault Zone (SLFZ) and owe their origin to subsidence within this zone (Blyth 1962, Dearman 1963). Holloway and Chadwick (1986) suggested that during the mid Eocene, the Sticklepath fault might have been active, where its movement could have led to the initiation of the strike-slip Petrockstowe and Bovey basins and was subsequently filled with fluvio-lacustrine

sediments. Bristow and Hughes (1971), and Bristow and Robson (1994) suggested that the southern boundary of the Petrockstowe Basin, was in part, formed due to a rejuvenated Variscan thrust fault that intersects with the western boundary faults, at a perpendicular angle south of Liverton (Figure 1.7). The SLFZ affected the northeast corner of the Bovey Basin and runs westwards through the Dartmoor granite. This fault forms part of a NW to NNW trending system of strike slip faults that cuts across western Britain and Ireland, with their history of reactivation linked to the Permian, Mesozoic and Cenozoic (Lake & Karner 1987). An example of this type of fault-bounded basin is the Lough Neagh Basin in Northern Ireland which also trends to the NE, and Rathlin Trough in Northern Ireland (Ziegler 1990). The Lough Neagh, Bovey and Petrockstowe basins have a similar sedimentary basin fill history (Wilkinson *et al.* 1980). Apart from this, Ruffell (2002) also stated that there was a complex wrench fault system that extended to the north of the Variscan Front to include the NW continuation of the SLFZ, the NW trending Coding Fault and the NNW trending Bann, Newry, Camlough and Markethill faults. To sum up, the offsets along the segmented SLFZ controlled the location of the early Cenozoic Bovey and Petrockstowe basins (Holloway & Chadwick 1986, Bristow & Robson 1994) and Lundy pull-apart basin (Arthur 1989, Quinn 2006). The continuous movement in the later part of the Palaeogene enabled the accumulation of thick clays in the basin similar to the Lough Neagh Basin (Quinn 2006). According to Blyth (1962) the Sticklepath – Lustleigh fault became active during the Paleogene, and most activity ceased before deposition of the upper part of the Bovey Formation. The Bovey Basin covers an area of approximately 50 Km^2 and is underlain by clays up to 1100 metres thick. The general geology of the Bovey Basin has been described by Vincent (1974), Edwards (1976) and Selwood *et al*. (1984).

1.6.3 Geological setting of the Petrockstowe Basin

The Petrockstowe Basin is located in the SW part of Chulmleigh district, near Newton Abbott, Devon, SW, England (Figure 1.6 &1.7). It is fault-bounded and over 600 m deep

(Freshney *et al.* 1979). It is located on the SLFZ. Movement within this faults zone (SLFZ) have been reported to be responsible for sedimentation and preservation of the Bovey Formation in the Petrockstowe Basin (Freshney *et al.* 1979). Shearman (1967), Freshney *et al*. (1979) and Cattell (1996) suggest that strike slip faulting was initiated during the Variscan Orogeny. The SLFZ and related faults might have moved dextrally (Shearman 1967, Cattell 1996) during and after the deposition of the Palaeogene sediments in the Petrockstowe Basin giving room to subsidence in the basin. The Palaeogene Petrockstowe Basin is situated on right offsets of the SLFZ and developed partly as a response to accommodation flexures, where the horizontal movement on SLFZ was transformed into vertical movements along the two sides of the SLZF through the granite (Bristow & Robson 1994). Bristow and Robson (1994) also proposed a structural model for the development of the basin – 'a pull-push' model – which suggested that the development was in two phases: an early, transitional phase, during which much of the sedimentation occurred, and a subsequent transpressional phase in which boundary thrust faults developed. The geometry of the basin margin faults is poorly understood, although Bristow *et al*. (1992) have proposed a model for the near surface geometry of the basin margin faults using both field data and exploration data. Crowell (1974) described pull-apart basins as deep rhomb shaped depression bounded on their sides by two, subparallel, overlapping strike-slip faults, termed transfer faults which link the two ends of the strike-slip faults.

A characteristic common to both Bovey and Petrockstowe pull-apart basins in SW England and the Lough Neagh Basin, is the thickness of their Palaeogene sedimentary fill (Quinn 2006). Allen and Allen (2013) defined a strike-slip fault as a linear to curvilinear in plan view and generally possess principal displacement zone (PDZ) along which the bulk of the shear strain is accommodated. Allen and Allen (2013) stated that structural pattern of strike slip faults are controlled by the following:

i) the kinematics (convergent, divergent, parallel) of the fault system

ii) the magnitude of the displacement

iii) the material properties of the rocks and sedimentary fills in the deforming zone

iv) the configuration of pre-existing structures

Based on geophysical measurements over the Bovey Basin, it is suggested that about 600 m of Palaeogene sediments may be present, confirmed by a borehole drilled by the British Geological Survey in the centre of the Petrockstowe Basin (Figure 1.8) which penetrated 660 m of sands and silts (Freshney *et al.* 1979).

Bristow (1968) stated that Paleogene sediments of the Petrockstowe Basin are likely to have been derived from weathering granite developed on Culm measures shale and sandstones under the warm temperate or sub-tropical conditions of early Paleogene times.

In the Petrockstowe Basin, Turner (1979) reported that pollen types indicated a boundary between the Oligocene and Eocene at about 120 m depth in British Geological Survey (BGS) Borehole No.1 and at about 240 m in Borehole No. 2 to the northwest; while pollen content in Borehole No. 3 was poor and could not be used in correlating the three BGS Boreholes biostratigraphically. A second method adopted by Turner (1979) for the correlation but not as an age control was heavy mineral analyses of the sands, which show abundant topaz and coarse fragmental reddish brown tourmaline between 305 m and 320 m, and in the sands and gravels below 550 m in BGS Borehole No. 1. In Borehole No.2, at 150 m to the northwest, an abundance of topaz occurred between 111 m and 133 m. The correlation of Turner (1979) at this horizon at 120 m in Borehole No. 1 accords best with the pollen evidence. The various correlations made using Borehole Nos 1 and 2 indicated an overlap at the north-west end of the basin, and is in accordance with the restriction of

lacustrine sediments to the northern half of the basin, with an indication of more rapid subsidence in the north than in the south.

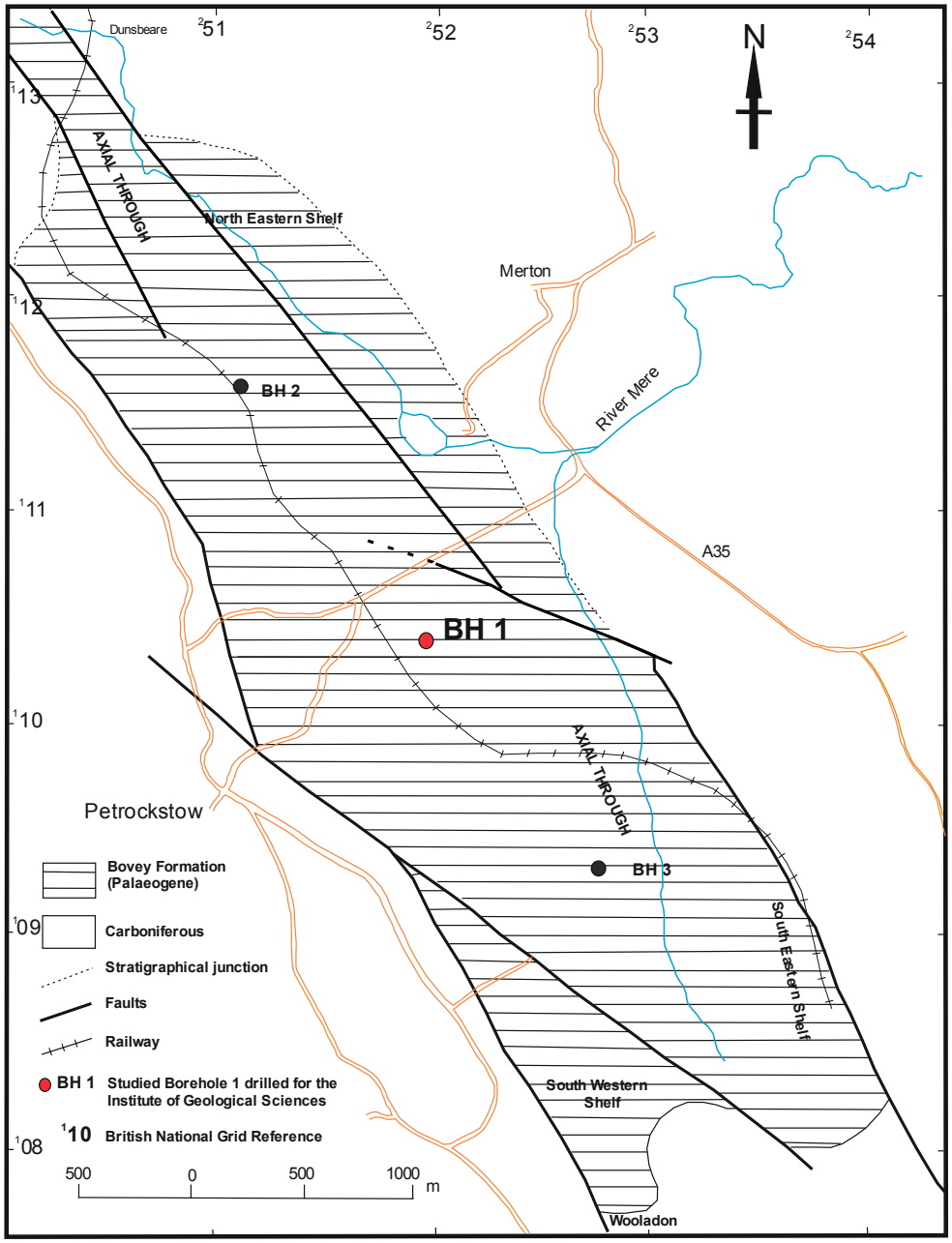

Figure 1.8: Geological map of the Petrockstowe Basin showing the location of Borehole 1 (cores 1A & 1B); [[1]10] British National Grids Reference, [modified from Freshney *et al*., 1979].

On the north eastern shelf of the basin, correlation of the shelf succession with the thicker sequence of the central trough seems to be difficult owing to facies changes (Freshney *et al.* 1979).

While Turner (1979) believes the shelf succession was wholly Eocene in age and therefore it should be correlated with beds below 235 m in Borehole No. 2, and between the depths of 110 m and 385 m in Borehole No. 1. These authors are of the opinion that sedimentation overlapped the internal shelf bounding faults and continued over a wider area at least into late Eocene times. The topmost Oligocene beds and some top Eocene strata are not restricted, as a result of erosion, to the axial trough area. Hence a possible estimate of maximum areal extent of deposition could be projected to be between 305 m and 350 m in the central part of the basin. Details of the events around the south-eastern marginal area (Meeth) and the south-western shelf area (Wolladon) (Figure 1.8) are contained in Freshney *et al*. (1979).

Many authors have stressed the significance tectonics has had on sedimentation within the basin (Freshney 1970, Edwards 1976, Reading 1980). The Petrockstowe Basin is mainly filled by kaolinitic clays, silts, sands, gravels and lignite of Paleogene age, which are correlated with the similar sediments of the Bovey Formation (Edwards 1976) in south Devon. Most workers agreed that these deposits are of Paleogene age, and work by Turner (1979), based on palynology indicates that the Petrockstowe sediments are dated to Oligocene and Eocene in age. A fining-upward sequence is observed which is suggestive of an alluvial environment, which is a prototype of the facies model as applied to fluvial deposits of Miall (1985). The gravels found at the bottom of each cycle might constitute a lag deposit, while the coarser sands more frequently found together with gravelly sands, fining upwards into silty sands, are probably representative of point bar and swale-fill deposits of a river system (Freshney *et al.* 1979). Based on palynological evidence, Turner (1979) suggested a subtropical climate with palms, ferns and heathers and many plants with swamp affinities. He noted that pollen from fagaceous trees probably derived from forest established on drier ground away from the river.

1.6.4 Geological setting of the Bovey Basin

The Bovey Basin is similar to the Petrockstowe Basin and is located between Newton Abbot, Kingsteignton and Bovey Tracey (See Figures 1.6 & 1.8). The Bovey Basin lies southeast of the Dartmoor granite and is roughly 7 km from east to west and 5 km from north to south (Figures 1.7 & 1.9). In the northern and eastern boundaries of the basin there are sedimentary contacts between the Dartmoor granite and the Upper Greensand and Aller Gravel, Aller Gravel and Lappathorn Member, Lappathorn and Abbrook clay-and-sand member these sediments dipped generally at low angle in the southwest or west.

The bulk of the basin is filled by a thick (~ 1200 m) sequence of Paleogene kaolinitic clays, silty clays, silts, lignites and sands, referred to as the Bovey Formation (Edwards 1976). The Bovey Formation is underlain along its eastern outcrop in the main basin and south of Newton Abbot by flint gravels of presumed Eocene age, the Aller gravel, and by shallow marine sands and gravelly sands of the Upper Greensand facies, which are Albian and Cenomanian in age; elsewhere it is faulted against or underlain by Devonian, Carboniferous or Permian rocks (Edwards 1976).

Edwards (1976) proposed a morphological sub-division of the basin into two parts, lying respectively to the north and to the south of Newton Abbot. The part between Bovey Tracey and Newton Abbot is considered as the main basin; the second part lies south of Newton Abbot and is referred to as Decoy Basin (Figure 1.9). Fashman (1971) gave 1245 m as the maximum thickness of the Bovey Formation based on gravity measurements while Vincent (1974) gave 1066 m based of drilled borehole record. Only the top 300 m are exposed at the surface and therefore studied. A borehole drilled at Teigngrace by the former Institute of Geological Sciences now British Geological Survey (BGS) around 1917 – 1918 proved 203.3m of Bovey Formation sediments and is the deepest borehole in the basin to date. Vincent (1971) studied another borehole drilled at the centre (in an area named Great Plantation) which achieved a depth of 260 m. The lithological succession of the Bovey

Formation is set out in Table 1.0 and the distribution is shown on the geological map (Figure 1.9).

Table 1.0: Lithostratigraphical units of the Bovey Formation (Edwards 1976)

Undifferentiated (mainly Blatchford Sand)	***Upper Bovey Formation***
	Woolley Grit Member
	Bovey Heath Member
	Green Plantation Member
	Heathfield Member
	Brimley Member
	Blatchford Sand Member
	Stover Member
	Twinyeo Member
Undifferentiated	***Middle Bovey Formation***
	Ringslade Clay Member
	Chudleigh Knighton Clay-and-Sand Member
Southacre Clay and Lignite	Southacre Clay-and-Sand Member
Abbrook Clay and Sand	Abbrook Clay-and-Sand Member
	Lappathorn Member
Undifferentiated	Staplehill Gravel Member
	Lower Bovey Formation
	(not exposed)
Woolley Grit	

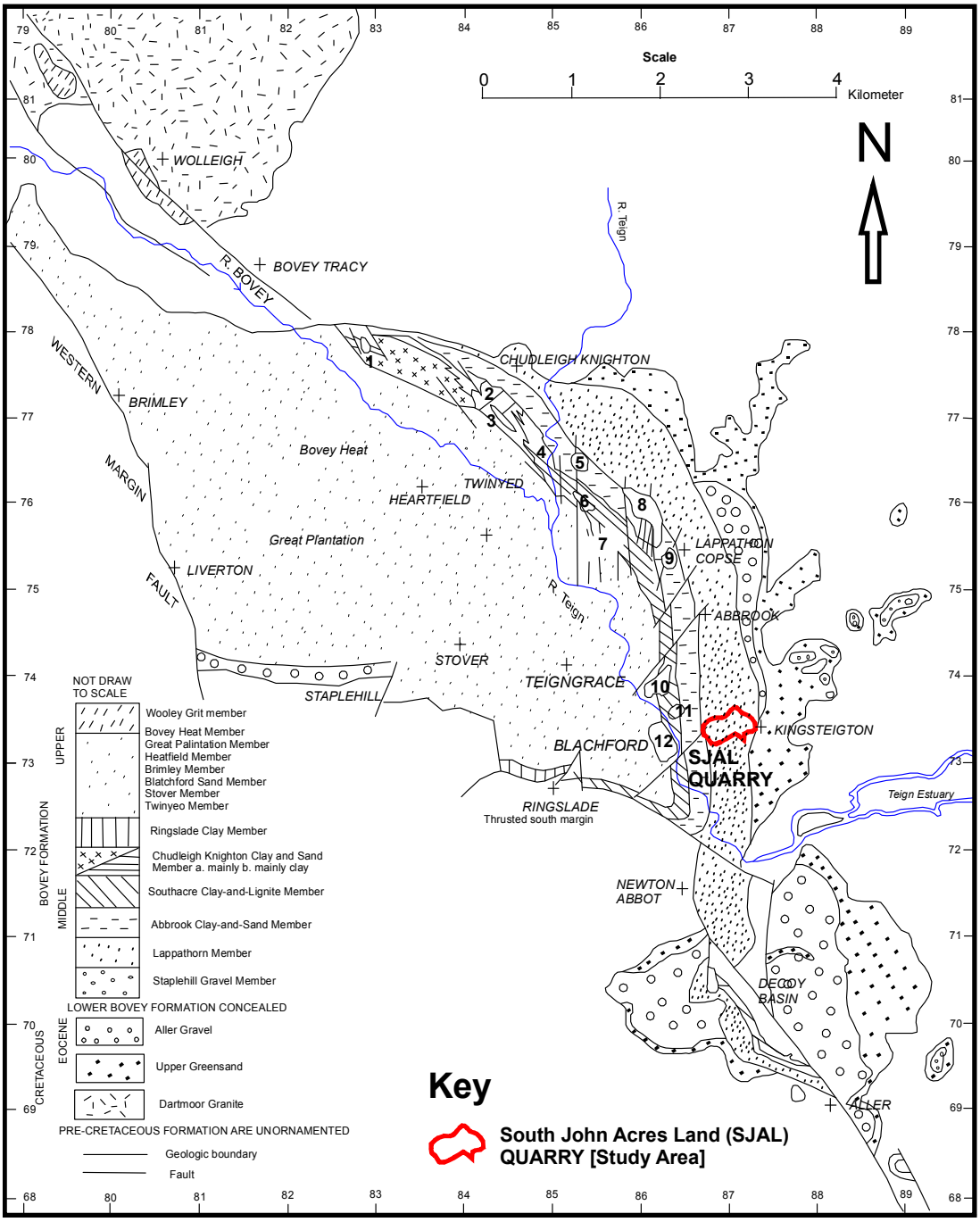

Figure 1.9: Geological map of the Bovey Basin showing the location of the South John Acres Lane (SJAL) Quarry modified from Selwood *et al.*(1984).

1.7 PALYNOLOGY

According to Traverse (1988), the late Palaeocene and early Eocene were typically very warm and were characterised by truly tropical floras in England. Traverse (1988) stated that maximum tropicality was at the early/middle Eocene boundary. The middle Eocene was considered as the palaeotropical maximum, as this was the time of greatest expression of the palaeotropical flora in the Northern Hemisphere.

The uppermost ca. 300m of the Bovey Formation based on borehole data in the Bovey Basin has been dated as early to middle Oligocene, with rare pollen grains at ca. 297 m depth suggesting the probability of Eocene sediments at greater depth (Wilkinson *et al.* 1980). Chandler (1957), Edwards (1976), Wilkinson and Boulter (1981), had earlier suggested that the Bovey Basin probably included Eocene and Oligocene strata, but dating was uncertain. Despite the fact that the Bovey Basin is a pull-apart type basin it is isolated and the lignites, clays and sands do not contain any faunal remains, although they are rich in flora in places. The deposits are only exposed in quarry sections where clay mining is ongoing.

In a related work, Freshney *et al*. (1982) observed that because the estimated depth of the Bovey Basin was 1100 m (Vincent 1974), then it can be argued that the lowermost ~ 700 – 800 m of the Bovey Formation could probably be assigned to Eocene. In addition, Curry *et al*. (1979) suggested that a late Eocene age for the lower part of the basin cannot be ruled out. Freshney *et al*. (1982) in their findings from the similar strike slip Dutson Basin, located southeast of Petrockstowe Basin, emphasised that out of the 26 genera range through the European Tertiary, *Nudopollis*, *Plicatopollis* and some of the spores are particularly characteristic of the Eocene, which show a great similarity with the present results which will be discussed in the subsequent sections.

Pollen and spores preserved in the Bovey Basin suggests an Oligocene or middle Oligocene age based on the key pollen and spore identified in this study, among which are *Arecipites*,

Inaperturopollenites, *Monocolpopollenites*, *Tricolporopollenites*, *Cicatricosisporites*, *Sequoaipollenites* and *Pompeckjoiaepollenites*. Wilkinson *et al*. (1980) reported a similar occurrence of these key Oligocene taxa in Washing Bay, Lough Neagh Clays, Northern Ireland to *Polypodiaceaesporites*, *Pitysporites*, *Inaperturopollenites*, *Arecipites*, *Monocolpopollenites*, *Tricolporopollenites*, *Tricolpopollenites* and *Polyvestibulopollenites*. These taxa were also found to be abundant in the Bovey section.

Palynofacies analyses was used in this present study to unravel the type of organic matter associated to the sediments as a means of determining the source of carbon reservoir in the basin and this is the first time such a method was used in both Petrockstowe and Bovey basins.

1.8 AIMS

Understanding the environmental changes that occurred during the early Palaeogene climate system especially those that took place in the early Eocene and the late Oligocene (e.g. Eocene – Oligocene transition and Oi-1 glaciation), with emphasis to the terrestrial realm, is of great importance investigating the Earth's climate system at this time period.

The aims associated with this research are:

1. To constrain the chronology of the Bovey and Petrockstowe basins using a combination of palynological and chemostrigraphic techniques.
2. To understand the changing palaeoenvironment of the Bovey and Petrockstowe basins and how this responded to climatic change during the Palaeogene
3. To investigate the regional response to transient and rapid climatic events such as hyperthermals and the Eocene – Oligocene boundary.
4. To generate the first absolute estimates of mean annual air temperature (MAAT) from the early Palaeogene, from Northern European terrestrial sections.

The techniques employed to achieve the stated aims included the following:

1. Sedimentary facies analysis of the Petrockstowe and Bovey basins

2. Total organic carbon (TOC) stable isotope analyses as a proxy for generating chemostratigraphic record ($\delta^{13}C_{TOC}$) in order to constrain the position and nature of the magnitude of the carbon isotope excursion
3. Palynofacies and palynological analysis as a proxy for palaeoenvironmental interpretation and dating of the sediments
4. Glycerol Dialkyl Glycerol Tetraether (GDGT) analysis for reconstructing palaeotemperatures using the MBT'/CBT proxy

CHAPTER 2 - METHODOLOGY

2.1 INTRODUCTION

This chapter outlines the research strategy and the main techniques employed throughout this thesis.

2.2 Petrockstowe Basin Logging

Two borehole cores from a registered borehole (Petrockstowe 1A & 1B) held by the core repository at the British Geological Survey (BGS), Keyworth, Nottingham, UK, were logged (Figure 2.1 – Figure 2.2). The sampled section was between 410 m and 240.52 m respectively (note the measurements were originally in non-metric units of inches but have been converted to standard units). Facies analysis was used to describe and interpret sedimentary data allowing for major depositional processes and environments of deposition to be interpreted within the basin. Facies analysis followed Miall's (1985, 1988) principles, with minor modifications. In the course of the logging in some instances part of the cores were missing, which was noted in the driller's notes and confirmed by my own observations. It is very important to note that the core was not cut or slabbed.

2.2.1 Sampling

In total 96 samples were collected for Total Organic Content (%TOC) and $\delta^{13}C_{TOC}$ analysis across the entire depth of the cores. The sampling spacing interval was at an average of 1 m, in some places less, while in others more. Based on the %TOC values obtained, 30 samples were chosen for the palynological analysis, especially within the region of the Eocene – Oligocene boundary as proposed by Turner (1979), and the CIE region, where high – resolution sampling for $\delta^{13}C_{TOC}$ was also carried out. Also, 16 samples were collected and analysed for the Gycerol Dialkyl Gycerol Tetraethers (GDGT).

Figure 2.1: Petrockstowe core samples in the BGS Keyworth core laboratory displayed for description, logging and sampling by the Researcher

Figure 2.2: Part of a zoomed core sample (the cores are not slabbed) showing the condition of the core material at the GBS Keyworth, core laboratory

2.3 Bovey Basin - South John Acres Lane (SJAL) Quarry Fieldwork

Centimetre (cm) scale logging of 48 m of the Abbrook Clay-and-Sand Member to the upper Lappathorn Member of the Bovey Formation was undertaken in the exposed working section at the John Acre Lane Quarry (Figures 2.3, 2.4, & 2.5). Concurrently, while generating the lithological log, samples were collected throughout the entire section with the objective of analysing them for $\delta^{13}C_{TOC}$ in order to determine the chronostratigraphic age of the sediments and any possible CIE which may be related to Eocene sediments as reported by earlier studies in this area (Wilkinson 1979). Approximately 500 g of sediments from each horizon was collected, and the sampling resolution was a minimum of 2 m, although this varied in some places depending on the length of the section. In total 70 samples were analysed for %TOC, $\delta^{13}C_{TOC}$, palynology and Glycerol Dialkyl Glycerol Tetraether (GDGT) extraction from the Bovey Formation.

2.3.1 Sampling

The method adopted during sample collection in all instances was virtually the same. Before sampling trenches were cut to ensure only fresh material were collected. The material was collected using a hammer. Upon return to Plymouth samples were oven dried at 30^{o}C for 24 hours to ensure complete dryness. After this the samples were ready for preparation for bulk $\delta^{13}C_{TOC}$, palynology and Glycerol Dialkyl Glycerol Tetraether (GDGT) extraction.

The purpose of description and interpretation of facies and depositional environments of the Bovey Formation, (Miall 1985, Miall 1988) method was adopted.

Figure 2.3: View of part of the section logged and sampled in the South John Acres Lane Quarry section, Bovey Basin showing Abbrook Clay-and-Sand Member to the upper Lappathorn Member of the Bovey Formation

Figure 2.4: View of the section logged and sampled in the South John Acres Lane Quarry section, Bovey Basin showing out cop of part of the Southacre Clay-and-Lignite Member

Figure 2.5: View of the South John Acres Lane Quarry section, Bovey Basin showing the out cropped Southacre Clay-and-Lignite Member comprising of lignites and carbonaceous brown and black clays, with subordinate grey to greyish brown silty clays and sands.

2.4 Total Organic Carbon (TOC) Stable Isotope Analyses

For the determination of total organic carbon (TOC) and $\delta^{13}C_{TOC}$ analysis, rock samples of ~ 20 g were homogenised by grinding. The samples were then decarbonated using aqueous hydrochloric acid (HCl; 10%, v/v). A small amount of material was transferred into a 100 ml glass beaker filled with HCl; (10%, v/v) and left to settle for a minimum of 24 hours. Once settled, excess HCl was decanted and the process repeated until no reaction was observed, indicating all carbonate material had reacted. Each sample was then washed with deionised water and left to stand for 24 hours; this procedure was repeated until the sample was completely neutralised as indicated by testing with Whatman Universal pH 1 – 11 indicator paper. The aqueous phase was then decanted and the residue was dried in the oven at 40^{o}C for 24 hours and powdered again.

Following decarbonation, dried and ground samples were analysed at the NERC National Isotope Geosciences Laboratories (NIGL) at Keyworth, UK. A small pellet of each sample was placed into a foil thimble. Quantities of material used for analysis were determined on the basis of their TOC content. TOC content was measured using a Carlo Erba 1500 elemental analyser with acetanilide used as the calibration standard. Replicate analyses showed that a precision of $\pm 0.1\%$ (1Standard Deviation, σ), in well-mixed samples for the analyses conducted during the period July 2011 to April 2012 (Appendix 1, Table 5.1 – 5.3). For $\delta^{13}C_{TOC}$ analysis, between 1 mg and 120 mg of sample was weighed into a tin capsule, the capsule was folded and placed into a Carlo Erba 1500 EA for analysis using an online VG Triple Trap Mass Spectrometer. This setup also included a secondary cryogenic trap in the mass spectrometer for the analysis of very low carbon samples. The $\delta^{13}C_{TOC}$ results were calibrated against Vienna Peedee Belemnite (VPDB) using the International Standards NBS-19, IAEA-CO-8 and IAEA-CO-9. Five standards were evenly distributed throughout the individual isotope runs to correct for daily drift. The mean standard deviation on replicate $\delta^{13}C_{TOC}$ analyses of laboratory standard (BROC1) and soil (SOILB) was between $\pm 0.1‰$ – 0.5‰ (1 Standard Deviation, σ) for $\delta^{13}C_{TOC.}$ The carbon isotope composition of the TOC within the samples is referred to as $\delta^{13}C_{TOC,}$ and the period of the analysis was from July 2011 to April 2012 (Appendix 1, Table 5.1 – 5.3).

Regression analysis was used to determine whether there was a significant correlation between $\delta^{13}C_{TOC}$ values and % weight of organic carbon (wt. % TOC) for Petrockstowe cores 1A, 1B and South John Acres Lane Quarry section (because of low R^2), temporary it is assumed that $\delta^{13}C_{TOC}$ values are independent of lithological facies change.

2.5 Organic Geochemistry

2.5.1 Glycerol Dialkyl Glycerol Tetraether (GDGT) Analysis

To reconstruct high resolution terrestrial palaeotemperatures in both the Bovey and Petrockstowe basins, a novel geochemical proxy based on branched Glycerol Dialkyl

Glycerol Tetraether (brGDGTs) found in bacterial membrane lipids was employed (Weijers *et al.* 2007a, Peterse *et al.* 2012). The Metheylation Branched Tetraether/Cyclization Branched Tetraether ratio (MBT'/CBT) proxy for the reconstruction of palaeotemperatures and past soil pH is based on the distribution of branched Glycerol Dialkyl Glycerol Tetraether (brGDGT) membrane lipids in soils, peats and lacustrine and coastal marine sediments (Schouten *et al.* 2013, Bauersachs *et al.* 2015). Weijers *et al*. (2007a) has shown that the worldwide distribution of different brGDGTs varies with mean annual atmospheric temperature (MAAT) and soil pH; where the number of cyclopentane moities has a direct relationship to soil pH, while the number of methyl branches is related to MAAT and to a lesser degree, also to pH. The relatively strong affiliation between brGDGT-Ia and pH demonstrates that the degree of methylation is to an extent dependant on pH (Weijers *et al.* 2007a, Peterse *et al.* 2012).

In order to determine CBT and MBT' indices which are based on brGDGTs, the calculation of CBT is according to (Weijers *et al.* 2007b) (Eq. 1)

$$CBT = -Log(\frac{Ib+IIb}{Ia+IIa}) \quad (1)$$

$$MBT' = \frac{[I+Ib+Ic]}{[Ia+Ib+Ic+IIa+IIb+IIc+IIIa]} \quad (2)$$

Eq. 2 is a modified calibration by Peterse *et al*. (2012) which is employed in the calculation of the reconstructed MAAT using equations 3 and 4.

$$pH = 7.90 - 1.97 \text{ x } CBT \quad (3)$$

$$MAAT = 0.81 - 5.67 \text{ x } CBT + 31.0 \text{ x } MBT' \quad (4)$$

The MBT'/CBT proxy has been applied as a MAAT proxy in several studies throughout the Cenozoic to reconstruct lakes and coastal marine environments that have a large proportion of terrestrial organic matter, (Weijers *et al.* 2007b, Schouten *et al.* 2008, Zink *et al.* 2010).

2.5.2 Branched and Isoprenoid Tetraether Index (BIT)

The Branched and Isoprenoid Tetraether (BIT) index is another organic proxy dependent on the relative abundance of brGDGTs, representing terrestrial organic matter, relative to Crenarchaeol, was dominant GDGTs in marine environment as contain in Figure 2.6 Hopmans *et al*. (2004) as a means of quantifying the relative abundance of terrestrial organic matter (OM). It is calculated using eq. 5 of Hopmans *et al*. (2004):

$$BIT = [Ia + IIa + IIIa] \,/\, [Ia + IIa + IIIa + Cren] \quad (5)$$

Where *Cren* = Crenarchaeol, and Ia, IIa, IIIa etc refer to specific branched GDGTs (Figure 2.7)

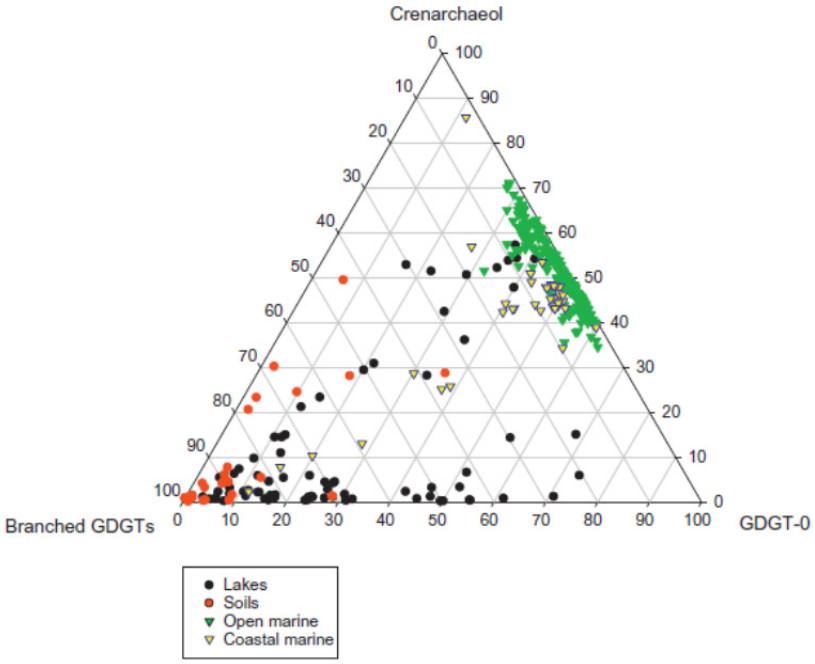

Figure 2.6: Ternary diagrams showing the distribution of GDGT-0, Crenarchaeol and total branched GDGTs in modern environments (Schoon *et al*. 2013).

Because the BIT index uses compounds of similar structure, it has the potential to be relatively insensitive to diagenetic bias (Hopmans *et al.* 2004). It can reach values ranging from 0, denoting no brGDGTs for open marine sediments, to 1, denoting no Crenarchaeol, for soil and peat samples. Hopmans *et al*. (2004) tested this novel index by applying it to

core top sediments from the Angola Basin near the mouth of the Congo River. They found that the brGDGTs are derived from ubiquitous organism living in soils and peats and are not selective for any particular vegetation type or climate (Hopmans *et al.* 2004). Kim *et al*. (2006), Herfort *et al*. (2006) and Kim *et al*. (2012) showed that the index was high (mainly >0.8) in river-suspended particulate matter and decreased in marine suspended particulate matter with increasing distance from the coast.

The structural definition of GDGT-1, GDGT-2 and GDGT-3 are as found in Weijers *et al*. (2007b) and Castaneda & Schouten (2011) which is shown in Figure 2.7. Isoprenoidal GDGTs are considered to be derived mainly from pelagic Thaumarchaeota (Brochier-Armanet *et al.* 2008); which is formally known as Crenarchaeota Group 1; (Sinninghe Damsté *et al.* 2012) and some Euryarchaeota, which are ubiquitous in marine sediments (Kim *et al.* 2008, Kim *et al.* 2010).

2.5.3 Extraction and analysis

Approximately 50 g of dry powdered sediment was extracted via a Soxhlet apparatus for 24 hours using dichloromethane/methanol (DCM/MeOH; 2:1; v/v) as the organic solvent. Solvent was removed from recovered total organic extract (TOE) by rotary evaporation under near vacum before transfer to a vial with washings and removal of solvent under nitrogen.

The TOE was further fractionated over Al_2O_3 into apolar and polar fractions using *n*-hexane: DCM (9:1; v/v; apolar) and DCM:MeOH (1:2; v/v; polar). The polar fraction containing GDGT was dissolved in *n*-hexane/*iso*-propanol (99:1; v/v) and passed through a 0.45µm PTFE filter. GDGT containing fractions were analysed using an Agilent 600 series High Performance Liquid Chromatography/Atmospheric Pressure Chemical Ionization – Mass Spectrometry (HPLC/APCI-MS) system. Normal phase separation was achieved on an Alltech Prevail Cyano column (150 mm x 2.1 mm; 3µm) with a flow rate of 0.2 ml min^{-1}.

Initial solvent was *n*-hexane/*iso*-propanol (99:1; v/v) eluted isocratically for 5 minutes, followed by a linear gradient to 1.8% *iso*-propanol over 45 minutes. Analyses were performed in positive selective ion monitoring (SIM) mode for protonated molecular ions $[M+H]^+$ to increase sensitivity. All samples were analysed using two SIM methods. Firstly, the ions at *m/z* 1302, 1300, 1298, 1296, 1292, 1050, 1036, 1034 and 1022 were measured and peak areas were integrated to provide the relative abundance of the major GDGTs and to calculate the BIT indices, although the samples under consideration are non-marine. Secondly, emphasis is on the second set, where the ions at *m/z* 1292, 1050, 1036, 1034, 1032, 1022, 1020 and 1018 were measured and peak areas integrated to provide the relative abundances of all branched GDGTs and to calculate MBT', CBT and BIT indices. Integration of peak areas was undertaking using XCalibur V.2.0.6 software.

Samples were only analysed once due to the limited concentration of GDGTs; therefore repeatability was not calculated. However, daily measurements of an in – house peat standard over the course of 5 months (during which brGDGTs within were measured) show (1 σ) of 0.05 for pH and 0.33 °C for MAAT which is lower compared to the original calibration error for soil pH and MAAT estimates of 0.7 and 5.0^{o}C respectively using the MBT' – CBT using Eq. 1 and 2 (Peterse *et al.* 2012).

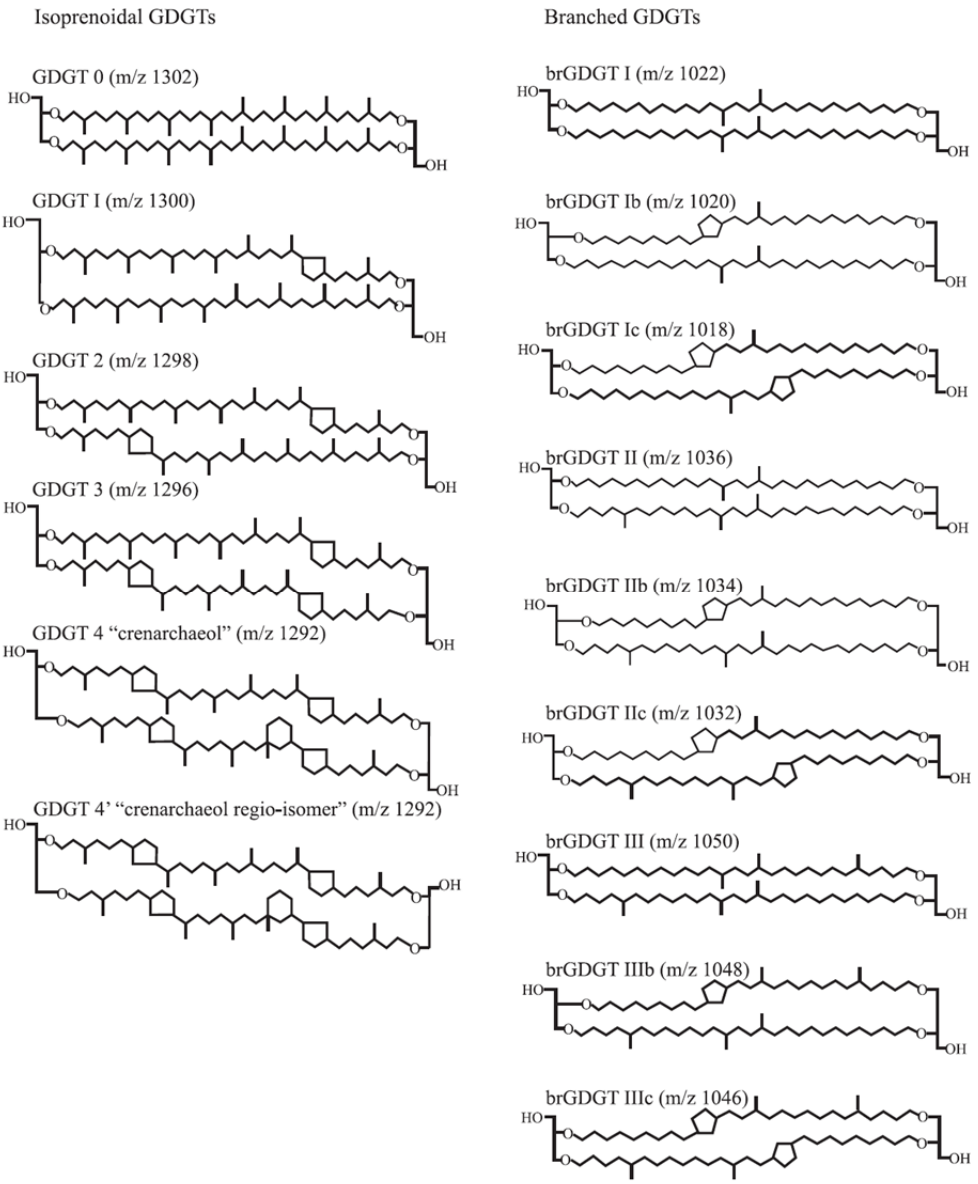

Figure 2.7: Molecular structure of isoprenoid Glycerol Dialkyl Glycerol Tetraethers (GDGTs) and branched GDGTs used for calculating of MBT'/CBT, BIT Index (Weijers *et al*. 2007b, Castaneda & Schouten 2011).

The samples for GDGTs analyses were analysed in two separate batches, with the first batch of samples prepared, processed and run at the Organic Geochemistry Laboratory (OGL), School of Chemistry, University of Bristol, UK (which involves pulverisation, Soxhlet extraction, fractionation into polar and apolar fractions, dissolution and passing through a 0.45μm PTFE filters). While the second batch of the samples were partly prepared at the Chemistry laboratory of the University of Plymouth, UK (which involved pulverisation, Soxhlet extraction of the organic lipid, fractionation into polar and apolar fractions,

dissolution and passing through a 0.45 µm PTFE filters). Then after this stage, all the samples from both batches containing the GDGTs fractions were analysed at the OGL, School of Chemistry, University of Bristol, UK by the use of an Agilant 600 series High Performance Liquid Gas Chromatography/Atmospheric Pressure Chemical Ionization – Mass Spectrometer (HPLC/APCI-MS).

2.6 Palynological sample preparation

The samples were prepared at the Palynology Laboratory of the BGS, Keyworth. The samples were first registered on entry to laboratory and allocated a BGS working laboratory code: MPA61578 -61587, MPA62269 - 62288, MPA63216 - 63260 (for n = samples, where n = 75). Samples from Petrockstow cores 1A & 1B and South John Acres Lane Quarry section, totalling 75, were collected and processed. A summary of the outline of the general procedure for palynological sample processing is given in Figure 2.8 for easy comprehension.

2.6.1 Removal of silicates and carbonates

All samples were prepared according to standard palynological techniques (Traverse 1988, Brown *et al.* 2008). In general the quantity of samples required for palynological preparation depends on the organic content of the samples; in this context 20 g was used and transferred into 150 ml bottles where ~75 ml of Hydrofluoric acid (HF) (40%) was added to dissolve the silicates. The samples were then left in the fume hood for one week and then sieved at 10 µm and placed in warm hydrochloric acid (HCl; 36%) with the aim of dissolving the carbonates. Caution was taken not to allow the samples to boil so that they didn't contaminate other samples. The samples were again sieved at 10 µm and the > 500 µm fractions were removed (Figure 2.8). The next step taken was to centrifuge and allow the samples to settle, decant off the HF while continuing the neutralisation with the addition of deionized water.

2.6.2 Heavy Liquid separation

A heavy liquid separation was carried out on samples: MPA63216, MPA63217, MPA63219, MPA63220, MPA63221 and MPA63233 where minerals still remained. Zinc bromide ($ZnBr_2$) solution with a specific gravity of 2.0 (76%, w/w) was added to 50 ml of the residue sample in centrifuge tubes and was agitated using a Vortex mixer for 1 minute. Separation occurred at 4000 rpm after 5 minutes of continues centrifugation (Figure 2.8). The merit of using $ZnBr_2$ is that it is, can be reclaimed easily and is less expensive than the other heavy liquids. The float was the predominantly organic fraction; disposable pipettes were used to extract this organic fraction, with a small amount of water added first to allow removal of the organic layer. At this juncture, oxidation was carried out on samples where necessary (see the section on oxidation). Samples that did not require oxidation were washed in distilled water prior to mounting. A few drops of the wet suspension were always previewed on a temporary slide before they were finally mounted to give an indication on the nature of the organic matter present.

2.6.3 Oxidized sample preparation

Oxidation was required in some sample where there seems to be too much organic matter present, or if the palynomorphs are too dark to be identified. Tschudy (1958) stated that oxidation gives a complete dispersal of pollen and removal of humic material. Oxidation was achieved by the addition of nitric acid (HNO_3) to the centrifuge mixture of the samples, decanted and mounted onto cover slips. Addition of the HNO_3 was made for different periods to some few samples depending on the sample requirement, which lasted up to 2 minutes. Proper oxidation is the point at which the pollen and spores are comparatively light and transparent.

2.6.4 Mounting of slide

One drop of Polyvinyl Alcohol (PVA) solution was added to the suspension from stage 2 and left on a warm plate for the water to evaporate. The residue was mounted onto cover slips. After curing and cooling, the slides were cleaned with acetone. By the adaptation of this method, all palynomorphs are settled onto the coverslip and should be in a similar plane when viewing the slide (Tschudy 1958, Collinson *et al.* 2009). This procedure was followed as shown in Figure 2.8 for every sample.

2.7 Palynological slides

Slides were studied using a Zeiss standard microscope, normally using standard transmitted light, but occasionally using phase contrast to determine palynological characteristics. A total of 67 samples were used for palynofacies analysis while 36 samples were used for palynological analysis. Out of the total samples processed, 8 from South John Acres Lane (SJAL) Quarry section and 1 from Petrockstow core 1B respectively were found to be barren for both palynofacies and palynological analysis. In the palynological analysis species were identified where possible. Counts were made using X40 objective, and where required a X100 objective was used to check morphological detail. The standard count of 300 species per slide was used. According to Buzas (1979), when ~ 300 counts are made the indices can very reliable and when comparison is made of the number of two populations with respect to the number of species that may contain the resultant number of individuals in the two populations should be the same.

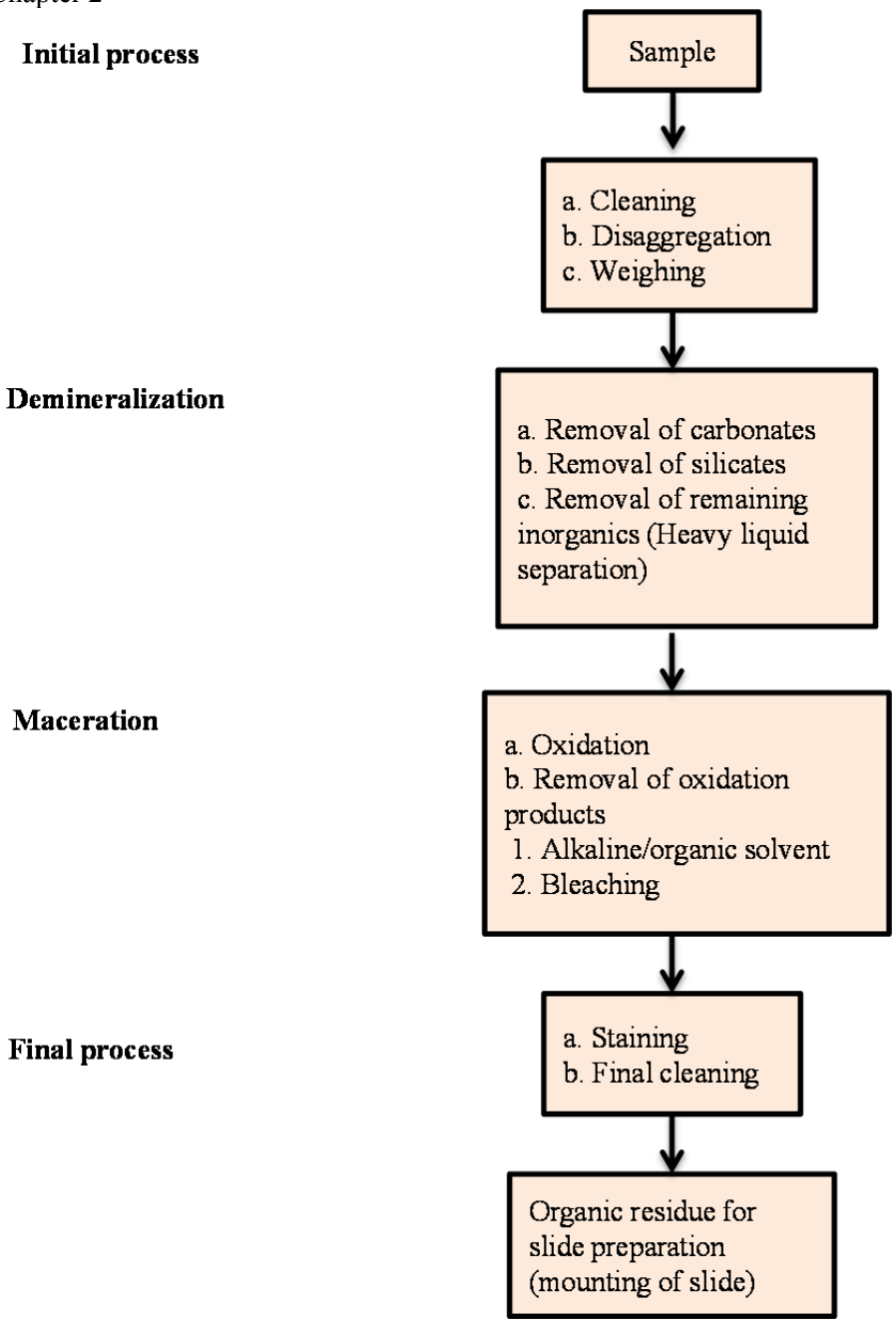

Figure 2.8: Schematic presentation of palynological sample processing (Traverse 1988).

2.8 Taxonomy of some selected form genus

A brief description of the taxonomy of key species is considered and presented as follows with some comment on their botanical affinity which has been adopted for this thesis.

Phylum – Bryophyta

Class – Musci

Order – Sphagnales

Form-genus: *Stereisporites* spp. The living species of Sphanagles are tropical to subtropical, with many representatives in temperate regions

Phylum – Pteridophyta

Class – Pteropsida

Order – Filicales

Family – Schizaeaceae

The spore Schizaeaceae is highly abundant in Eocene deposits. The living species of the family are largely tropical, less often subtropical and temperate.

Form-genus: *Cicatricosisporites* spp.; it has a natural affinity of Schiaeaceae, Anemia/Mohria which is a fossil type. It has a lateral pyramidal shape and single/radial symmetry. Length in view 47.0µm; the type of aperture is laesura, pointed at the end.

Family – Polypodiaeceae; the living species of polypodiaceae are widely tropical, subtropical and temperate habitats. Their spores are mostly and often very commonly represented in the Eocene deposits

Form-genus: *Polypodiaceoisporites* Potonie, 1953; with natural affinity of Pteris (Pteridaceae) in a fossil form. The shape is polar and triangular in form of a single grain with radial symmetry. The type of aperture existing is

laesura/trilete. The sporoderm has one layer, cingulum with a thickness of 4 – 6 μm.

Form-genus: *Laevigatisporites* Potonie & Gell 1933

Family – Taxodiaceae, taxodium

Form-genus: *Inaperturopollenites* hiatus Potonie, 1931b; it has an affinity with conifers/gymnosperm of fossil type. The shape is equatorial with a diameter of 35.0 μm and monad grain. The exine is psilate and very thin ~1 μm. The aperture is *Inaperturopollenites*.

Form-genus: *Sequoiapollenites* sp.

Class – Dicotyle donopsida

Family – Nyassaceae; the living species of the Nyassaceae are tropical and subtropical trees. Their pollen is particularly abundant in the middle Eocene deposits

Form-genus: *Tricolporopollenites* spp. (Brenner, 1968); with an equatorial pollen shape to subprolate, monad grain and bilateral symmetry at times is iso/anisopolar. The exine layer type is tectate where the nexine is very thick, dense and shows sculpture that is micropitted. The aperture type is tricolporate with a narrow ectocolpi. It shows a large endopore that is distinct. The affinity of these taxa is mainly angiosperm.

Family – Meliaceae

Form-genus: *Tetracolporopollenites* sp. Natural affinity is angiosperm; the shape is equatorial with a diameter of 23.0

μm. The equatorial pollen shape is prolate, monad grain; symmetry is radial which is iso/anisopolar. The exine layer is tectate, thick nexine and gradually thickens toward equatorial region. The sculpture is psilate, aperture type is tricolporate, ectolpi is costate, endoaperture is endpores; colpi is long which almost reaching the pores with straight boarders and pointed end.

Form-genus: *Plicapollis pseudopollenites*

Form-genus: *Minorpolli*

CHAPTER 3 – FACIES ANALYSIS

3.1 INTRODUCTION

The term Facies was introduced by Gressly (1838) and defined by Walker (1992) as a body of rock characterized by a particular combination of lithology, physical and biological structures that are different from the bodies of rock above, below and laterally adjacent. A facies association is defined as a group of facies that are genetically related to one another, and which have some environmental significance (Collinson 1969). Although different facies may represent different depositional processes, these different processes can occur together or very near each other in space and time in the same depositional environment. Hence, a facies association represents a specific depositional environment.

Facies analysis is the analysis of the vertical and lateral relationships between facies associations, that can be used to reconstruct the spatial and temporal changes in the depositional environment of sedimentary rocks, and reconstruct the controls upon these.

In this chapter, facies analysis will be used as a tool to:

- establish the depositional environments;
- reconstruct and isolate the accommodation (tectonic/base-level) and climate controls on sedimentation; and
- establish the potential occurrence of unconformities (sequence boundaries), which may be of importance when evaluating the continuity of records of temporal change provided by geochemical and palynological analyses within the Petrockstowe Basin and Abbrook Clay-and-sand and Southacre clay-and-lignite members of the Bovey Basin.

3.2 FACIES ANALYSIS OF PETROCKSTOWE 1A AND 1B CORES AND THE ABBROOK CLAY-AND-SAND MEMBER AND SOUTHACRE CLAY-AND-LIGNITE MEMBER, BOVEY FORMATION, JOHN ACRES LANE QUARRY, BOVEY BASIN

In the Petrockstowe Basin, the facies are described from two boreholes (1A and 1B, GR SS 5200 1040 and SS 5202 1041 respectively). A sedimentary log generated from the Petrockstowe cores 1A and 1B through the Bovey Formation are presented in Figures 3.1.1 – 3.1.7. The sediments/lithology of Petrockstowe Basin has previously been described in (Freshney 1970, Edwards 1976, Edward Cameron Freshney *et al.* 1979). No detailed facies analysis (*sensu stricto*) of Petrockstowe Basin sediments has yet been published. In the John Acres Lane Quarry, Bovey Basin (GR SX 286270 75020) the descriptions are from exposures. A sedimentary log measured through part of the Abbrook Clay-and-sand and Southacre clay-and-lignite members is shown in Figure 3.2.0. Aspects of the sedimentary facies of the Abbrook Clay-and-sand Member and South Acre Clay-and-lignite Member of the Bovey Formation have previously been described by (Edwards 1971, Vincent 1974, Edwards 1976, Selwood *et al* (1984).

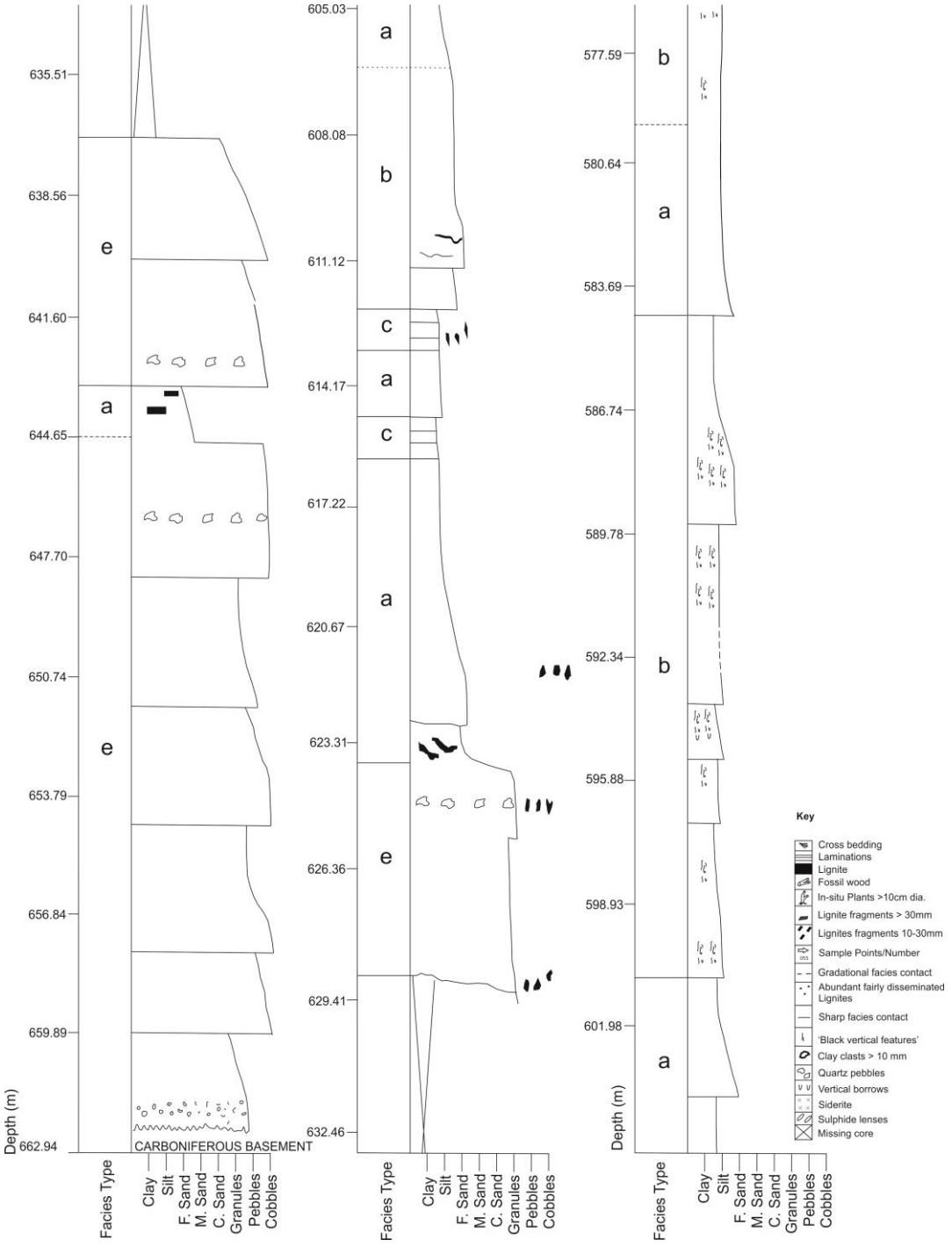

Figure 3.1.1: Composite sedimentary log through Bovey Formation, Petrockstowe core 1B

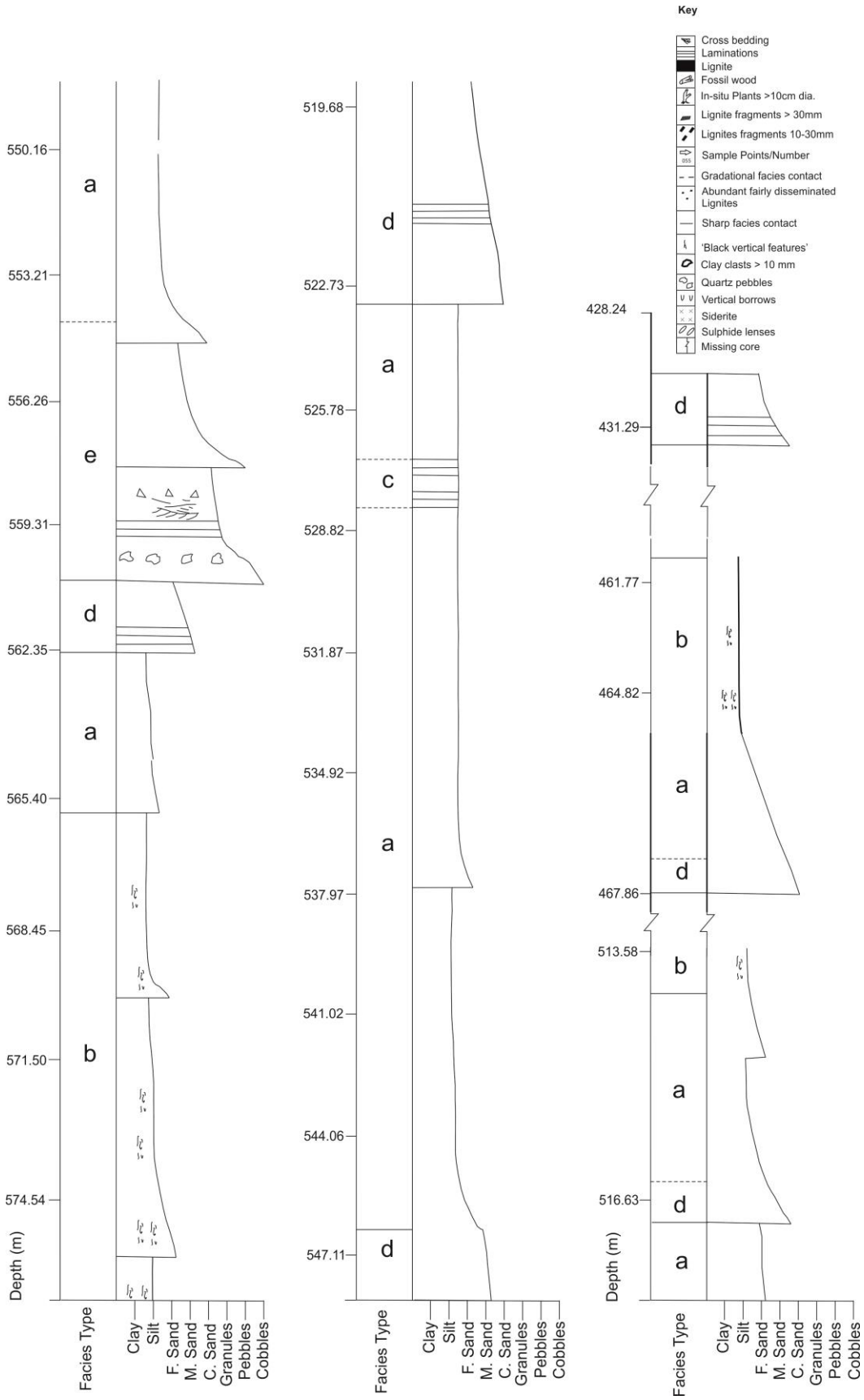

Figure 3.1.2: Composite sedimentary log through Bovey Formation, Petrockstowe core 1B

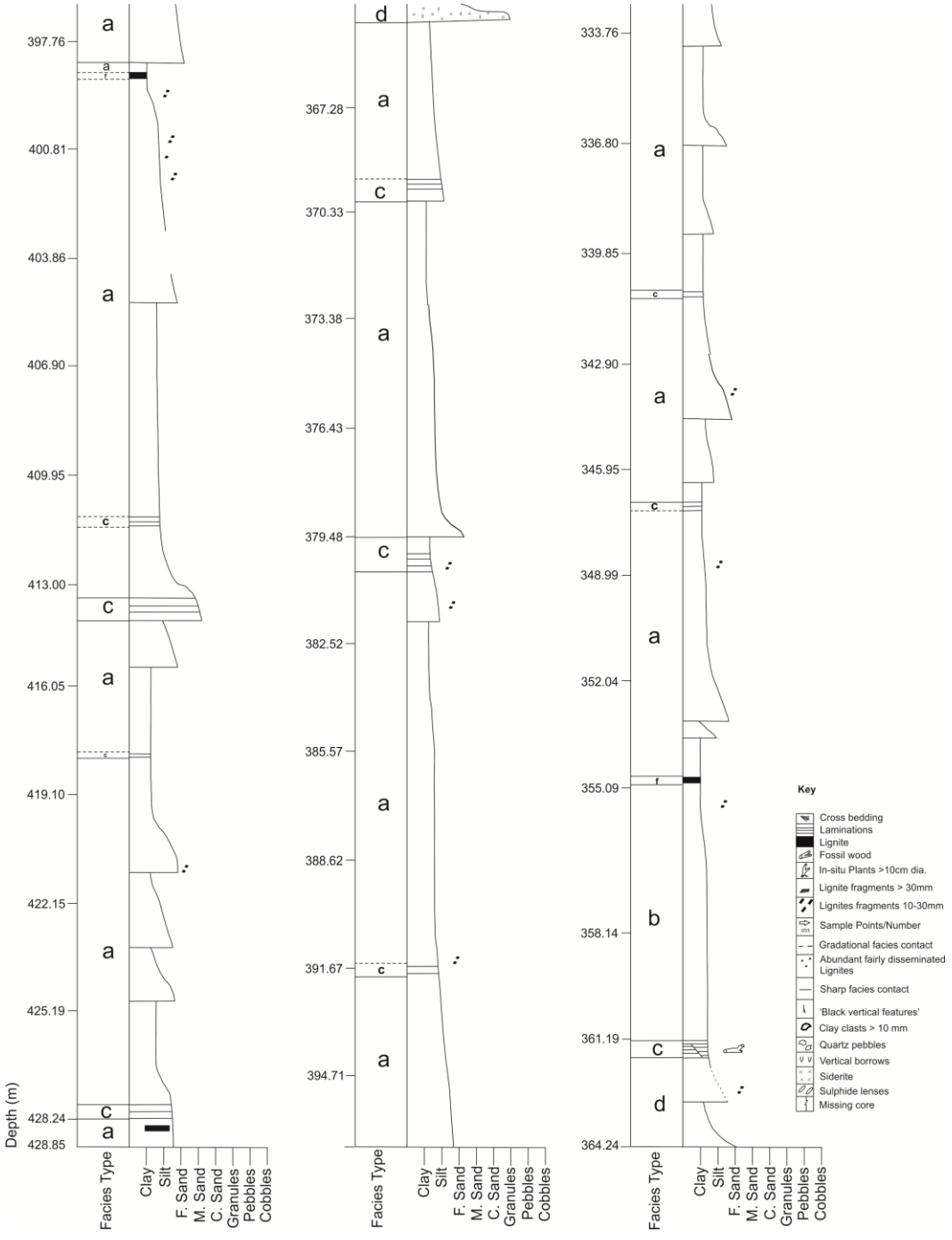

Figure 3.1.3: Composite sedimentary log through Bovey Formation, Petrockstowe core 1B

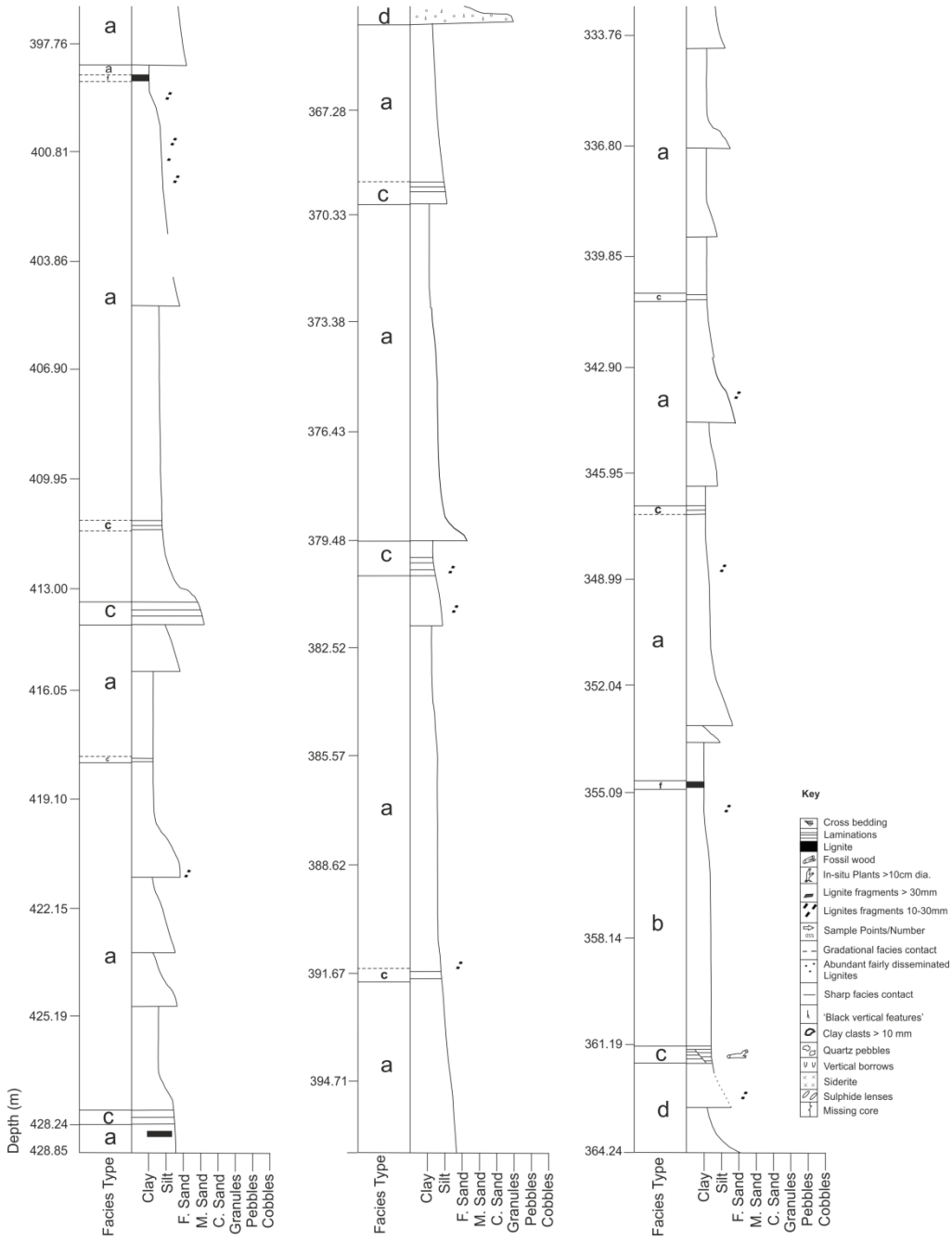

Figure 3.1.4: Composite sedimentary log through Bovey Formation, Petrockstowe core 1A

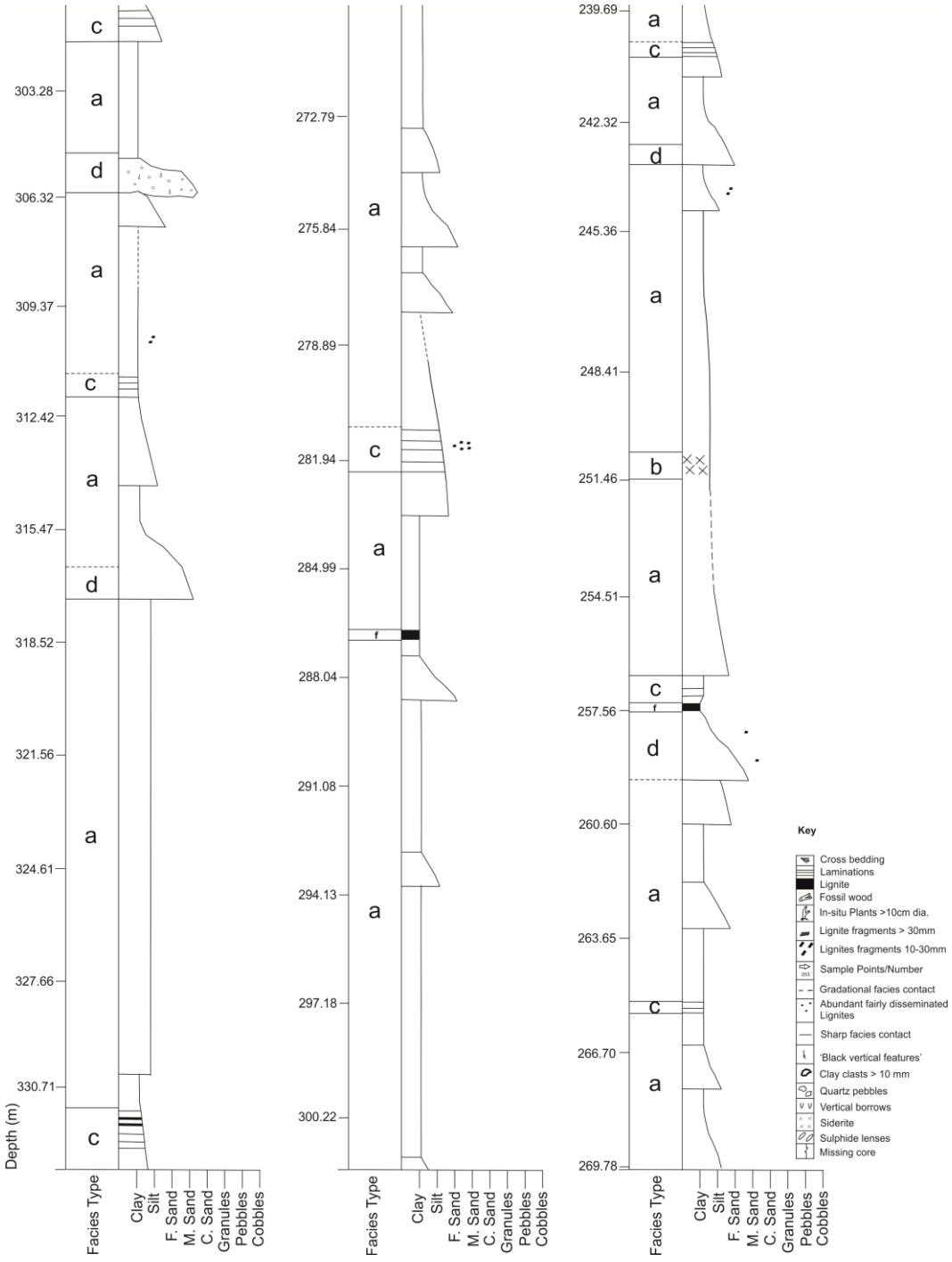

Figure 3.1.5: Composite sedimentary log through Bovey Formation, Petrockstowe core 1B

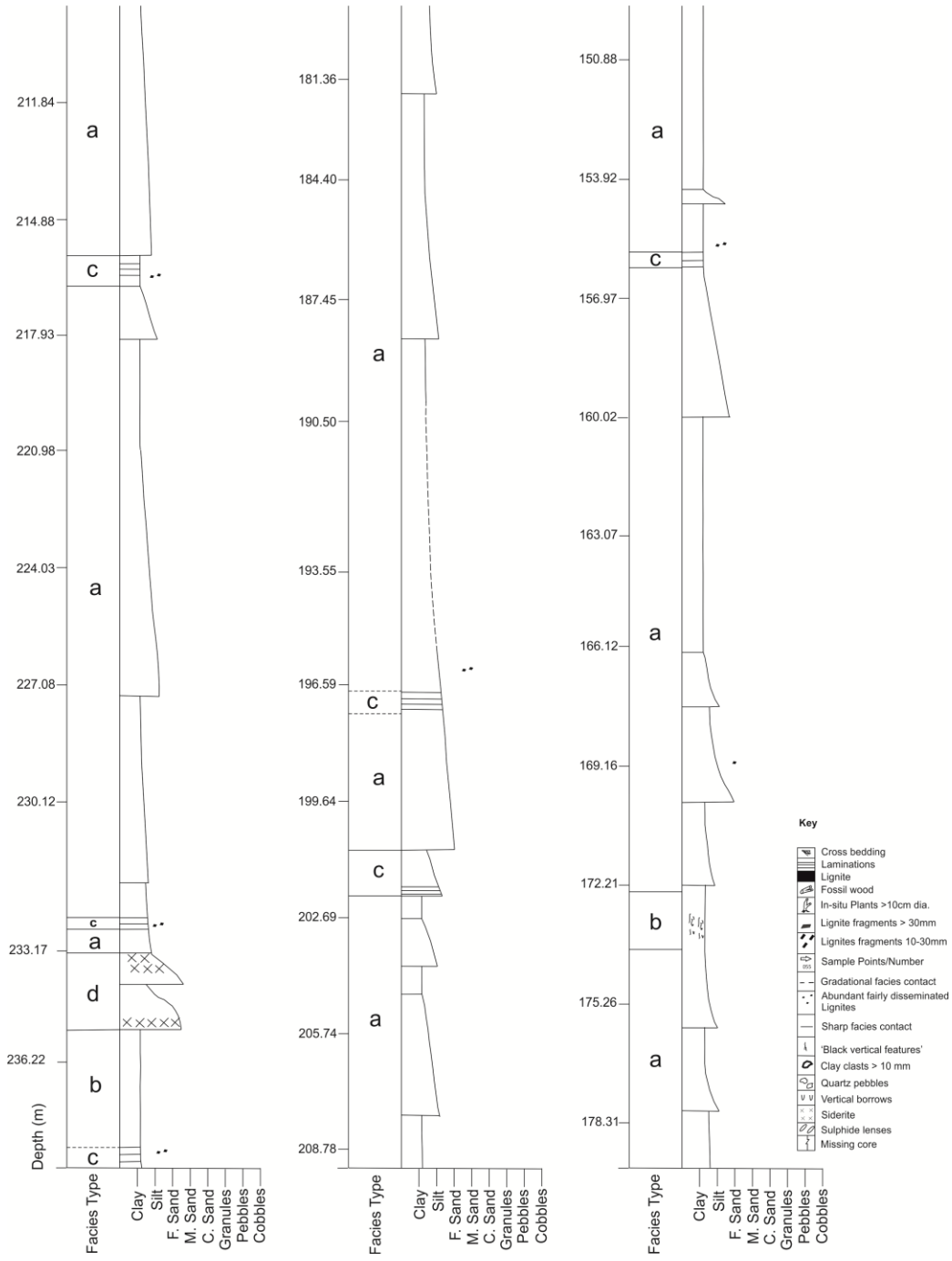

Figure 3.1.6: Composite sedimentary log through Bovey Formation, Petrockstowe core 1A

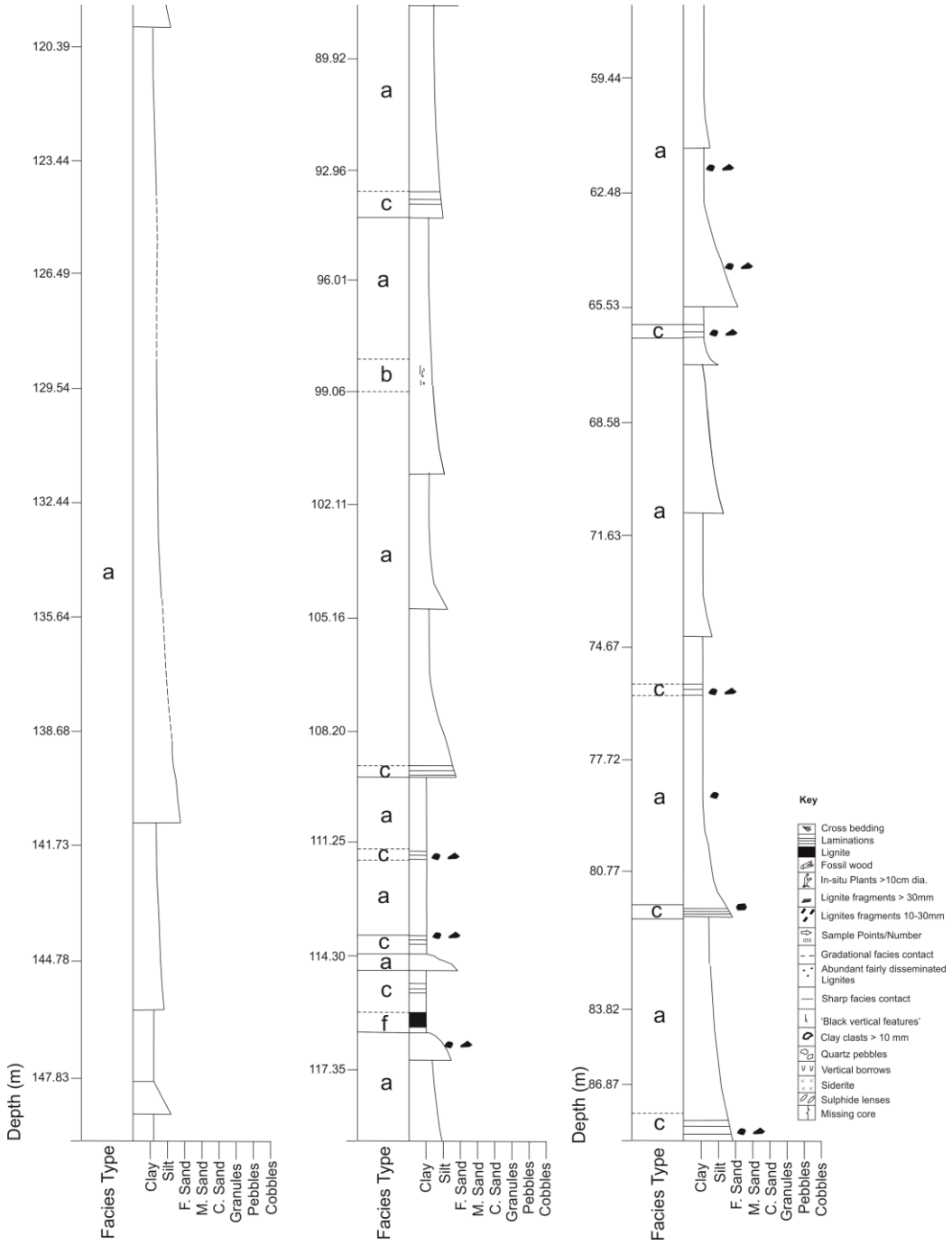

Figure 3.1.7: Composite sedimentary log through Bovey Formation, Petrockstowe core 1A

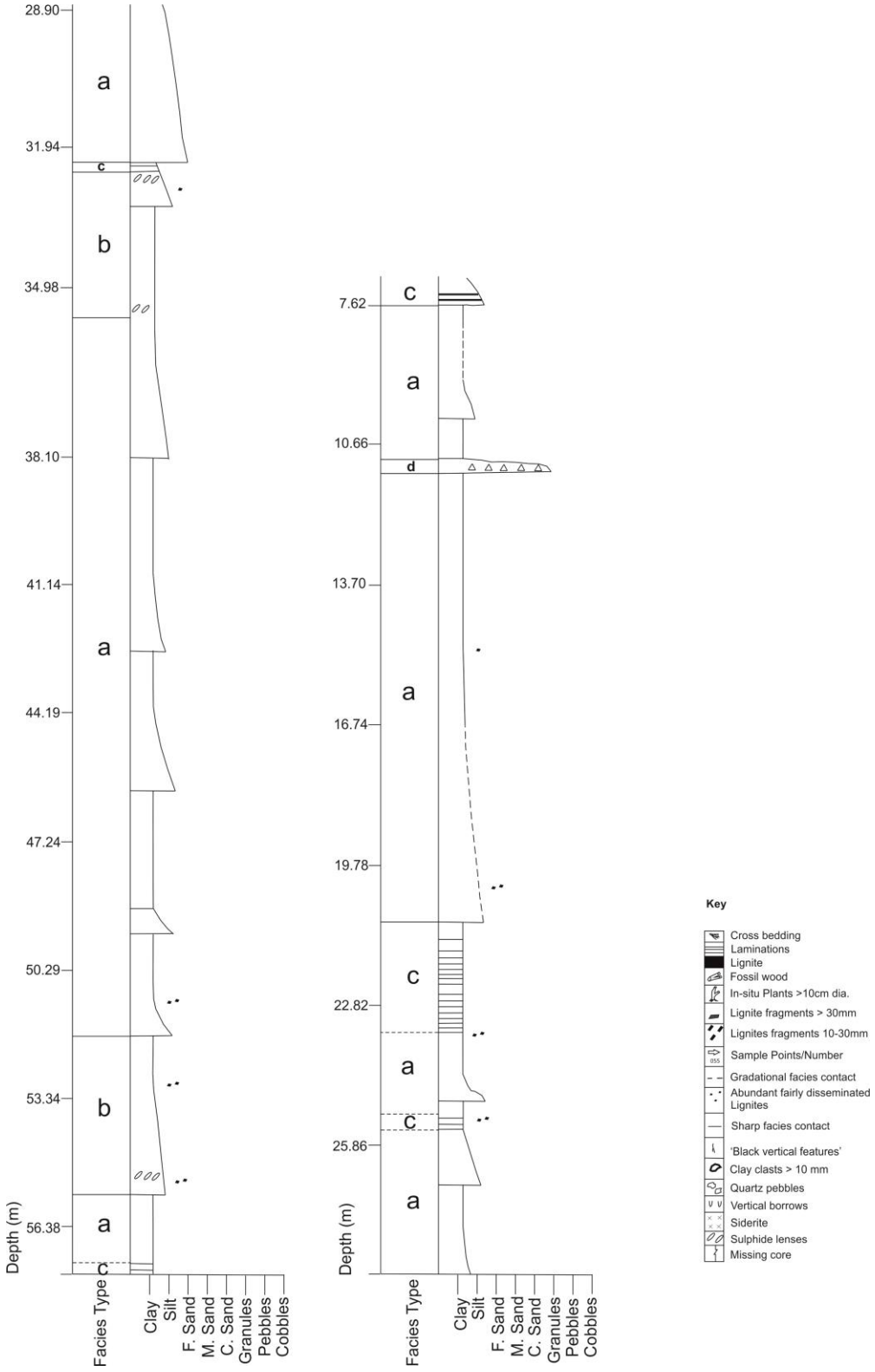

Figure 3.1.8: Composite sedimentary log through Bovey Formation, Petrockstowe core 1A

3.2.1 Description and interpretation of facies

Lithofacies a: Silty clay

A massive lithofacies of pale to mid-grey/olive claystone, or yellow-brown silty to very silty clay is present at the Petrockstowe cores. But in the John Acres Lane Quarry of the Bovey Basin, in places it contains ironstone or ferruginised silty clay horizons up to a thickness of 10 cm (Figure 3.1.9 G). Also in John Acres Lane Quarry, there are subordinate silt and rare sand-grade quartz (Figure 3.2.1 D). There is presence of irregular, dark brown to black vertical features occurring sporadically within the facies, which resemble rootlets, but may be bitumen on fractured surfaces. Rare laminations are defined by thin lignitic drapes that are often disturbed. This facies occurs in single or repeated fining-up packages of up > 45m thick (Figures 3.1.5 & 3.1.6). This lithofacies is interbedded with other lithofacies and in some places is gradational while in other places it has a sharp and erosional contact with lithofacies (c), (d), (e), (f) and (i). In the quarry, this lithofacies occurs in a homogenous bed up to 4 m thick that are laterally extensive at the scale of the quarry (at least 500 m). Unlike in the core, this lithofacies is interbedded with and is gradational with lithofacies (b), (c) and (i). It has sharp, erosional contact with the bases of lithofacies (d) and (e).

The significant thickness of this lithofacies represents considerable periods of low energy sedimentation dominated by fall-out from suspension in a subaqueous setting. The general absence of lamination and the disturbed nature of lamination when it occurs or the occurrence of disseminated quartz grains throughout may be indicative of extensive bioturbation and reworking of discrete coarser layer that may be deposited under high energy conditions. In addition the scarcity of body fossil *Diplocynodon* or *Hyracotherium* is an indicative of anoxia or rapid sedimentation.

Lithofacies b: Mottled and sideritic clay

In the Petrockstowe core, this lithofacies is a massive yellow, orange to dark red homogenous or mottled plastic silty clay, or hard, siderite-cemented claystone (Figure 3.1.9 B). And in the John Acres Lane Quarry, it occurs once and is a massive pale grey to buff or olive coloured silty clay with bright salmon to red mottling and joint surfaces weather buff to yellow (Figure 3.2.1B). In the core, this lithofacies contains, in places, yellow to red horizons up to 5 cm thick of "sand grade" ferruginised material, and scattered siderite in the form of spherules usually between 1 and 2 mm diameter. The siderite spherules occasionally aggregate into spherical concretions. Vertical burrows up to 2 cm occur in the silty clay, and are picked out by infillings of clay of slightly different colours. This lithofacies occurs in fining-up successions 20 – 25m, thick and interbeds and is gradational with lithofacies (a), and (c). There is a sharp contact between lithofacies (a) and (c) (Figures 3.1.1, 3.1.2 & 3.1.6). The Mottled clay lithofacies occurs in a bed 50 cm thick which is laterally persistent at the John Acres Lane Quarry (> 500 m) and it interbeds and gradational with lithofacies (a) and (g). Edwards (1976) have given an extensive description previously of Marcasite nodules as part of this facies.

The fine-grained, laminated nature of this sediment is indicative of suspension fall-out in a subaqueous setting or the mottling may be representing a suspension settling of clay and silt under low or zero current velocities. Siderite is a common early diagenetic mineral in fine-grained, organic rich sediments that were subject to anoxia; highly reducing conditions release Fe^{2+} from clays and carbonate during the anaerobic decomposition of organic material (Berner 1981, Pye *et al.* 1990, Middleton & Nelson 1996). Siderite granules have been generally interpreted as forming in meteoric waters (Faure *et al.* 1995, Catling 1999), but it have also been shown experimentally to form under conditions of extreme evaporation and

hypersalinity (Rajan *et al.* 1996). Freshney (1970) interpreted this lithofacies as a palaeosol based on the frequent occurrence of "rootlets", although distinct root-like morphological features were not observed in this facies as part of this study. Siderite cements and concretions are commonly described in palaeosols (Berner 1981, Pye *et al.* 1990, Collinson 1996, Ludvigson *et al.* 1998, Loope *et al.* 2012), and the reducing conditions are provided by zero sulphide activity, low Eh (-0.25 to -0.35 volts), and severely restricted circulation, microbial activity and its subsequent diagenetic alteration (Curtis & Spears 1968). However, the context of this facies, commonly gradationally interstratified with clearly subaqueous lithofacies b and c, does not support a subaerial origin for the siderite formation and mottling in this lithofacies.

Lithofacies c: Laminated silty clay

This is a massive pale to buff/ brown or white claystone with lignitic and woody horizons. Parallel laminae draped with organic material occur repeatedly in places in alternating "rhythmites", although in some cases the laminae are wavy or normally faulted (throws of centimetres) (Figure 3.1.9 C). The thickness of this facies ranges from 0.2 m to 2 m. This lithofacies is interbedded and gradational to lithofacies (d), (f), (a) and (b).

The fine-grained, laminated nature of this sediment is again indicative of suspension fall-out in a subaqueous setting. The repeated, rhythmytic alternations of clay and organic-rich drapes are similar to "varves", commonly described from lake sediments (Sturm & Matter 1978, Tye & Coleman 1989, Reading 1996, Postma 1997) (de Geer, 1912). Fresh water inhibits clay flocculation, so subtle changes in grainsize during the input from diluted density currents and settling out of clay suspension are better recorded in lacustrine settings. Changes in grainsize recorded by varves have been interpreted as seasonal changes in basin sediment input

(Reading 1996). Rhythmites are also commonly described from tidally - modulated environments (Ashley 1975) but changes in current velocity in tidal systems more usually lead to sand/mud interlaminae (Reading 1996), in contrast to those described in this facies. It is difficult to determine whether the micro normal faults are syn-sedimentary. If they are, they may be evidence of tectonism (Freshney 1970) or deposition on a slope at the time of sedimentation.

Lithofacies d: Silty Sand

This lithofacies comprises a distinctly white to mid grey, poorly sorted fine sand with a distinct subordinate silt and clay. Silt grains comprise quartz, organic flakes and rare tourmaline. The finer fraction is largely made of kaolinite; which is supported by the x-ray diffraction analysis conducted on Bude Formation revealed that kaolinite peak becomes increasingly sharper denoting increasing lattice order (Bristow & Robson 1994). This lithofacies contains plant material in fragments up to 30 cm. The lithofacies occurs in sheets that are laterally extensive at the John Acres Lane Quarry (<500 m). Sedimentary structures are not evident, however beds are up to 3 m thick, are sharp-based and erosional into lithofacies (a) and fine-upward to lithofacies (a). Lithofacies (e) is interbedded with this lithofacies.

The context of this facies, associated with lithofacies (a) suggests that it represents subaqueous deposition. The fact that this lithofacies contains lenses of lithofacies (e) nested within it indicates that the facies represents protracted sedimentation, probably in the form of settling from unconfined homopycnal flows that are characteristic of freshwater depositional environments (Reading 1996). Abrupt initiation of sedimentation may be represented by distributary avulsion at a more proximal (to the lake margin) site, and the overall fining-up motif may indicate choking or abandonment of the distributary.

Lithofacies e: Minor Sand and gravel

This lithofacies in the Petrockstowe cores comprises fine to coarse sand, granule and pebble grade material. Clasts are of quartz, and to a lesser degree, chert, up to 2 cm in diameter, mainly angular to sub angular (see Figure 3.1.9 D). Because of the large pore space between grains, much of this lithofacies is poorly cemented mainly by silica cement, and is associated with considerable core-loss. Hence, many sedimentary structures cannot be identified. However, upper phase plane bed lamination and cross bedding are defined by lignitic drapes in grey to brown sands. Laminae are occasionally disrupted by steep normal faults with centimetres of throw. This facies occurs in fining-up successions 0.32 - 3.05 m thick, and this lithofacies interbeds or is gradational with lithofacies (a), (b), (c) and (e).

In the South John Acres Lane Quarry, the lithofacies occurs as rather homogeneous, very poorly sorted lenses of medium-to-coarse to gravel-grade angular to sub angular quartz and tourmaline sand in a pale to grey clay matrix (about 50%) Figure 3.2.1 D. Sand-grade disseminated organic material occurs throughout. The lenses are up to 1 m across and up to 10 cm thick. This lithofacies lacks visible sedimentary structures. The lenses occur within lithofacies (a) and (d).

Structures associated with this facies in the cores are cross-bedding and upper phase plane beds are indicative of unidirectional flow in the lower and upper flow regime. The possible interpretation given in the context of this facies as observed in core is typically interstratified with lithofacies (a) and (b) implies deposition in a subaqueous setting. Following the definition of Miall (1985), this facies may be suggestive of bars forms.

While in the South John Acres Lane Quarry section this facies is seen as lenses within facies (a) and (d) imply deposition into a standing body of water. The poor sorting suggests these may be the products of small debris flows (i.e. high density flows). Although, the clay may

have settled between intra-granular spaces subsequently, apparently resulted to poor sorting; and this facies might likely be a product of minor turbidity currents (or hyperpycnal flows, i.e. low density flows).

Lithofacies f: Major Sandstone

This lithofacies refers to most coarse sandstone bodies greater than 1 m in length and 10 cm thick. Poorly sorted angular to sub-angular quartz, tourmaline and organic flakes of coarse sand to granule-grade occur in a clay matrix (about 50% clay), (Figure 3.2.1 E). This lithofacies occurs in beds up to 3 m thick, can be laterally extensive at the John Acres Lane Quarry (<500 m), but also pinched-out at the exposed section. Trough and tabular cross-bedding is picked-out by foresets enriched in tourmaline or organic flakes in places, but this is generally poorly defined. In one instance, large-scale cross-sets up to 2 m occur. The orientation of the dip of the foresets, towards the margin of the channel implies these may be lateral accretion cross-sets. The facies is erosional into lithofacies (a) and has a sharp, planar, upper contact with lithofacies (a) and (b). Recumbent, pyritized tree logs up to 1m in length, and scattered carbonaceous plant debris occur at the base of the sandstones (see Figure 3.2.1 E).

Trough and tabular cross bedding are indicative of unidirectional sediment transport in the lower flow regime. The occurrence of lateral accretion cross-sets is indicative of helicoidal flow in high sinuosity (i.e. meandering) channels. Thus, this facies represents the deposits of unidirectional currents, confined to low-gradient channels. This facies may be equal to the architectural element LA of Miall (1985).

Lithofacies g: Coarse sand and granules

This is a massive lithofacies which occurs at the base of Petrockstowe 1B core, forming the bottom of the Palaeogene sediments which unconformably overlie a weathering profile developed on the Carboniferous Bude Formation(Fenning & Freshney 1968, Freshney *et al.* 1979, Bristow & Robson 1994). It is a pale grey poorly sorted soft sandstone comprising coarse sand- to pebble-grade clasts and containing interstitial clay. The grains are mostly sub-angular to sub-rounded quartz up to 20 mm, and lignitic flakes are common (Figure 3.1.9 A). Poor lithification of this facies has resulted in poor preservation of core and many sedimentary structures (if present) have been lost. Some cross bedding organised in to sets 0.20 – 0.40 m thick are observed, and upper phase plane beds with lamina spaced typically 10 - 20 mm apart occur in successions up to 0.20 m thick. Body and trace fossils are not observed in this facies. This lithofacies occurs in single or multiple fining-up packages up to 5 m thick. This lithofacies interbeds and is gradational with lithofacies (b) and has sharp base with facies (c) and (d) Figures 3.1.1, 3.1.2. This lithofacies is similar to facies St, Sp and Gm of Miall (1985), but is not diagnostic of any specific architectural element. The large grainsize is indicative of high energy transport of the sediment, and could suggest a depositional site in the deeper parts of fluvial channels (Bridge *et al.* 1986, Bridge *et al.* 1995).

Lithofacies h: Lignitic Clay

This lithofacies is massive to weakly laminated pale brown to black claystone and siltstone. Disseminated organic material, coarser than 0.1 mm is set in a clay matrix, or as a carbonaceous colloidal coating to clay and possibly mica particles. More rarely, bedding parallel, elongate lenses of laminated lignite measuring up to 20 cm, and horizons of fossil wood up to 30 cm occur. The clays are generally free from quartz grains of silt and sand

grade. The dark, irregular vertical features described in lithofacies (a) occur in this lithofacies too. Body and trace fossils are absent. This lithofacies is characterised by tabular beds up to 50 cm thick, which are laterally extensive throughout the quarry (>500 m). This facies is consistently interbedded with and is gradational with lithofacies (a) and (i). Also, Vincent (1983) observed the presence of fine grained non-graded and non-banded clays containing plant remains could suggest floating vegetation collected at the further end of the lake within a back swamp environment might have led to the formation of lignitic clay.

This lithofacies represents shorter periods of settling from suspension of clays and silts along with the ready input of abundant organic material, including rafts of peat. The abundance of preserved organic material, and the scarcity of trace and body fossils is indicative of anoxia and/or rapid sedimentation.

Lithofacies i: Lignite

This lithofacies comprises brown, light brown to black, brittle, fissile lignite, in beds 1 – 2 cm thick, or concentrated in irregular beds (see Figure 3.1.9 F). In the John Acres Lane Quarry the lignite bed is up to 1 m thick and laterally persistent (>500 m) with compressed wood fragments measuring up to 30 cm thick and 50 cm length are readily identifiable within the lignitic body (Figure 3.2.1 F).

This lithofacies interbeds and alternates with lithofacies (a) and (a), (a) and (h) or (h) and (h) in the South John Acres Lane Section and either (a) and (c), (a) and (b), (e) and (e) in the Petrockstowe cores with which it has gradational or a sharp contact. In this study, from the field evidence observed there is presence of rootlets beneath the beds in the South John Acres Lane Quarry section which strongly suggests that the lignites were potential *in-situ* accumulation.

Lignite (or coal) typically represents the preserved remains of peat which represent *in situ* accumulation of dead plants in wholly terrestrial environments known as

mires (Diessel 1992). However, Chandler (1964) and Edwards (1976) consider the bulk of the plant material in the lignites to have been transported from outside the depositional area, based on palaeobotanical evidence. For example, *Sequoia couttsiae*, which is a common Palaeogene flora in the southern England, is commonly broken and fragmented and is represented by small fragments obviously transported from a distance. *Sequoia couttsiae* is in great abundance in Bovey Basin (Chandler 1964)represented by masses of wood which *Osmunda* forms the bulk of the lignite seams in this basin. In a similar work, Jones (1994) has documented the only known example thus far of fossil wood of Oligocene age from this facies by the use of microscopic and chemical techniques. Jones (1994) suggested that the depositional environment was an acidic fresh water lake, which might have influenced directly or indirectly the cell wall homogenisation. However, in the Petrockstowe core the presence of rootlet bearing beds occurring beneath the lignite suggests *in situ* peat accumulation in mires.

Figure 3.1.9: Photographs of facies types in the Petrockstowe 1A and 1B cores, Petrockstowe Basin. (A) = example of Lithofacies (g); (B) = example of Lithofacies (b); (C) = example of Lithofacies (c); (D) = example of Lithofacies (e); (E) = example of Lithofacies (c) showing "wavy lamination cross-cut by a small fault"; (F) = example of Lithofacies (i); G = example of Lithofacies (a); and (H) = example of Lithofacies (b)

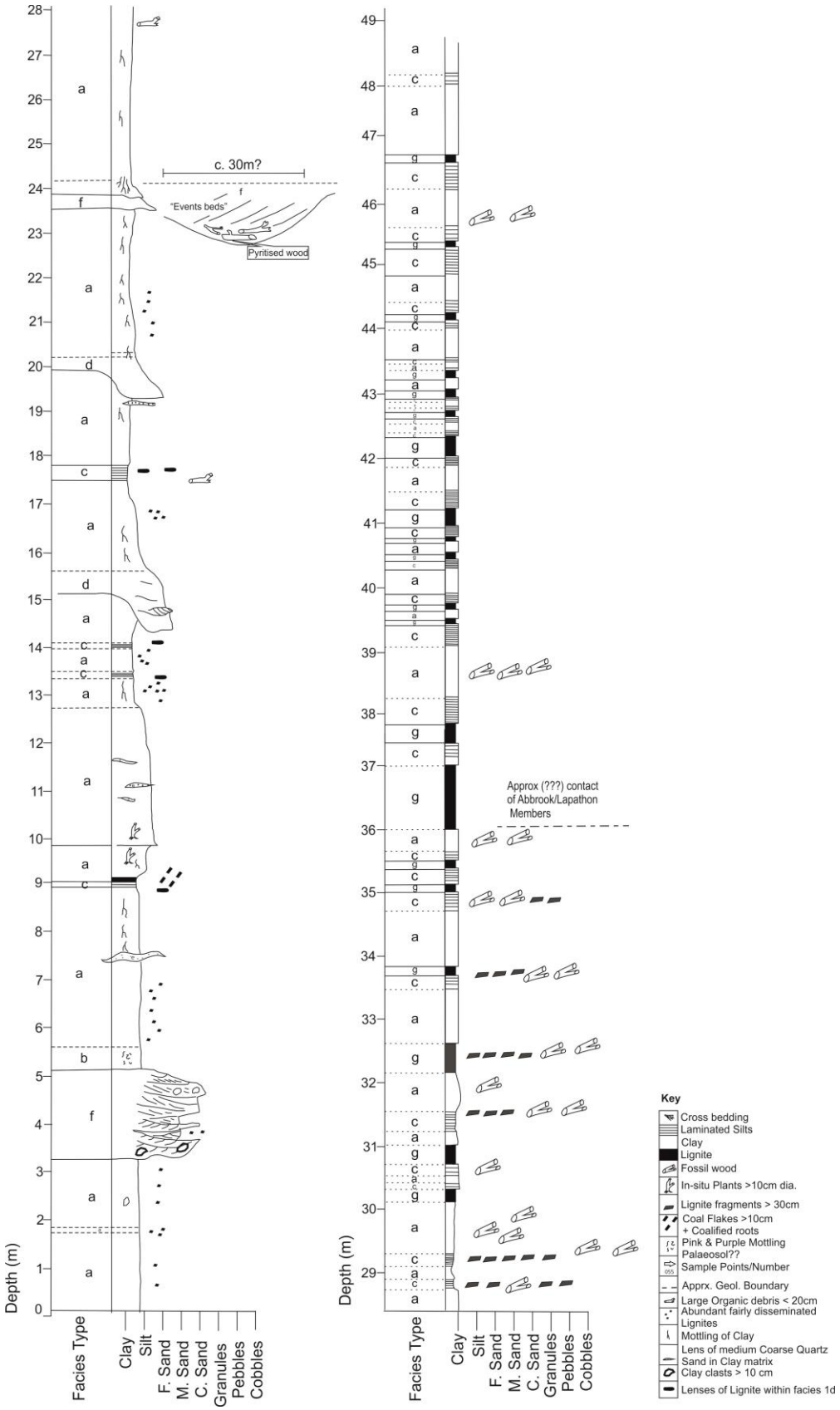

Figure 3.2.0: Sedimentary log through the Abbrook Clay-and-Sand Member and Southacre Clay-and-Lignite Member, Bovey Formation, South John Acres Lane Quarry, Bovey Basin

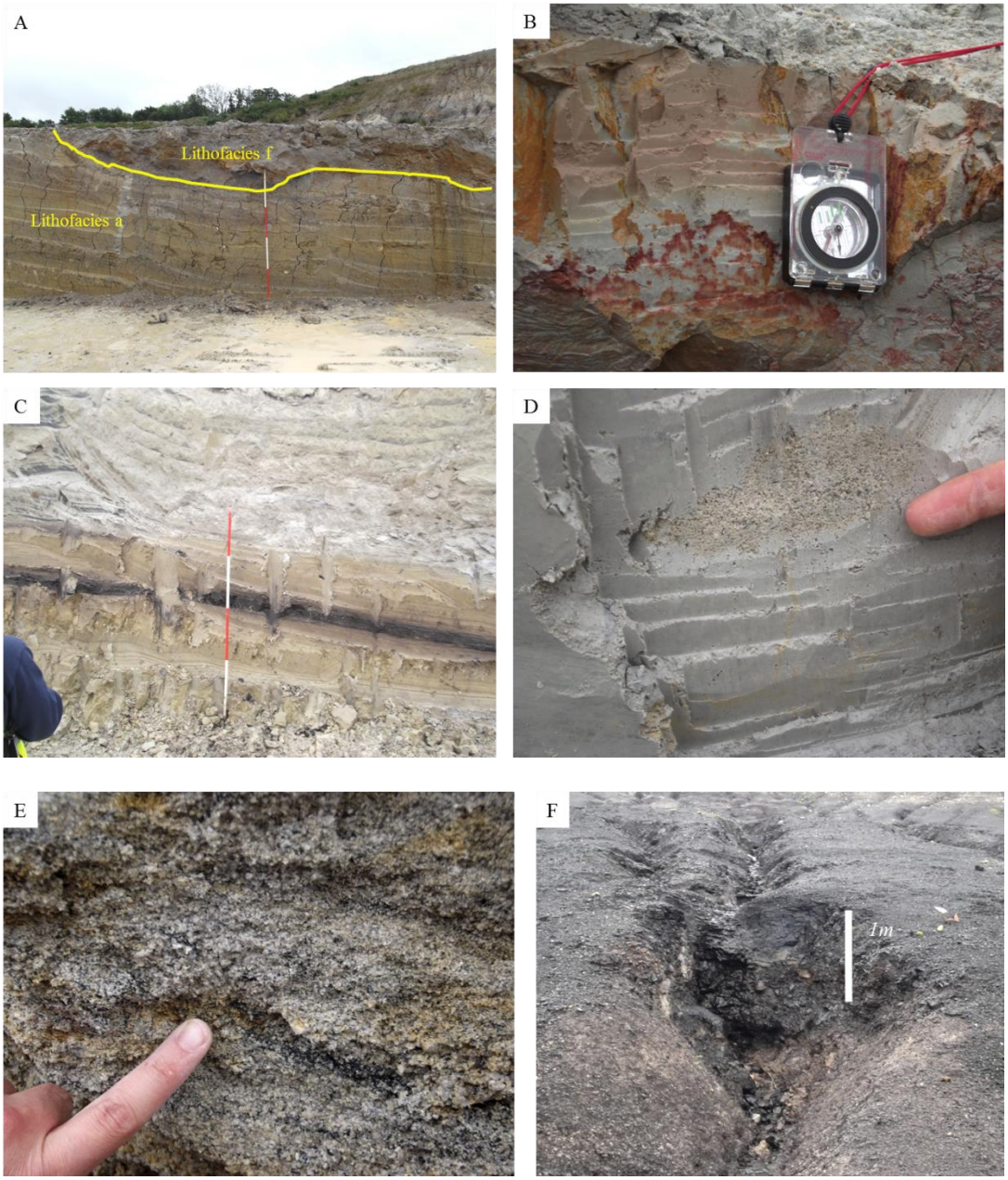

Figure 3.2.1: Photographs of facies types in the Abbrook Clay-and-sand Member and Southacre Clay-and Lignite Member, Bovey Formation, John Acres Lane Quarry. (A) Detail of the erosional contact between Lithofacies (a), *Silty clay* and Lithofacies (f), *Major sandstone*. Pole is 2 m tall. (B) Lithofacies (b), mottled and sideritic clay: olive-to-pink coloured claystone with deep red-to-purple mottling by iron oxides. Compass clinometer is 10 cm long. (C) Detail of planar contact between Lithofacies (a), Silty Clay and Lithofacies (h) Lignitic Clay. (D) Lens of Lithofacies (e), Minor Sand and gravel occurring within Lithofacies (a), Silty Clay. (E) Detail of lithofacies (g), Major sandstone: poorly sorted coarse-grained sandstone, comprising quartz and tourmaline. Concentrations of tourmaline define forsets of large-scale cross-bedding. (F) Thick lignite bed (Lithofacies (i)) associated with Lithofacies (a), Silty Clay and Lithofacies (h), Lignitic Clay.

3.3 Facies Associations

This section deals with the organisation of facies described in section 3.2.1. A wide range of associations have been ascribed to the deposits of the Bovey Formation in Petrockstowe 1A and 1B cores, which have been interpreted as deposits of "turbid suspension in rivers", "temporary lake", "mixed bed load" and "sand filled channels with flood plain clays" environments (Freshney *et al.* 1979).

The deposits of the Abbrook Clay-and-Sand and Southacre Clay-and-Lignite Members have previously been interpreted as deposited in 'fluviatile' 'flood-plain', "lacustrine", 'back swamp' and 'mudflat' environments (Edwards 1976), a 'fluviatile' environment, 'flood-plains and to a lesser extent… lakes' (Selwood *et al.* 1984), under conditions that were 'damp or humid', 'warm and swampy' (Selwood *et al.* 1984). The main argument that subaqueous deposition was lacustrine is based on the palaeobotanical data of Chandler (1964). In this context, the following tentative facies associations are suggested:

3.3.1 Long-lived lake or Lake Centre

Three rhythmically interbedded lithofacies, Lithofacies (a), (e), and (g) form this facies association. Lithofacies (a) and (h) record protracted periods of suspension fall out (Figure 3.30). The greater preservation of organic material in Lithofacies (c) represents shorter periods of suspension fall-out under conditions (i) which were more anoxic, or (ii) in which the sedimentation rate was faster, or (iii) where there was a greater supply of organic material. Lithofacies (i) either represents the formation of terrestrial mires or represent the products of suspension-settling of water-logged plant material in a low-energy, subaqueous environment. The latter interpretation is preferred, following Chandler (1964) and Edwards (1976). This is because, (i) this is more similar in terms of processes to the two lithofacies with

which Lithofaces (i) is interbedded, and (ii) there does not appear to be any evidence for shallowing, such as coarsening-up, between Lithofacies (a) and (h) and Lithofacies (i).

Thus, this facies association represents the deposits of a permanent standing body of water i.e. lake after (Chandler 1964), characterised by settling-from-suspension of fines and organic material. There was marked cyclicity in the supply rate and/or preservation of clay and organic material to this lake, as recognised by Edwards (1976). It is possible that the lake was stratified into an upper, oxic level and lower, anoxic level. The lake may have experienced changes in the position of the stratification, probably ultimately driven by climate change, which influenced the preservation potential or organic material supplied to the lake. Alternatively, cyclic climate change may have led to changes in the supply of organic and/or clastic material to the lake. The thick successions of clays characteristic of this facies association suggest that they accumulated under low pH conditions. Low pH conditions lead to the formation of clay flocs which results in the rapid deposition of large volumes of clay (Vincent 1974, Staub & Cohen 1979). Many of the individual facies within this association (i.e. a, h, and i) show little internal banding, grading and lamination, which is characteristic of deposition following flocculation. Additionally, there is little evidence for vertebrate and invertebrate body fossils, supporting the notion that acid waters and turbid conditions limited preservation (Vincent 1983).

3.3.2 Ephemeral lake or Lake Margin

Lithofacies (a), (b), (c), (d), (e) and (i) occur in this facies association. Lithofacies (a) records long term suspension fall out and a stagnant body of water. Lithofacies (c) records preservation of organic material and represents a short period of suspension

fall out under the conditions (i) which were more anoxic, (ii) in which there was variation in subsidence and sedimentation rate, (iii) where there was variation in supply of organic material. The lake seems to have occurred at intervals. Lithofacies (b) records periods of restricted water circulation in the silty clays and high water table. This might have resulted in the formation of siderite. Lithofacies (i) represents the formation of terrestrial mires (Figure 3.40). Again, lithofacies (d) and (g) represent periods of coarser sediment supply to the standing body of water by means of density flows, possibly associated with distributary avulsion processes outside of the exposed area. The density flows may have been unconfined, and travelled down a pro-delta slope. Lithofacies (b) records periods of subaerial exposure, oxidation and pedogenesis of sediments that were formerly subaqueous. Lithofacies (g) records the incision of low-gradient, high sinuosity channels. The low gradient required to generate high-sinuosity channels is not typical of subaqueous, density flow processes (Collinson, 1996), and thus this lithofacies records subaerial exposure of sediment that were formerly subaqueous. These channels may be analogous to tidal creeks that form in the intertidal areas during falling tide. These channels subsequently became conduits for coarse sediment passing through the zone which was formerly covered in water.

Thus, this facies association tends to suggest a standing body of water i.e. lake, as earlier proposed by (Chandler 1964). However, unlike the facies association interpreted above, the standing body of water subjected to periodic subaerial exposure, and occasional the input of coarser material. Hence, the standing body of water was either shallower than facies association 3.3.1, and/or was subjected to more major changes in the relative position of the lake (i.e. it was ephemeral?). The presence of irregular, dark brown to black vertical features more or less rootlets may suggest subaerial exposure to the lake floor too. Distinct shallow-water indicators

such as wave ripples are not present, probably due to the small size of the basin which might have prevented the development of a significant wave-base.

3.3.3 Sand filled fluvial channels

Repeated cyclic fining-up facies are the common characteristics of this lithofacies (g) and facies association. Lithofacies (g) records a point bar fill deposit, which unconformably overlies the Carboniferous Bude Formation and fines upward with some preserved lignitic flakes. Lithofacies (g) represents the incision of low gradient, high sinuosity channel. This channel subsequently became a conduit for coarser sediment passing through the zone which was formerly covered with water (Figure 3.30).

3.3.4 Flood plains

Lithofacies (a), (c), (e) and (i) occur in this facies association. Lithofacies (a) records long term suspension fall out and a stagnant body of water. Inter bedding of Lithofacies (e) within lithofacies (a) repeatedly may represent velocity fluctuations during a single flood and/or several floods. This lithofacies association represents flood plains with sedimentation occurring mainly during flooding and is mostly from suspension material deposited during low velocity (Figure 3.30). In some instances, flood waters escape from through flowing river channels.

3.4 Facies association succession and Sequence Stratigraphy of Petrockstowe 1A and 1B cores, Petrockstowe Basin

In the Petrockstowe 1A and 1B cores, a succession of Sand-filled fluvial channels 662 – 500 m) ~ 160 m thick is followed by an Ephemeral lake or lake margin succession ~ 400 m thick. This represents an overall deepening-up succession. From a sequence stratigraphic view point, non-subsidence and constant sediment supply, or sedimentation exceeding subsidence, will results in an overall shallowing-up succession. The observed succession reflects a long-term overall trend of basin subsidence outpacing sediment supply. This is very typical of strike-slip bounded basins, e.g. dextral wrench fault-bounded basins of the South Island, New Zealand (Miall 1985, Allen & Allen 2013).

According to Emery & Myers (1996), a high accommodation rate has the tendency to promote the preservation of complete fining upward channel units associated with more rapid flood-plain aggradation. This period may be associated with poorly drained soils, flood-plains peats and development of high water tables, which potentially is being observed in Petrockstowe and Bovey Basins as the major similarity common to the two basins. A high accommodation rate may also be responsible for the preservation of cyclic alternation of facies a, b, c, e and i in the Petrockstowe cores 1A and 1B, which may be present can be associated with rapid base-level rise, which tends to lead to increased flood-plain aggradation, and this subsequently resulted to deposition of clay, silty clay succession or sedimentation might have been controlled by contemporaneous fault movement, which was mostly in the NW to SE line (Freshney 1970). Similarly, the channel fills/mouth bars seen at the bottom of the Petrockstowe core 1B could be due to the slow base level rise, as very little accommodation is available for the over bank areas (Catuneanu 2006). Also, the potential channel stacking during reduce accommodation as noted in the

Bovey Basin section at around ~ 3 – 5 m, 15 m, 20 m and 24 m (Figure 3.30) may be accompanied by frequent avulsion, which promotes spread of excess sediment laterally (Holbrook 1996).

The succession in Petrockstowe 1A and 1B cores may be subdivided into five, shorter durations of stratigraphic sequences (SEQ), (sensu Van Wagoner *et al.* 1990). Each sequence contains conformable sediment package, bounded by a surface of erosion or non-deposition. These sequences are named SEQ1-5. SEQ1 occurs unconformably above the Carboniferous Bude Formation to 500m, and is characterised by Sand fluvial filled channels (i.e. lithofacies a, b, e and f). The occurrence of an unconformity above the Carboniferous Bude Formation marked the lower sequence boundary (SB) of SEQ 1 and the upper boundary is marked by the sharp contact between the minor sand and gravel with the mottled/sideritic clay occurring at about 500 m depth.

SEQ 2 has a SB occurring at about 420 m immediately above the minor sand and gravel package than the underlying succession (Van Wagoner *et al.* 1990) and fining up into a lignitic thin bed representing the maximum flooding surface (mfs) terminating at the upper SB within a silty clay facies. Then, the succession began to become shallow towards the upper SB. This sequence has a thickness of ~ 110 m. SEQ 2 is characterised by lithofacies (a), (b), (c), (d), (e) and (f) denoting an ephemeral lake or lake margin.

SEQ 3 also has a SB boundary at the bottom that commence with a transgressive lag marked by granules facies which could suggest an incise valley channel overlying SEQ 2. The package deepens upwards reaching the mfs occurring within a clay facies, and then terminating at the upper SB marked by clay facies. Also, towards the upper SB, mottled/sideritic clay occurs suggesting a possible sub-aerial exposure.

This sequence has a thickness of about 90 m, and is characterised by the following lithofacies a, c, d and e.

SEQ 4 SB occurs by the presence of granules and coarse grained sandstone overlain sharply by the claystone facies succession of SEQ 3. This is the thickest package in the succession, which is ~ 110 m and is considered to be the prograding lake facies association, probably the deepest part of the lake. The mfs is associated with vertical borrows and the upper SB occurred within the lignitic facies. This also suggests an ephemeral lake/marginal lake.

SEQ 5 is the last stratigraphic sequence in the succession towards the top. The lower part of SEQ 5 is bounded by thin lignitic bed which continued to fine upwards with an auto cyclic sedimentation pattern. This package has a thickness of ~ 100 m. The upper SB is marked by sandy granules which may represent an erosional surface and this SEQ is characterised by lithofacies a, b, c and f.

In the subsequent chapters of this thesis, a section will be devoted in linking the facies association succession to the biostratigraphy, where a possible age of the sediments will be deduced.

3.5 Facies association successions and Sequence Stratigraphy of the Abbrook Clay-and-Sand Member and Southacre Clay-and-Lignite Member, Bovey Formation, South John Acres Lane Quarry, Bovey Basin

In the logged section through the Abbrook Clay-and-Sand and Southacre Clay-and-Lignite members of the Bovey Formation, a succession 26 m thick of a Long-lived lake or lake centre is followed by a succession 28 m thick representing Ephemeral lakes or lake margins. Overall in this succession, the rate of sediment supply has outpaced the space and generally a fining upward trend is observed or shallowing-up trend.

3.6 Correlation of Petrockstowe core and South John Acres Lane Quarry section, Bovey Basin

Chandler (1957), Wilkinson and Boulter (1981) and Edwards (1976) all share same opinion on the presence of Eocene – Oligocene transition within the Bovey Formation encountered in the Bovey Basin while Turner (1979) reported Eocene – Oligocene boundary in the Petrockstowe Basin using pollens/spore record. On this basis and lithofacies analysis, a correlation of the two basins is hereby presented (Figure 3.50). The depositional environment for the two sections suggested a long lived lake or lake centre and towards the top of South John Acres Lane Quarry section, is an ephemeral lake or lake margin

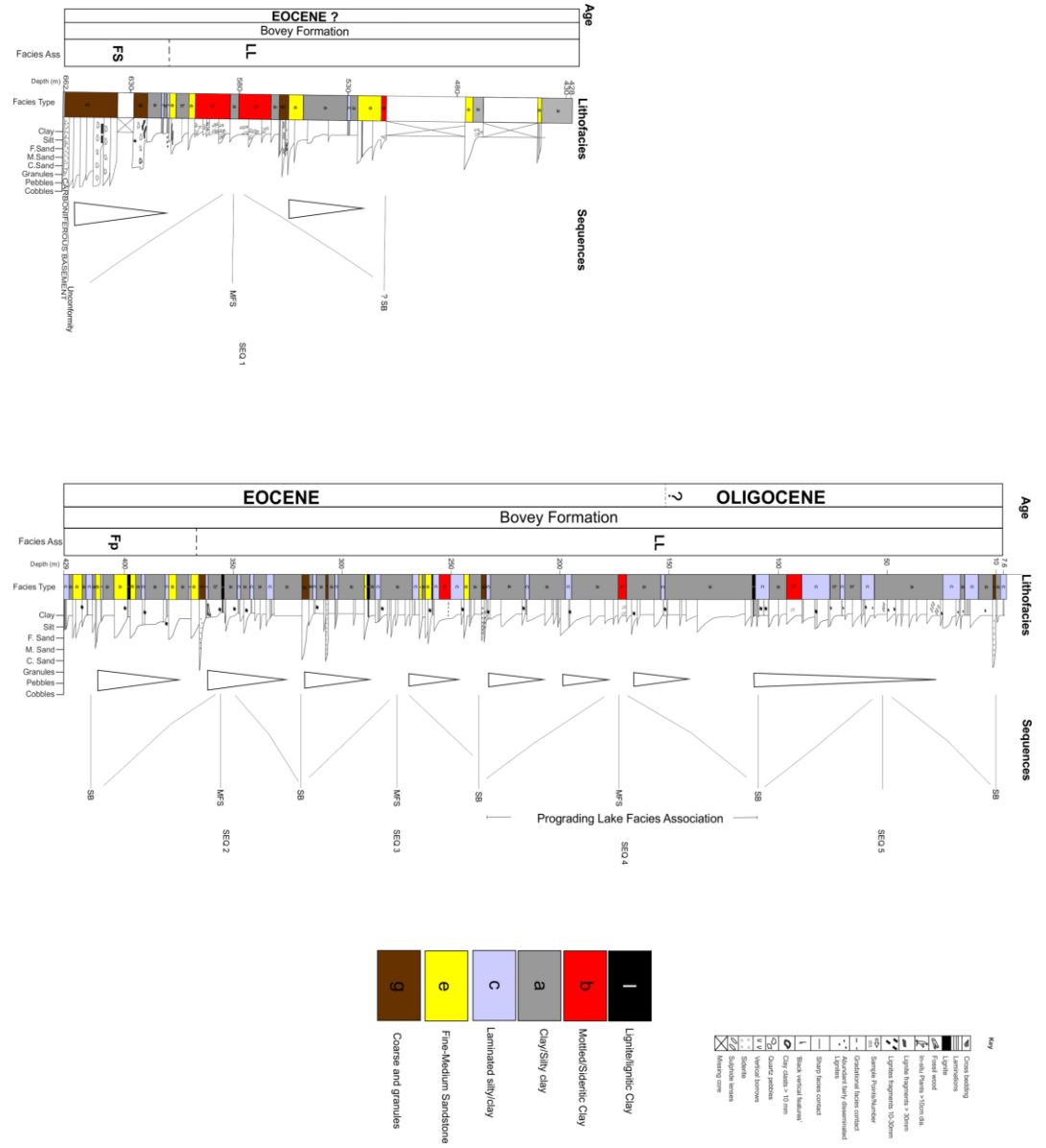

Figure 3.30: Depositional model for the Petrockstowe 1A & 1B, Petrockstowe Basins, Southwest, UK

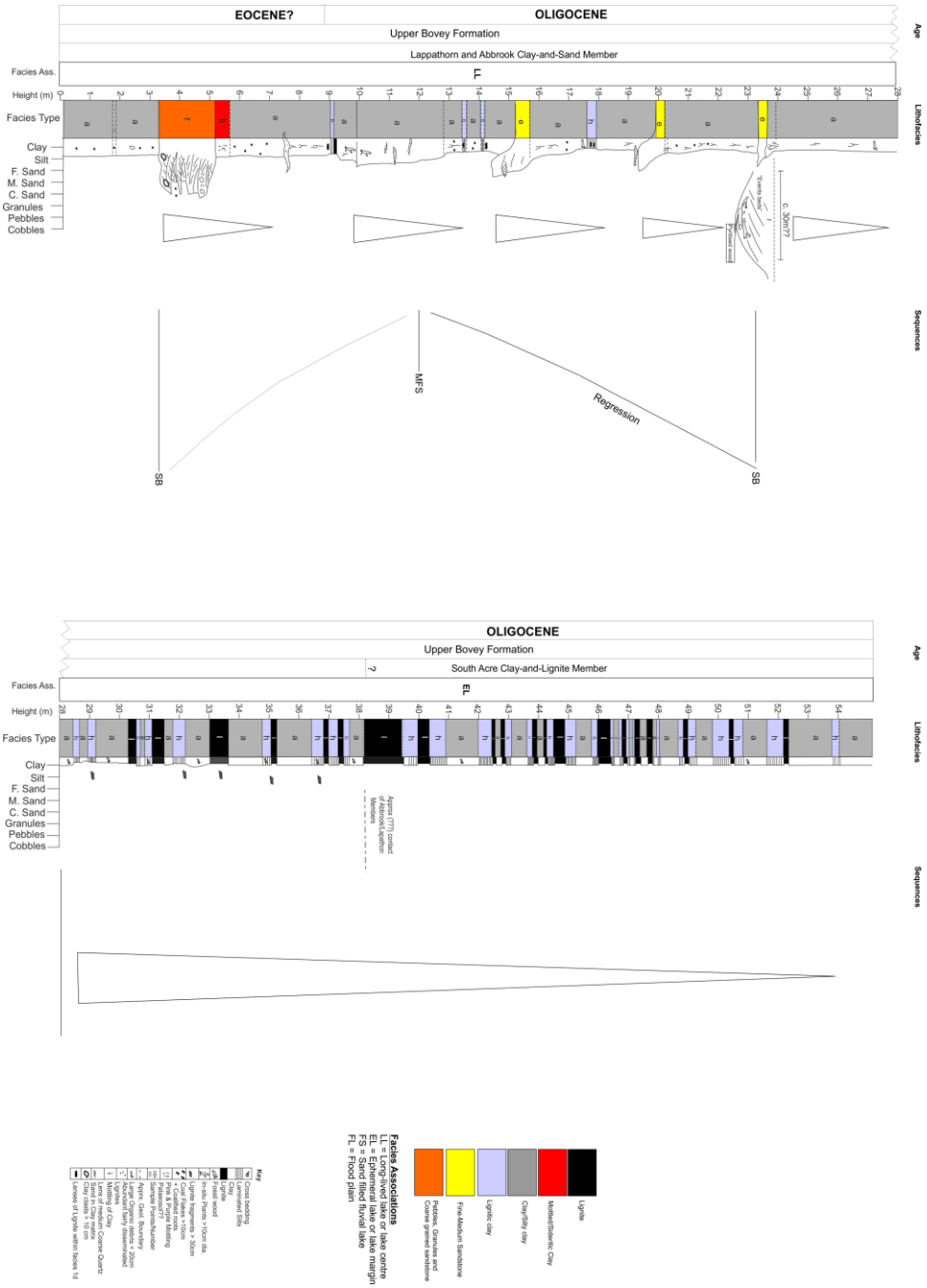

Figure 3.40: Depositional Model for the South John Acres Lane Quarry section, Bovey Basin, Southwest, UK

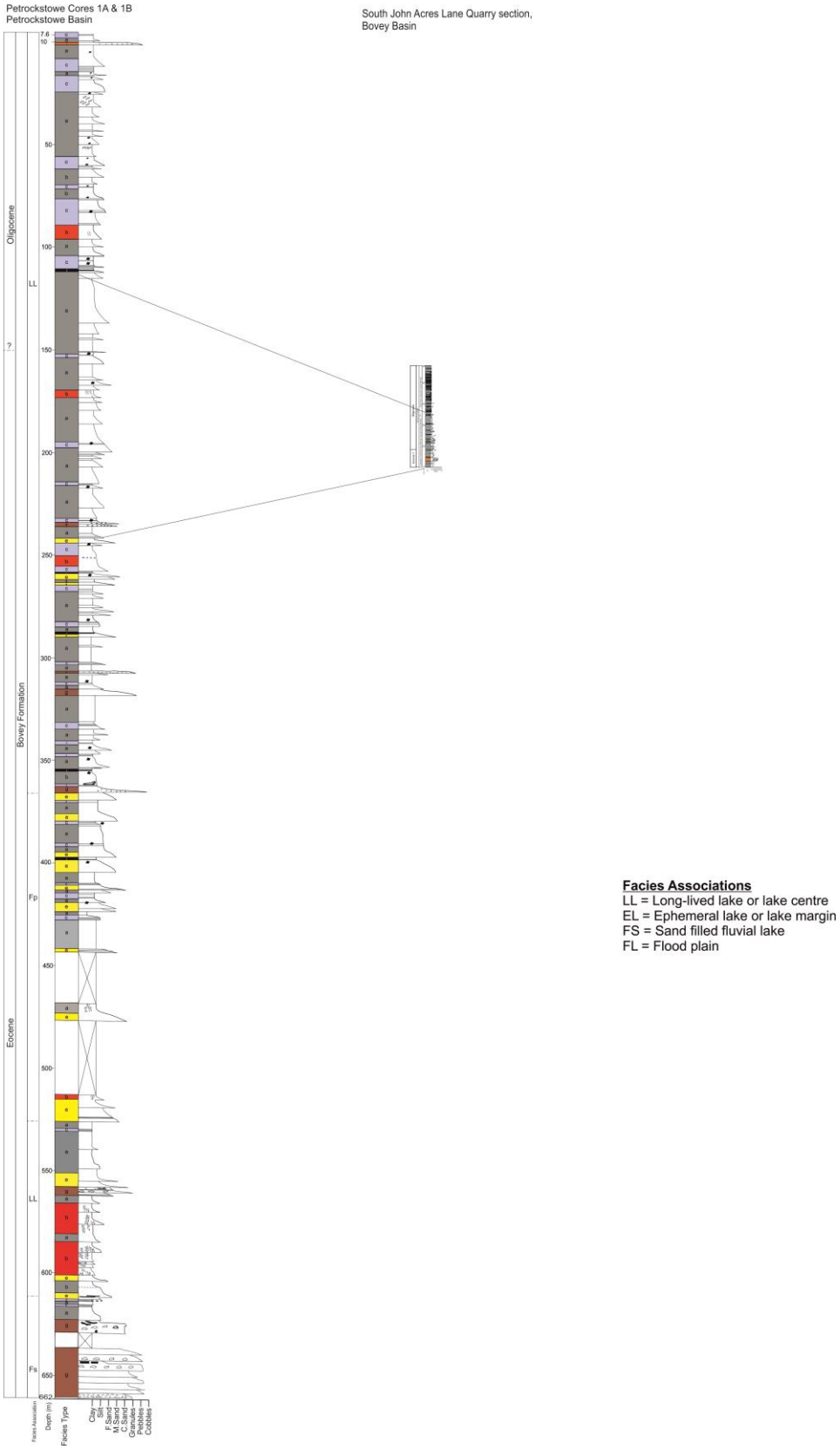

Figure 3.50: Correlation between Petrockstowe cores 1A & 1B, Petrockstowe Basin and South John Acres Lane Quarry, Bovey Basin, Southwest, UK

3.7 Palaeogeography of the depositional settings in the Bovey and Petrockstowe Basins in the Eocene – early Oligocene

Palaeogeographic models for the Bovey and Petrockstowe basins are presented in (Figures 3.60 – 3.90). In the Petrockstowe Basin, as determined from facies analysis, the earlier part of the deposition in the Eocene was via rivers in which sands and granules represent mainly channel sands deposited as either channel lag deposits, channel bar deposits or point bar deposits with possibly flood deposits of silty clays and silty sands that was controlled by contemporaneous fault movement, of which most was in the NW to SE directions and these faults might have led to the division of the present basin axially into deep central trough of over 2200 ft (~670 m) with flanks shelf areas to the NE and SW (Freshney 1970). In the upper part, deposition occurred in the Oligocene. It is important to note that in the second phase of the deposition, the river deposition extended over a wide area due to the fact that the central faulting became less active. Also, the channels sands and gravels are much more restricted to the area of the trough while the overbank deposits became much more extensive, especially in the shelf area of present Morton village and SE of Petrockstowe (Freshney 1970, Freshney *et al.* 1979).The presence of organic fragments may point to deposition in quite waters (small lakes and ponds) around the NW. Low relief and sluggish stream surrounding the Petrockstowe Basin during the Palaeogene times might have led the general fineness of the grains. In summary, Fresheny *et al*. (1979) in their words "in Palaeogene there could have been a Cornubian peninsula with rivers flowing NW and SE from its spine towards the marine areas in the present Celtic Sea, the English Channel and the Hampshire Basin".

On the other hand, earlier workers like Key (1862) considered the shape of the Bovey basin to have been elongate, but got contracted in the middle and the lake was fed by a rapid river entering the lake from its upper end and having tributaries in granite hills covered with forest trees. The said tributaries carried clays derived from decomposed feldspars, siliceous sand and gravel, vegetable matter and stones and boulders of various types. The Palaeogeography of the Bovey Basin is a complex one with many reviews by (Chandler 1957, Vincent 1974, Edwards 1976). The sediments of the Bovey Basin were presumed to have covered far greater area than its present limit (Maw 1864) and Scott (1929) attributed the "connection between the lake in which the Bovey beds were deposited and the Eocene river which gave rise to Bournemouth beds". Jukes-Browne (1909) in his opinion said the Bovey Basin has a tectonic origin and its present limit was not far removed from the original lacustrine area. Jukes-Browne (1909) further argued that during the Eocene, the western part of England was a land surface, where eastern Devon was covered by a sloping table of chalk that was later removed to Peniplain topography via subaerial detrition. Throughout the so called Bagshot times, Southern England sunk slowly, leading to the spread of the shallow Bournemouth beds further west ward that led to the formation of lagoon, lakes and swamps on the low lying plains adjoining the rivers which flowed into the bay. Bovey Basin was probably part of the lake and swamp area. It was assumed that Dartmoor Granite was exposed although, it may have less relief than the present time and possibly the ground to the south was higher (Edwards 1971, Vincent 1974).

Similarly, towards the end of Cretaceous there was an uplift in the western part of England, which continued into the Eocene and later gave rise to the land westward while the sea margin retrieved eastward gradually Scott (1929). Scott suggested that the drainage lines in Eocene seem to have been in an eastern direction and most

likely the clays in Dorset might have their origin from Dartmoor via the eastern flowing rivers. Again, in the Oligocene, the referred uplift continued, resulting to the eastern recession of the sea. A rift valley with N-W and S-E trend developed across western margin in the middle Oligocene.

Chandler (1957) suggested that during the Oligocene Bovey Tracey lake basin lignites accumulated plant debris much of which were swept from a steep warm valley into an associated lake basin lying in Palaeozoic strata. The lake was surrounded by marshland tree covered slope which contributed to the fossil flora. The Bovey beds had fill a gap in the British Stratigraphic column, by implication large column of strata existed below the sequence, probably over 2000 ft (> 606 m) in thickness in the centre and thin towards the shelf area, mostly consist of Palaeogene and partly Cretaceous and this means that the Bovey Basin may have been filled over considerable time, most likely representing part of the Palaeogene period Vincent (1971) From the above, one could speculate that the Bovey Basin was much deeper than 600 m.

Details of the description of the Abbrook Clay-and-Sand Member is contained in (Vincent 1971, Edwards 1976).The depth of the lake was not constant during the time of deposition which gave rise to its variation and concentration of suspended sediment occupied limited areas, and expansion was difficult to fill the whole sedimentary area. The deposition of clays and silty clays in the lower and middle Abbrook was in the lacustrine environment. There was a general coarsening trend to the N-W which may suggest the likely source was towards the present-day river Bovey (i.e. along the Sticklepath Lustleigh Fault). Also, the coarse material seemed to be granitic in origin, suggesting the Dartmoor Granite was exposed fairly close to the sedimentary area.

The area of sedimentation began to shrink towards the N-W during the upper Abbrook times and the whole area covered by fans, which ultimately gave rise to gravelly muddy sands with abundant pieces of lignite and occasional lakes that were anoxic (see Figures 3.60 & 3.70 Palaeogeographic map both lower/upper Abbrook times).

In the lower Southacre time, shallow lakes were dominant in the NE, stretching from the present Chudleigh Knigton Heath to Clay lane and Newbridge. In the upper Southacre times, the depositional environment became complicated while sedimentary area extended further to the south over much of the western part of the then Bovey Basin with the existence of shallow lake. Towards the end of the upper Southacre, the southern lake shrunk northwards, and eventually the Southacre pit was reached, and most of the upper clays in the pit were found to the south. It was at this time that the large thick lignites were build up as a back swamp with occasional lacustrine inversion (Vincent 1971).

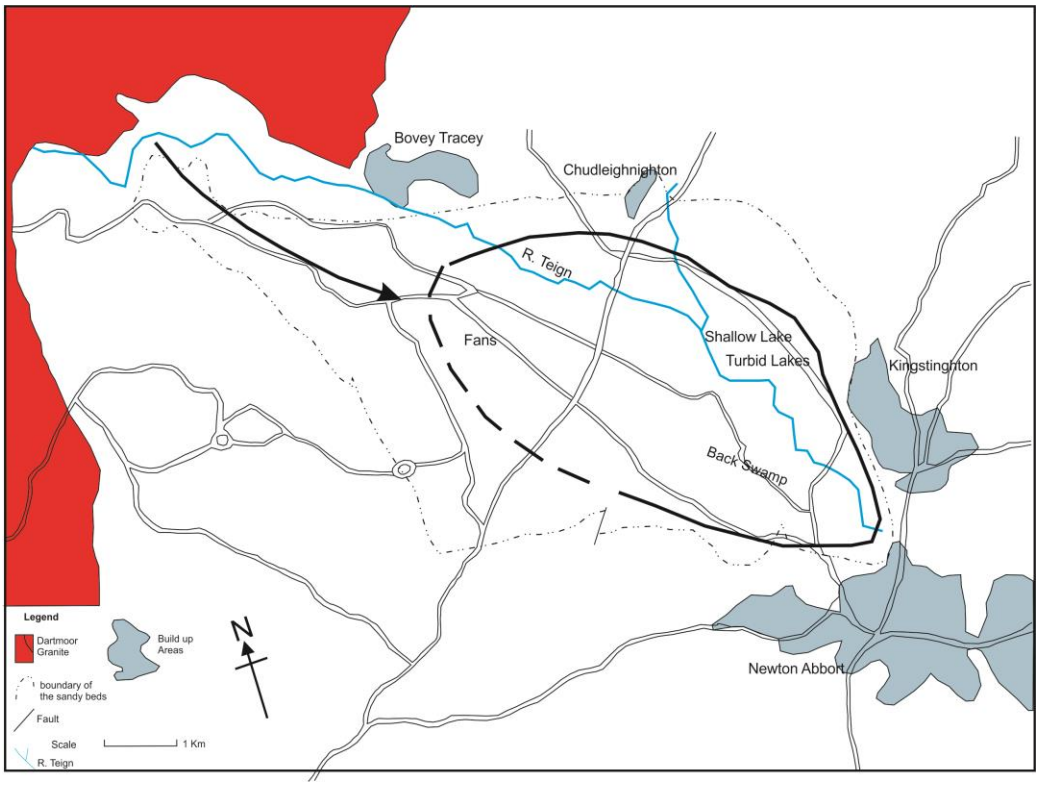

Figure 3.60: Palaeogeography of Carboniferous Abbrook Times, Bovey Basin (from Vincent, 1974)

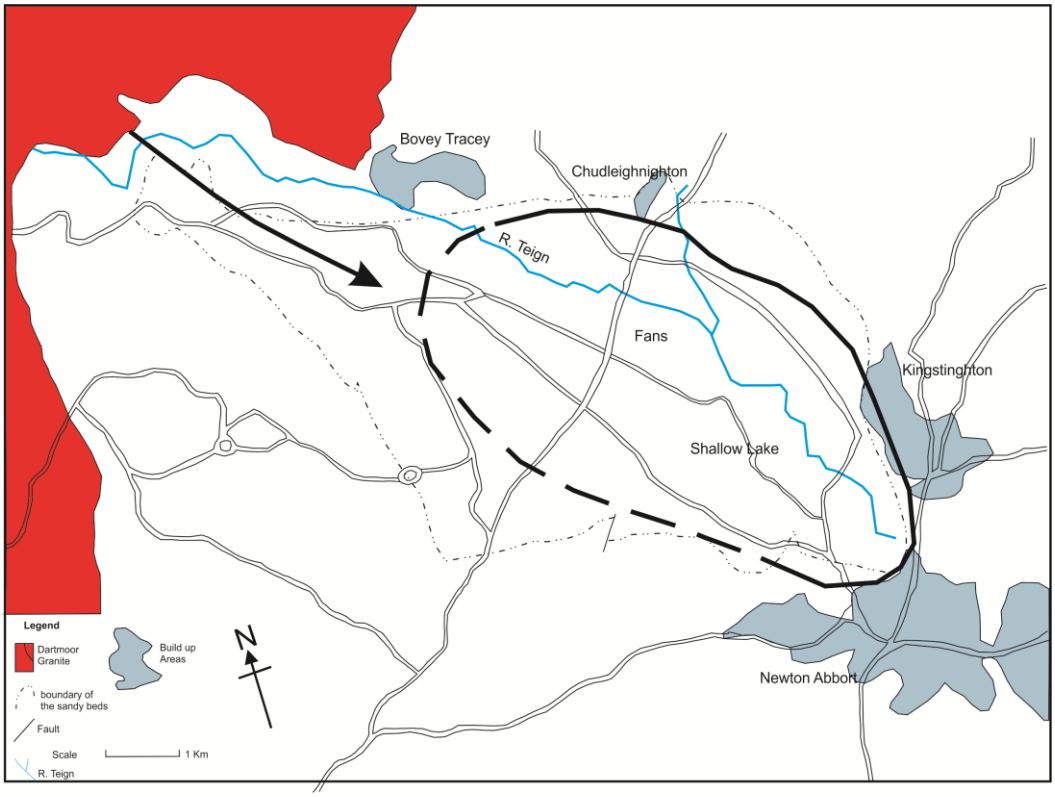

Figure 3.70: Palaeogeography of lower to middle Abbrook Times, (from Vincent, 1974)

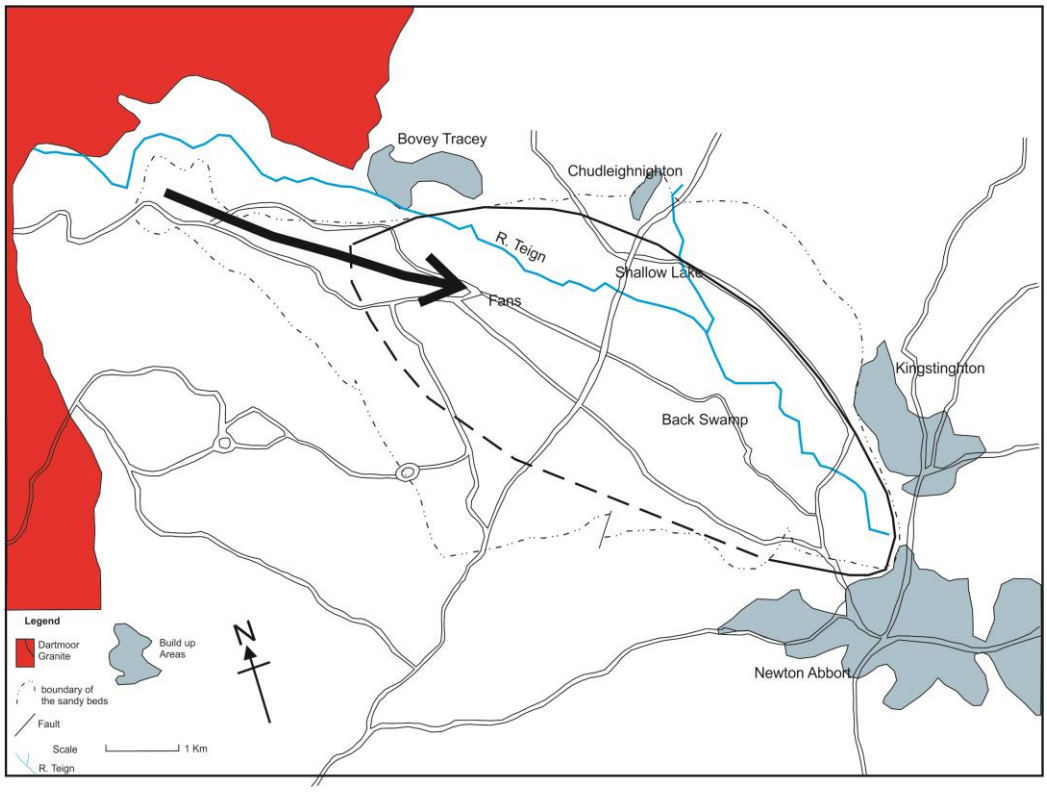

Figure 3.80: Palaeogeography of lower Southacre Times, (from Vincent, 1974)

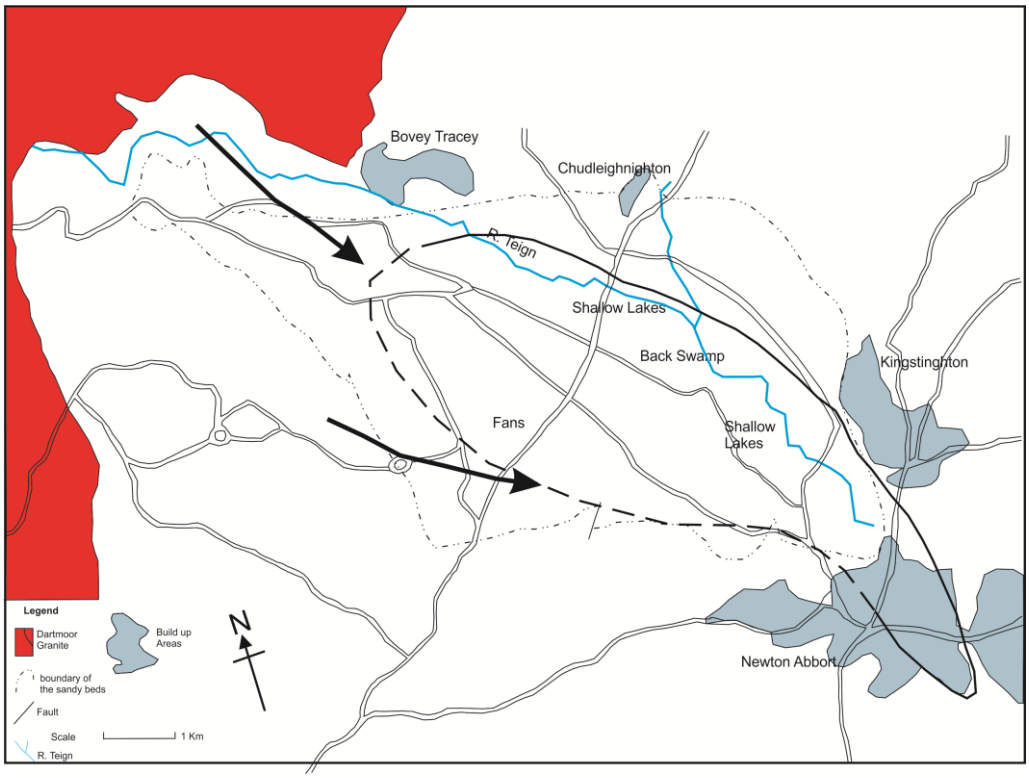

Figure 3.90: Palaeogeography of Upper Southacre Times (from Vincent, 1974)

CHAPTER 4 – PALYNOFACIES AND PALYNOLOGICAL ANALYSIS

4.1 INTRODUCTION

The most pronounced hyperthermal events associated with the Palaeogene are the Palaeocene Eocene Thermal Maximum (PETM), Early Eocene Climate Optimum (EECO) and recently secondary hyperthermal Eocene Thermal Maximum – 2 (ETM-2 ~53.5 Ma). These short periods of global warming in the marine sections are recorded by faunal and floral changes, isotope shifts and biomarker data, while in the terrestrial sections, such increase in atmospheric temperatures is recorded by changes in the composition of plant communities as a result of migration of floral elements and evolution (Crouch *et al.* 2001, Wing & Harrington 2001, Gingerich 2006, Sluijs *et al.* 2006, Agnini *et al.* 2009, Jaramillo *et al.* 2010, Zachos *et al.* 2010). Also, reconstructed temperature and hydrographic responses to abruptly increased atmospheric CO_2 concentrations were similar from ETM-2 ~53.5 Ma and the better-described PETM 55.5 Ma(Sluijs *et al.* 2006, Sluijs *et al.* 2009). Emphasis was put on the (EMT-2) ~ 53.5 Ma being associated with a rapid increase in atmospheric CO_2 content, although the impact was only documented locally (Nicolo *et al.* 2007, Stap *et al.* 2009).

Steurbaut *et al*. (2003) using integrated data based on sedimentology, micropalaeontology and carbon isotope analysis of the Palaeocene – Eocene boundary of Belgium sequence in northern Europe identified a different series of biotic and tectonic events which are associated with brief global episode of hyperthermal events of Initial Eocene Thermal Maximum (IETM), which was formally regarded as Last Eocene Thermal Maximum (LPTM) and established their succession. Results showed that the onset of the carbon isotope excursion (CIE) found at the base of the Tienen Formation coincides with the onset of *Apectodinium* abundance and also coincides with the development of deeply incised palaeovalleys. They concluded that despite the extreme warm climate and tectonic instability

of the area, the vegetation across the IETM was relatively stable and showed low extinction and first-occurrence rates.

Similar studies from the northern hemisphere on palaeoclimatic reconstruction estimates Eocene to Oligocene transition on the basis of bioclimatic analysis of terrestrially derived spores and pollen from marine sediments from the Norwegian-Greenland Sea. Elderett *et al*. (2009) showed that the cooling of ~5^{o}C in cold months has a mean temperature of 0 – 2^{o}C and a continued increased seasonality prior to Oi-1 glaciation event. Hence, the data have shown that the cooling temperature component is indeed incorporated into the $\delta^{18}O$ shift along the Eocene – Oligocene transition.

The age of the deposits in the Petrockstowe and Bovey basins is not precisely known, with only evidence of plant fossil remains in the lignite and the absence of animal fossils proved difficult in preservation in the turbid and acidic condition which prevailed (Vincent 1983). In the light of the above a multiproxy approach will be adopted in attempting to determine the age of the sediments in this chapter.

Reid (1911) and Chandler (1957) showed that the long ranging plant fossils (e.g. *Stratiotes websteri, Potamogeton tenuicarpus and Rubus microspermus*) appeared the first time in the Oligocene, their upper geological limit is not known despite the fact that the Bovey lignites have drawn considerable attention from many workers. Palynological investigations conducted by Freshney *et al* (1979) suggested that the Petrockstowe sediments are Eocene in age with a part of the strata belonging to the Oligocene. This dating remains debatable among palynologists, but Vincent (1983) reported that the Bovey Basin covers the time range from Upper Eocene to the Middle Oligocene, yet final sedimentation in the western side of Bovey Basin might be much younger in age.

In another work by Collinson *et al*. (2009) on the Cobham Lignite Bed (Cobham, Kent, UK) using high-resolution palynological studies, results indicated vegetation response to rapid climate warming at the onset of the PETM. It clearly demonstrated that the lower laminated lignite recorded a negative CIE at the onset of the PETM in the bulk material while the upper blocky lignite represented the estimated 4-12 Kya after the PETM onset.

In a similar study Hodgson *et al*. (2011) in south east England revealed that Palaeogene strata of the Hampshire basin was found to contain a CIE in the Upnor Formation followed by a positive recovery of yet another CIE found in the overlying Reading Formation. Hodgson *et al*. (2011) showed the CIE recorded in the Upnor Formation predates the PETM and the recovery at the base of the Reading Formation is unrelated to it.

Globally the Middle Eocene is regarded as representing a "greenhouse" climate and in the UK, southern England was covered by paratropical vegetation type characterised by coastal *Nypa* which was dominated by mangrove swamps bordering the land (Collinson & Cleal 2001). The taxon *Cyclanthus lakensis* seed in the UK is generally found in fresh water facies while in Messel Germany the seeds are very abundant in the siliciclastic facies of site SMF-7 and its presence in Messel seems to justify its growth around fresh water lakes and rivers (Collinson 1996, Smith *et al.* 2007). *Nypa* mangrove palms and *C. lakensis* serve as a diagnostic element of the middle Eocene European vegetation (Collinson & Cleal 2001). In the Hampshire Basin, southern England, *C. lakensis* is found to be the most widespread plant fossil and is geographically recorded from Thrasher's Heath in the west to Bracklesham Bay in the east (Smith *et al.* 2007). This fossil provides more evidence for the link between European and South American present day floras.

In a related work on specific faunal study and preliminary palynological study from the Isle of Wight, southern England shows an onset of cooling earlier in the Eocene (Savin 1977, Collinson *et al.* 1981). Fruit, seeds, pollen and spores from the Palaeogene deposits of the London and Hampshire Basins conform to a continuous sequence from the Early Eocene, indicating no evidence for sudden climate change at the end of the Eocene where the base was considered to be the Bembridge Marls in the Hampshire Basin. Established evidence was for two major periods of floristic change suggesting gradual cooling that commenced in the latest Early Eocene.

In addition to the earlier findings relating to the nonmarine Solent Group of sediments of the Hampshire Basin that span the Eocene and earliest Oligocene, results proved that it is rich in biota, including mammals and charophytes with only few fully marine, time diagnostic

intervals (Hooker *et al.* 2009). Hooker *et al*. (2009) emphasised that there was a major sea-level fall associated with polar ice at the Oligocene isotope event commonly referred to as Oi-1 glaciation close to the start of the Oligocene, represented in the Hamstead Member of the Bouldnor Formation due to the falling stage of system tract followed by an unconformity prior to the next maximum flooding surface.

These proxies are employed in determining whether the PETM exists in the lower Petrockstowe Basin, and reconstructing the mean annual air temperature in both Bovey and Petrockstowe basins for the first time.

Due to the fact that the precise age of these basins remains unresolved, an attempt is made to date the sediments of these basins using biostratigraphy (palynology) and chemostratigraphy (stable carbon isotopes $\delta^{13}C_{TOC}$). Also to find out if the Eocene – Oligocene cooling event affected these basins locally or regionally.

4.2 PALYNOFACIES ANALYSIS RESULTS

The term palynofacies was first introduced by Combaz (1964) to mean "all organic material which is clearly identifiable in palynological slides". In other words, "palynofacies" is defined as "a distinct assemblage of specific HCl and HF insoluble organic matter whose composition reflects a specific sedimentary environment" (Powell *et al.* 1990); while Habib (1982) and Tyson (1995) define palynofacies as "representing a specific aspect of an organic facies or palynologically defined organic facies".

The aim of this chapter is to discuss the palynofacies analysis carried out on the Petrockstowe and Bovey basins samples and the subsequent palaeoenvironmental reconstructions achieved from these analyses. To achieve this, counts of >300 organic matter of each sample was made. In order to have a coherent analytical output, the classification system of Tyson (1995) was adopted. This states that:

1. Palynomorphs: Tyson (1993) defined palynomorphs as a parameter that constitutes pollen, spores and undifferentiated forms (mainly poorly preserved), though there

are different standards of preservation and degrees of colouration suggesting that some might be reworked (Figure 4.1).

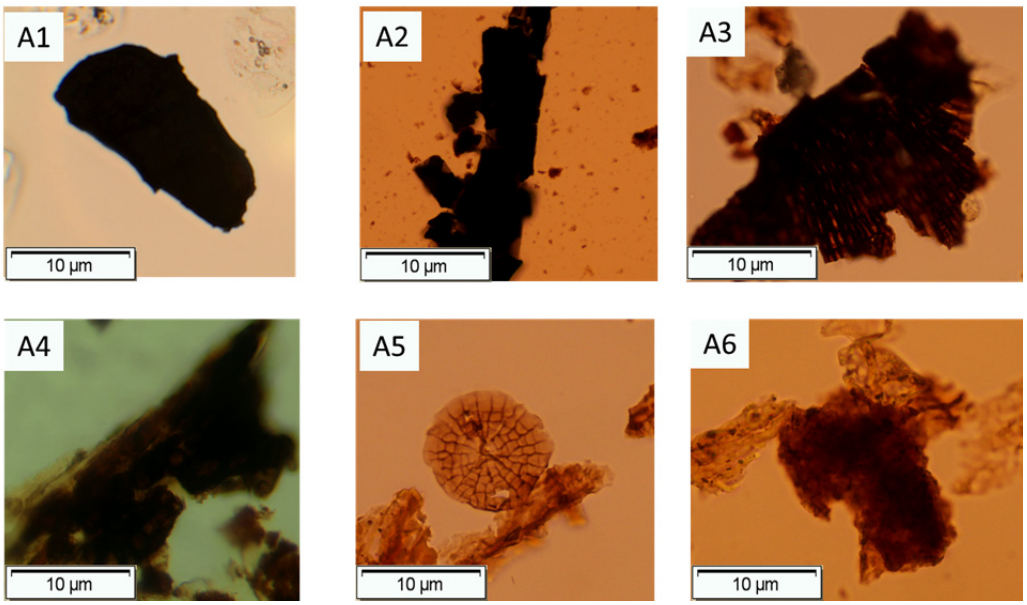

Figure 4.1: Example of phytoclasts (opaque), phytoclast (fungal) and amorphous organic matter (AOM). (A1) Opaque lath-shaped phytoclast; sample MC95 [slide: MPA62274]. (A2) Large lath opaque phytoclast; sample MC3 [slide: MPA61578]. (A3) Multicellular fungal 'fruiting body'; sample MC19 [slide: MPA61582]. (A4) Tangle masses of melanised fungal hyphae; sample MC58 [slide: MPA62270]. (A5) Multicellular fungal 'fruiting body' (because is discrete, is considered a palynomorph and not a phytoclast; sample MC19 [slide: MPA61582]. (A6) Well preserved AOM seen in transmitted white light; sample SJAL029 [slide: MPA63240].

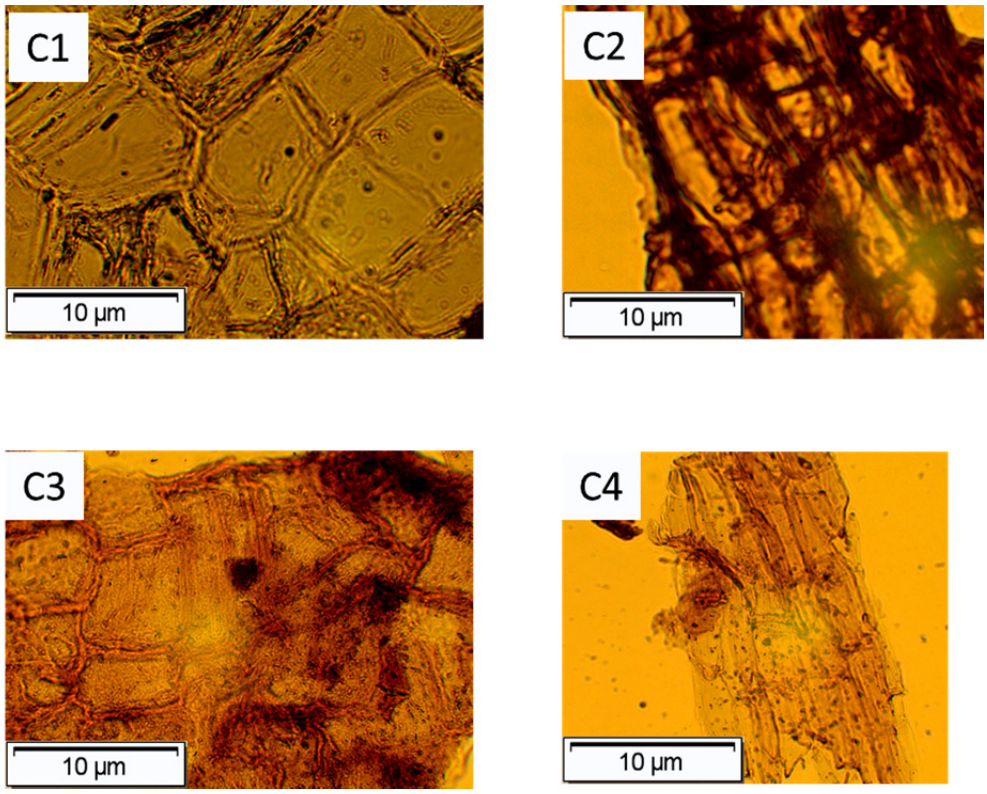

Figure 4.2: Example of phytoclast group-translucent cuticle and membranous tissues. (C1) Dispersed cuticle phytoclast showing regular rectangular cell outlines (most likely gymnosperm origin); sample SJAL026 [slide: MPA63237]. (C2) Dispersed cuticle phytoclast; sample SJAL040 [slide: MPA63248]. (C3) Structured phytoclast, cross hatched structure of the phytoclasts with thicken ribs rough at right angles to one another; sample SJAL027 [slide: MPA63238]. (C4) Dispersed cuticle phytoclast showing undulate rather than straight cell boundaries, a spiked out by the curticular flanges; sample SJAL027 [slide: MPA63238].

2. Phytoclasts: This group is made up of both black and brown well-lignified tracheid material, poorly lignified, tissue fragments derived from higher plants (Bostick 1971) and carbonized charcoal like "black wood" (Figure 4.1) following Burges (1974), Claret *et al*.(1981) and Tyson (1993) classification schemes. Also, belonging to this group is the translucent sub-group of phytoclasts that is basically made of land plant tissues and cuticle fragments (see Figure 4.2) as contained in Correia (1970).
3. Amorphous Organic Matter (AOM) group and other palynodebris of humic gel/resin. Under transmitted white light, it appears grey, pale yellow or brown in colour, partly translucent masses of variable thickness and with no cellular detail (see Figure 4.3). The AOM group probably originates from bacteria, phytoplankton,

and degraded organic aggregates. Their size varies from <5 to about 45 µm in diameter. This type of organic matter is linked to anoxic conditions and its preservation in sediments is dependent on the presence of an anoxic water layer. Boulter and Reddick (1986) supported the idea that amorphous matter is associated with low energy basin deposits regardless of the fact whether it is related to diagenesis or not.

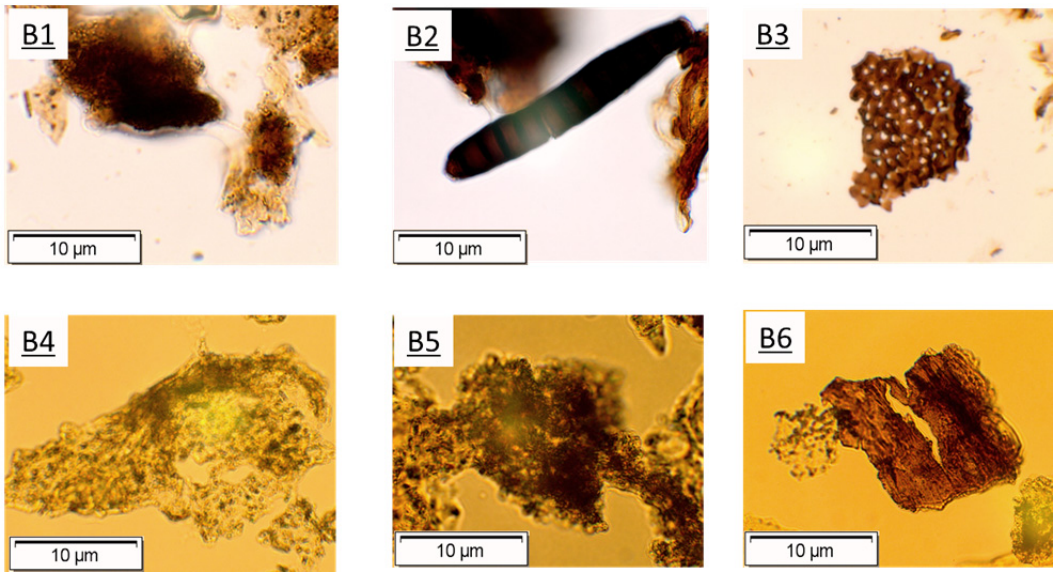

Figure 4.3: Example of -Amorphous Organic Matter (AOM) group and phytoclast group (mainly translucent). (B1) Humic gel and plant cuticle as seen in transmitted white light; sample MC60 [slide: MPA62271]. (B2) is an example of multicellular); sample MC58 [slide: MPA62270]. (B3) Phytoclast (biostructured) composed of at least two gymnosperm tracheids; sample MC76 [slide: MPA62288]. (B4 & B5) are well preserved AOM seen in transmitted white light; samples SJAL002 [slide: MPA63217] and sample SJAL023 [slide: MPA63235]. (B6) is a cross section of plant fragment sample SJAL013 [slide: MPA63225].

4.2.1 Petrockstowe Core (1A and 1B), Petrockstowe Basin

Based on the organic composition, analyses throughout the cores of the Petrockstowe Basin, three main groups of the organic matter were observed amorphous organic matter (AOM), phytoclast and palynomorphs as contained in Tyson (1995) see Tables 4.1a & 4.1b and Table 4.2. Detailed counts of all the sub-groups are found in Appendices 1 & 2, Tables 4.3.1 – 4.3.4.

Table 4.1a: Percentage of Amorphous Organic Matter (AOM), palynomorphs (Palyno) and phytoclast (phyt) groups in sample throughout core 1A, Petrockstowe Basin

Sample ID	Slide No (BGS)	Depth (m)	AOM (%)	Palyno (%)	Phyt (%)
MC3	MPA61578	23.5	10.2	4.6	85.1
MC12	MPA61579	65.8	21.3	36.3	42.5
MC13	MPA61580	75.5	37.3	42.5	20.2
MC18	MPA61581	109.4	28.9	27.4	43.8
MC19	MPA61582	111.3	24.0	58.9	17.1
MC20	MPA61583	116.0	21.4	58.7	19.8
MC27	MPA61584	202.3	18.5	73.2	8.3
MC35	MPA61585	257.3	23.9	66.7	9.4
MC42	MPA61586	311.2	10.2	79.6	10.2
MC48	MPA61587	354.8	9.9	79.8	10.3
MC-54	MPA62269	405	0.7	23.0	76.3

Table 4.1b: Percentage of Amorphous Organic Matter (AOM), palynomorphs (Palyno) and phytoclast (phyt) groups in sample throughout core 1B, Petrockstowe Basin

Sample ID	Slide No (BGS)	Depth (m)	AOM (%)	Palyno (%)	Phyt (%)
MC-58	MPA62270	432	1.7	40.3	58.0
MC-60	MPA62271	523	0.0	38.3	61.7
MC-61	MPA62272	540	6.0	51.3	42.7
MC-63	PMA62273	569	5.7	83.0	11.3
MC-95	MPA62274	586	9.0	1.0	90.0
MC-64	MPA62275	586	4.0	3.3	92.7
MC-101	MPA62276	587	0.0	0.3	99.7
MC-102	MPA62277	588	2.0	6.3	91.7
MC-103	MPA62278	590	0.0	1.3	98.7
MC-104	MPA62279	591	1.0	1.0	97.7
MC-65	MPA62280	593	5.7	3.3	91.3
MC-96	MPA62281	596	3.7	6.3	90.0
MC-97	MPA62282	596	2.7	24.0	73.3
MC-66	MPA62283	598	4.0	3.3	92.7
MC-67	MPA62284	604	6.1	3.0	90.9
MC-68	MPA62285	605	7.0	5.7	87.3
MC-70	MPA62286	607	1.3	3.3	95.3
MC-73	MPA62287	611	1.3	42.7	56.0
MC-76	MPA62288	616	1.0	35.3	63.7

From the palynofacies analyses dataset generated, a palynofacies zonation scheme is proposed which is labelled ‘A’, ‘B’, ‘C’ and ‘D’ (Figures 4.4 & 4.5). The zonation scheme is based on the different palynofacies groups. This zonation is analogous to the physical stratigraphic interval. The organic matter in each zone is presented as a percentage for each organic component. The description of the individual samples analysed can be found in Appendix 1 with the results summarised in Tables 4.3.1 and 4.3.2. From base to top beginning at 616 m, palynofacies zones are characterised as follows:

Palynofacies Zone A (616m – 586m)

Description

This interval shows a palynofacies distribution dominated by phytoclasts with highest occurrence of ~100% towards the upper end of the zone. Within the interval of 616 mm – 586 m the distribution rises from 56% to 100 % phytoclasts; comparatively AOM and palynomorphs record low occurrences mostly below 10 % with the exception of three samples that had distribution of < 42%.

Interpretation

This zone is made up of phytoclasts particularly the opaque/black type suggesting a strong terrestrial influx and deposition near the fluvial system, which indicates a proximal suboxic-anoxic environment. Also, because they are highly degraded this may suggest pre- and post-depositional alteration may be related to some extent to sub aerial oxidation due to water column fluctuation and transport (Tyson 1993,1995).

The distribution of phytoclasts group is variable from low to high and probably took place over different successive sedimentary cycles of different magnitude, e.g. suspension settling or terrestrial mire. It is clearly observed that the percentage of palynomorphs tends to

decrease greatly while the percentage of the phytoclasts increases. The interpretation is that the high values of phytoclasts represent periods of high woody fragments contributing to the basin as a result of increased run-off (Tyson 1995).

Palynofacies Zone B (586m – 523m)

Description

In this interval, there is an increase in the palynomorph group from 1% at 586 m to 83% at 569 m and then a decrease to 15% at 523 m to mark the end of this zone. Of particular interest is the AOM group with a 6% distribution at 593 m which decreases to 0% at 523 m. Similarly, the phytoclast group abundance decreases from 93% at 586 m to 61% at 523 m Between zones 'A' and 'B', there is sharp fall in the phytoclast and the AOM groups while the palynomorphs group rise, although towards the end of the zone it fall to below 50% there about.

Interpretation

It is observed that the distribution of the various palynofacies categories corresponds to changes in the sedimentary facies through cyclic pattern from silty clay to coarse sandy material where the palynomorphs are more related to the fine sediments that favours good preservation/high recovery, and back into clayey material again, a typical fining upward sequence (Figure 4.5). This is also associated with long lived lake depositional system.

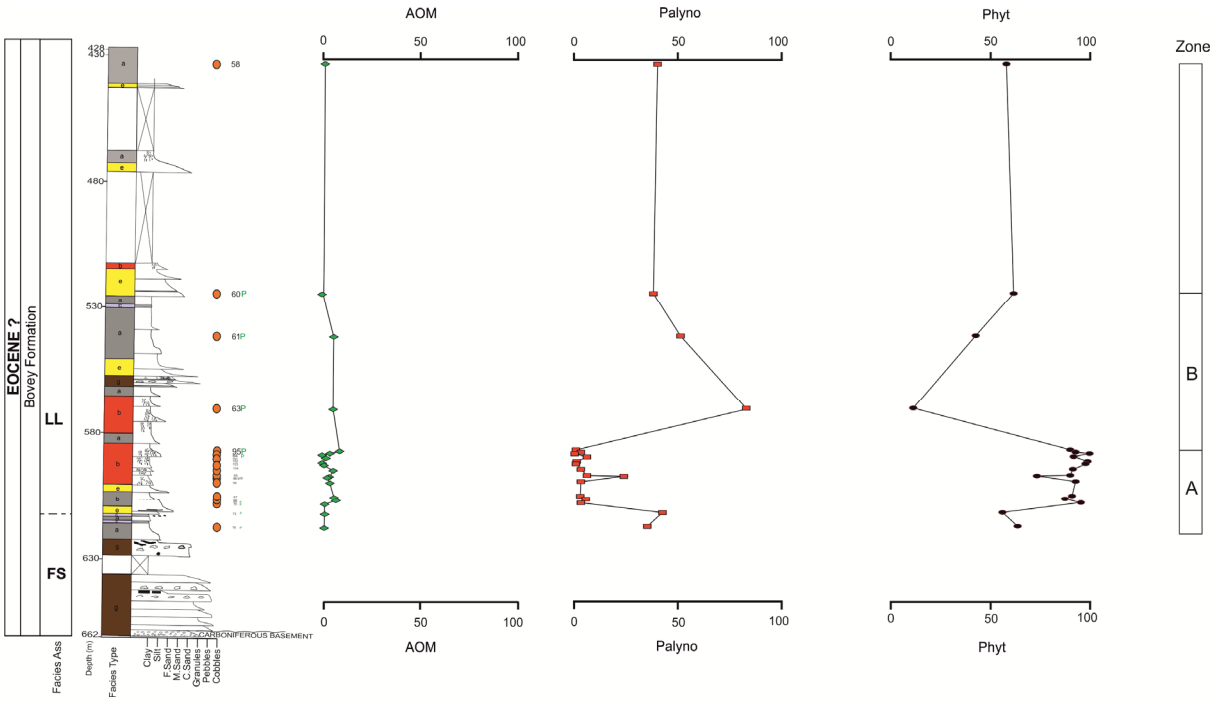

Figure 4.4: Data from Petrockstowe core 1B, Petrockstowe Basin, (a) age, (b) depth, (c) lithology, (d) distribution and percentage occurrence AOM, Palyno, Phyt

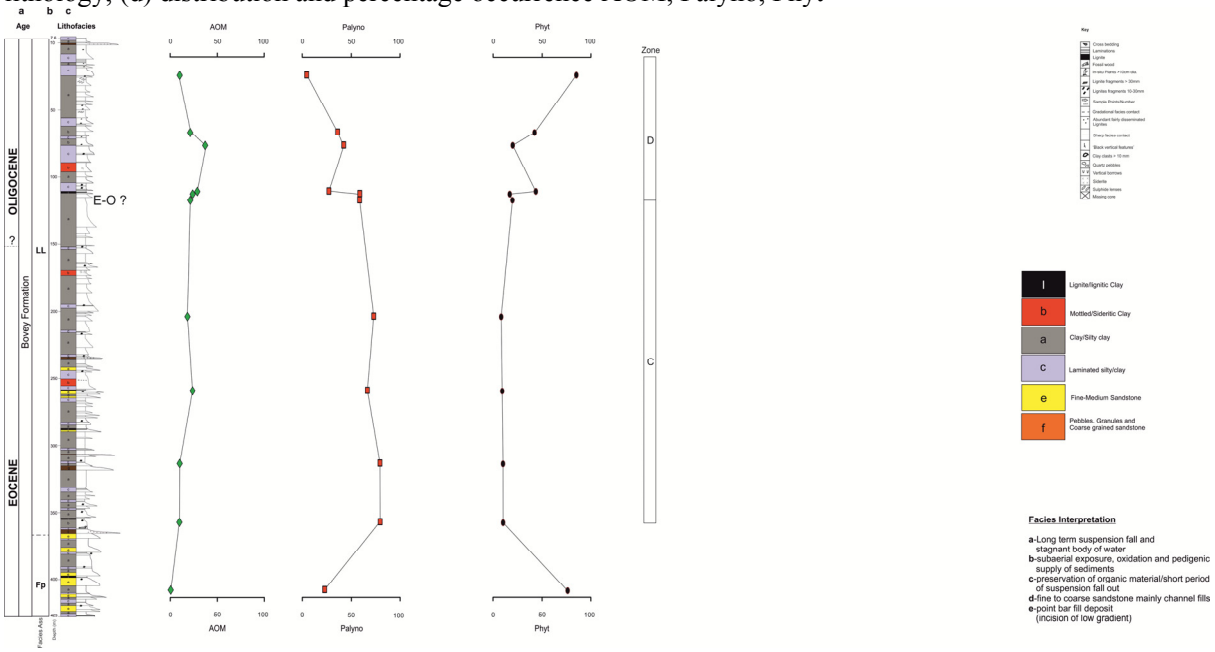

Figure 4.5: Data from Petrockstowe core 1A, Petrockstowe Basin, (a) age, (b) depth, (c) lithology, (d) distribution and percentage occurrence AOM, Palyno, Phyt

Palynofacies Zone C (354m – 109m)

Description

This palynofacies zone is characterised by high percentages of palynomorphs that have 79% maximum distribution in the lower part of core 1A from 354 m to 109 m and a minimum of 59%, which is consistent in distribution through this interval. The next most abundant group

is AOM reaching 23% at 257 m with a minimum distribution of 10% at a depth of 354 m. The palynomorphs show variability in their state of degradation within the zone. And lastly the phytoclast group has < 10% in its distribution all through the zone.

Interpretation

It is observed that the distribution of the palynomorphs increase while the phytoclasts decrease and this phenomenon could be related to the progradation of the lake level which supports preservation of palynomorphs (Fig. 4.5).

Palynofacies Zone D (109m – 23.5m)

Description

In this palynofacies zone the percentage distribution of the AOM, the phytoclast and the palynomorph groups overwhelmingly dominate the samples, where a sharp rise in the phytoclast group from 20% to 85% is noticed within the fine lithology. This suggests that the abundance of AOM in a depositional environment could be as a result of degradation of organic materials like algal remains (Oboh-Ikuenobe *et al.* 2005). This high value is not constant throughout the zone because fluctuation of the high and low values of AOM continues throughout the core. Other groups, the phytoclasts and palynomorphs, show similar fluctuations of high and low values between 109 – 23.5 m depth (Fig. 4.5).

Interpretation

The relative fluctuations in the distributions of the AOM, the palynomorphs and the phytoclast groups, despite the general falling trend in the distribution of the AOM and the palynomorphs the phytoclasts show an increase towards the top of the core with respect to the cyclic pattern of the lithofacies; this could suggest a long-term suspension fall out, restricted water circulation in the silty clay and a high water table. The depositional environment could probably be related to an ephemeral lake or lake margin.

4.2.2 South John Acre Lane Quarry Section, Bovey Basin

The same methodology adopted in the zonation of the Petrockstowe cores is applied to the South John Acres Lane Quarry section, Bovey Basin. The palynofacies zonation in the Bovey Basin is coded 'I – M'and 'A – D' in the Petrockstowe Basin, resulting in five palynofacies zones. The results are summarised and presented in Tables 4.2 and Appendix 1, Tables 4.3.3 – 4.3.4.

Palynofacies Zone I (0.05m – 7.70m)

Description

In this interval the AOM group has the most dominant composition, reaching 65% at 1.75 m height and a minimum distribution of 36% at 2.8 m. In between 0.05 – 7.70 m some samples that did not contain any organic matter are categorised as barren samples (marked Ba in the table). The barren samples found in this zone include the following: SJAL002, SJAL004, SJAL006, SJAL011, SJAL0012 and SJAL014. The phytoclast group is comprised of lath and equidimensional sized particles, with a distribution ranged between 7 – 62%, reaching the maximum at 2.80 m. (Figure 4.6). The palynomorph group shows a range of 2 – 28%, and the majority are not well preserved within this zone.

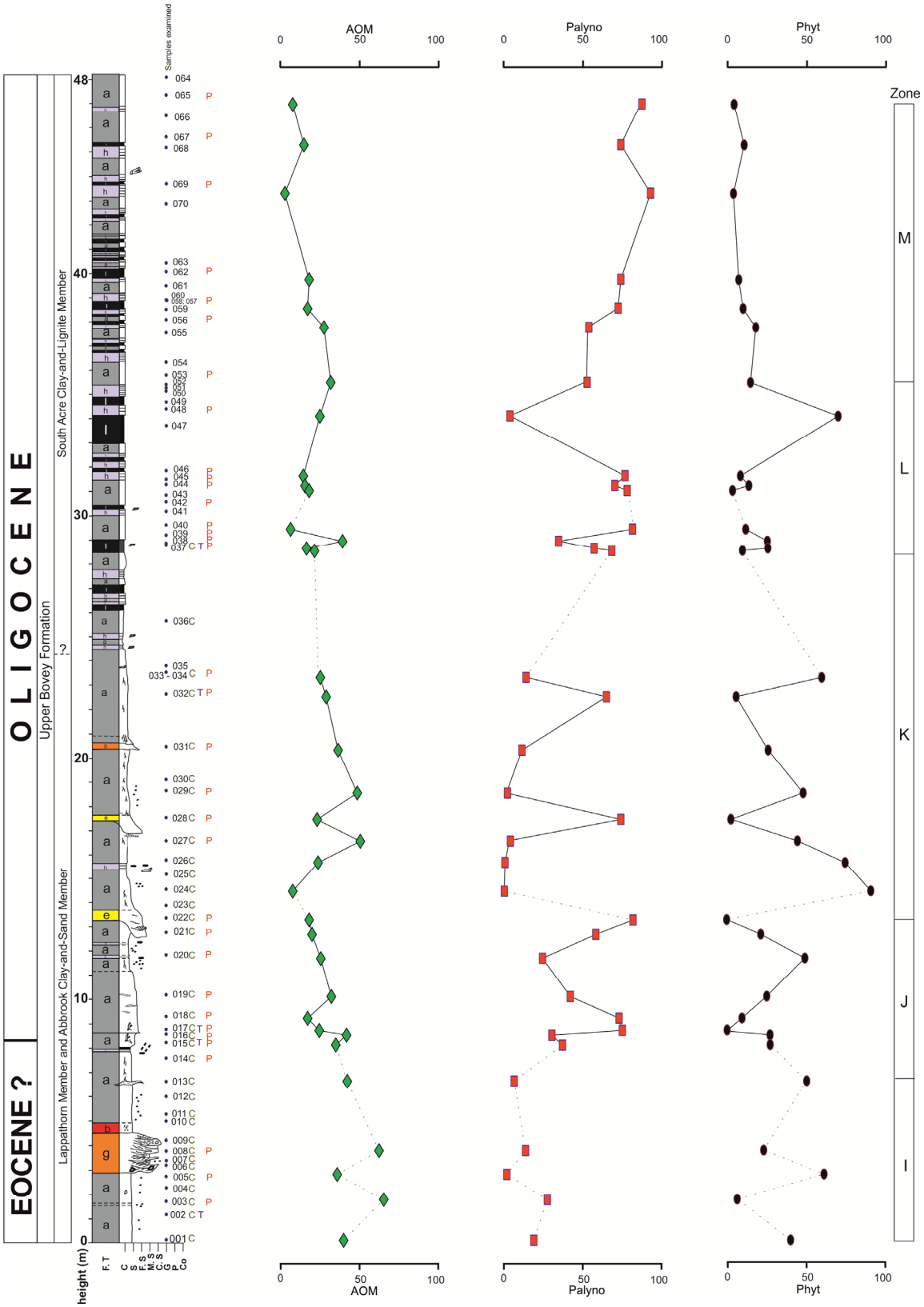

Figure 4.6: Data from South John Acres Lane Quarry Section, Bovey Basin, Southwest (a) age, (b) depth, (c) lithology, (d) distribution and percentage occurrence AOM, Palyno, Phyto.

Table 4.2: Percentage of Amorphous organic matter (AOM), palynomorphs (Palyno) and phytoclast (phyt) groups in samples throughout the South John Acres Lane Quarry section, Bovey Basin, (Ba: Barren samples, where no organic matter was observed)

Sample ID	Slide No (BGS)	Depth (m)	AOM (%)	Palyno (%)	Phyt (%)
SJAL065	MPA63260	47.40	8.3	87.0	4.7
SJAL067	MPA63259	45.70	15.3	73.7	11.0
SJAL069	MPA63258	43.70	3.3	92.3	4.3
SJAL062	MPA63257	40.10	18.7	73.7	7.7
SJAL060	MPA63256	38.90	17.7	72.0	10.3
SJAL056	MPA63255	38.10	28.0	53.7	18.3
SJAL053	MPA63254	35.80	32.3	52.6	15.1
SJAL048	MPA63253	34.40	25.4	4.2	70.4
SJAL046	MPA63252	31.90	15.0	76.3	8.7
SJAL045	MPA63251	31.50	16.0	70.0	14.0
SJAL044	MPA63250	31.30	18.7	77.7	3.7
SJAL042	MPA63249	30.60	Ba		
SJAL040	MPA63248	29.70	7.0	81.0	12.0
SJAL039	MPA63247	29.20	39.7	34.7	25.7
SJAL038	MPA63246	28.90	17.0	57.0	26.0
SJAL037	MPA63245	28.80	22.0	68.0	10.0
SJAL036	MPA63244	25.70	Ba		
SJAL034	MPA63243	23.50	25.7	14.3	60.0
SJAL032	MPA63242	22.70	29.3	64.7	6.0
SJAL031	MPA63241	20.50	36.8	11.7	26.2
SJAL029	MPA63240	18.70	49.0	2.7	48.3
SJAL028	MPA63239	17.60	23.7	73.7	2.7
SJAL027	MPA63238	16.70	50.9	4.5	44.6
SJAL026	MPA63237	15.80	24.2	1.0	74.7
SJAL024	MPA63236	14.60	8.3	0.7	91.0
SJAL023	MPA63235	13.90	Ba		
SJAL022	MPA63234	13.40	18.7	81.3	0.0
SJAL021	MPA63233	12.80	20.4	58.1	21.5
SJAL020	MPA63232	11.80	26.0	24.7	49.3
SJAL019	MPA63231	10.20	32.7	42.0	25.3
SJAL018	MPA63230	9.30	17.7	72.7	9.7
SJAL017	MPA63229	8.80	25.0	74.7	0.3
SJAL016	MPA63228	8.60	42.2	30.5	27.3
SJAL015	MPA63227	8.20	35.4	37.2	27.4
SJAL014	MPA63226	7.70	Ba		
SJAL013	MPA63225	6.70	42.7	6.8	50.5
SJAL012	MPA63224	6.00	Ba		
SJAL011	MPA63223	5.30	Ba		
SJAL008	MPA63222	3.80	62.7	14.0	23.3
SJAL006	MPA63221	3.20	Ba		
SJAL005	MPA63220	2.80	36.3	2.2	61.5
SJAL004	MPA63219	2.30	Ba		
SJAL003	MPA63218	1.75	65.7	27.7	6.6
SJAL002	MPA63217	1.20	Ba		
SJAL001	MPA63216	0.05	40.4	19.2	40.4

Interpretation

Generally, due to the lithological changes in this zone, it tends to be accompanied by a greater diversity in organic facies with high percentage of the AOM group, and according to Tyson (1993) high percentages of AOM reflect enhanced preservation in reducing conditions. In general terms, dominance of AOM reflects low energy, stagnant, oxygen-depleted environments (Tyson 1993). The phytoclast content was moderate to high due to sediment input signifying proximity to the source and could suggest a depositional environment associated to ephemeral lake or marginal lake.

Palynofacies Zone J (7.7m – 13.90m)

Description

This interval (~7.7 – 13.90 m) is characterised by the dominance of the palynomorph group which shows a gradual upward increase in the section although, it decreases before increasing again and a sudden break between 10.2 m and 11.8 m results in disruption in the distribution of the organic matter (Figure 4.6); this coincides with a brief change in lithology from fine grained-sand to silty clay. A greater percentage of the palynomorph group is composed of degraded spore and pollen. The AOM and the phytoclast groups have an opposite distribution pattern, with the AOM ranging from 18 – 42% while phytoclast is between 0 – 49% at heights 8.20 – 14.0 m respectively.

Interpretation

The high percentage of palynomorphs, and phytoclasts and other preserved structured tissues are characteristic of a fluvio-deltaic environment, which may be associated with point bar deposits Tyson (1995).

Palynofacies Zone K (13.9m – 25.7m)

Description

The greater part of this interval is dominated by the AOM and the phytoclast groups while the palynomorph group has a low distribution with two points showing high abundance. The

AOM group has a minimum occurrence of 8% at 14.6 m and a maximum of 51% at 16.7 m, and decreases towards 23% at 17.6 m. The palynomorphs show no significant trend in distribution compared to the AOM; where one of the highest occurrences (74%) in the palynomorph group also coincided with low occurrences of the phytoclast and the AOM marking changes in lithofacies from fine sandstone to laminated clay, rich in plant remains around 17.6 m height. The phytoclast and AOM groups continue to decline towards the upper part of the zone and similarly the palynomorph group increases before it again decreases close to the end of the zone (Figure 4.6).

Interpretation

The high occurrence of the AOM group (comprising a large proportion of living or dead bacteria, or organic matter from bacterial degradation of plant material) (Bryant *et al.* 1988, Tyson 1995, Ekwenye *et al.* 2014) in this horizon is associated with clay and points to reducing environments. Also, the high occurrence of the phytoclast group comprising mainly of translucent grains/particles which are mostly cuticle, suggest a typical long lived lake or lake centre (Tyson 1995).

Palynofacies Zone L (25.7m – 30.60m)

Description

This palynofacies zone is the thinnest compared with the other palynofacies zones and has a similar trend with the previous zone K. At the lower boundary of the zone it is noted that when the AOM and phytoclast groups are experiencing high distribution, the palynomorph group shows low distribution and vice versa towards the middle and the upper part of the zone. In this interval the samples reflect a high diversity of palynomorphs (with a record of 7 species) in one sample (SJAL 040), reaching 81% abundance at around 29.7 m height. At the base of this zone, it shows lesser abundance of 67% at 28.8m. There is high occurrence of 40% and 70% of the phytoclast group observed despite the fact that sedimentologically, this interval is silty clay and laminated clays. Hence, the biodegradation by microbial

activity has the influence of reducing the palynomorph count especially in the clayey environments Ekwenye *et al*. (2014).

Interpretation

The high abundance of the AOM group may partly be due to masking, is highly associated with bacterially - degraded origin signifying restricted circulation levels during deposition. Also, the large number of palynomorphs observed in this zone tends to reflect lower energy environments than many impoverished woody assemblages (Batten & Stead 2005). The depositional environment in this zone could be considered to an ephemeral lake or marginal lake.

Palynofacies Zone M (30.6m – 47.40m)

Description

This interval is characterised by high occurrences of the palynomorph group, not less than 53% and reaching a maximum of 92% before decreasing towards the upper end of the zone, while the phytoclast and the AOM groups show low abundances (Fig. 4.6). The AOM and the phytoclast groups recorded abundance of 3 - 28% and 4 - 18% respectively.

Interpretation

There is less AOM than in the previous zone; this part of the section could be related to a bacterially-degraded origin, which indicates restricted circulation levels at the time of deposition. The presence of Chlorophyta (*Botryoccus* and others) in this interval is indicative of fresh water lakes and lagoons (Tappan 1980), the occurrence of which shows no apparent association to sequence or lithology.

4.3 PALYNOLOGY RESULTS

The aim of this section is to present the results of palynology data generated from the two sections. Out of the 75 samples analysed (11 samples from Petrockstowe core 1A; 19 from

Petrockstowe core 1B and 45 from South John Acres Lane Quarry section) investigated the majority were largely productive, yielding spore and pollen although some samples contained only very limited numbers of palynomorphs (see Appendix 2, Tables 4.3.5 – 4.4.0). Pollen and spores were counted from the prepared slides, as described in section 2.7. Counts of 300 pollen and spore grains were made per slide where possible. A significant number of the samples analysed produced very poor counts of pollen/spores from rare, to very rare, which could be due to poor preservation of the pollen/spores, dispersal or transport means, and lithology type. By definition, the following are adopted in the context of this thesis: rare – very rare < 5 specimens; rare – sparse 5 – 10 specimens; 10 – 25 very few specimens; common 20 – 49 specimens and abundant > 50 specimens (Crouch & Brinkhuis 2005).

4.3.1 Palynomorphs

All palynomorphs identified are listed, and the nomenclature adopted for their identification follows that of Thomson and Pflug (1953) for pollen, that of Krutzsch (1959) for spores, Jansonius and Hills (1976) for pollen/spores, and Punt *et al*. (2007) for pollen and spores. In applying this nomenclature to this study, the following factors were considered:

1. with some of the palynomorphs identified there was difficulty in relating the fossil forms to extant genera; while other species it was possible to relate them to their botanical affinities by grouping the forms according to extant families.
2. it is more consistent to make comparisons with similar forms when using the same nomenclatural system

It is very important to note that in using such definitions, some morphological genera could have a wide range and thus include a number of different species in a single form species. A variety of spores, pollen grains and fresh water algae were encountered in the slides examined. The morphological groups of the taxa identified are:

I. Monolete spores

Arecipites Woodhouse monosulcate pollen

Laevigatisporites sp Wilson & Webster 1946; *Laevigatisporites haardti* Potonie & Ven.1934, Thomson & Pflug, 1953

II. Trilete spores

Cicatricosisporites form species; *Schizaea Schizaea* (Dudar) Potonie & Gelletich, 1953[natural affinity: Schizaeaceae, Anemia/Mohria; fossil]

Cyathidites sp

Gleicheniidites senonicus Ross 1949, fossil

Polypodiaceoisporites spp. (Potonie & Gelletich, 1933) Kedves 1961a sub-fsp. Minor Kedves 1961a (Dorog)

III. Bisaccate pollen type

Pinuspollenites spp (Potonie, 1931b) Thomson & Pflug, 1953

IV. Inaperturopollenites pollen types

Inaperturopollenites hiatus (Potonie, 1931b) Thomson & Pflug, 1953, Taxodiaceae = affinity, *Taxodium* or *Glyptostrobus (Dorog)*

Sequoiapollenites spp.

V. Monocolpate pollen type

Cycadopites

Monocolpopollenites form species. A *Palmae (Dorog)* Pflug & Thomson, 1953

VI. Triporate pollen types

Plicapollis pseudoexcelsus (W.Kr.1958a) W.Kr.1962 subsfp *turgidus* Pflug, 1953, (Dudar); *Triporate*

Pompeckjoidaepollenites subhercynicus (W.Kr. 1954) (W.Kr.1967)

VII. Tricolporate pollen type

Ilexpollenites spp.

Porocolpopollenite Pflug, 1953

Retitricolporopollenites spp

Tiliaepollenites, *Tiliae* Potonie, 1931 extant *Tilia* pollen

Tricolporopollenites spp; *Tricoloporopollenites Kruschi* (Potonie, 1934) Thomson & Pflug, 1953 subfsp. Accessorious Potonie, 1934b, *Nyassaceae* (Oroszlany)

Trudopollis spp.

VIII. Tetracolporate pollen type

Tetracolporopollenites

4.3.2 Palynological analysis

Throughout Petrockstowe cores 1A & 1B and the South John Acres Lane (SJAL) Quarry section, the palynomorph assemblages are grouped into spores, angiosperm, gymnosperm, fungi, unidentified palynomorphs as shown in Table 4.3 and Tables 4.4, 4.5 and 4.6 show their distribution is presented in Figures 4.7 - 4.9. Because the two sections are purely terrestrial, there was no record of any dinoflagellate cysts which are usually an indicator of a marine environment.

The important key palynomorphs assemblage from both sections are presented in Plates 1 – 6, they vary in their degree of preservation, some are reworked and degraded evident by their dark colour and broken parts; the scale bars are 10 μm.

Table 4.3: Main groups of palynomorphs in the Petrockstowe core 1A & 1B, Petrockstowe Basin and the South John Acres Lane Quarry section, Bovey Basin

Spores	Angiosperm	Gymnosperm
Sterreisporites spp.	Arecipites spp.	Bisaccate
Cicatricosisporites spp.	Cycadopites spp.	Inaaperturopollenites spp.
Cingulatisporites spp.		Monocolpopollenites spp.
Polypodiaceisporites spp	Plicapollis spp.	Sequoaipollenites spp.
Laevgatisporites spp.	Plicapollis pseudopollenites	
	Tricolpate sp.	
	Tricoporopollenites spp.	
	Tricolpopollenites spp.	
	Triletes spp.	
	Triporopollenites spp.	
	Tetraporopollenites spp.	
	Pompeckjoidaepollenites spp.	
	Porocolpopollenites spp.	
	Minorpollis spp.	
	Salixpollenites	
	Pityosporites spp.	
	Ilexpollenites spp.	

Table 4.4: Percentage of spore, gymnosperm, angiosperm, fungi and unidentified palynomorphs in samples throughout the core 1A, Petrockstowe Basin

Smaple No	Slide Number (BGS)	Depth (m)	Spore % of total	Gymnosperm pollen % of total	Angiosperm pollen % of total	Fungi % of total	Unidentified % of total
MC3	MPA61578	23.5	0.0	0.0	72.7	0.0	27.3
MC12	MPA61579	65.8	2.7	21.8	60.9	1.8	12.7
MC13	MPA61580	75.8	0.7	27.9	68.0	0.0	3.4
MC18	MPA61581	109.4	2.2	27.5	59.3	6.6	4.4
MC19	MPA61582	111.3	22.3	45.1	29.5	0.0	3.0
MC20	MPA61583	116.0	50.0	31.4	15.1	0.0	3.5
MC27	MPA61584	202.3	4.8	51.8	40.5	1.6	1.3
MC35	MPA61585	257.3	34.3	49.5	5.7	7.6	2.9
MC42	MPA61586	311.2	72.8	22.2	3.1	0.6	1.3
MC48	MPA61587	354.8	0.0	0.0	0.0	0.0	0.0
MC54	MPA62269	405.1	47.6	405.1	52.4	0.0	0.0

Table 4.5: Percentage of spore, gymnosperm, angiosperm and fungi in samples throughout the core 1B, Petrockstowe Basin., cells highlighted in grey indicate where samples were barren

Smaple No	Slide Number (BGS)	Depth (m)	Spore % of total	Gymnosperm pollen % of total	Angiosperm pollen % of total	Fungi % of total
MC58	MPA62270	431.6	6.7	34.9	49.0	9.4
MC60	MPA62271	523.0	4.2	33.6	54.6	6.7
MC61	MPA62272	540.1	47.9	17.6	34.2	0.3
MC63	MPA62273	569.1	42.9	0.0	57.1	0.0
MC95	MPA62274	585.5	0.0	50.0	50.0	0.0
MC64	MPA62275	586.4	0.0	50.0	50.0	0.0
MC101	MPA62276	587.0				
MC102	MPA62277	588.3	41.7	0.0	50.0	4.2
MC103	MPA62278	590.1				
MC104	MPA62279	591.0				
MC65	MPA62280	593.1				
MC96	MPA62281	595.6	0.0	0.0	0.0	100.0
MC97	MPA62282	595.9	33.3	33.3	33.3	0.0
MC66	MPA62283	598.0				
MC67	MPA62284	603.8				
MC68	MPA62285	605.0	54.5	18.2	27.3	0.0
MC70	MPA62286	606.6	50.0	0.0	50.0	0.0
MC73	MPA62287	610.5	6.4	23.4	44.7	25.5
MC76	MPA62288	616.0	6.3	27.1	37.5	25.0

Table 4.6: Percentage of spore, gymnosperm, angiosperm, fungi and unidentified species in samples throughout the South John Acres Lane Quarry, Bovey Basin

Smaple No	Slide Number (BGS)	Height (m)	Spore % of total	Gymnosperm pollen % of total	Angiosperm pollen % of total	Fungi % of total	Unidentified % of total
SJAL065	MPA63260	47.40	33.6	54.3	10.0	0.7	1.0
SJAL067	MPA63259	45.70	24.1	61.0	13.0	0.6	1.3
SJAL069	MPA63258	43.70	39.0	52.4	8.3	0.0	0.3
SJAL062	MPA63257	40.10	23.5	57.0	19.1	0.0	0.4
SJAL060	MPA63256	38.90	25.7	48.2	21.5	1.6	0.3
SJAL056	MPA63255	38.10	46.3	50.3	10.9	0.0	6.8
SJAL053	MPA63254	35.80	25.6	42.4	16.0	0.0	16.8
SJAL048	MPA63253	34.40	25.0	25.0	12.5	37.5	0.0
SJAL046	MPA63252	31.90	50.2	40.3	7.1	0.9	1.4
SJAL045	MPA63251	31.50	37.4	41.2	15.0	0.0	5.3
SJAL044	MPA63250	31.30	57.8	39.2	6.3	0.7	1.9
SJAL042	MPA63249	30.60	12.4	77.5	10.1	0.0	0.0
SJAL040	MPA63248	29.70	29.9	59.9	10.2	0.0	0.0
SJAL039	MPA63247	29.20	39.2	45.4	15.5	0.0	1.0
SJAL038	MPA63246	28.90	37.5	67.8	1.3	12.5	1.3
SJAL037	MPA63245	28.80	54.6	49.7	3.6	1.3	0.0
SJAL034	MPA63243	23.50	25.0	56.8	18.2	0.0	0.0
SJAL032	MPA63242	22.70	12.7	65.3	17.9	0.0	0.6
SJAL031	MPA63241	20.50	22.2	38.9	22.2	0.0	0.0
SJAL029	MPA63240	18.70	0.0	40.0	60.0	0.0	0.0
SJAL028	MPA63239	17.60	20.2	54.5	23.7	0.0	0.4
SJAL027	MPA63238	16.70	13.3	26.7	46.7	6.7	0.0
SJAL022	MPA63234	13.40	47.4	33.2	19.4	0.0	0.0
SJAL021	MPA63233	12.80	78.0	11.0	5.0	0.0	0.0
SJAL020	MPA63232	11.80	57.3	16.0	25.3	0.0	1.3
SJAL019	MPA63231	10.20	79.7	11.0	8.5	0.0	0.8
SJAL018	MPA63230	9.30	25.3	18.2	50.5	1.0	5.1
SJAL017	MPA63229	8.80	45.0	67.4	16.7	0.0	5.8
SJAL016	MPA63228	8.60	0.0	23.2	58.0	2.9	15.9
SJAL015	MPA63227	8.20	9.1	4.5	18.2	63.6	4.5
SJAL014	MPA63226	7.70	0.0	28.6	64.3	0.0	7.1
SJAL008	MPA63222	3.80	25.9	11.1	22.2	25.9	14.8
SJAL005	MPA63220	2.80	0.0	100.0	0.0	0.0	0.0
SJAL003	MPA63218	1.75	4.8	47.6	23.8	0.0	23.8
SJAL001	MPA63216	0.05	0.0	0.0	100.0	0.0	0.0

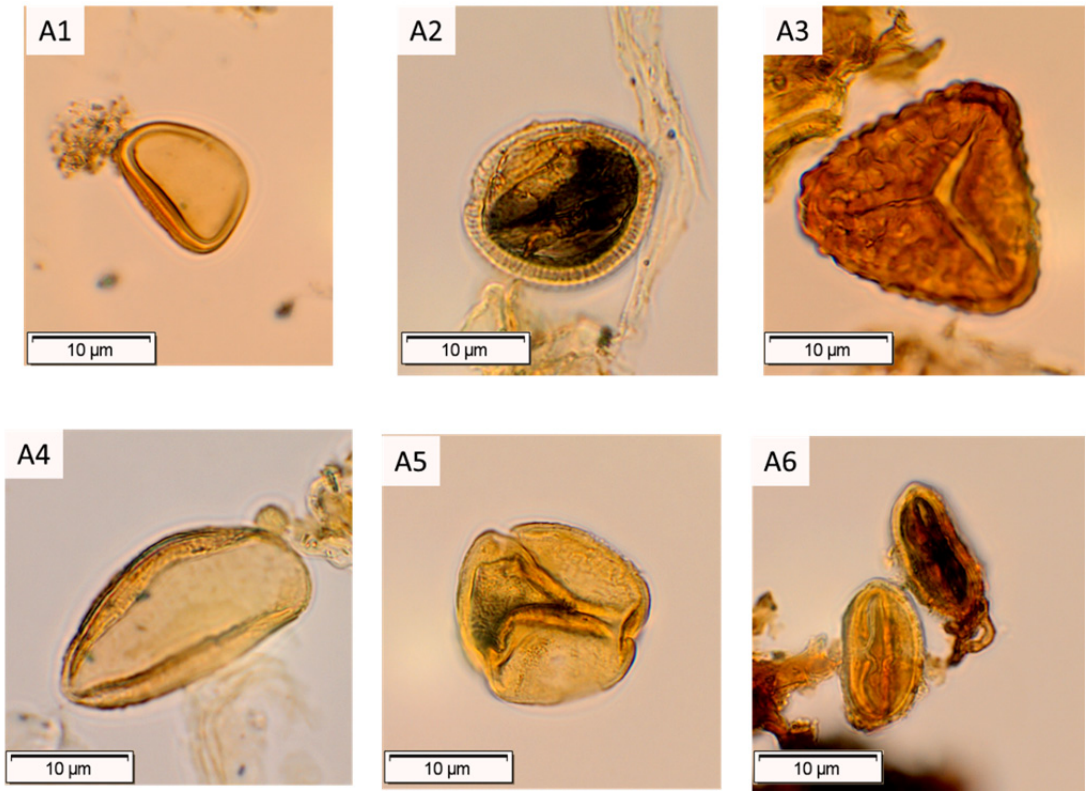

Plate 1: Palynomorphs identified in core 1B of the Petrockstowe Basin

(A1) *Laevigatisporites* spp., sample MC-61 [slide: MPA62272]

(A2) Tricolporate (*Ilexpollenites* spp.), sample MC-73 [slide: MPA62287]

(A3) *Polypodiaceoisporites* spp., sample MC-61 [slide: MPA62272]

(A4) Monocolpates spp., sample MC-61 [slide: MPA62272]

(A5) Tricolporate (*Retitricolporopollenites* spp.), sample MC-76 [slide: MPA62288]

(A6) Tricolporate (*Retitricolporopollenites* spp.), sample MC-73 [slide: MPA62287]

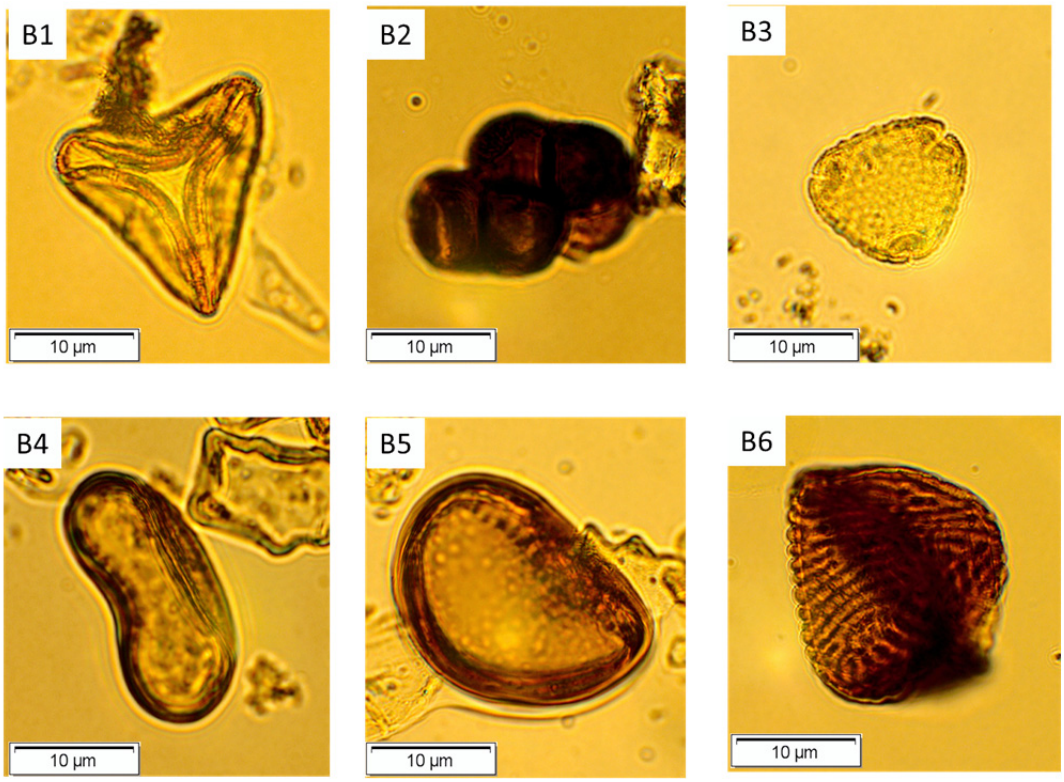

Plate 2: Palynomorphs identified in South John Acres Lane Quarry of the Bovey Basin

(B1) *Gleicheniidites senonicus*, sample SJAL003 [slide: MPA63218]

(B2) Fungal spore (Dicellate), sample SJAL026 [slide: MPA63227]

(B3) *Tiliaepollenites* spp., sample SJAL020 [slide: MPA93232]

(B4) *Laevigatisporites* spp., and particles of translucent woody fragments, sample SJAL037 [slide: MPA63245]

(B5) Polypodiisporites spp.??), sample SJAL037 [slide: MPA63245]

(B6) *Cicatricosisporite*s spp., sample SJAL037 [slide: MPA63245]

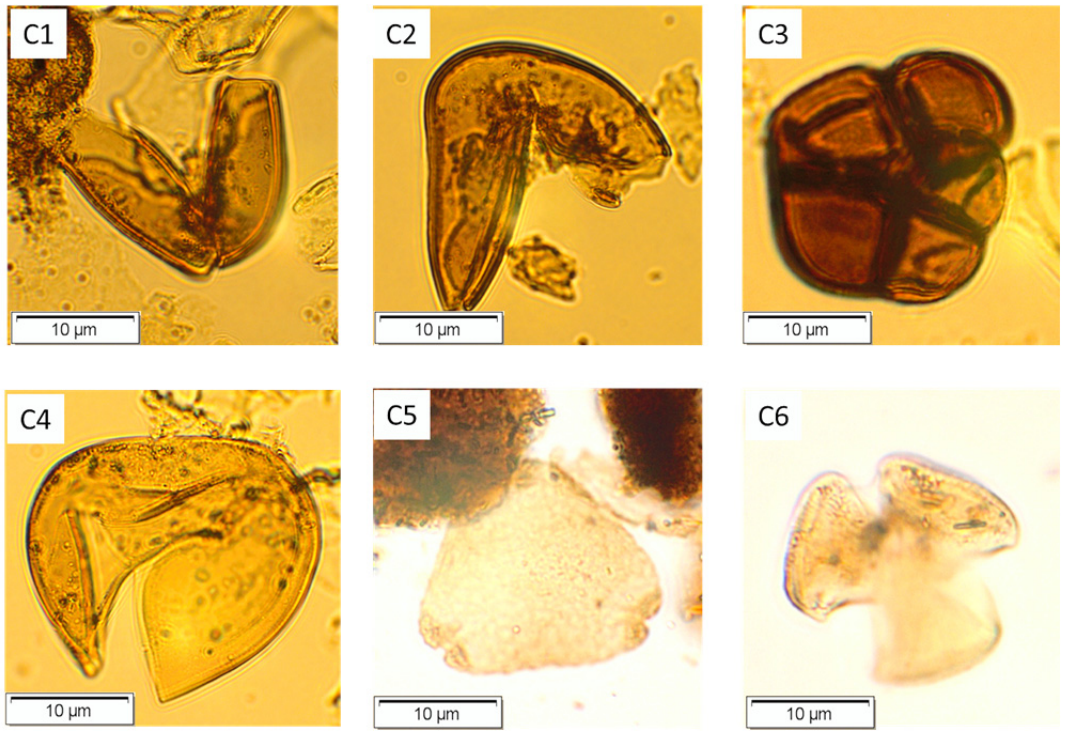

Plate 3: Palynomorphs identified in South John Acres Lane Quarry of the Bovey Basin

(C1) Broken trilete spore surrounded by dark brown AOM as a result of poor preservation conditions, sample SJAL038 [slide: MPA63246]
(C2) Broken trilete spores (cf. *Cyathidites* spp.), sample SJAL039 [slide: MPA63247]
(C3) Fungal cluster, sample SJAL038 [slide: MPA63246]
(C4) Trilete spore (cf. Cyathidites spp.), sample SJAL040 [slide: MPA63248]
(C5) *Tiliaepollenites* spp., humic gel, dark brown AOM, dark brown phytoclasts and translucent woody fragments, sample SJAL046 [slide: MPA63252
(C6) Trilete spore (cf. *Retitricolpites* spp.), sample SJAL044 [slide: MPA63250]

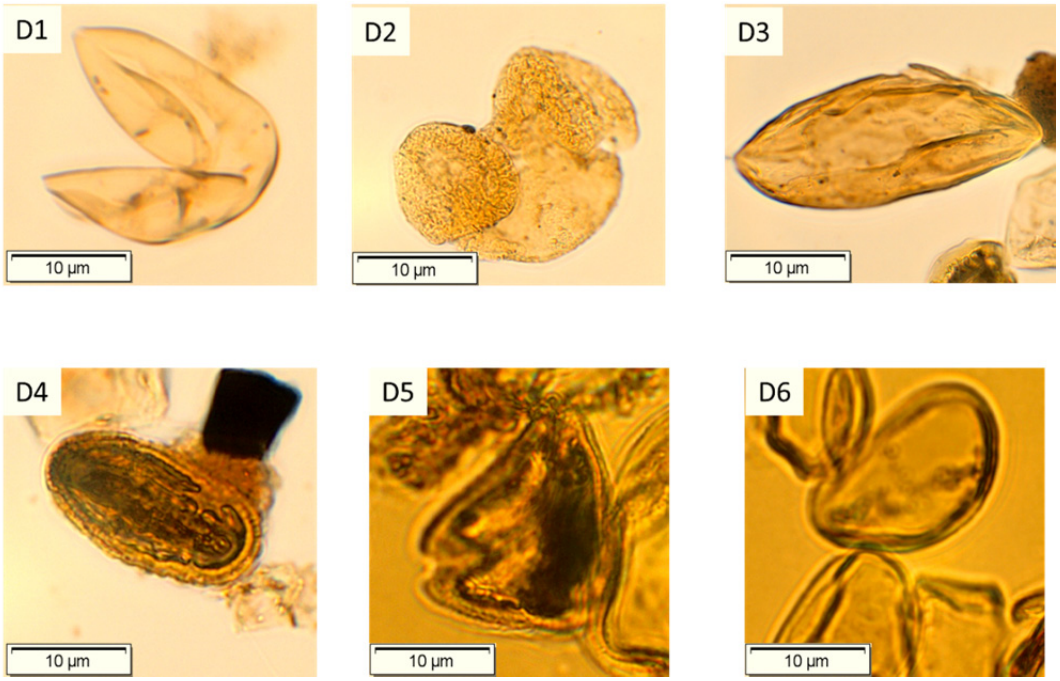

Plate 4: Palynomorphs identified in South John Acres Lane Quarry of the Bovey Basin

(D1) *Inaperturopollenites hiatus* or (Taxadiaceae spp.), sample SJAL054 [slide: MPA63254]
(D2) Bisaccate or (*Pinuspollenites* spp.) yellow to translucent colour, sample SJAL056 [slide: MPA63255]
(D3) Monocolpate pollen, sample SJAL056 [slide: MPA63255]
(D4) Trilete spore (cf. *Retitricolporopollenites* spp.), black or opaque phytoclasts, humic gel, sample SJAL056 [slide: MPA63255]
(D5) *Trudopollis* spp., black to dark brown in colour, sample SJAL060 [slide: MPA63256]
(D6) Cluster of *Laevigatisporites* spp., light yellow to translucent colour, sample SJAL069 [slide: MPA63258]

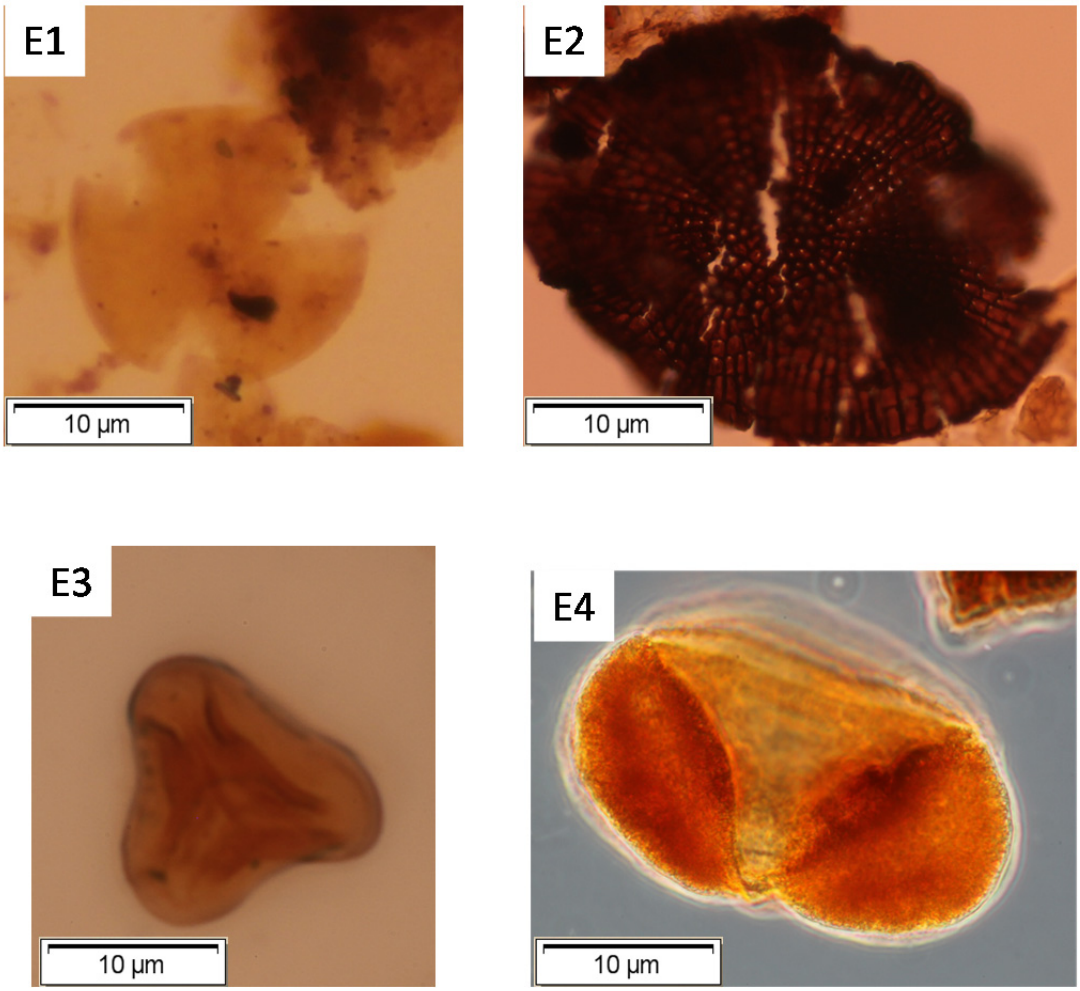

Plate 5: Palynomorphs identified in core 1A of the Petrockstowe Basins

(E1) *Tricolpites* spp., translucent colour surrounded by dark brown phytoclasts and humic gel/translucent woody fragments, sample MC-13 [slide: MPA61580]

(E2) Fungal fruiting body (Hyphae), dark brown, sample MC-19 [slide: MPA61582]

(E3) Trilete (cf. *Leotriletia* spp.), sample MC-19 [slide: MPA61582]

(E4) Bisaccate pollen (cf. *Pinuspollenites* spp.), sample MC-27 [slide: MPA61584]

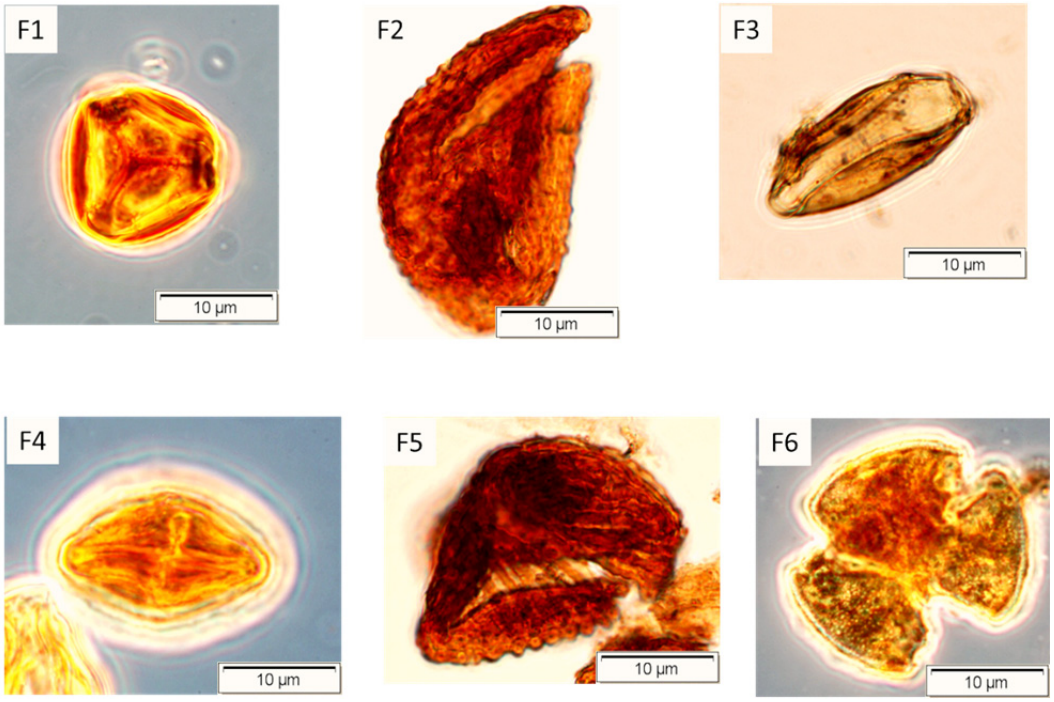

Plate 6: Palynomorphs identified in core 1A of the Petrockstowe Basin

(F1) *Plicapollis pseudoexcelsus* as seen under oil immersion, sample MC-20 [slide: MPA61583]
(F2) *Polypodiaceoisporites* spp., sample MC-42 [slide: MPA61586]
(F3) *Monocolpopollenites* spp., sample MC-42 [slide: MPA61586]
(F4) *Tricolporopollenites* spp., as seen under oil immersion, sample MC-42 [slide: MPA61586]
(F5) *Cicatricosisporites* spp., sample MC-42 [slide: MPA61586]
(F6) *Tricopites* spp., as seen under oil immersion, sample MC-27 [slide: MPA61584]

The palynological quantitative analysis of the samples from the cores in the Petrockstowe Basin and the South John Acres Lane Quarry section, Bovey Basin showed the following grouping: spores included *Stereisporites* spp., *Cicatricosisporites* spp. (Plate 2, B6), *Cingulatisporites* spp., *Polypodiaceisporites* spp. (Plate 1, A3) and *Laevigatisporites* spp. (Plate 1, A1); gymnosperm pollen composed of Bisaccate (Plate 4, D2, Plate 5, E4), *Inaperturopollenites* spp. (Plate 4, D1), *Monocolpopollenites* spp., *Sequoaipollenites* spp. and angiosperm pollen composed of *Arecipites* spp, *Cycadopites* spp., *Monolete* spp., *Plicapollis* spp. (Plate 6, F1), *Plicapollis pseudopollenites*, *Tricolpate* spp. (Plate 1, A2, A5,

A6), *Tricolporopollenites* spp. (Plate 6, F4), *Tricolpopollenites* spp., *Triletes* spp., *Triporopollenites* spp., *Tiliaepollenites* spp., *Tetraporopollenites* spp., *Pompeckjoidaepollenites* spp., *Porocolpopollenites* spp., *Minorpollis* spp., *Salixpollenites* spp., *Pityosporites* spp., *Ilexpollenites* spp.; and lastly the fungi/algae group.

The assemblage *Laevigatisporites* spp., Bisaccate, *Inaperturopollenites* spp., *Monocolpopollenites* spp. and *Tricolporopollenites* spp. have shown high abundance throughout the core/section in both basins with the exception of *Tricolporopollenites* spp. which was not observed in the South John Acres Lane Quarry, Bovey Basin.

Laevigatisporites spp. (Plate 2, B4) first occurs in the Petrockstowe core at a depth of 616 m with 6% abundance decreasing to 4% within a short interval and rising to 50% and then remains stable before it disappeared in the core top at around 23 m. Comparatively, in the South John Acres Lane Quarry section, *Laevigatisporites* spp. has its first occurrence in sample SJAL003 with 5% abundance and continues to increase to 78% in sample SJAL019, while five samples from this section proved to be barren yielding no palynomorphs. The samples are SJAL001 – 002 (0.1 – 1.2 m), SJAL004 (1.8 m), SJAL006 (3.2 m), SJAL011 - 013 (5.3 – 6.7 m) and SJAL023 – 026 (13.9 – 15.8 m).

Bisaccate pollen first occurs in sample MC 73 with 2% abundance at 610 m. At 595 m it disappears and only to reappear with of 33% abundance in sample MC97. Between 596 m – 569 m, Bisaccate pollen disappears again to reappear in sample MC61 at 540 m with abundance of 1% and then shows an increase of up to 36% around 202 m. After this interval, the abundance falls to <5% between 116 – 111 m which marked its last occurrence (Figure 4.6). In the South John Acres Lane Quarry, this pollen has its first occurrence in sample SJAL034 with 11% abundance, which is also the peak of its distribution. The last occurrence is in sample SJAL060 with 1% occurrence. In between the first and last occurrences the maximum distribution reached is not >3% meaning very rare and some samples encountered were barren.

Inaperturopollenites spp. is a conifer pollen and is similar to that produced by modernTaxidium and usually represents a warm and swampy environment (Boulter & Craig 1979, Collinson *et al.* 1981, Collinson 1992) and being deposited in-situ (i.e. not far from its place of growth). *Inaperturopollenites* spp. is first observed in the lower part of the core 1B around 616 m with 4% very rare abundance decreasing to 2% at 610 m. After this interval, no record of it is observed until around 540 m with 12% sparse abundance which continues to decrease to 8% rare abundance at around 311 m; toward the upper part of the core the distribution of the species is variable which is very rare to rare switching between 15-3%. This short break could be associated with the Eocene – Oligocene boundary proposed by Turner (1979) which he suggested to be at a depth of 120 m in this core on the basis of pollen data. This floral change coincided with a fall in the reconstructed MAAT from 19.5^{o}C to 15^{o}C. In the South John Acres Lane Quarry section, Bovey Basin, the taxa first occurs in sample SJAL003 with a common abundance of 48%, and a series of breaks as marked by the barren samples between depths of 5.3 m – 6.7 m and 14.6 m – 15.8 m. It shows a sharp decline in abundance at around 10.2 – 12.8 m represented by samples SJAL019-021. Thereafter the abundance remains sparse at around 15% till the top of the section. *Inaperturopollenites* spp. is one of the species that marks the Eocene – Oligocene boundary as reported by Machin (1971) from the Palaeogene of the Isle of Wight. There is no sharp break to demonstrate a transition to “cooler” floras, with only a gradual loss of warm/tropical plants. This time period still maintains species richness. In addition to that, the disappearance of *Inaperturopollenites*, *Monocolpopollenites* and the sudden increase in high percentage of *Tricolpopollenites* suggest a change in temperature in the Upper Oligocene (Boulter 1980).

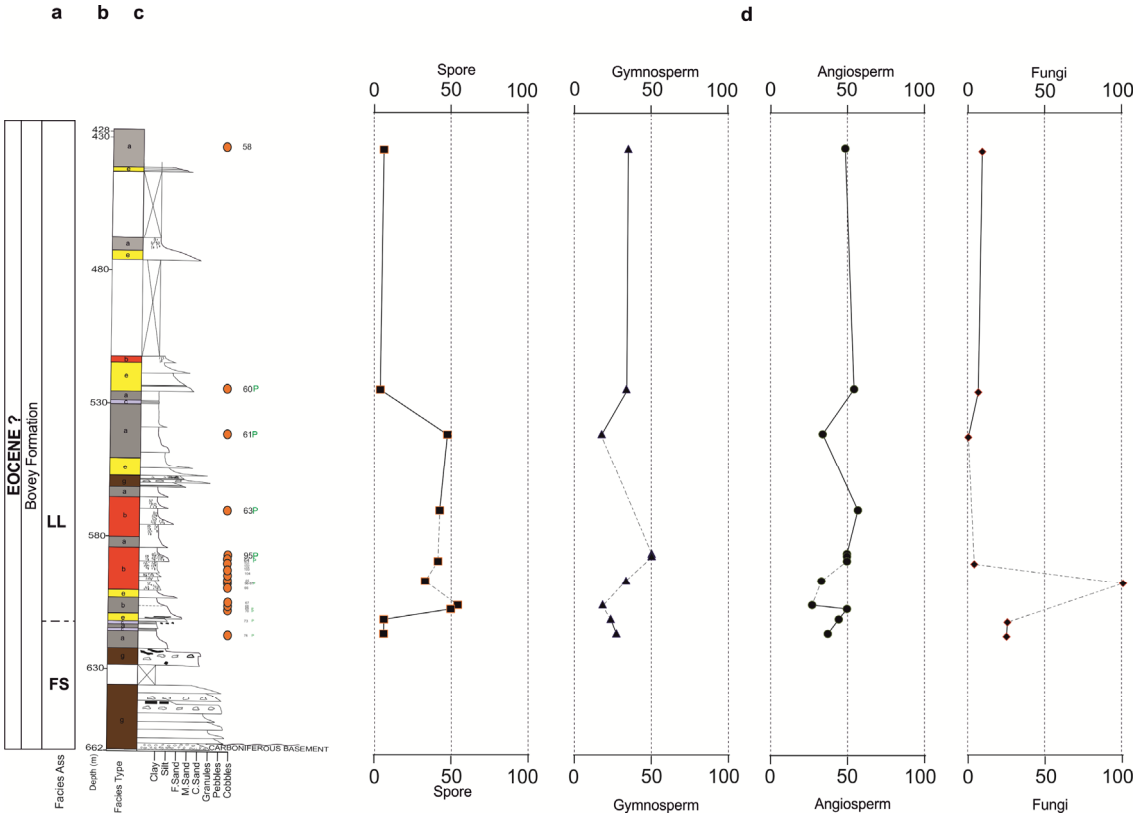

Figure 4.7: Palynomorphs from Bovey Formation, Petrockstowe 1B core, Petrockstowe Basin, Southwest, United Kingdom.

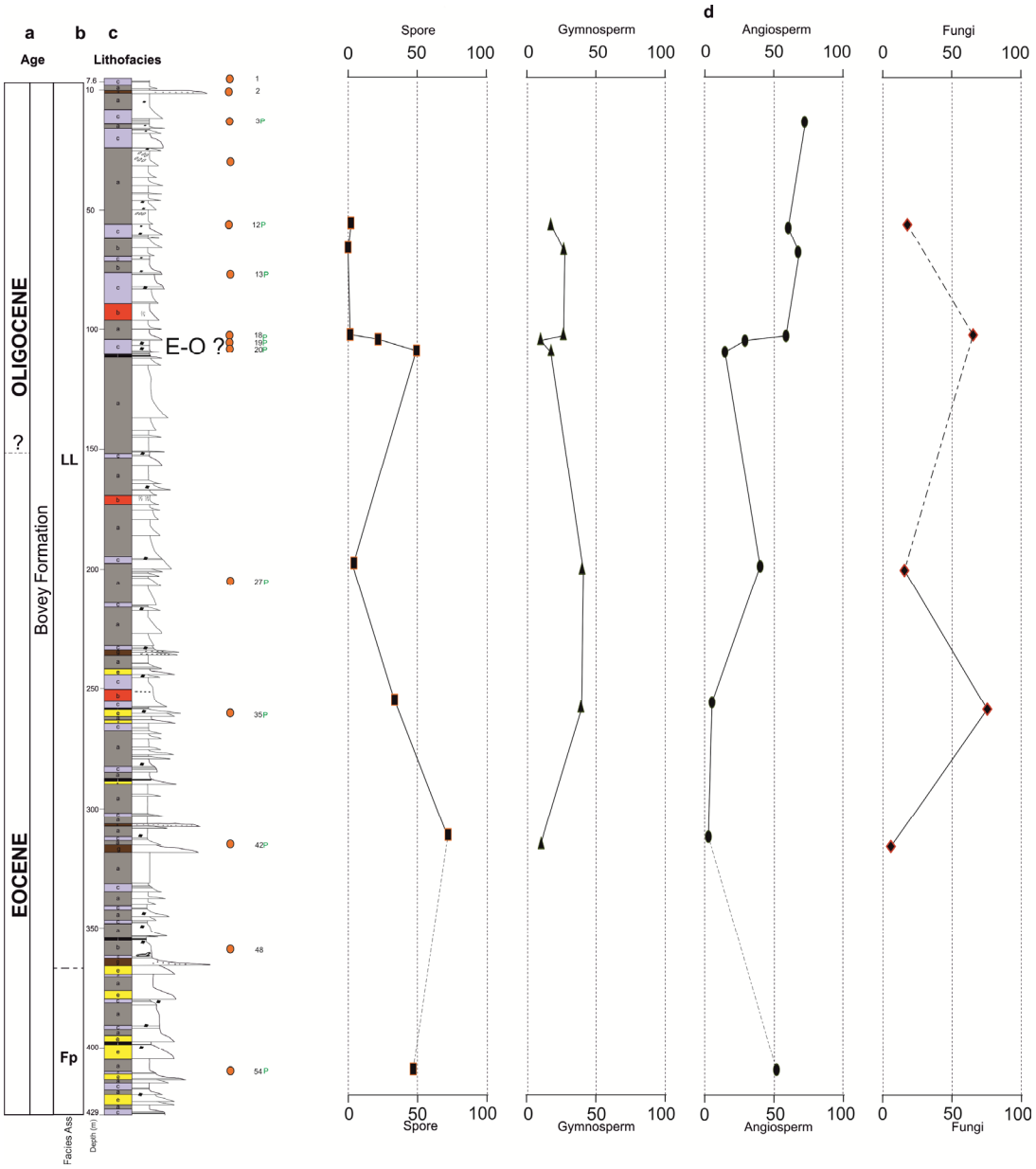

Figure 4.8: Palynomorphs from Bovey Formation, Petrockstowe 1A core, Petrockstowe Basin, Southwest, United Kingdom.

Monocolpopollenites spp. (Plate 6, F3) has its first occurrence in the core in sample MC76 at 616 m with 23% sparse abundance decreasing to 18% at 605 m. Between 603 m – 587 m it was not observed. It becomes common with an abundance of 30% at around 575 m and with16% recorded at 523 m, moving upwards the abundance becomes common reaching 47% and decreases to 14% at a depth of 116 m (Figures 4.7 – 4.8). In the South John Acres Lane Quarry section *Monocolpopopollenites* spp. has its first occurrence in sample SJAL005 with an abundance of 50%. Then there are two different breaks as a result of barren samples

and its re-occurrence yields very rare abundance of 4%. This cyclic manner of occurrence, no occurrence and barren samples repeats itself a number of times before becoming sparsely distributed (6 – 24%) covering the interval 5.3 m – 47.7 m (Figure 4.7). Wilkinson (1979) reported that *Monocolpopollenites* spp. and *Arecipites* spp. are considered to have characteristics of palm pollen, which when compared to distribution maps of modern flora, suggests that the climate at the time of its deposition was frost-free.

Tricolporopollenites spp., occurs for the first time in sample MC76 at 616 m in the core sparsely (27%) and increases to common abundance 47% after 588 m it shows a rapid increase to abundant distribution (50%) at 585 m. Thereafter the percentage fluctuates between very rare to common (2 – 46%) up to the point of its last occurrence at 65 m. In the section *Tricolporopollenites* spp. has its first occurrence in sample SJAL008 sparsely with 19% abundance and no occurrence within the barren part of the section. After the barren region, it re-occurs with very rare to sparse distribution (3 – 15%) from 7.7 m to 13.4 m. Its next appearance is in sample SJAL027 with a 13% abundance, which increases to common abundance (20%) at 17.6 m, which then forms the highest level of its occurrence. Subsequently values decline while in some parts no occurrence is recorded towards the upper part of the section as seen in samples SJAL-37, 040-041, and 045-048. Finally, the last occurrence of about 5% was at the top of the section in sample SJAL065. *Tricolporopollenites* spp. is another species with a similar trend of abundance like *Plicapollis* spp., but is not as abundant as *Plicapollis* spp.

Triletes spp. (Plate 5 - E3; Plate 3 – C4 & C6; Plate 4 – D4) is an angiosperm species, unlike the previous species, has its first occurrence in sample MC61 at a depth of 540 m in the core with sparse abundance of 14% which then decreases to very rare 1% at 257 m. At 116 m the abundance is rare to sparse 10% and in the upper part of the core the abundance declines to very rare 1% at around 109 m. A re-occurrence of this taxon is observed at the top of the core with 18% sparsely abundant. In the John Acres Lane Quarry section *Triletes* spp. had

its only occurrence in sample SJAL003 with a sparse abundance of 24% mainly found at the bottom of the section.

Salixpollenites spp. has its first occurrence in sample MC73 at 610 m at 2% to reach a maximum of 4% at around 431 m. The last occurrence was noted in sample MC13 at 75 m (Figure 4.8). Similarly, in the South John Acres Lane Quarry section *Salixpollenites* spp. first occurred in sample SJAL019 with 2% abundance and its last occurrence of 1% at most. Generally, this taxon has a very rare to sparse distribution in the two sections.

Tiliaepollenites spp. (Plate 3, C5) is another angiosperm species that generally has a very variable occurrence in the entire core length, with the first occurrence observed in sample MC72 which is very rare to rare abundance of 2% and 9% in sample MC68 over a depth of 616 – 605 m. The subsequent occurrence is in sample MC60 with an abundance of 2.5%. There is another break in the abundance of this species between 431 – 257 m with the appearance in sample MC27, and it continues to oscillate between rarely and very rare i.e. 10% and <2% up to the top of the core. At 116 m depth of the core, there is a change from low abundance to massive abundance, corresponding to the 120 m depth of palynological change as earlier noted by Turner (1979) (Figure 4.8). Unlike in the core, in the South John Acres Lane Quarry section, the distribution has no specific trend for this taxa *Tiliaepollenites* spp., it shows a very rare abundance of <4% just before the top of the section at around 35.8 – 47.7 m.

Cicatricosisporites spp. (which has an affinity to Schizaeaceae, Anemia/Mohria) has its first occurrence in sample MC68 at 605 m with a 9% rare to sparse abundance covering 603 – 569 m of the core depth. Thereafter it becomes abundant 61% in sample MC42 and eventually decreases to very rare <3% at 116 m which marks its last occurrence in the core. *Cicatricosisporites* spp. is only dominant over a short interval in the core. Unlike in the core *Cicatricosisporites* spp. has its first occurrence in sample SJAL019, with a common abundance of 41%. It then ceases to occur until the middle part of the section recording a

10% sparse distribution in sample SJAL037. An increase to 20% was observed then it declines to 6% at 31.3m, to the point of last occurrence in sample SJAL056 with 17% sparse abundance at 38.1 m recorded. This species stratigraphically has a long age range occurring from Cretaceous to Oligocene (Wilkinson *et al.* 1980, Boulter & Manum 1996, Rull 2003), therefore it cannot be used to constrain the age of these sediments, but rather it is a broad age range indicator. For instance, Collinson (1996), Sweet *et al*. (1999) and Collinson *et al*. (2003) have shown that *Cicatricosisporites* spp. spores were found in abundance in Cobham Lignite, which are comparable to fern spore abundances considered as "fern spikes" or "fern spore abundance" that marked the Cretaceous – Palaeogene (K/Pg) boundary. The abundance of the *Cicatricosisporites* spp. fern spore suggests the ease with which spore bearing plants adjusted in the course of colonising the disturbed terrains as it was a peculiar feature of the Cobham Lignite Bed. The appearance of *Cicatricosisporites* spp. in both the Petrockstowe and Bovey Basins could probably suggest reworking due to degradation of the species.

Stereisporites spp. 2 – 18%, *Cingulatisporites* spp. <3%, *Monolete* spp. 50%, *Pityosporites* spp. 0.3 – 1% and *Tetraporopollenites* spp. 1% all have their first and last occurrence in the pre CIE region identified in the core 1B, lower Petrockstowe Basin with the exception of *Polypodiaceoisporites* spp. 29%, which has it first and last occurrence in the post CIE region. In the South John Acres Lane Quarry section *Stereisporites* spp. has its first occurrence in sample SJAL019 with an abundance of 2% and last occurrence in sample SJAL065 with an abundance of 1%. In between the first and the last occurrence all other occurrences were <2%.

Fungi/algae is another group of palynomorphs studied in the cores, with their respective abundance seemingly common between 616 – 430 m and absent from 430 m to the top of the core with its last occurrence at around 8m.

The remaining pollen was only encountered in the South John Acres Lane Quarry section, Bovey Basin. *Porocolpopollenites* spp. has its occurrence in sample SJAL018 and last occurrence in sample SJAL020 which are 6% and 4% respectively.

Plicapollis spp. is an angiosperm is recorded only in the South John Acres Lane Quarry section with first occurrence in sample SJAL014 with 64% abundance and shows a stepwise decrease through 14% and 38% down to 2%. Thereafter, the samples are barren between 13.9 m – 15.8 m followed by 7% abundance in sample SAJL027, and then increased to 60%. The trend in the distribution of *Plicapollis* spp. in the section shows two major peaks occurring at 7.7 m and 18.7 m (Figure 4.9).

Pompeckjoidaepollenites spp. is an angiosperm pollen and is among the important key Eocene indicators Wilkinson (1979) which occurs in the Bovey Basin at a depth of ~ 290 m. In this present study its first occurrence is recorded in sample SJAL016 8.6 m with 9% occurrence, which increases upward towards the middle of the section to about 27% and thereafter gradually decreases to the point of its last occurrence, which is 1% at 45.7 m sample SJAL067, corresponding to the top of the section.

Cycadopites spp. is an angiosperm pollen which first occurs in sample SJAL040 with 9% abundance and the last occurrence in sample SJAL067 with 2% abundance. Most of the occurrences of this species are found in the upper part of the section.
Minorpollis spp. first occurred in sample SJAL021 with an abundance of 6% which increases to 17% in the middle of the section and began to decrease to the point of its last occurrence in sample SJAL060 with 3% abundance at around 38.9 m. Between 28.9 m to 35.8 m interval of the section, *Minorpollis* spp not has been observed.

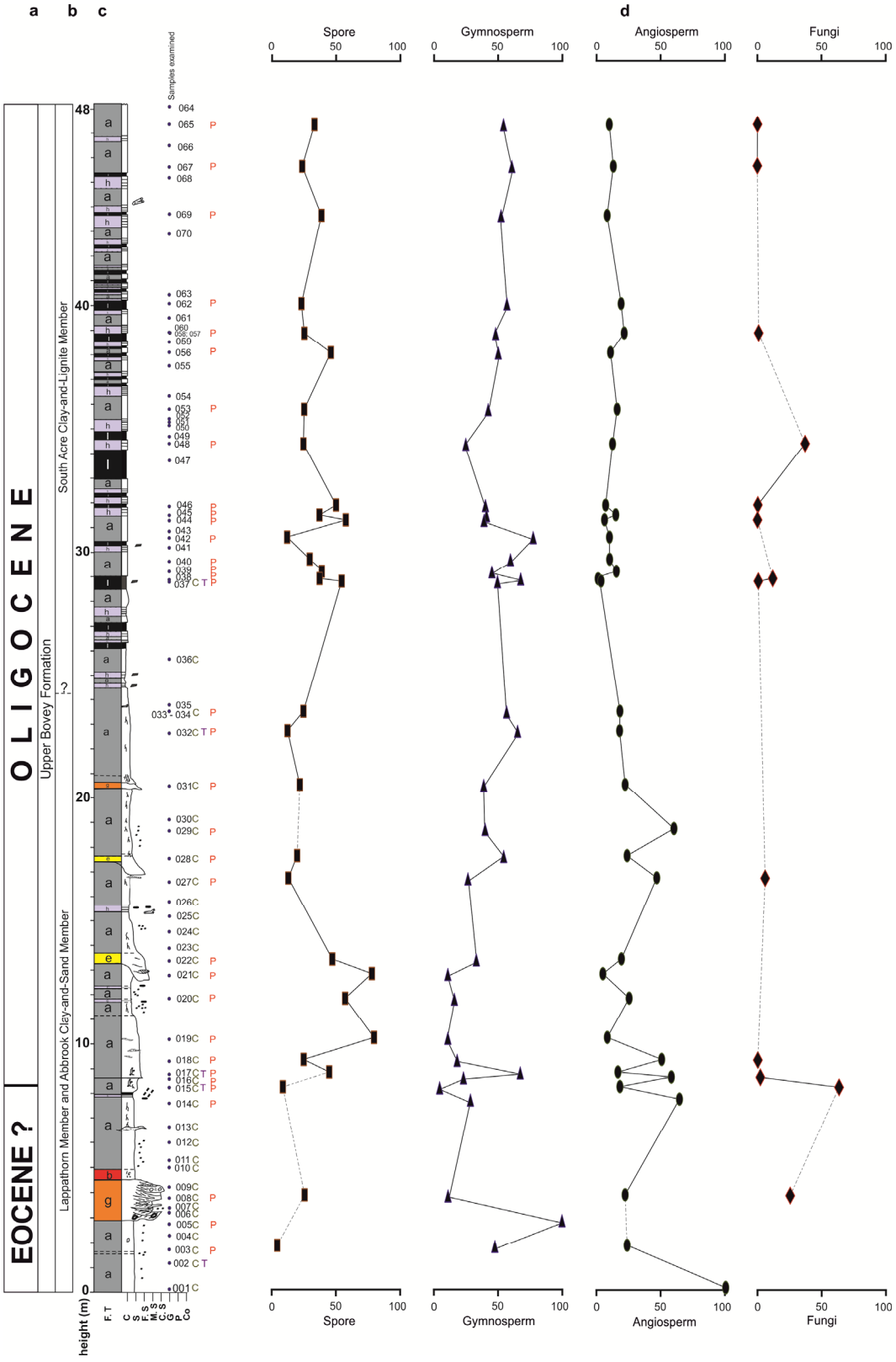

Figure 4.9: Palynomorphs from Bovey Formation, South John Acres Lane Quarry section, Bovey Basin, Southwest, United Kingdom.

4.4 QUANTITATIVE ANALYSIS OF PALYNOLOGICAL DATA

In order to determine the significance of species that tend to co-occur in samples and which group together samples of similar taxonomic composition, Hierarchial Agglomerative Clustering (CLUSTER analysis) was applied to the data generated for both the Petrockstowe and Bovey Basins. Again, similarity percentage analysis (SIMPER) Clark and Warwick (1994) was carried out to determine which species were responsible for similarity within group of samples. Diversity indices and CLUSTER analysis were performed with (PAST) software (Hammer *et al.* 2001). The technique is a permutation test of a null hypothesis for a specified set of samples which are not in a priori divided into groups, and are not different from each other in the multivariate structure. With this particular set of data, 1000 runs of permutations were used to calculate a mean profile with 999 simulated profiles, and the significance level of choice considered was 5%. Subsequently, the resulting clusters of samples were analysed through similarity within the groups (details of SIMPER methods are contained in Clarke 1993). The expectation of this analysis is for the species to be identified as typifying each group to be:

1. Those that occur at a consistent abundance in each sample within the group, so that the deviation of their contribution (SD) is low
2. Those where the ratio between the average similarity within the group (Similarity) and SD is low.

This method as employed enabled the identification of groups of samples that contain a similar suite of taxa in similar proportions and more so to identify their characteristic species.

Appendixes 3 - 9 shows the result of the Cluster analysis and similarity profile test which did not prove to be statistically significant, therefore the results of this analysis did not prove to be significant with respect to palaeoecological reconstruction. The lack of statistically significant Cluster analysis and similarity profile results could suggest the possibility of two scenarios associated to the reconstruction of the palaeoecology in the study area, either the original assemblage has been altered due to diagenesis or there was no existence of

relationship originally between groups of the samples in the first place. Alternatively, it might be as a result of switching over from one facies association succession to the other.

4.5 AGE MODEL

4.5.1 Is PETM preserved in the lower Petrockstowe Basin?

A change in spore/pollen assemblages in a terrestrial realm reflects changes in palaeovegetation, albeit processes like transportation, preservation and sedimentation can have an effect (Tyson 1995, Traverse 1988). A comparison of the microflora assemblages of the Cobham Lignite and the lower Petrockstowe sediments shows little notable changes with the exception of the 'blocky lignite' strata that are probably more diverse due to generic lumping of the taxa in palynomorph assemblages in the Cobham Lignite the (Collinson *et al.* 2009).

The Cobham Lignite lithology is characterised by the abundance of unique taxa like *Pentapollenites*, *Pistillipollenites*, *Liliacidites*, which are present in the CIE however these taxa are absent in the Petrockstowe Basin. Very rare *Tricolpates* and *Polycolpates* occur in both Cobham Lignite and Petrockstowe Basin (Tables 4.3.5 – 4.3.78, Appendix 2).

The pre-boundary (Palaeocene) succession at Cobham is typified by a significant number of *Tricolpopollenites* (only abundant in the basal clay), *Pentapollenites* (entire pre-PETM and disappears above laminated clay shortly after PETM), *Cicatricosisporites* (high occurrence before the PETM, and is related to the distribution of charcoal) (see Figures 4.10).

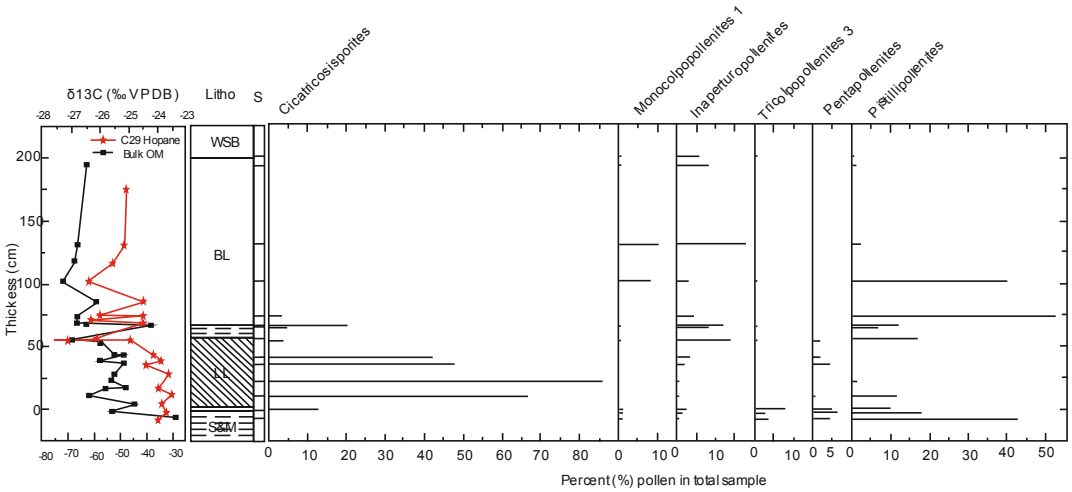

Figure 4.10: Pollen diagram showing the distribution and abundance of some taxa through the Cobham Lignite Bed demonstrating the CIE using the carbon isotopes and the sample that defined the PETM (Collinson *et al*. 2009).

In comparison, the Cobham Lignite rare taxa pollen are diverse and somewhat different to the rare taxa from the lower Petrockstowe cores. There are only few elements occurring in both areas (*Monocolpopollenites* Fig. 5C, *Inaperturopollenites* Fig. 5F – I, *Laevigatisporites* Fig. 6A, Trilete Fig. 6E, Bisaccate conifer pollen Fig. 6I, *Monocolpopollenites* Fig. 6R, *Tricolporopollenites* Fig. 8HH and are found in Collinson *et al.* 2009).

Terrestrial palynoflora from the northern Tethyan realm at St. Pankraz, Austria, (Hofmann *et al.* 2011) can be distinguished from lower Petrockstowe by the lack of and low presence of Cupressaceae/Taxodiaceae (these are related to pollen of coniferous trees e.g. Bisaccate grains and Inaperturate grains). According to Hofmann et al. (2011) the rareness of the Taxodiaceae at St. Pankraz can be related to the swampy habitats that were not present in the vicinity of the depositional site.

Tricolpoporopollenites spp. has significant occurrences in the Petrockstowe sediments (50%). This taxa is a key species that is normally found in mesothermal to temperate taxa

within Lower Eocene strata, and is comparable to the occurrence of *Tricoloporopollenites* Macrodurensis (Vitaceae), *T.krushi* (Nyssa like), *T.edmundi* (Mastixiaceae) and *Sparganiaceaepollenites* reticulatus (Sparganiaceae) to have occurred at St. Pankraz, Austria signifying Lower Eocene age (Hofmann *et al.* 2011).

Therefore, due to the strong similarity of the palynofloral data of this present study and the Krappfield section (Hofmann *et al.* 2011), leads to the conclusion that the present data-set in conjunction with the magnitude of the carbon isotope excursion places it more appropriately at the EMT2. This could represent a much warmer and humid climate. Many taxa from the palynological sample of the lower Petrockstowe core 1A analysed, comprised of fern spores (*Polypodiaceae*, *Normalpolleplicatopollis*, *Pompeckjadeopollenits*) and high diversity megathermal elements, for example palm pollen types *Tricolpoporopollenites*, *Monocolpopollenites*, *Inaperturopollenites*, monocots.

How does this fit with the change during the PETM in terms of vegetation and environment as observed by Wing *et al*. (2005); Harrington and Jaramillo (2007) in the Northern and Southern hemisphere? There is similarity between the ETM2-H2 recorded from the palaeosol carbonate in the Upper Deer (characterised by two negative carbon isotope excursions of -3.8‰ and -2.9‰) and Gilmore Hill sections (characterised by one negative carbon isotope excursion of -2.7‰) in the Bighorn Basin (Abels *et al.* 2012) with the results obtained from the lower Petrockstowe core which is found within the red mottled clay with a -2.0‰ CIE

In the lower Petrockstowe section, *Pentapollenites* and *Pistillipollenites* are absent in pre-CIE. Taxa like *Cicatricosisporites*, *Monocolopopollenites*, *Inaperturopollenites* and *Tricolpopollenites* all occurred in pre-CIE. Contrary to the high occurrence of *Monocolpopollenites*, *Inaperturopollenites* showing high percentage in the PETM in Cobham lignite, *Monocolpopollenites*, *Inaperturopollenites* are absent in the CIE of the

lower Petrockstowe Basin but, *Inaperturopollenites* appeared to be of high percentage post CIE and *Monocolpopollenites* has high percentage of distribution all through the section. *Tricolpopollenites* has significant abundance during and after CIE with much abundance post CIE. *Cicatricosisporites* also, becomes dominant in post CIE but mainly in sample MC42 with 61% abundance. Other elements occurring in the lower Petrockstowe Basin during the CIE are Triletes which appeared during and after the CIE, and then tend to decreased towards the middle part of the section. *Laevigatisporites*, *Stereisporites*, Tricolpate, *Pompeckjoidaepollenites*, *Plicapollis pseudopollenites*, Bisaccates and Monolets all occurred during the CIE of the Petrockstowe Basin.

It is very important to stress that despite the similarity of taxa like *Tricolpopollenites*, *Inaperturopollenites*, *Monocolpopollenites* occurring in both Petrockstowe and Cobham Lignite bed, the absence of key taxa *Pistillipollenites* and *Pentapollenites* in the Petrockstowe Basin does not qualify the section to be assigned to the PETM. But, this observation is consistent with the views of Sluijs *et al*. (2009) which stated that "ETM2 and PETM shared qualitatively similar climate response on land and in shallow deep oceans". While in Cobham Lignite there is the disappearance of *Cicatricosisporites*, *Tricolpopollenites* and *Pentapollenites* after the pre-CIE in the lower Petrockstowe section these taxa are seen all through the section.

Generally, it is observed that the onset of boundary and synboundary succession are characterised by Taxadiaceous swamp vegetation containing related elements (Collinson *et al.* 2009).

4.5.2 Is the Eocene - Oligocene boundary preserved in the Bovey and Petrockstowe basins?

Chandler (1957), Wilkinson and Boulter (1981) and Edwards (1976) all agreed that Eocene - Oligocene strata exist in the Bovey Basin but the degree of certainty relating to the age remains unconfirmed. In order to fill the gap in the dating of these sediments, a palynological analysis was conducted. Emphasis is placed in comparing the results obtained

in the present study with those of previous authors and similar related studies in Europe and possibly global sections.

The pollen and spores preserved in the South John Acres Lane Quarry section of the Bovey Basin sediments offer a unique opportunity for a glimpse of mid latitude flora that suggests an Oligocene or middle Oligocene age. The key pollen and spores that were identified in the area which are either sparse or common include: *Arecipites*, *Inaperturopollenites*, *Monocolpopollenites*, *Tricoloporopollenites*, *Cicatricosisporites*, *Sequoiapollenites,* and *Pompeckjodaepollenites*. *Inaperturopollenites* belongs to smaller conifer pollen, that is similar to that produced from modern Taxodium (swamp taxa) and are usually deposited near to the place of growth (Wilkinson *et al.* 1980). *Inaperturopollenites* is one of the conifer pollen that is abundant with good preservation both dark to light brown, which suggests a warm and swampy environment that led to the formation of peats (Teichmüller & Teichmüller 1968). *Arecipites* is a palm pollen with affinity of tropical to sub-tropical forms could suggest that the climate at the time of their deposition was almost frost free. When compared to modern distribution maps *Monocolpollenites* has a tropical to sub-tropical source. Wilkinson *et al*. (1980) in their study of Washing Bay in the Lough Neagh Clays, Northern Ireland, documented that the occurrence of key Oligocene taxa for example *Polypodiaceaesporites*, *Pityosporites*, *Inaperturopolenites*, *Arecipites*, *Monocolopopollenites*, *Tricolporopollenites*, *Tricolpopollenites*, and *Polyvestibulopollenites* . All of these taxa were recorded from sparse to abundant occurrence in the South John Acres Lane Quarry section, Bovey Basin, strongly suggesting that the sediments were deposited in the Oligocene. In another related study Boulter and Manun (1996) documented palynological evidence from site 908, Hovgard Ridge, in Greenland which had the following suite of assemblages (*Gleichniidites*, *Lycopodium*, *Polypodiaceaesporites*, *Sequoiapollenites*, *Inaperturopollenites*, *Sciadopityspollenites*, *Tsugaepollenites*, *Piceapollenites*, *Pityospoirtes*, *Polyporopollenites*, *Juglandspollenites*, *Alnipollenites*) which are similar to the assemblages (*Arecipites*, *Inaperturopollenites*, *Monocolpopollenites*,

Tricoloporopollenites, *Cicatricosisporites*, *Sequoiapollenites*, *Pompeckjodaepollenites*) from this current work.

To this end, the deductions presented here are based on comparison with literature from earlier works conducted in some parts of the Bovey Basin, Mochras, and Lough Neagh in Northern Ireland. Table 6.3.1 shows the abundance count data from the South John Acres Lane Quarry section of the Bovey Basin and when these results are correlated to those of Palaeogene assemblages from other European sections, (e.g., Belgium, (Gorin 1975) and France, (Chateauneuf 1972) there are similarities in floral composition and palaeoecology. According to Kotthoff *et al*.(2014), swamp vegetation was widespread during the Eocene to the early Oligocene with less significant palaeobotanical changes from this set of assemblages. Hence, based on these similarities and the present data set, it would strongly suggest these sediments are of Oligocene to middle Oligocene age.

In comparing the pollen/spore assemblages in the Bovey Basin with the pollen and spore assemblages that are well preserved in the Petrockstowe Basin, the following suite of assemblages (*Arecipites*, *Tricolporopollenites*, *Tiliaepollenites*, *Triletes*, *Pompeckjodaepollenites* and Bisaccates) are common to both basins. Importantly, the only minor difference between the suite of assemblages in the upper Petrockstowe Basin and the previously discussed spore and pollen assemblages in the Bovey Basin is the occurrence of *Tiliaepollenites*, *Triletes* and Bisaccate pollen.

Tricolporopollenites is a pollen type from trees and herbs with broad affinity and coincidently it blooms towards the upper part of the Petrockstowe core. Boulter (1980) described *Tricolporopollenites ipilensis* to have occurred from Neogene of Europe as well as Palaeogene and was considered to be of special significance for representing a low temperature zone in the upper Oligocene, where it was found to be abundant. The occurrence of this taxa as one of the key elements in the upper Petrockstowe core, strongly suggest Oligocene age.

Furthermore, *Tiliaepollenites* has shown similar trend in the upper part of the Petrockstowe core and is considered a key pollen taxon of the Oligocene strata in Europe, for example *Tiliaepollenites insculptus* (Mai 1976). Likewise, Bisaccate conifer pollen showed an increase in abundance, but because they are known to be easily transported by wind and water, their value for drawing palaeoenvironmental conclusions is restricted. The association of fern-conifer is a key feature of palynological assemblages and this can be compared to similar assemblages observed in the Headon sediments of the Hampshire basin (Collinson *et al.* 1981). The Headon sediments are well calibrated Palaeogene sediments.

Although, there is no significant palynoforal shift in the two studied sections, earlier studies by Machin (1971) documented similar findings with no sharp breaks in the transition to cooler floras, gradual loss of warm/tropical plants with rich species as evident in the Isle of Wight Palaeogene microfossils. Furthermore, Roche & Schuler (1976) emphasised the presence of *Caryapollenites simplex*, *Bifaciatisporites spp* and *Retitriletes franforttensis* in a Belgium section to support the EOT. On the basis of previous results and the current data from the two section, it is strongly suggested that the Eocene – Oligocene boundary is preserved in the Bovey and Petrockstowe basins.

4.6 PALAEOENVIRONMENTAL INTERPRETATION

The aim of this section is to discuss how the palynofacies are related to the lithofacies in the two basins and possibly to generate information on the prevailing environmental conditions during the deposition of the sediments.

4.6.1 Petrockstowe Basin

Often, fine grained sediments host large quantities of organic matter provided they were deposited in essentially anoxic conditions (Batten 1982). Organic rich beds are common in the lower Petrockstowe succession, corresponding to palynofacies zone A, which contains

siltstones and clays and which yielded good quantities of palynomorphs. A good example is the phytoclast group which has a high percentage of up to 95%, while other palynofacies groups palynomorphs 50%, AOM <10%, were sparsely observed, reflecting deposition in distal settings with low yield of organic matter. The bulk of the associated phytoclast or 'woody material' suggests that deposition occurred in an oxidising environment. Contrary to the abundance of phytoclasts in the interval (585 – 575 m), the palynomorphs, AOM, were less. Among the pollen and spores recorded in this zone, although less abundant, include: *Laevigatisporites*, *Mocolpate*, *Cicatricosisporites*, *Plicapollis*, *Stereisporites* and Bisaccate pollen, which is floating pollen and is usually pollinated by wind and water, suggesting a regional element not local.

Palynofacies zone B, is characterised by high percentage of palynomorphs (80%), followed by <10% each of AOM and phytoclast, translucent and fungi. From the boundary of palynofacies zone A to B.

In the upper part of the section corresponding to palynofacies zone C and D, AOM and palynomorphs dominate the distribution of the palynofacies which could indicate restricted circulation of water (Tyson *et al.* 1979) signifying that there is restricted water circulation rather than productivity, which may serve as the controlling factor for the organic rich sediment accumulation in a depositional environment. Also, the percentage ratio of palynomorphs to AOM, could suggest diverse source of areas of the organic matter (Martín-Closas *et al.* 2005). Evidence from the microscope work tends to prove that phytoclasts were dominated by the non-opaque degraded type, which could suggest to some extent pre- and syn-depositional alteration, related, for instance, to sub-aerial oxidation due to water column fluctuation and transport (Tyson 1995, Mendonça Filho *et al.* 2012).

4.6.2 Bovey Basin

Palynofacies zone I shows a high abundance of AOM components, together with low percentage of palynomorphs, which indicates a low energy environment after a period of high fluvial flow with the deposition of phytoclasts. The AOM group could also be associated with the TOC content of the sediments, and the highest TOC content recorded in this zone is 1.8 wt.%. Therefore, it probably indicates a suspension water environment. This interpretation is consistent with the results of Mendonca Filho *et al*. (2010) from Oligocene lacustrine system in the Cenozoic Taubate Basin, Brazil. In a related studies Batten & Stead (2005) showed that there was a typical association of *Botryococcus* with non-marine AOM in the English Channel, offshore UK.

In palynofacies zones J and K, the phytoclast and AOM groups showed a decreasing trend while the palynomorphs increases, and with breaks in places which suggests a strong terrestrial influx and deposition near active fluvio-deltaic systems (Tyson 1995).

Palynofacies zones L and M shows the palynomorph group to be >60% with high occurrence of pollen and spores like *Laevigatisporites*, *Inaperturopollenites*, *Monocolpopollenites* and *Sequoiapollenites* with most of them being dark to light brown. Also, there is presence of algae, specifically fresh water types like *Botryococcus* in this zone. This tends to suggest a lake environment (possibly tropical to sub-tropical) with low salinity that is stable ((Tyson 1995). Also, Tiercelin (2009) found that *Botryococcus* was among the abundant phytoplankton remains seen in the sample of the lacustrine facies of the Cenozoic rift basin of East Africa. Hence, this is evidence to show that the depositional environment under review is a lake.

In addition, this zone possibly suggests deposition in a suspension water body environment, with reducing conditions. Therefore, the organic material might have experienced a slow process of organic decomposition, which is highly connected to swampy environment (peat forming) as result of high turnover of terrestrial matter. The presence of *Laevigatisporites*,

Inaperturopollenites, *Monocolpopollenites* and *Sequoiapollenites* could suggest deposition in a humid climate and as characteristic of proximal depositional environment.

In a similar analogy, palynofacies zone M, which has a low percentage of AOM and phytoclasts respectively could indicate a non-turbulent water regime. This also suggests strongly that the environment of deposition is terrestrial and proximal to the source area. This interpretation is in agreement with an ephemeral lake or marginal lake as contained in section 3.3.2.

4.6.3 $\delta^{13}C_{TOC}$ versus palynofacies relationship in the Petrockstowe Basin

From the results of $\delta^{13}C_{TOC}$ and palynofacies analyses, as presented in Figure 4.4, the most dominant palynofacies group corresponding to the CIE in the lower part of Petrockstowe core is the phytoclasts. The AOM and palynomorphs groups were less abundant. At the pre-excursion stage phytoclasts had a high abundance of almost 80%, which then dropped to 40% at the onset of the CIE. During the CIE it increased again and reached a maximum abundance of 95%. The characteristics shown by the phytoclast group is not directly proportional to the $\delta^{13}C_{TOC}$ values of the sediments, suggesting that the source of the $\delta^{13}C_{TOC}$ carbon might be atmospheric. This is further evidenced by the distribution of the palynofacies group within the body of the CIE, which is consistent, corresponding to the upper part of palynofacies Zone A. When considering the upper part of the Petrockstowe core, the $\delta^{13}C_{TOC}$ values show wide variability with no significant negative isotope shifts. In some horizons, depth intervals of 360 − 350 m, 265 − 245 m and 55 − 8 m, $\delta^{13}C_{TOC}$ values correspond to variation in the grain size of the sediments (fine sand to medium sand, clay to medium to coarse sand and silty clay to clay to coarse sand) and the $\delta^{13}C$ values might therefore be related the carbon contents source of the sediments. Between the depth range of 360 − 350 m, there was no palynofacies change encountered while the horizons between 265 − 245 m and 55 −8 m all the palynofacies groups have a consistent distribution (Figures 4.4 & 4.5), which suggest that the negative isotope shifts seen in these horizons has no direct

relationship to the sources of its carbon. In palynofacies zone C and D, the abundance of the palynofacies group has also been consistent with the natural variability of the $\delta^{13}C_{TOC}$ values but, at ~120 m there was a significant $\delta^{13}C_{TOC}$ shift away from the mean -26.0‰ to -27.5‰ and this isotopic shift corresponds to a change in the abundance/distribution of the palynofacies group with a switched over from 20% to 40% Amorphous group, 50% to 40% Palynomorphs group and 10% to 40% phytoclasts group. This sudden change in the abundance of the palynofacies groups and the shift in $\delta^{13}C_{TOC}$ corresponds to the suggested Eocene – Oligocene boundary of Turner (1979), which is consistent with current findings.

4.6.4 $\delta^{13}C_{TOC}$ versus palynofacies relationship in the Bovey Basin

Lithofacies interpretations were discussed in sections 3.3 – 3.5, which serve as the primary tool in identifying the depositional conditions under which these sediments were deposited, while the palynofacies is a secondary tool, as the palynological samples were from the fine grained silty clay facies which were more likely to host the preserved organic matter. These sediments usually contained dispersed organic matter which are either transported or produced in-situ. The results of the $\delta^{13}C_{TOC}$ analysis for the South John Acres Lane Quarry section presented in section 5.3.2 have a mean value of -26‰ with three cyclical shifts (Figure 4.6), which could possibly reflect a change in sediment source. The beginning of the carbon isotope shift starts with coarse grained particles, which correspond to a higher distribution of AOM, which then decreases with an increase in the phytoclast ratio within the finer particles, while the palynomorphs remains abundant as the lithofacies changes to clay/lignitic clay towards the upper part of the section. Palynofacies zones “I”, “J”, and “K” are occurring within the Lappathorn Member and Abbrook-Clay-and-Sand Member of the Upper Bovey Formation which has all three cycles related to the changes in $\delta^{13}C_{TOC}$ and grain size, while zones “L” and “M” occurred within the South Acre Clay-and-Lignite Member which has a more or less natural variability of $\delta^{13}C_{TOC}$ values with the exception of one data point (-22.0‰). At this horizon the AOM shows a significant decrease, palynomorphs increase, while phytoclasts remain fairly constant for some meters. This could

be related to local palaeohydrological changes which controlled diagenesis of the autochthonous terrestrial fraction. When water levels are low, it favours biodegradation of phytoclasts because the formation of AOM particles involves aerobic process (Sebag *et al.* 2006). In summary, the $\delta^{13}C_{TOC}$ values in this part of the Bovey Basin appear to be positively skewed towards the coarse grained particles of the sediments while the more negative $\delta^{13}C_{TOC}$ values are found within the finer particles. In other words in the Bovey Basin the $\delta^{13}C_{TOC}$ could be suggested to be controlled by the grain size of the sediments.

CHAPTER 5 –TOTAL ORGANIC CARBON (%TOC) AND STABLE CARBON ISOTOPE ($\delta^{13}C_{TOC}$)

5.1 INTRODUCTION

The Palaeogene (~65 – 23 Ma) (which consists of the Palaeocene, Eocene and Oligocene epochs) is a period of major climatic reorganization and understanding the temperature changes that occurred during this time period, especially those that occurred in the continental record is of great importance. The early Palaeogene is characterised by a series of short lived hyperthermal or transient periods of warming, with high sea levels and the lack of significant polar ice and profound shifts in biotic communities (Zachos *et al.* 2008, Zeebe *et al.* 2009, McInerney & Wing 2011). It has been suggested that these hyperthermal events may serve as one of the best analogues for a future warmer world. The most prominent of these events is the Palaeocene Eocene Thermal Maximum (PETM) (~55.5 Ma) which is characterised by a 5 – 8 ^{o}C temperature increase, and a 3 – 5 ‰ negative carbon isotope excursion (CIE). After the PETM the Eocene Thermal Maximum 2 (ETM-2) event (~53.5 Ma) is the next most prominent hyperthermal event in the Palaeogene and is characterised by a CIE of >1.5‰ (Lourens *et al.* 2005). Both of these events are considered to be associated with the geologically rapid injection of $\delta^{13}C$ depleted carbon to the ocean – atmosphere system (Zachos *et al.* 2005, Lourens *et al.* 2005, Nicolo *et al.* 2007, Littler *et al.* 2014). The ETM-2 event is further followed by the smaller H2 event, around 100 thousand years later (Cramer *et al.* 2003, Lourens *et al.* 2005, Abels *et al.* 2012).

The only available evidence for ETM-2 surface warming available are those from the subtropical south eastern Atlantic ocean with an ~0.8‰ negative oxygen isotope excursion in calcite of surface dwelling foraminifera interpreted as being caused by a ~ 3^{o}C warming (Lourens *et al.* 2005). In the upper Deer Creek (UDC) and Gilmore Hill (GH) sections of the Bighorn Basin, Wyoming the ETM-2 event is characterised by two negative $\delta^{13}C_{pc}$

excursions; the former of between – 3.8‰ and – 2.9‰ and the latter of – 2.7‰ in the GH section (Abels *et al.* 2012).

The exact age of the Bovey Formation sediments in the Petrockstowe Basin remains controversial; Turner (1979) assigned an Eocene – Oligocene age to the upper part of the formation and believes that much older sediments could be encountered in the deeper part of the basin.

In this study, chemostratigraphy ($\delta^{13}C_{TOC}$) was used to re-evaluate the age of these sediments, to see if these sedimentation extend back into Palaeocene. This is the first time a high resolution $\delta^{13}C_{TOC}$ record across the Petrockstowe cores 1A and 1B and South John Acres Lane Quarry section have been generated to ascertain if there are any CIE's in these sections. This will be used to propose an age model to link the CIEs of these basins to the hyperthermal events (PETM, ETM-2) the CIEs would be associated within the basins.

5.2 Percentage Total Organic Carbon (%TOC)

5.2.1 *Petrockstowe Basin*

The sediments from the Petrockstowe core have highly varying %TOC values ranging from 0.02 to 42.7 %TOC with a mean of 3.2 ±7.0 %TOC (1 σ one standard deviation), (Table 5.1 & 5.2; Appendix 10). Figures 5.1& 5.2 show the %TOC results against the lithological section of cores 1A and 1B. The highest %TOC values coincide with the darkest clay or laminated silty clay facies, or with lignite or plant remains.

5.2.2 *Bovey Basin*

The total organic carbon (%TOC) values from the South John Acres Lane Quarry section, Bovey Basin, are shown in (Table 5.3; Appendix 10). As shown in Figure 5.3 the sediments have %TOC values ranging from 0.1 to 61.8 %TOC with a mean of 12.4 ±18.3 %TOC (1 σ one standard deviation). As for the Petrockstow Basin, the highest %TOC values coincide with either lignitic, silty clay or laminated silty clay facies. More coincidence of high %TOC

to lignite, lignitic clay, or silty clay facies are apparent in the South John Acres Lane Quarry section and in the Petrockstowe Basin.

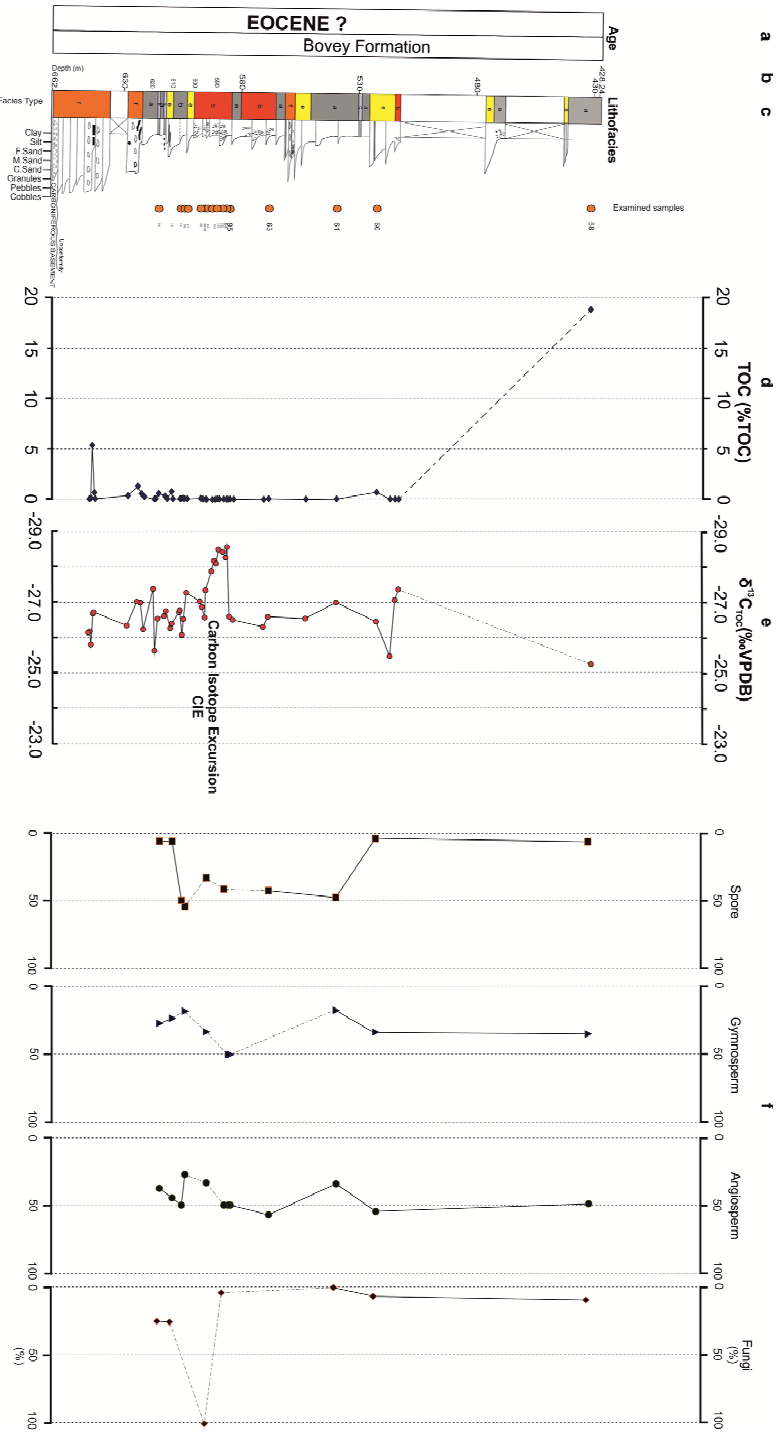

Figure 5.1: Data from core 1B, Petrockstowe Basin (a) Age, (b) Depth, (c) Lithology, (d) TOC, (e) $\delta^{13}C_{TOC}$ (‰VPDB) and (f) distribution and percentage occurrence of Spores, Gymnosperm, Angiosperm and Fungi. Error bar reflects long-term reproducibility based on replicate analysis of standard of BROC 2 standard. All results are adjusted to 0.02‰, the size of the error bars are smaller than the data points.

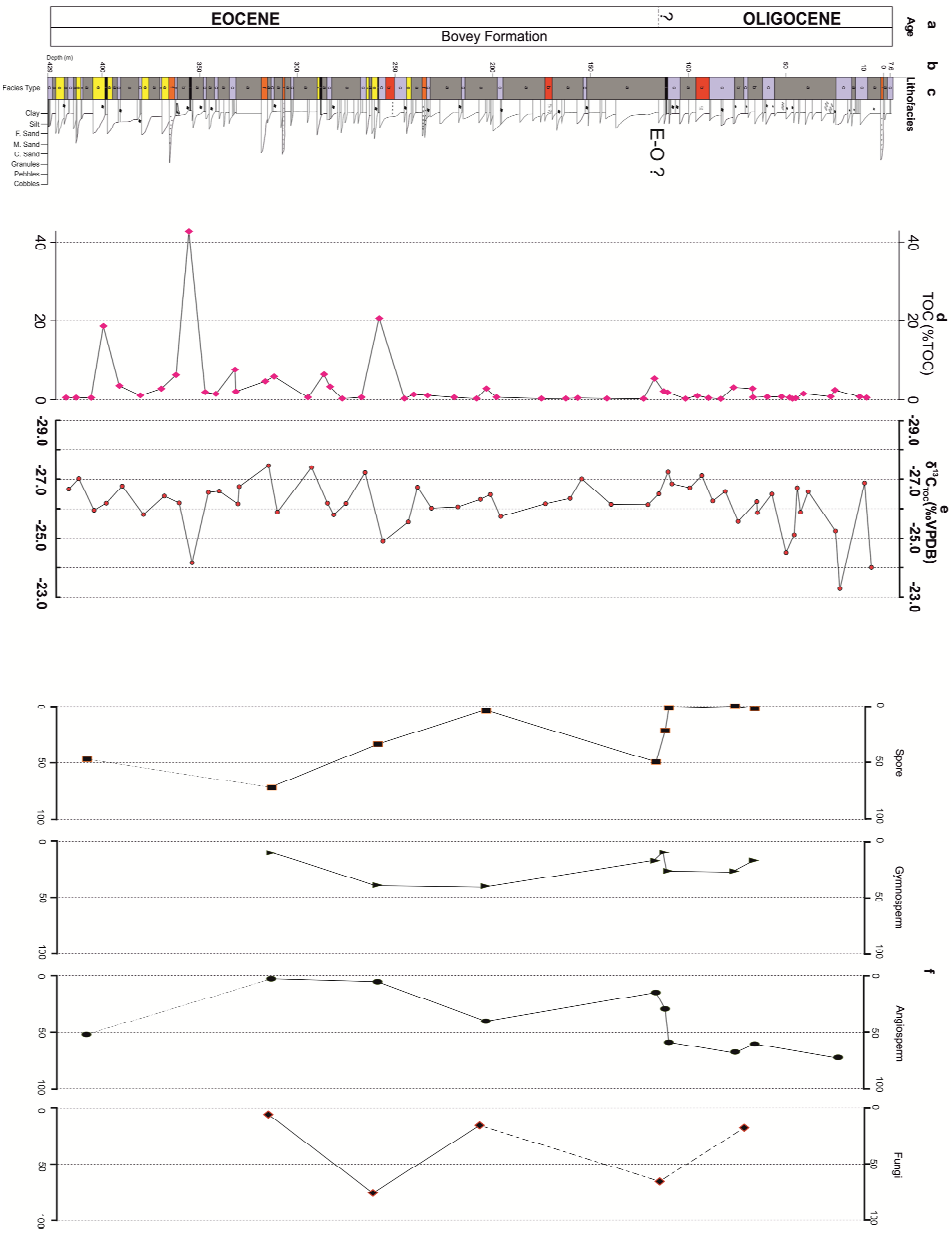

Figure 5.2: Data from core 1A, Petrockstowe Basin (a) Age, (b) Depth, (c) Lithology, (d) TOC, (e) $\delta^{13}C_{TOC}$ (‰VPDB) and (f) distribution and percentage occurrence of Spores, Gymnosperm, Angiosperm and Fungi. Error bar reflects long-term reproducibility based on replicate analysis of standard of BROC 2 standard. All results are adjusted to 0.02‰, the size of the error bars are smaller than the data points.

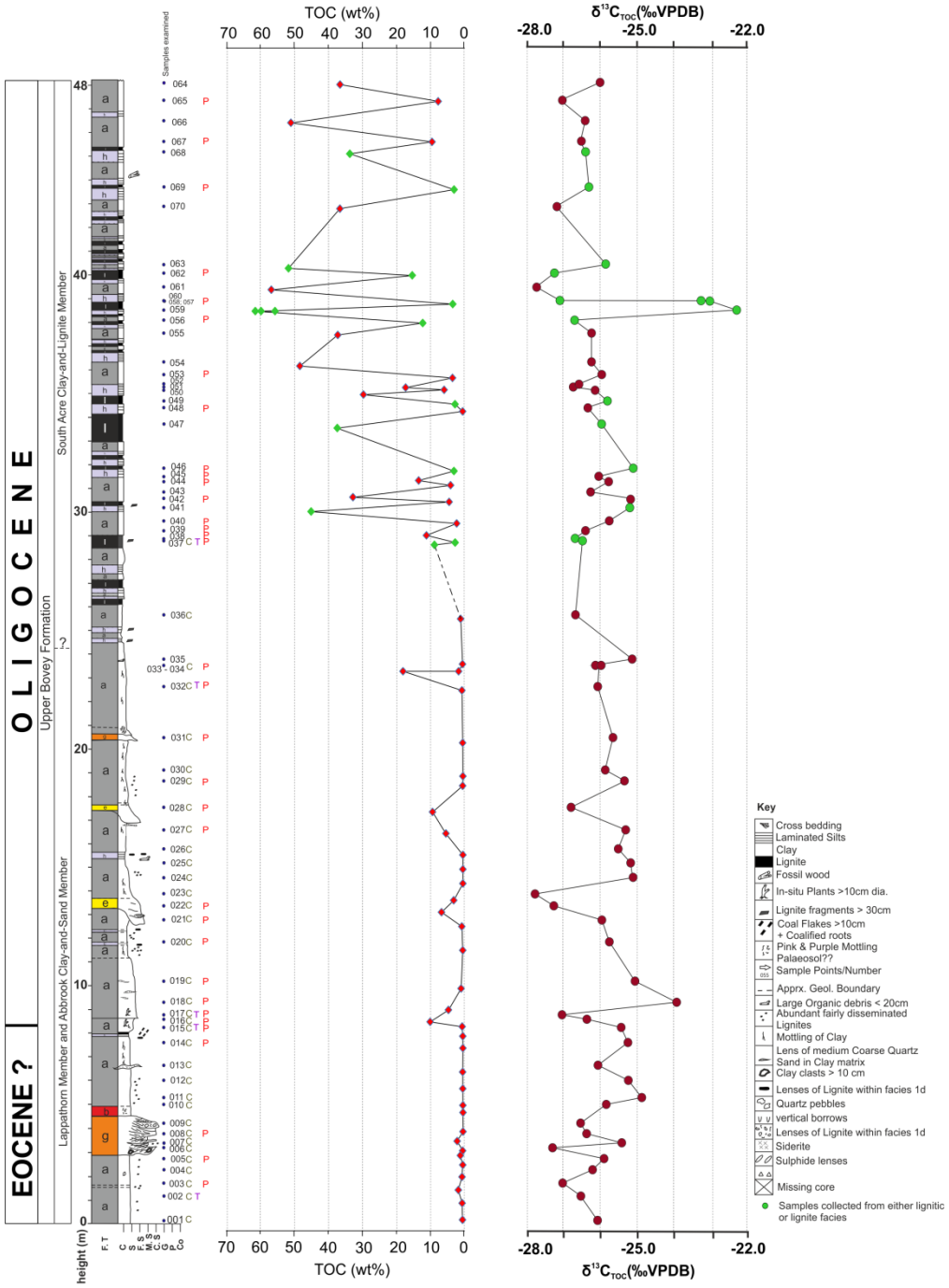

Figure 5.3: Data from South John Acres Lane Quarry section, Bovey Basin showing Age, Height, Lithological section, (d) TOC, (e) $\delta^{13}C_{TOC}$ (‰VPDB). Error bar reflects long-term reproducibility based on replicate analysis of standard of BROC 2 standard. All results are adjusted to 0.02‰, the size of the error bars are smaller than the data points.

5.3 Stable carbon isotope ($\delta^{13}C_{TOC}$) record

5.3.1 *Petrockstowe Basin*

The $\delta^{13}C_{TOC}$ values of samples in the Petrockstowe cores range from -28.5‰ to -24.0‰ with a mean value of -26.0 $\pm$0.8‰ (1 σ one standard deviation).

As can be seen in Figure 5.2, values at the base of core 1B start off with a $\delta^{13}C_{TOC}$ value of ~ -26.6‰ at 655 m. A carbon isotope excursion with a magnitude of ~2.0‰ can be seen from ~ 580 m depth with $\delta^{13}C_{TOC}$ values reaching a minimum of -28.6‰. The entire excursion occurs over a thickness of ~7.0 m, from 586 – 593 m. The data then shows a return to pre-excursion values of -26.2‰ at 580 m (Figure 5.2). Thereafter, the $\delta^{13}C_{TOC}$ remain relatively consistent between 584 m and 571m with $\delta^{13}C_{TOC}$ in the range of -26.5‰ and -26.3‰. Notable variability in $\delta^{13}C_{TOC}$ outside the CIE could be due to organic carbon source variation, sediment mixing or other local effects. It is important to note that the core was lost between 513.59 m to 431.60 m; hence no core was recovered from this interval.

According to Magioncalda *et al*. (2004), reliability of organic $\delta^{13}C_{TOC}$ values in chemostratigraphic investigations depends upon the organic compounds in sediment being well mixed. It is generally known that $\delta^{13}C_{TOC}$ values can rapidly change with changes in the carbon source as a result of isotope fractionation at the time photosynthetic fixation of carbon occurred (Diefendorf *et al.* 2010). The reason for this is that $\delta^{13}C_{TOC}$ values may be influenced by factors including organic matter degradation, bacterial growth, selective preservation and the effect of Rayleigh distillation with depth (Wynn *et al.* 2005). Different isotopic fractionation values for different organic material plays a great role. For example, for type C3 and C4 plants the $\delta^{13}C_{TOC}$ ranges between – 20‰ to – 35 ‰ and – 10 ‰ to – 14‰ respectively (Cerling & Harris 1999, Tipple & Pagani 2007) while the isotopic fractionation for leaves and wood trees is - 20 ‰ to – 30 ‰ (McCarroll & Loader 2004). This shows that trees are depleted in $\delta^{13}C_{TOC}$ relative to air and the degree of fractionation controlled by the response of the trees to their environment (McCarroll & Loader 2004).

A plot of %TOC versus $\delta^{13}C_{TOC}$ shows that no significant correlation exists between TOC and the $\delta^{13}C_{TOC}$ as $R^2 = 0.15$ (Figures 5.4). The lack of correlation suggests that the isotopic values are not influenced by the TOC of the sediments and, hence the $\delta^{13}C_{TOC}$ values are likely to be representative of the vegetation at that time. Also, Tyson (1995) has demonstrated that the potential sources of variation in bulk $\delta^{13}C_{TOC}$ values, for example contemporary leave versus wood $\leq$ 3‰ lighter; C3 versus C4 plant organic matter $\leq$ 15‰ lighter.

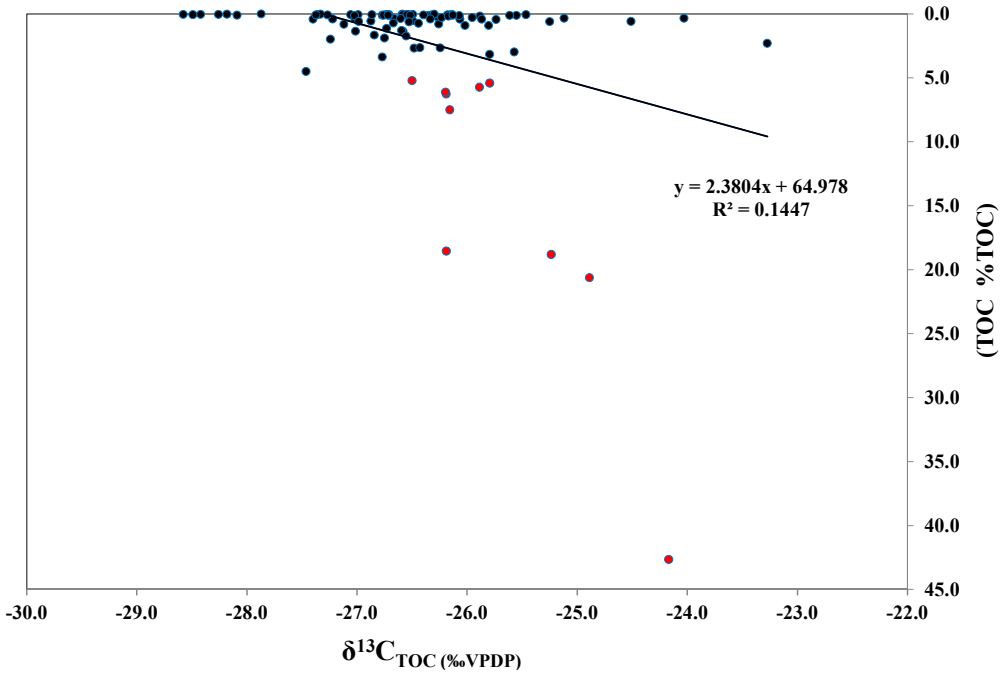

Figure 5.4: Correlation of TOC versus δ^{13}CTOC from the Petrockstowe cores 1A and 1B, Petrockstowe Basin (with all TOC data set from 0.00 - 42.65 %TOC; the data points highlighted in blue-black have TOC ≤5 %TOC).

In the upper part of the Petrockstowe 1A core, the $\delta^{13}C_{TOC}$ values generally oscillate around -26.0‰.This could be due to the natural variability of $\delta^{13}C_{TOC}$ within the sediments. However, at three different horizons more positive $\delta^{13}C_{TOC}$ values are recorded (354 m, 257 m, 25 m with corresponding $\delta^{13}C_{TOC}$ values of -24.2‰, -24.9‰ and -25.2‰ respectively). At about 111.4 m, there is a significant shift of $\delta^{13}C_{TOC}$ which coincides with a floral change with a decrease in the abundance of spores from 50% to almost 0%, and with an increase in

abundance of gymnosperm from <20% to 40% and angiosperm from 20 to 60% respectively and lastly fungi fall in abundance from 60% to <20%. The Eocene – Oligocene boundary proposed by Turner (1979) was placed around 120 m and in this study the isotopic shift recorded from 122 m to 111 m is highlighted in blue. There is a general trend to more positive values above 60 m in the core. The major $\delta^{13}C_{TOC}$ shifts recorded at 354 and 257 m are defined by a single value and correspond to a significant peak in %TOC, which could be woody fragments. Large positive correlations between sediments $\delta^{13}C_{TOC}$ and TOC in some facies may reflect an increase in the ratio of phytoplankton to terrestrial organic matter, as well as changes in productivity-related isotopic fractionation (Middelburg 1991, Tyson 1995).

5.3.2 *South John Acres Lane Quarry section, Bovey Basin*

The $\delta^{13}C_{TOC}$ values of samples from the South John Acres Lane Quarry section, Bovey Basin range between -27.8‰ − -22.5‰ with a mean value of -26.0‰ ± 1‰ (1 σ standard deviation) (Figure 5.3). In this section, there are two notable carbon isotope shifts which could represent a possible sedimentological response as they match lithofacies changes. The first shift occurs at 9 – 12 m height corresponding to $\delta^{13}C_{TOC}$ values of -23.9‰ to -27.8‰. The second $\delta^{13}C_{TOC}$ shift was recorded at 38 – 39 m height with a spike of -22.5 to -23.1‰ within laminated silty clays to lignitic band. This negative $\delta^{13}C_{TOC}$ may be unconnected to the type of depositional environment (lignite facies) probably because lipid preservation is great under anoxic condition. Nevertheless, it is generally assumed that the contents of the lipids are too small to explain the bulk isotopic effect observed in the course of diagenesis (Dean *et al.* 1986). Also, a lack of fractionation that is often apparent under oxic conditions reflects an indiscriminate degradation of isotopically heavy constituents.

There are carbon shifts observed in the South John Acre Lane Quarry section, Bovey basin at around 9 -12 m and 38 -39 m (Figure 5.3) but they are related to palynological changes,

i.e. carbon source changes and not atmospheric $\delta^{13}C$ changes like that seen in Petrockstowe cores.

Two correlation coefficients were calculated for the dataset. The first with TOC ≤ 5 %TOC, gave an R^2 value of 0.015 (Figure 5.4), and the second with all TOC from 0.0 – 62.0 %TOC, gives an R^2 value of 0.052 (Figure 5.5). The second (Figure 5.5) is similar to the regression calculated in section 5.3.1 for the Petrockstowe cores and suggests no relationship between $\delta^{13}C_{TOC}$ and %TOC.

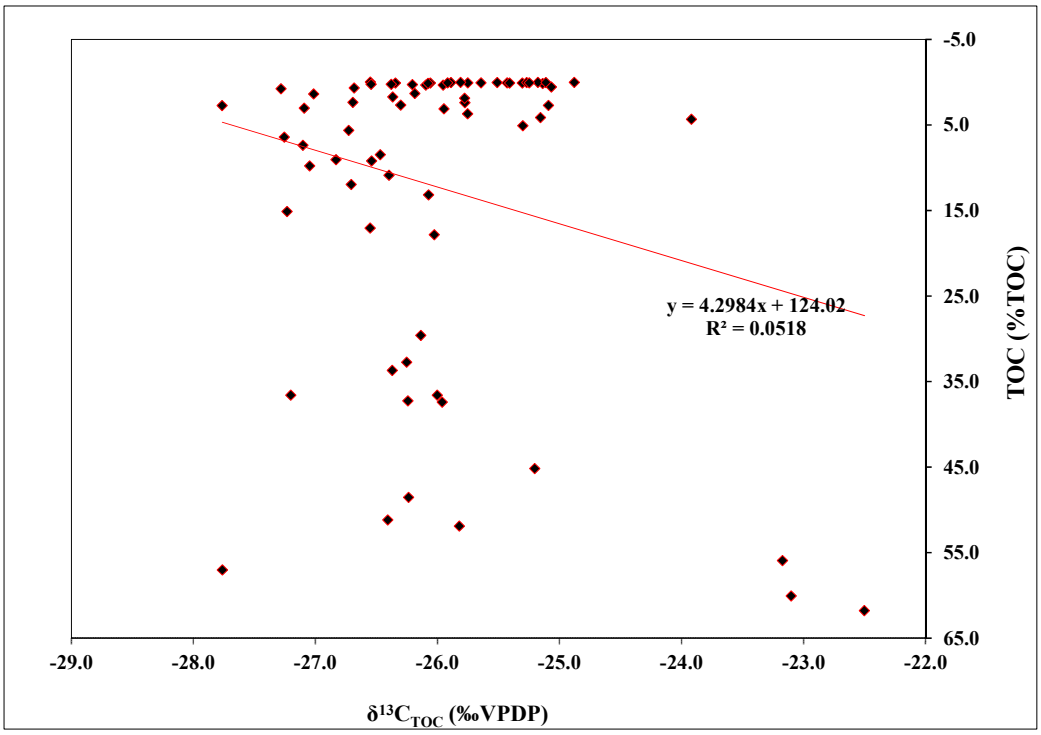

Figure 5.5: Correlation of TOC versus $\delta^{13}C_{TOC}$ from the South John Acres Lane (SJAL) Quarry section, Bovey Basin (where TOC ≤5 %TOC).

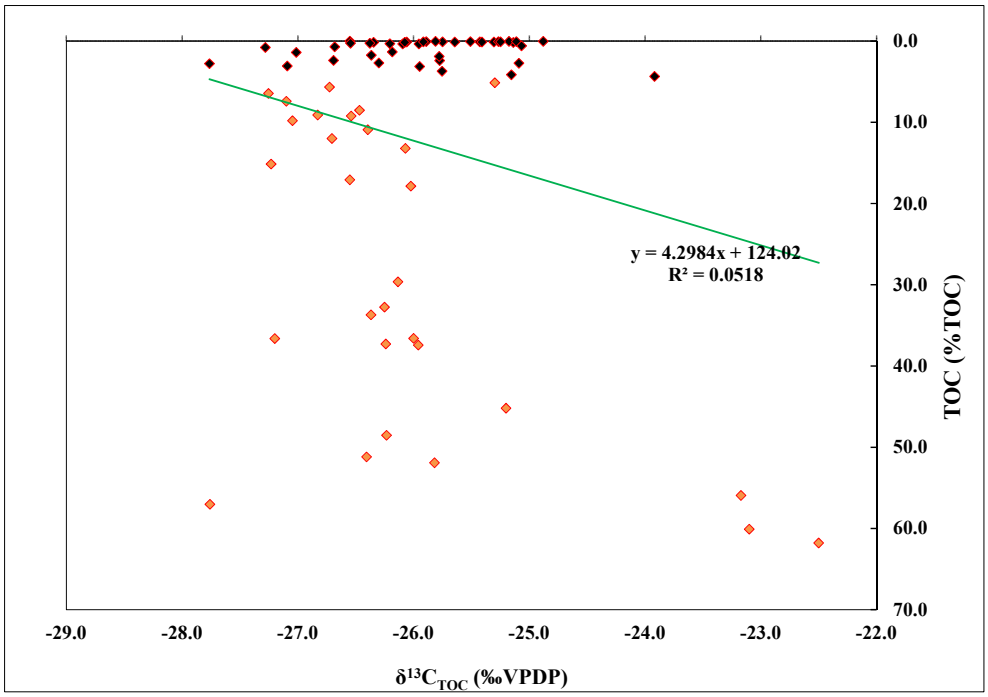

Figure 5.6: Correlation of TOC versus δ ^{13}CTOC from the South John Acres Lane (SJAL) Quarry section, Bovey Basin (with all TOC data set from 0.0 - 62.0 %TOC represented by black-red data points while orange data points have TOC ≤ 5 %TOC).

5.4 Carbon Isotope Excursion (CIE)

5.4.1 Petrockstowe Basin

In identifying the magnitude of a CIE, at ~590 m (Figure 5.2) the onset in the section has to be determined first. Domingo *et al*. (2009) proposed two methods for calculating the magnitude of any CIE. The first is considering the average $\delta^{13}C_{TOC}$ value preceding the CIE, which is subtracted from the mean of $\delta^{13}C_{TOC}$ values occurring in the CIE. The second is the 'maximum CIE' method which identifies the most positive $\delta^{13}C_{TOC}$ value before the negative $\delta^{13}C_{TOC}$ shift and the most negative $\delta^{13}C_{TOC}$ at the base of the excursion. In this study, the 'maximum CIE' method is adopted in examining the CIE in the lower Petrockstowe Basin. With this method, the onset of the CIE was placed within the silty clay facies of the lower Petrockstowe Basin at around 616 m, and is defined by a negative $\delta^{13}C_{TOC}$ isotope shift of at least 2‰ to a minimum value of < -28.5‰.

The magnitude of the Petrockstowe CIE is similar to the PETM CIE that has been identified in the Cobham Lignites in the south east UK (Collinson *et al.* 2003, Collinson *et al.* 2009). These in turn correlates to the carbon isotope profiles of the Bighorn Basin, Wyoming, USA, based on palaeosols carbonates that are characterised by a temperature rise of 5 – 9^{o}C in ten thousand years and a gradual declined to pre-excursion values in ~100 – 200 thousand years (McInerney & Wing 2011). This results in a CIE of 2 – 6.5‰ pointing to the release of > 2000 Gigatons of Carbon (Koch *et al.* 1992, Bowen *et al.* 2001, Cramer *et al.* 2003, Panchuk *et al.* 2008, Zeebe *et al.* 2009, McInerney & Wing 2011). Considering a CIE of ~-2‰ from the lower part of Petrockstowe core 1B, this CIE magnitude falls within the lower limit of that is associated with the PETM, suggesting it may be related to this hyperthermal event. However, biostratigraphically there is an absence of Palaeocene pollen/spore e.g. *Pistillipollenites* pollen, *Platycaryapollenites platycaryoids* or *Triatriopollenites caryophaenus* as commonly found in the Cobham Lignite (Collinson *et al.* 2003, Collinson *et al.* 2009) in the Petrockstowe core suggesting that this CIE is unlikely to be the PETM.

From the magnitude of the CIE in the lower part of the Petrockstowe core 1B; the magnitude could potentially suggest an isotopic perturbation which may be associated with one of the other transient carbon isotopic shifts that occurred after the PETM i.e. either the ETM-2 or ETM-3. The magnitude of the CIE (- 2‰) recorded in the lower Petrockstowe core 1B is similar to the (- 3.8‰) CIE documented as ETM-2 and H-2 in the continental succession of the McCullough peaks, Bighorn Basin, Wyoming, USA. Using palaesol carbonate carbon isotope stratigraphy Abels *et al*. (2012) show that the CIE magnitudes of - 3.8‰ and - 2.9‰ which are comparable with that seen in Petrockstowe. The ETM-2 and H2 of the Bighorn Basin only show lithologic changes. No major biostratigraphic faunal change similar to those during the PETM (Koch *et al.* 1992, Bowen *et al.* 2002, Abels *et al.* 2012) occurred. This particular evidence for the absence of major biostratigraphic change is similar to that seen in the lower Petrockstowe core 1B which shows few elements changing, like *Monocolpopollenites* sp., *Inaperturopollenites* sp., *Laevigatisporites* sp., Bissacate and some

conifer pollen. In addition there is lack/low presence of Cupressaceae/Taxodiaceae which could be related to swampy habitats. There is unfortunately no magnetostratigraphic record from this core, which could have served as an additional piece of evidence to support the proposed age model, i.e. ETM-2. In the present study the CIE is potentially associated with a long-lived lake or lake centre and fold plain facies association while the early Eocene sediments of the Willwood Formation, Bighorn Basin, Wyoming, USA shows that they were deposited in a meandering river system characterised by fine grained overbank deposits with distinctive colour bands that could be related to ancient soil horizons that have different maturity styles and spacing (Kraus & Riggins 2007, Aziz *et al.* 2008).

At the base of the section which coincides with the identified CIE, Gymnosperm and Angiosperm species are virtually on the average distribution ranging from 30 – 50 % while spores proportions constitute 45 – 52% and Fungi are constantly at the lowest abundance 0 – 20%. Also, coincident with the CIE onset Angiosperm proportion was on the rise reaching 50% while Gymnosperms fall to 30%. Throughout the body of the CIE Angiosperm and Gymnosperm proportion gradually increased, despite the variability from 50 – 30 % while the spores decrease from 52 – 45%.

The present palynological data set shows no significant changes in organic matter source throughout the CIE interval. The interval is mainly dominated by phytoclast and equal proportions of AOM and palynomorphs, suggesting that the CIE is not carbon source related as indicated by the presence of mesothermal conifers species (e.g. Taxodium and/or *Metasequoia* or *Sequoiapollenites*) and Angiosperm e.g. *Pompeckjoidaepollenites* sp. The abundance of these taxa remains unchanged towards the upper part of core 1A, which suggests there was the presence of moderately diverse mixed conifer vegetation. The occurrences of Cycads, *Tricolpopollenites* sp. that has an affinity to modern palm vegetation could suggest coldest months mean temperatures >5^{o}C in the modern world (Greenwood &

Wing 1995). On the other hand, the minute shift observed by the increase in the abundance of the Gymnosperms and Angiosperms while the spores decrease within the body of the CIE would be associated with tropical to warm temperature wet climates where a large number of spores are ferns and it is well known that epiphytic ferns in the late Palaeogene were associated with extreme warmth and the expansion of tropical biome towards the mid-latitudes (Eldrett *et al.* 2014).

The present study is the first high resolution $\delta^{13}C_{TOC}$ data generated from this section, in conjunction with palynology data as presented in Chapter 4, pages 128 −129, although only a minute shift was observed in the abundance of Gymnosperms and Angiosperms with a decrease in spores suggesting that the CIE was related to tropical warm temperature wet climates. Unlike the work of Abels *et al*. (2015), in identifying the five younger hyperthermals recorded in the Bighorn Basin, due to lack of palynology data they resorted to used procession forcing over the 7 m thick overbank – avulsion sedimentary cycles and the ~ 100 – 405 Kyr eccentricity forcing related to the carbon cycle changes in the ETM2 to I2 stratigraphic interval.

An age model for the lower part of the Petrockstowe Basin is hereby proposed on the basis of the magnitude of the $\delta^{13}C_{TOC}$ excursion, which is similar in absolute value to the magnitude the CIE recorded for the Eocene Thermal Maximum-2 (ETM-2; ~53.6Ma) with a magnitude of -3.8‰ in the Bighorn Basin. On this note, it would be strongly suggested that an age of ~53.6Ma – i.e. ETM-2 be recommended for this section of the Petrockstowe Basin.

5.5 Eocene – Oligocene Boundary

One of the most prominent abrupt climatic events in the Cenozoic is the Oi-1 glaciation occurred in the Oligocene. The decent into it occurred across E – O boundary (Kennett & Shackleton 1976, Zachos *et al.* 1996, Lear *et al.* 2000). The Oi-1 glaciation is considered to

represent the initiation of major permanent Palaeogene ice sheets on Antarctica; however the debate is ongoing as to what caused this glaciation event. This event is marked by a ~1.5‰ shift in the oxygen isotope ratio of carbonate from deep sea benthic foraminifera (Zachos *et al.* 2001). According to Coxall *et al*. (2005) ODP site 1218 proved to have the best record across the E – O boundary and a correlation has been made here in trying to investigate the presence of the E – O boundary in the Petrockstowe core 1A using $\delta^{13}C_{TOC}$ to confirm the proposed boundary, based on pollen data, made by Turner (1979). However, even though global $\delta^{13}C$ records from benthic foraminifera show decrease by 1.4‰ within less than 500 000 yr to the lowest $\delta^{13}C$ values in the deep ocean across the E – O boundary. This cannot be used a chemostratigraphic marker for the E – O boundary in the Petrockstowe Basin as the sediments in this basin are terrestrial.

Chandler (1957) noted plant species of Palaeogene age from Blue Waters Mine, Heathfield Clay pit and Kingsteignton in the Bovey Basin were assigned to the middle Oligocene. The presence of *Microdiptera parva* and *Brasenia ovula* proved that the Bovey Formation was not older than the Highclif Sands or Bournemouth Marine Series. Similarly, Chandler (1964) documented *Potamogeton temicarpus*, *Rubus microspermus* and *Stratiotes websteri* that first appeared in the Oligocene. Despite the assignment of an Oligocene age to the Blue Waters mines Chandler (1964) still speculates that at a considerable depth Eocene sediments could be present. This was justified by the presence of Eocene indicators like *Anacolside* and *Pompeckjoidaepollenites* from Borehole 839 857, near Heathfield that penetrated 185 m of Upper Bovey Formation, 69 m of South Acre clay-and-Lignite and 51 m of Abbrook Clay-and-Sand and from below 290 m depth, Selwood *et al*. (1984) deduced that the beds above were lower to middle Oligocene age. From the new pollen data generated from the South John Acres Lane quarry section, it has been revealed that between 28.9 m to 30.6 m of the lithological section a change in lithofacies, which coincides with the disappearance of *Pokmpeckjoidaepollenits* taxa occurred, with a brief carbon isotope excursion of about 2‰ (-27.5 to -25.0‰). It should be noted that towards the upper part of the John Acres Lane

Quarry section of the Bovey Basin, there is an increase in abundance of the following species *Salixpollenites*, *Tiliaepollenites*, *Plicapollis*, *Sequoiapollenites*, and *Cycadopites* which remains constant all through the section. *Tricolporopollenites* (associated with trees, shrubs and herbs of broad affinity), *Inaperturopplenites*, *Arecipites* and *Monocolpopollenites* (reflects characetristics of palm pollen) might suggest that the climate at the time of deposition was probably frost free. Also %TOC suddenly increased from <10wt% to >40w%t, which tend to be in line with the palynological change. Because of the earlier correlation presented by Chandler (1957, 1964) and further emphasis by Selwood *et al*. (1984) on the presence of Eocene – Oligocene boundary in this section, the $\delta^{13}C_{TOC}$ excursion recorded support the earlier views on the Eocene – Oligocene boundary being present. This also agrees with similar findings from Hampshire Basin, UK (Collinson *et al.* 1981b, Hooker *et al.* 2004) although, Collinson *et al*. (1981a) have found no evidence of sudden climatic change at the end of Eocene but have observed two major periods of floristic change, pointing to more gradual cooling that might have started in the latest Eocene.

5.5.1 Conclusion

In conclusion, the CIEs recorded in Petrockstowe core 1B suggest an age model of ETM-2 (~53.6Ma), and biostratigraphically the observed increase in the abundance of Gymnosperm and Angiosperm with the decrease in spores, suggest a warmer climate and show probable evidence of the hyperthermal event.

There is no chemostratigraphic marker in the $\delta^{13}C_{TOC}$ for the E-O boundary, though one does exists in Bovey, but this is due to a carbon source change associated with a cooling.

The EOT in the Petrockstowe Basin show a $\delta^{13}C$ shift of ~ -1‰ which is considered to be due to atmospheric carbon source, coincided with floral change.

CHAPTER 6 – ORGANIC GEOCHEMISTRY

6.1 INTRODUCTION

The reconstruction of palaeothermometry gives a valuable contribution to the understanding of Palaeogene climate which is a known period of a major climatic reorganization. In this chapter, the aim is to apply the Branched and Isoprenoid Tetraether (BIT) index and Methylation Branched Tetraether/Cyclization Branched Tetraether Ratio (MBT'/CBT) proxy (a new novel proxy) for the reconstruction of palaeotemperature and pH, based on the distribution of Branched Glycerol Dialkyl Glycerol Tetraether (brGDGT) membrane lipids to the Palaeogene sediments in the Petrockstowe and Bovey basins.

6.1.1 METHYLATION BRANCHED TETRAETHER/CYCLIZATION BRANCHED TETRAETHER RATIO (MBT'/CBT)

The MBT'/CBT proxy (defined in eq. 1 & 2, in Chapter 2, page 42) for the reconstruction of palaeotemperature and past soil pH (eq. 3, in Chapter 2, page 42) is based on the distribution of brGDGT membrane lipids. The brGDGTs usually vary in the amount of methyl branches (4 - 6) in the GDGT molecule, which can also contain up to two cyclopentane moieties (Sinninghe Damste *et al.* 2000, Hopmans *et al.* 2004). The CBT index is related to soil pH while the MBT' index is a function of both soil pH and mean annual air temperature (MAAT) (Weijers *et al.* 2007b, Tierney & Russell 2009, F. Peterse *et al.* 2012b).

The MBT'/CBT proxy has frequently been applied to coastal marine sediments (Hopmans *et al.* 2004, Huguet *et al.* 2007) with the brGDGTs deposited as part of river transported soil organic matter. In addition, palaeoclimatic reconstructions have been made on tropical Central Africa (Weijers *et al.* 2007b), the Lomonosov Ridge in the Arctic (Weijers *et al.* 2007c), Greenland (Schouten *et al.* 2008) and the Amazon Basin (Bendle *et al.* 2010) by the application of this novel proxy.

Weijers *et al*. (2007c) and Schouten *et al*. (2008) applied the MBT'/CBT proxy in their studies to investigate the E – O boundary and Oligocene – Eocene (O – E) boundary respectively in the Artic region. Both studies lead to the reconstruction of mean annual air temperatures (MAAT). The MAAT data obtained by Weijers *et al*. (2007c) were comparable to the TEX_{86} record of Sluijs *et al*. (2006) in terms of timing and magnitude of the temperature change, where a 8^{o}C warming was recorded in the P – E with MAT estimate of >20^{o}C.

The MBT'/CBT proxy has also been used to reconstruct MAAT from Greenland-Norway, which has found substantial cooling at the E – O transition of the order of ~3 – 5^{o}C coincidentally matched with a reconstructed pollen record from the same region (Schouten *et al.* 2008). In the Miocene, the MBT'/CBT proxy has also been applied to the reconstruction of the MAAT in northern Europe and showed a cooling trend consistent with palynological data (Donders *et al.* 2009).

The brGDGT proxy has also been used in Pliocene peat deposits from the Canadian Arctic, and the results showed that the Arctic air temperature during the Pliocene time was like (Ballantyne *et al.* 2010) while the brGDGTs was employed in the study of loess-paleosol sequence in the China loess plateau, which gave the timing and magnitude of deglacial atmospheric warming in East Asia (Peterse *et al.* 2011). When the MBT'/CBT proxy was applied to lake sediments, the distribution of brGDGTs in sediments of Lake Challa West Africa and Lake Towuti in Indonesia, the results differed significantly from that of the surrounding soils (Damsté *et al.* 2009, Tierney & Russell 2009) suggesting that the brGDGTs might have been produced insitu in the aquatic environment. Thus, it has influence on the application and interpretation of the MBT'/CBT for lake or lacustrine samples. Tierney & Russel (2009), also noted in their study that there were dramatic changes in the characteristics of GDGTs within a single lake.

In another study to test the potential of the MBT'/CBT proxy to stalagmites Yang *et al*.(2011) got different MBT'/CBT values for the stalagmites than those from the overlying soil. This lack of relationship in MAATs indicates that brGDGTs were produced during stalagmite formation. Also, the application of the MBT'/CBT proxy to a terrestrial environment of recent peat and ancient coal in particular, revealed MAAT estimates which did not compare well with actual data or reconstructed MAAT. Factors other than temperature, for example past vegetation change, could likely influence the results (Weijers *et al.* 2011).

The MBT'/CBT palaothermometry proxy, in conjunction with terrestrial palynology, was also applied to a new sedimentary record from the Wilkes Land margin, East Antarctic, which was recovered by the Integrated Ocean Drilling (IODP Expedition 318, site U1356). The results of this study showed that the data served as a framework for a terrestrial climatic reconstruction for the early Eocene of Antarctic (Pross *et al.* 2012).

Peterse *et al*. (2012a) have observed a certain level of error in the application Weijers *et al*.(2007b) calibration; they argued that caution is required in the interpretation of the absolute reconstructed values using the MBT/CBT proxy. Hence, Peterse *et al*. (2012b) revised Weijers et al (2007b) calibration to MBT'/CBT (eq. 2, in Chapter 2, page 3) and tested the revised MBT'/CBT calibration for palaeotemperature reconstruction on the records of atmospheric warming in tropical Africa (Weijers *et al.* 2007b) and southeast Asia (Peterse *et al.* 2011) over the last deglaciation and the onset of the long term cooling near the Eocene – Oligocene boundary (Schouten *et al.* 2008) and during the PETM (Weijers *et al.* 2007c). The Peterse *et al*. (2012b) and Hopmans *et al*. (2004) calibration were used throughout this present study to reconstruct palaeotemperature. The application of MBT'/CBT proxy to ancient sediments is influenced by diagenesis and maturity. This is evidenced by the re-examination of the distribution of the GDGTs in artificial maturation experiments (Schouten *et al.* 2004) with results showing the tendency of the MBT' index to

decrease during artificial maturity, while the CBT index increases with maturity, particularly above 24^{o}C. This could suggest that the brGDGTs containing cyclopentane moieties are thermally less stable and this may be the same with isoGDGTs (Schouten *et al.* 2013).

The variation in the distribution of brGDGT's influencing MBT'/CBT values, for sediments deposited under oxic and anoxic conditions in a small lake in the USA, showed they are attributed to different producers of both the br-iso GDGTs to small lake sediments which included soil organic matter and *in situ* production (Tierney *et al.* 2012). Tierney *et al*. (2012) emphasised that evidence for the preferential *in situ* production of the more methylated brGDGTs within a lake sediment column, showed both the large proportional representation of the type III iso-brGDGTs as well as potentially the peculiar subsurface peak in the concentration of type III brGDGTs. The resultant effect of *in situ* production of type III GDGTs lowers the MBT'/CBT indices in surface sediments which could be the reason for the "cold bias" observed when translating MBT'/CBT values into temperature associated with lacustrine environments.

6.1.2 BRANCHED AND ISOPRENOID TETRAETHER (BIT) INDEX

Hopmans *et al*. (2004) defined the BIT index as a means of quantifying the relative abundance of GDGTs which would serve as a proxy for the determination of relative abundance of terrestrial organic matter as contained in eq. 5 in chapter 2 page 43. The idea of the BIT index originated from the fact that the brGDGTs were found to be occurring predominantly in the terrestrial environment while Crenarchaeol GDGTs were dominant in marine environments.

Originally, the BIT index was conceptualised for tracking the input of soil organic matter to marine sediments but now it is mostly applied in the lacustrine environment (Schouten *et al.* 2013). It could be applied as well as a potential indictor for the input of soil organic matter and soil erosion as evidenced by the positive correlation by lake records of Lake Challa from

West Africa where high records of BIT index tends to indicate the influence of increased rainfall and consequently an increased in soil erosion and input to the lake (Verschuren *et al.* 2009, Schouten *et al.* 2013). Again, results from Challa Lake showed that BIT was determined by the changing Crenarchaeol concentration instead of those of brGDGTs (Sinninghe Damsté *et al.* 2012).

The BIT index has been successfully applied in the determination of the onset of active river outflow during the last deglaciation in northern Europe (Ménot *et al.* 2006) and at several sites which demonstrated decreased sea level and increasing distance to river mouth during the Palaeocene Eocene Thermal Maximum – PETM (Sluijs *et al.* 2008a). The BIT index was also conveniently applied in the investigation of the implication of TEX_{86} in sea surface temperature reconstruction across early Cretaceous interbedded pelagic and shelf-sourced turbiditic sediments from two Deep Sea Drilling Project (DSDP) sites in the Western North Atlantic, where results showed that the offset in TEX_{86} ratio was small, but was consistent to temperature difference ~ 1 – 2 ^{o}C that occurred between interbedded lithologies of similar ages (Littler *et al.* 2014). Also, the index has been applied to investigations of some lakes. For example Sinninghe Damste *et al*. (2009) reported that the greatest flux of brGDGTs in the Lake Challa was during the short rainy season while Verschurea *et al*. (2009) used the index on Lake Challa sediments to constrain previous precipitation intensity from Mount Kilimanjaro. In addition, the BIT index has been applied to the study of modern surface sediments in the present coastal areas. Example are these are the of Washington Margin (Walsh *et al.* 2008), Gulf of Lion (Kim *et al.* 2006, 2010) and the Mediterranean Sea (Leider *et al.* 2010).

The BIT index is associated with some limitations in its application which have been identified by several authors in different studies and details are contained in Weijers *et al*. (2006a); Leininger *et al*. (2006); Tierney *et al*. (2009); Peterse *et al*. (2009); Huguet *et al*. (2010a); Kim *et al*. (2010a).

Among the outstanding issues to the application of the BIT index in the Palaeogene palaeoclimate that have remain unresolved is to understand whether BIT signals are representing allochtounous soil input or whether it depends on the type of the lake environment and its surrounding as well as on the Crenarchaeol abundance.

6.2 BIT Index, pH, CBT and MBT' Results

6.2.1 Petrockstowe Cores 1A & 1B, Petrockstowe Basin

A summary of the geochemical data for Petrockstowe cores 1A and 1B are presented in Tables 6.1a & b following Weijers *et al*. (2007b) calibration as modified by Peterse *et al*. (2012). The reconstructed palaeotemperature data are plotted against the lithological log in Fig. 6.1 & 6.2 and the detailed geochemical data is presented in Appendix 10 – Table 6.1a b. In all, 67 samples were analysed, 31 from Petrockstowe core 1A, 10 from Petrockstowe core 1B and 26 from the South John Acres Lane Quarry section. Of these only 51 yielded sufficient GDGTs and 41 of the samples were analysed from Petrockstowe cores 1A & 1B. Also, in Petrockstowe cores the MAAT temperatures were reconstructed from 20 samples only due to poor content or absence of GDGT's in them. In Petrockstowe core 1A, samples MC5, 12, 20 and 50 contained both isoprenoidal and brGDGTs, while the remaining samples contain either Isoprenoid or brGDGTs only. The reconstruction MAAT obtained in the core 1A was in the range of 11.9^{o}C to 27.5^{o}C with a mean value of 17.3 ^{o}C (1SD $\pm$ 4.7^{o}C), and in core 1B there were only two data set generated due to the poor content of the GDGTs, and has a minimum and maximum values of 14.5^{o}C and 19.5^{o}C respectively.

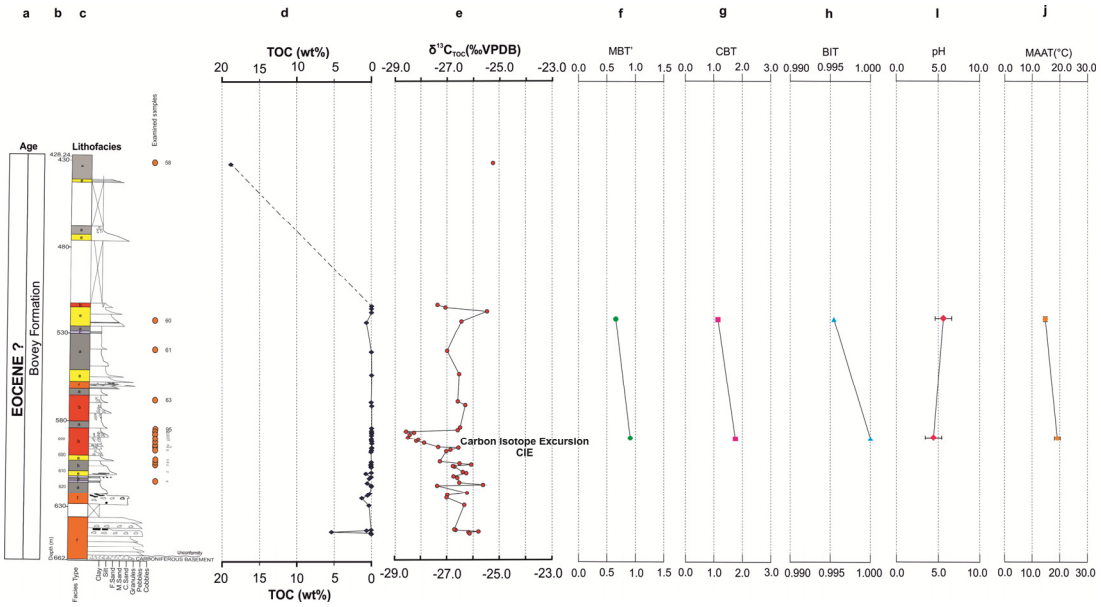

Figure 6.1: Data from core 1A, Petrockstowe Basin, Southwest UK (a) age, (b) Depth, (c) lithology, (d) TOC, (e) $\delta^{13}C_{TOC}$ (‰VPDB) and (f) MBT', (g) CBT, (h) BIT, (i) pH and (j) reconstructed mean annual air temperature (MAAT) using the MBT/CBT proxy. Error bars reflects long-term reproducibility based on replicate analysis of standard of BROC 2 standard. All $\delta^{13}C_{TOC}$ results have been adjusted to 0.1%, the size of the error bar.

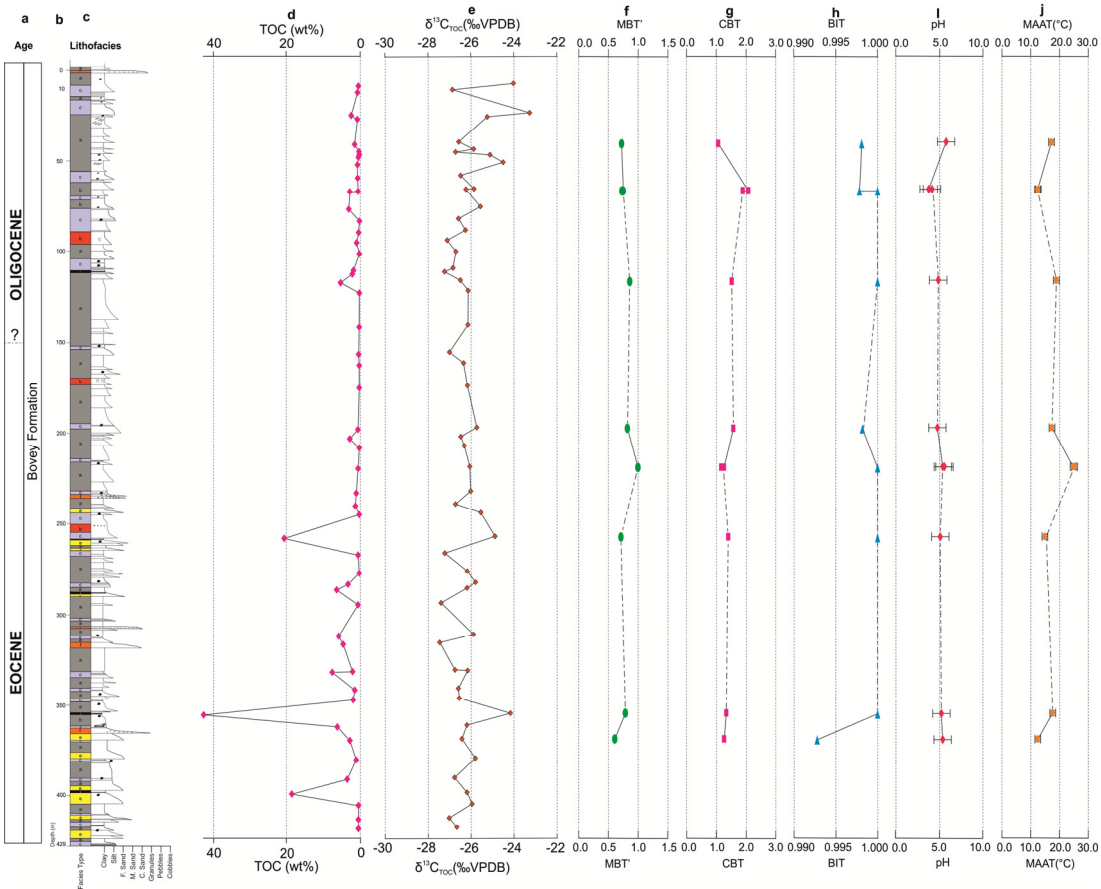

Figure 6.2: Data from core 1B, Petrockstowe Basin, Southwest, UK (a) age, (b) Depth, (c) lithology, (d) TOC, (e) δ13CTOC (‰VPDB) and (f) MBT', (g) CBT, (h) BIT, (i) pH and (j) reconstructed mean annual air temperature (MAAT) using the MBT/CBT proxy. Error bars reflects long-term reproducibility based on replicate analysis of standard of BROC 2 standard. All $\delta^{13}C_{TOC}$ results have been adjusted to 0.1%, the size of the error bar.

BIT Index

The BIT Index values from Petrockstowe and Bovey basins regardless of the type of lithology, was < 1.00 or very close to 1 in all the samples, and this confirms that the sediments have a very strong terrestrial influence (as opposed to marine) and a fluvial source to the brGDGTs (Hopmans *et al.* 2004, De Jonge *et al.* 2014, F. Peterse *et al.* 2012b). This is consistent with the palynological and palynofacies analysis data presented in Chapter 4. Also, this result is consistent with brGDGT's being resistant to diagenesis, which are predominantly produced in soils and show the traces of organic matter (Smith *et al.* 2012). Also, the BIT values derived from samples of the ODP site 913B which is of late Eocene to early Oligocene age, have values which range from 0.17 – 0.98. These values though they did not show a clear trend they did suggest high terrestrial input of organic matter and are in agreement with the BIT values from Petrockstowe and Bovey basins being in the range of near 1. Because the BIT values obtained are all close to 1, this suggests that they are resistant to diagenesis. This is contrary to results from some soils that had BIT values of 0.15 from estuarine and open marine environments (Francien Peterse *et al.* 2012a, Zhang *et al.* 2012). BIT values are not only determined by the concentration of brGDGTs but also by that of Crenarchaeol. This is typified by some samples from the South John Acres Lane Quarry section (Table 6.2a). Therefore, BIT values may vary with changes in the concentration of Crenarchaeol, and the concentration of brGDGTs may remain unchanged. Some factors like seasonal stratification, *in situ* productivity, as well as diagenetic effects, could affect the concentration of Crenarchaeol GDGTs, which could also have the potential to affect the terrestrial carbon reconstructions in a wide variety of marine and aquatic environment (Smith *et al.* 2012).

CBT

The cyclization of branched GDGTs (CBT) varies from 0.76 – 3.16 for the Petrockstowe sediments. A CBT value of 1.26 was observed at the bottom of Petrockstowe core 1A which

increased to 3.16 at 240 m depth. It suddenly decreased to 1.57 at 195 m depth. At 195 m, there is a significant shift in the CBT record, where the value then drops from 1.57 to 0.75 within a 40 m interval. Towards the top of the core, CBT values are in the range of 1.41 to 1.06 (Figure 6.1 & 6.2). In Petrockstowe core 1B, CBT values were only obtained from two samples and because of this reason the trend in MBT' could not be inferred. The CBT index is heavily dependent on the relative abundance of brGDGT-Ic. Where this group of GDGT is less than 2% of the total GDGTs in the sample, because the samples were from the lignite facies, this is consistent with results from the humid tropics where a 2% minimum and 6% maximum were recorded (Peterse *et al.* 2012) (see Figure 6.4 – 6.6 for the distribution of GDGT- Ic in some samples).

pH

The majority of the pH values reconstructed from Petrockstowe core 1A are in the range of 1.67 - 6.41, which tends to suggest that deposition of the sediments were under acidic conditions. This might possibly explain why there are no carbonates preserved in the Petrockstowe samples. Weijers *et al*. (2007a) has shown that in acid and neutral soils, brGDGTs dominate over the isoGDGTs. The results obtained from the Petrockstowe Basin tend to show strong similarity with those 134 soil samples from 90 globally distributed locations (Weijers *et al.* 2007a) (Figure 6.1 & 6.2). Similarly, abundant rainfall and humid soil conditions, in conjunction with acidic soils, might facilitate the development of anoxic niches, enhancing the growth of the brGDGT-producing bacteria (Peterse *et al.* 2009). As seen in Table 6.10, the brGDGTs I, II and III are found to be most abundant in the sediments that are highly related to the acidic sediments, with the maximum concentration being in Ia followed by II. The cyclic brGDGTs, particularly IIb and IIc occur in low concentrations or are below detection limit. GDGTs Ib is usually the most abundant cyclic brGDGT, followed by III and I. The abundance of the cyclic branched GDGTs in the Petrockstowe Basin samples are in agreement with earlier evidences of *in-situ* production of brGDGTs in several large rivers as reported by Kim *et al*. (2012), Yang *et al*. (2013) and De Jonge *et al*. (2014).

MBT'

The MBT' values for the Petrockstowe sediments vary from 0.41 to 0.99, which is similar to the range of global soils as reported by Peterse *et al*. (2012). Only two of the samples have MBT' values of less than 0.50 while the rest are > 0.50. The MBT' value is normally believed to change in response to the temperature in soils and lakes (Weijers *et al.* 2007a, Peterse *et al.* 2009, Sun *et al.* 2011). It is observed that the higher temperatures correspond to greater MBT' and low methylation in brGDGTs. The MBT' record shows an oscillation from 0.61 – 0.87 at the bottom to the upper horizon, though there is a marked increase at around 218 m with value ascending to 1.00. This observation is contrary to observations from the global data set, where low values of MBT', especially <0.1, were mainly found in soils from very cold and dry regions, e.g. the Arctic (Peterse *et al.* 2009) and the Tibetan Plateau (Liu *et al.* 2014), implying that very low MBT' values may be typical for global arid and cold regions. This suggests that the Petrockstowe section might probably be warmer than what is seen in very cold regions. The MBT' record differs from the CBT record in that it remains consistent with no significant shift, except at 94 m.

6.2.2 South John Acres Lane Quarry section, Bovey Basin

A summary of the geochemical data for the South John Acres Lane Quarry section is presented in Table 6.2b and the reconstructed palaeotemperatures are plotted against the lithological log in Figure 6.3. There were 26 samples analysed from this section and out of this total number only 23 samples had their MAAT reconstructed because the rest of the samples did not have enough GDGTs for analysis. Samples SJAL 12a & 12b, and 60b had no GDGTs detected in them. Samples SJAL 17b, 29b, 37b, 42b, 60b, and 69b contain isoprenoid and brGDGTs while samples SJAL 34a & 34b, 38a & 38b, 42a, 60a and 65a & 65b have isoprenoid and brGDGTs but their peak heights were too low or were too noisy to

be integrated. Because of this reconstructing MAAT from these samples failed (see Figure 6.4).

It is important to note that samples SJAL049, 062, and 067B from the Bovey Basin and samples MC12, 19, 35 and 48 from Petrockstowe Basin all occurred within the lignitic facies and also show cooling to reconstructed MAAT values of 3 – 5^{o}C and 11 – 18^{o}C respectively (see Table 6.2b). These values are very low and may be so due to the limited occurrence of, or absence of the brGDGTs in these samples. For example, SJAL049 presented poor peak areas for GDGTs IIa, IIb that were below integration limit, while Ia and IIb are absent which lead to them not being included in the MAAT data plotted against lithology. However, because these GDGTs are associated with different environments which supported the preservation of either the bacteria or archaea, which subsequently affects the distribution of the GDGTs preserved in the sediments, it could be suggested to some extent that the reconstructed MAAT, have some elements of covariance to the facies that supported the preservation of these GDGTs. This may be why Schouten *et al*. (2008) cautioned that results of MAAT reconstructed during the Palaeogene using the MBT'/CBT proxy should be interpreted with care as there may be potential bias due to seasonal difference.

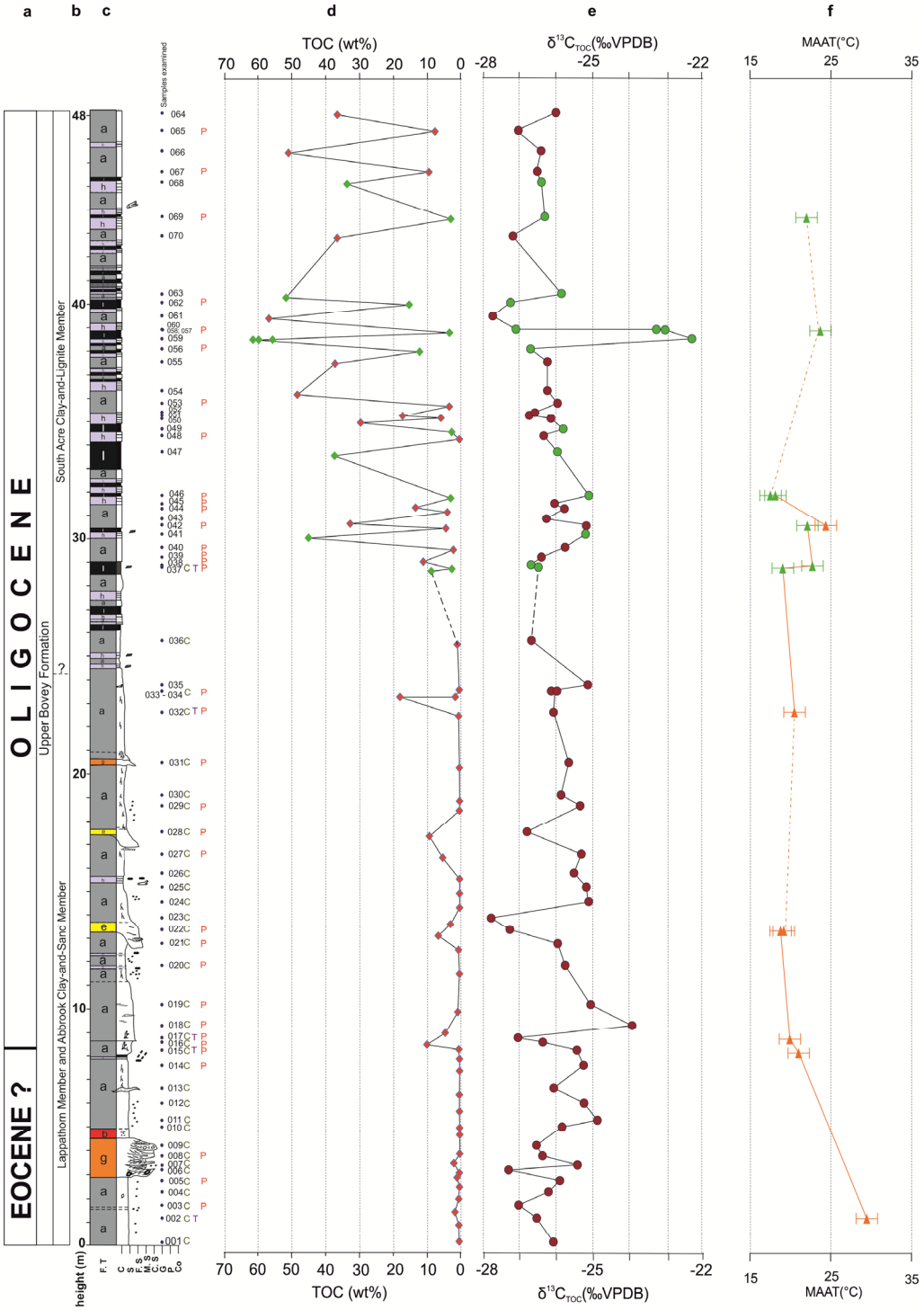

Figure 6.3: Data from South John Acres Lane Quarry section, Bovey Basin, Southwest, UK (a) age, (b) height, (c) lithological section, (d) total organic carbon, (e) stable carbon isotope (δ13CTOC), (f) reconstructed mean annual air temperature using the MBT'/CBT proxy. Error bars reflects long –term reproducibility based on replicate standard of BROC 2 standards. All $\delta^{13}C$ results have been adjusted to 0.1‰.

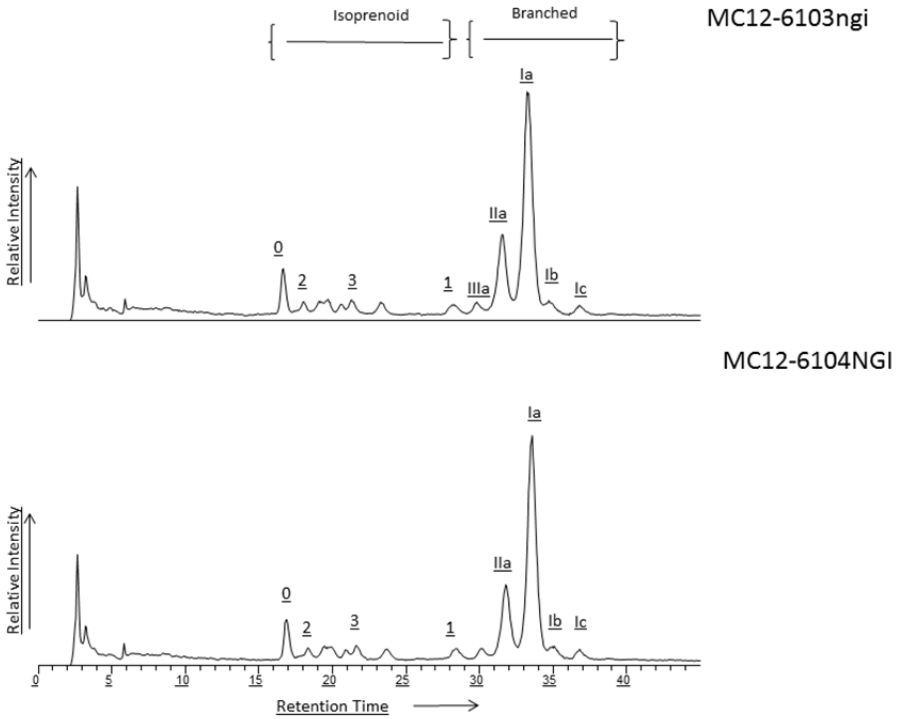

Figure 6.4: High Performance Liquid Chromatography/Atmospheric Pressure Chemical Ionization-Mass Spectrometry (HPLC/APCI-MS) base peak chromatograms of a polar fraction showing relative abundance and distribution of both isoprenoidal and branched GDGTs. GDGT-0 to GDGT-4 refer to isoprenoidal containing 0 -4 cyclopentane moieties respectively; Roman numerals refers to branched GDGTs. These are typical example of results from MC12a & b where most of the GDGTs were detected in these samples

CBT

CBT values in the South John Acres Lane Quarry section of the Bovey Basin were in the range of 0.42 – 1.67. At 1.20 m depth the CBT was 0.42 and increased to 1.67 corresponding to a depth of 8.50 m, and suddenly decreases to 1.42 at 28.80 m within the lignitic clayey part (Figure 6.7). After this point the CBT rises once again to 1.60 at 30.5 m and then decreases again to 1.18. Finally, the CBT rose to 1.40 at 43.70 m which happens to be the last sample in this section.

pH

The pH values reconstructed from the Bovey Basin are in the range of 4.60 – 5.57, which may suggest that deposition was under less acidic conditions than in the Petrockstowe Basin. This pH value is indicative of a specific environment as well as fitting within the depositional environment, indicated in the facies analysis i.e. peat swamps in a lake or delta plain. That is, this pH range is similar to values found in other peat and coals (Weijers *et al.* 2011). However, it should be noted that only a small section of the Bovey Basin was analysed. With this in mind the less acidic conditions could have had some influence on the distribution of the GDGTs. Table 6.2 shows that samples SJAL12a & 12b and SJAL060b have no GDGTs present, probably either due to lithology or poor preservation conditions. BrGDGTs I & II shown in Figure 6.5 are found to be the most abundant in the sediments, which could be related to the acidic nature of the sediments, where the maximum concentration is Ia followed by IIa. The cyclic brGDGTs especially Ic & IIa are either below detection limit or absent. BrGDGT Ia is usually the most abundant cyclic brGDGT followed by Ib, Ic and IIIa. The isoGDGTs are somewhat abundant in the Bovey Basin, especially isoGDGT-0. IsoGDGTs are abundant, with maximum concentration being in isoGDGT-0, followed by isoGDGT-1 and GDGT-2, while low concentrations were observed in GDGT-3 and GDGT-Cren or (GDGT-4). The GDGT-Cren' has not been detected in any of the samples from the Bovey Basin.

MBT'

The MBT' values for South John Acres Lane Quarry sediments are in the range of 0.30 to 1.00 and are within the range of those reported by Peterse *et al*. (2012) in their global record. Results of MBT' for sediment from the Bovey Basin are all > 0.50. Only sample SJAL29b has a lower MBT' value, with that of 0.30. A similar single value like this was also noted in the Petrockstowe sediment.

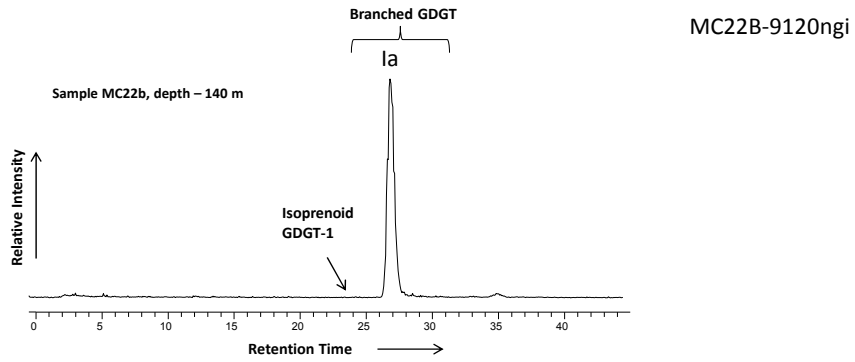

Figure 6.5: High Performance Liquid Chromatography/Atmospheric Pressure Chemical Ionization-Mass Spectrometry (HPLC/APCI-MS) base peak chromatograms full scan of a polar fraction of samples MC22 at a depth of 140 m showing relative abundance of branched GDGTs with only one isoprenoidal GDGT. Roman numerals refer to branched GDGTs.

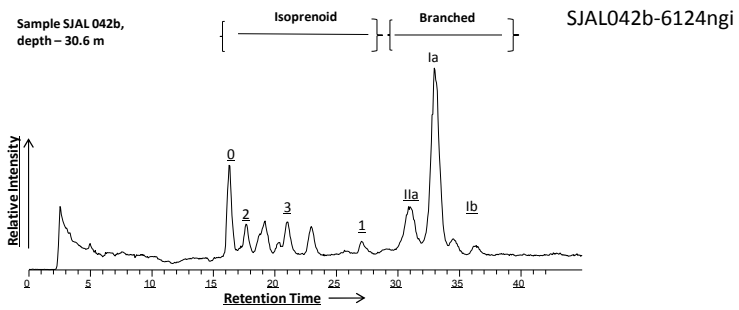

Figure 6.6: High Performance Liquid Chromatography/Atmospheric Pressure Chemical Ionization-Mass Spectrometry (HPLC/APCI-MS) base peak chromatograms full scan of a polar fraction samples SJAL60A at a depth of 38.9 m and SJAL 042b at a depth of 30.6 m respectively showing relative abundance of isoprenoidal and branched GDGTs. GDGTs-0 to GDGT-4 refer to

isoprenoidal GDGTs containing 0-4 cyclopenatne moties Cren' (Sinninghe et al. 2002); Roman numerals refer to specific branched GDGTs (Figure 2.7).

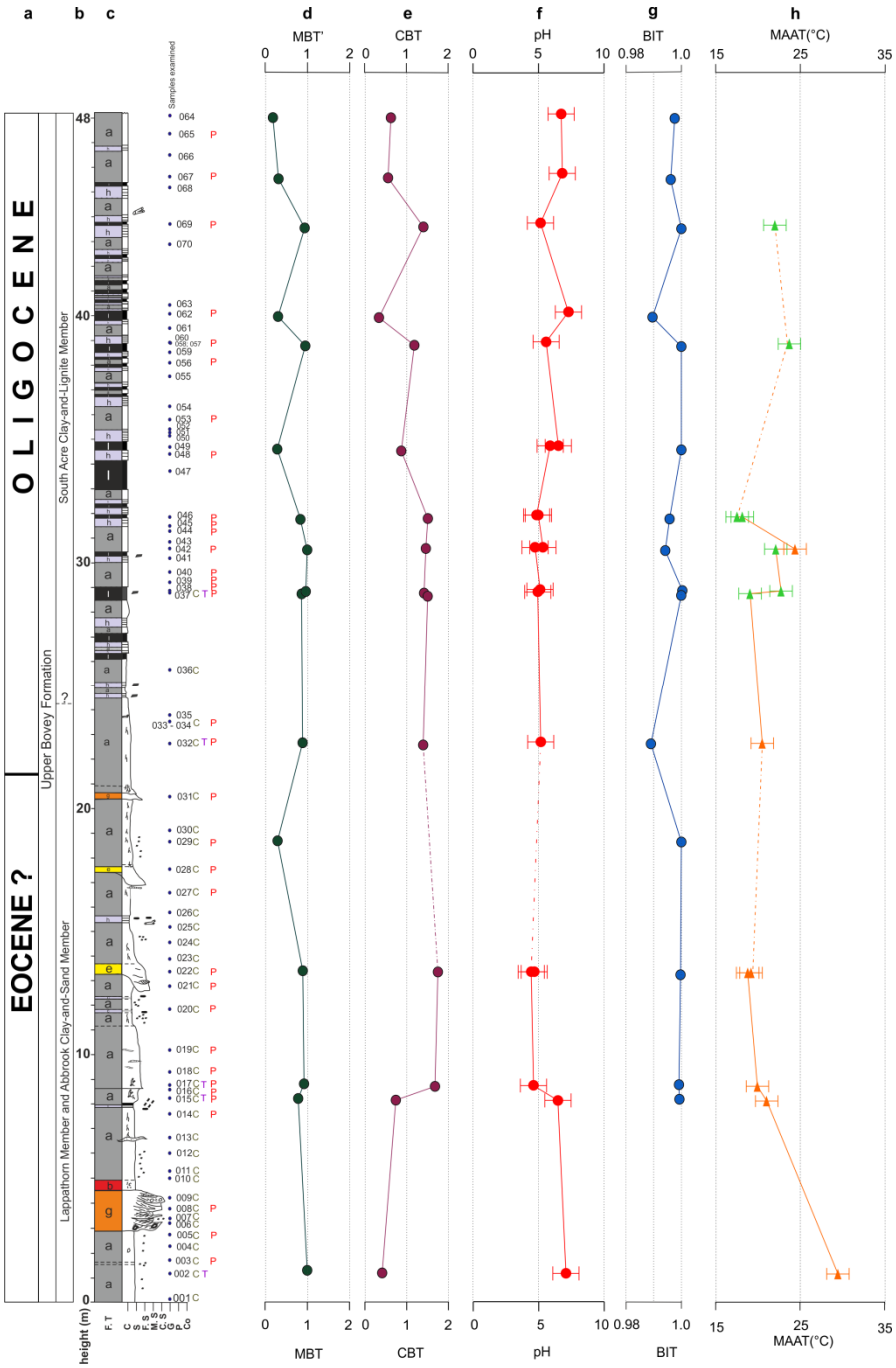

Figure 6.7: Data South John Acres Lane Quarry, Bovey Basin, Southwest, UK (a) age, (b) height, (c) lithological section (d) MBT', (e) CBT, (f) pH, (g) BIT, and (h) reconstructed MAAT using MBT'/CBT proxy.

6.3 Reconstructed Mean Annual Air Temperature (MAAT)

There is a poor terrestrial temperature record for the northern mid latitude of Europe through the Palaeogene. This new study therefore adds to this limited data set in a significant way. Results from this study show reconstructed MAAT obtained for the Petrockstowe Basin varied between 14 and 20^{o}C during the Eocene – Oligocene (Figure 6.1j & 6.2). Interestingly, towards the proposed Eocene – Oligocene boundary (Turner 1979), the data show that MAATs dropped gradually, probably during the early Oligocene, to 18 −12^{o}C (Figure 6.1j & 6.2). This suggests a significant cooling of ~ 4 - 5^{o}C within South West England. This is backed up by the palynology results shown in Chapter 4, pages 48 - 50 of this thesis. This new data from the Petrockstowe Basin shows a similar trend to those data reconstructed in the Greenland Basin during the late Eocene and early Oligocene (Schouten *et al.* 2008) although the absolute temperature values were not the same, they exhibit a similar cooling trend where they recorded a cooling of 3 - 5 ^{o}C linked to the Eocene – Oligocene climate transition. The cooling trend observed in this study is similar to those recorded in Hampshire Basin obtained using clumped isotope indicated that land temperatures from northern Europe decreased by an average of ~4 – 6°C from the late Eocene to the early Oligocene (Hren *et al.* 2013). Comparing results of Hren *et al*. (2013) with the continental North American data (Zanazzi *et al.* 2007, Zanazzi *et al.* 2015), suggest that there was a similar cooling trend on both sides of the Atlantic.

In a study carried out on a new sedimentary record from the Wilkes Lang Margin, East Antarctica, during the Integrated Ocean Drilling program (IODP Expedition 318 Site U1356) using the MBT'/CBT proxy, warm terrestrial temperatures during the early Eocene were followed by a marked cooling during the mid-Eocene (Pross *et al.* 2012). Soil temperatures of ~24 - 27^{o}C for the early Eocene and ~17 - 20^{o}C for the mid-Eocene were determined (Pross *et al.* 2012). These temperatures in terms of absolute values are similar to the reconstructed MAAT record obtained from the South John Acres Lane Quarry section of

the Bovey Basin which is in the range of 24 −18^{o}C. The results of the MBT'/CBT reconstructed temperature of this study, suggest a warmer climate in the mid latitudes of Northern Europe during the Eocene greenhouse world tend to be slightly colder than the MMST predicted climate models (Huber & Caballero 2011).

The new MAAT data in this study have also been compared with records of TEX_{86}, $UK^{k'}_{37}$ and reconstructed SST for the early Eocene and middle Eocene obtained from the Ocean Drilling Project Leg 189 Site 1171, from the South Atlantic (Bijl *et al.* 2009). This comparison shows that current MAAT data from both Petrockstowe and Bovey basins fall below the majority of the data set in the northern latitude reconstructed from bivalve-shell $\delta^{18}O$, TEX_{86} and SST for the early and mid-Middle Eocene from Seymour Island, East Tasman, New Zealand, Tanzania and DSP site 277 and ODP sites (1090, 925, 336)(Figure 6.8). This suggests that the MAAT data reconstructed from MBT'/CBT proxy from the present, albeit warmth but not as high as those recorded in the early Palaeogene climates which was forced by high atmospheric greenhouse gas concentration (Zachos *et al.* 2008). The MAAT record from this study, despite being of a lower magnitude than that observed at high southern latitude suggests cooling during the Eocene (Bijl *et al.* 2009, Hollis *et al.* 2009).

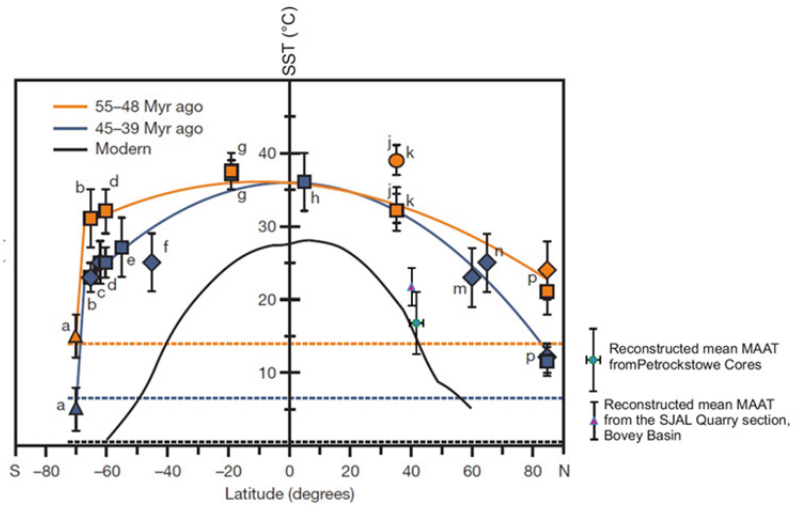

Figure 6.8: Comparison of the early and middle Eocene latitudinal SST gradients with reconstructed MAAT data from the Petrockstowe and Bovey Basins. A combination of bivalve-shell δ18O (triangles), TEX86 (squares), UKk'37 (diamonds) SST reconstructed for the early Eocene and mid-middle (blue) Eocene (data from Seymour Island (a); the East Tasman Plateau (b); Deep Sea Drilling project (DSDP) Site 277 (c); New Zealand (d); DSDP Site 511 (e); Ocean Drilling Project (ODP) Site 1090 (f); Tanzania (g); ODP Site 925 (h); New Jersey (j, k; circle represent peak PETM SSTs); ODP Site 336 (m); ODP Site 913 (n) and the Arctic Ocean (p). Black and dashed lines represent the present-day zonally averaged latitudinal temperature gradient and age-specific deep-sea temperatures respectively modified from (Bijl *et al.* 2009).

CHAPTER 7: SYNTHESIS

The aims of this research were to:

- Constrain the chronology of the Bovey and Petrockstowe basins using a combination of palynological and chemostratigraphic techniques.
- Understand the changing palaeoenviroment of the Bovey and Petrockstowe basins and how they responded to climatic change during the Palaeogene.
- Investigate the regional response to transient and rapid climatic events such as hyperthermals and the Eocene – Oligocene boundary event.
- Generate the first absolute estimates of mean annual air temperature (MAAT) from the early Palaeogene, from Northern European terrestrial sections.

To achieve these aims sedimentary facies analysis, chemostratigraphic analysis (using $\delta^{13}C_{TOC}$), palynological analysis and MBT'/CBT techniques were used to reconstruct the palaeotemperature for two terrestrial basins: the Bovey and Petrockstowe.

7.1 Age model for the Petrockstowe and Bovey basins

Based upon the results of this study two separate age tie points have being suggested as being present within the two basins: The Eocene Thermal Maximum - 2 (ETM-2) and the Eocene – Oligocene transition (EOT) in the Petrockstowe Basin and the EOT in the Bovey Basin. The first of these, ETM-2 is based upon a carbon isotope excursion (CIE) of around -2‰ which is recorded in the lower part of the Petrockstowe Basin. The $\delta^{13}C_{TOC}$ shift falls within the limit of the global terrestrial CIE for ETM-2 as recorded in global locations like the Bighorn Basin where a CIE of ~ 3.8 and ~ 2.8 magnitude were documented using carbon isotope records from palaeosol carbonates (Abels *et al.* 2012a, Abels *et al.* 2015, Lauretano *et al.* 2015).

Turner (1979) suggested that the Eocene – Oligocene transition occurred in the upper part of the Petrockstowe Basin based upon pollen data. Furthermore, Early Oligocene sediments

were first reported by Chandler (1957, 1964) to be present in the Bovey Basin. The presence of Eocene indicators like *Anacolside* and *Pompeckjoidaepollenites* were encountered at ~185 m into the upper Bovey Formation (Chandler 1964). Selwood *et al*. (1984) on the other hand recorded lower to middle Oligocene sediments 290 m below the Abbrook Clay-and-Sand Member of the Bovey Basin.

The previous studies placed the EOT in the Bovey Basin at below 185 m (Chandler 1957, Chandler 1964) while Wilkinson & Boulter (1981) places it at around 138 m and suggested that further downward the sediments are probably older and therefore considered them to be of Eocene age. This is against the evidence recorded in the present study which places the EOT boundary at a higher level of ~143 m using the deepest borehole record drilled in Bovey Basin with OS Grid Reference 8527 7297 which has penetrated the Upper Bovey Formation down to the boundary between Abbrook Clay-and-Sand Member and Southacre Clay-and-Lignite Member (Figure 7.1). Although it should be noted that there is a slight palynological shift, as evidenced by the disappearance of one of the main Eocene markers (*Pompeckjoidaepollenites*) and the increase in abundance of species related to trees, shrubs and herbs of broad affinity and palm pollens for (example *Inaperturopollenites*, *Arecipites*, and *Monocolpopollenites*) that suggests cooling towards the early Oligocene may have started at a greater depth ~300 m. In the Petrockstowe Basin the EOT boundary was placed at ~ 110 m (based upon biostratigraphy and MAAT) which is consistent with the previous results of Turner (1979) which was designated to be at around 120 m. In the Petrockstowe Basin ETM-2 was identified at around 595 m, but in the Bovey section it can only be inferred because an equivalent depth was not encountered in this study. As shown in Figure 7.2 Wilkinson & Boulter (1981) presented an earlier correlation of two basins in the south west England (Petrockstowe and Bovey), one in Wales (Mochras) and two in Northern Ireland (Washing Bay and Mire House) with, Mire House and Mochras being younger than the Bovey Basin. The new age model of the EOT for both the Petrockstowe and Bovey show similar cooling trend of about 10 – 12 °C which is similar to what is documented in

other terrestrial EOT's (Table 7.1) (Grimes *et al.* 2005, Pearson *et al.* 2008, Sheldon *et al.* 2012, Hren *et al.* 2013).

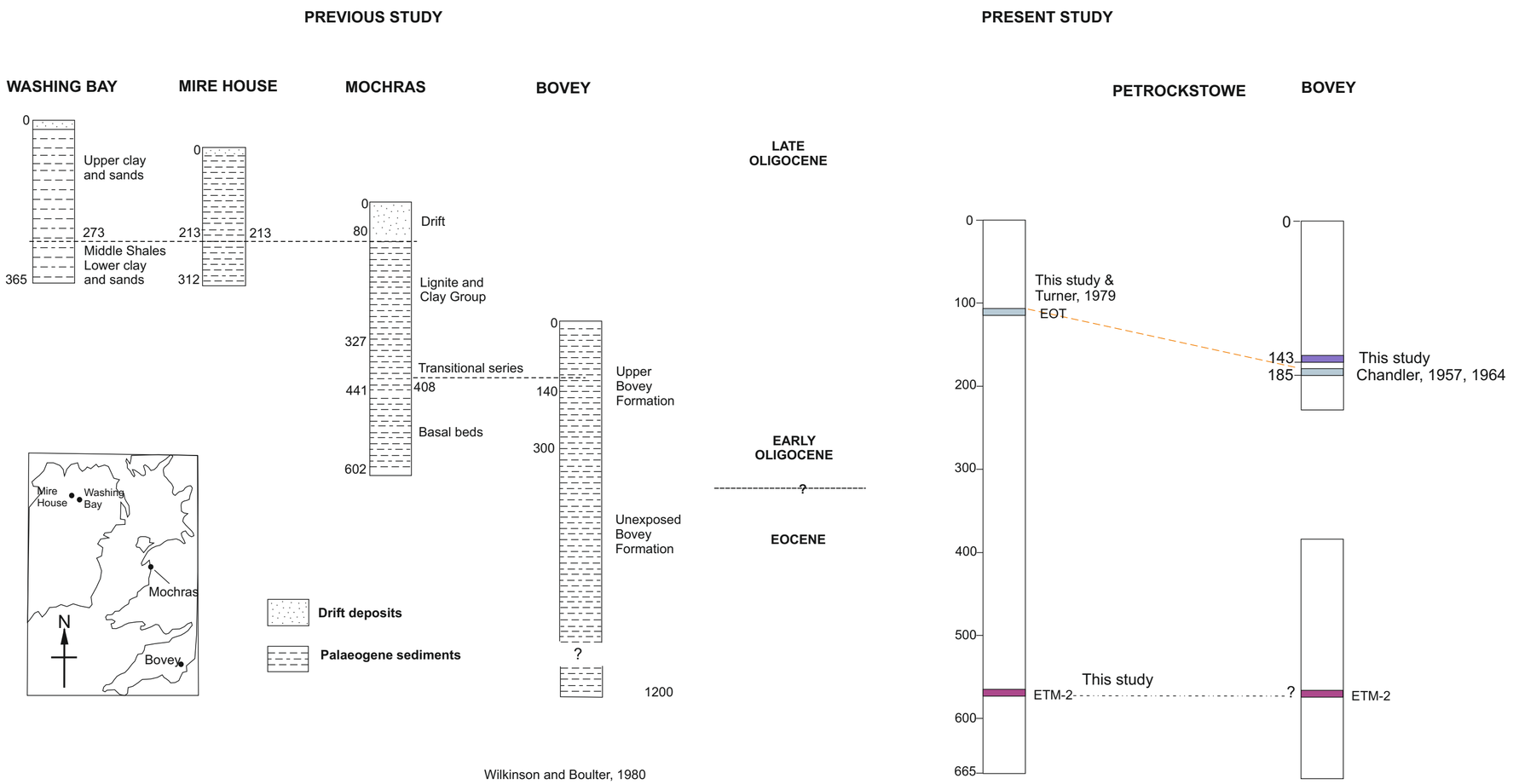

Figure 7.1: Chronostratigraphic correlation of the EOT in the Petrockstowe and Bovey basins based on integrated data from the present study and Chandler, 1957, 1964 and Wilkinson & Boulter, 1980.

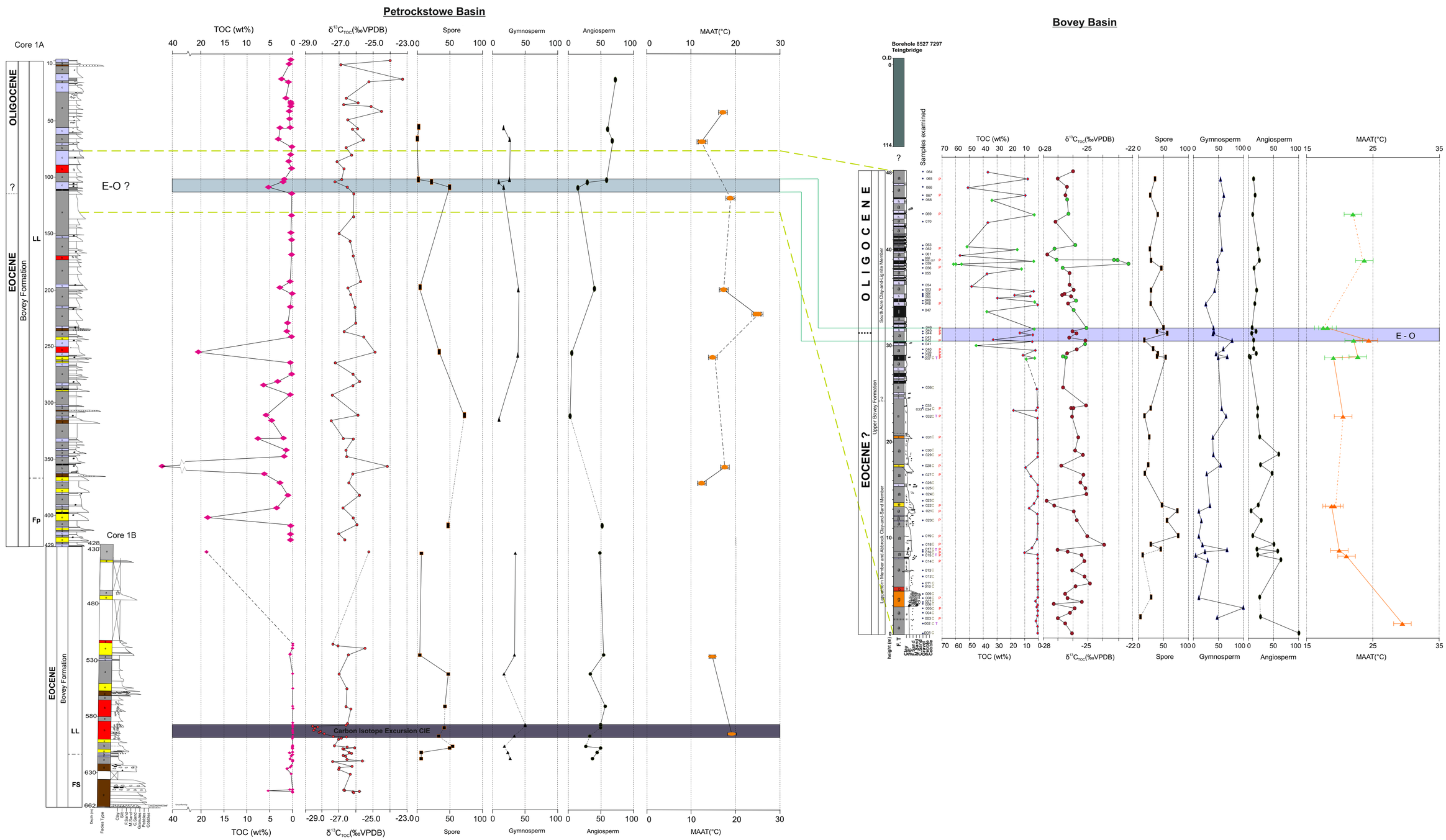

Figure 7.2: The Eocene – Oligocene boundary in the Petrockstowe and Bovey basins an dthe ETM-2 in the lower Petrockstowe core 1B, TOC (%TOC), stable carbon isotope ($\delta^{13}C_{TOC}$), Spores (%), Angiosperm (%), Gymnosperm (%), reconstructed mean annual air temperature (MAAT). Error bars reflects long-term reproducibilty based on replicate analysis of standard of BROC 2. All $\delta^{13}C_{TOC}$, results have been adjutsed to 0.02‰, the size of the error bar are smaller than the data points.

7.2 Long-term palaeoenvironmental changes during the Palaeogene in the Petrockstowe and Bovey Basins

In the Petrockstowe Basin sand-filled fluvial channels, a flood plain and an ephemeral lake or lake margin succession have been modelled as the depositional environments of these sediments, representing a deepening up succession. While in the Bovey Basin, an overall shallowing trend has been established in the succession evidenced by either constant sedimentation and subsidence for a long time or by sedimentation exceeding subsidence suggesting tectonism might be responsible for variation in the lithofacies. The presence of extensive lignitic beds in the South John Acres Lane Quarry section, Bovey Basin, represents an excellent archive of environmental change, which is predominantly composed of in-situ plant material that preserved changes in the atmospheric carbon budget over time. Four main facies associations were modelled for these basins, the long-lived lake or lake centre, ephemeral lake or lake margin, flood plain and sand filled fluvial channels. The various facies associations, show different responses to climate as demonstrated by the various proxies used.

Correlation of the two basins has indicated that the lower part of the South John Acres Lane Quarry section, Bovey Basin, and the upper part of the Petrockstowe core fall within the long-lived lake or lake centre while the upper part of the Bovey section is occurring within the ephemeral lake or lake margin associations. The upper part of the South John Acres Lane Quarry section is composed mainly of the South Acre Clay-and-Lignite Member, which correlates well with the Eocene-Oligocene deposits in the Petrockstowe Basin (Turner 1979) (see Figure 7.1).

The palynological data from the Bovey and Petrockstowe basins were used in determining how the depositional environment influenced the palynofacies type and whether there is a floral change that may be coincident with the onset of the CIE (Smith *et al.* 2007) in the lower Petrockstowe core. Similarly, to determine if there is any floral change and

temperature variation in the upper Petrockstowe core and South John Acres Lane Quarry section of the Bovey Basin coincident with the Eocene – Oligocene transition. These data were accompanied by MBT'/CBT proxy data. In summary the CIE was dominantly composed of phytoclast palynofacies and equal proportions of AOM and palynomorphs. The different palynofacies could be a representation of the different plant material that was deposited into the basin throughout the stratigraphic record and served as potential source of the organic matter contribution.

In order to assess whether a change in flora occurred coincident with the onset of the hyperthermal event, the relative abundance of Gymnosperm, Angiosperm, spores and fungi was compared to the CIE in the Petrockstowe Basin (Figure 7.1). In the lower part of the Petrockstowe core there was evidence of the predominance of Gymnosperm and Angiosperm population against low occurrences of spores and fungi recorded. Changes in vegetation coincident with the CIE are associated with terrestrial environment and this could also be related to increased $\delta^{13}C$ fractionation (Smith *et al.* 2007). The little vegetation or floral changes occurring within the body of the CIE, has not influence the magnitude of the CIE.

7.3 The ETM-2 in the Petrockstowe Basin

The 'Maximum CIE' method of Domingo *et al*. (2009) was applied to determine the CIE in the lower Petrockstowe core 1B where there is a significant shift in $\delta^{13}C_{TOC}$ values of - 2‰, which is within the range of terrestrial CIEs recorded globally for ETM 2 (Koch *et al.* 1992, Bowen *et al.* 2002, Abels *et al.* 2012b). The corresponding absence of *Pistillipollenites* pollen, *Platycaryapollenites playcaryoids* sp. and *Triatriopollenites caryophaenus* sp. while the presence of *Monocopopollenites* sp. *Inaperturopollenites* sp. *Laevigatisporites* sp, Biassacate, also suggests that the CIE is associated with ETM-2. This investigation suggests also that there is no systematic variation between CIE and depositional environment recorded in the lower Petrockstowe core because the CIE occurred within the same lithofacies (i.e. silty clay) (Figure 7.1). There is no defined trend of the MAAT within the

main body of the CIE, as there were only two data points that were integrated due to lack of the presence of GDGTs contents in most of the samples found in the part of the core.

7.4 The E-O boundary at the Petrockstowe and Bovey Basins

The Eocene – Oligocene transition has been proposed in the upper Petrockstowe Basin which is in agreement with the earlier opinion of Turner (1979) based upon pollen data. The reconstructed mean annual air temperature (MAAT) revealed that palaeotemperatures dropped from 28^{o}C to 12°C showing that there is a significant cooling coincident with this boundary. The temperature observed in this study is similar to the cooling recorded in the Solent Group, Hampshire Basin, UK where the clumped isotope methodology was adopted to measure the Δ47 of aragonite shells of fresh water gastropod *Viviparus lentus* (Hren *et al.* 2013). Hern *et al* (2013) observed a decrease of ~10°C of growing season temperature during the EOT; this corresponded to ~ 4 – 6°C decrease in MAAT from the late Eocene to the early Oligocene, yet it does no directly influence seasonality. The cooling recorded is also consistent with other documented marine and terrestrial biotic changes from Greenland (Schouten *et al.* 2008) and from east Antarctica where temperatures reconstructed using MBT'/CBT gave a conservative estimate in the range 24 and 27°C for the early Eocene suggesting the coldest mean summer temperature (MST) (Pross *et al.* 2012). This result is similar although, slightly warmer compared to the terrestrial MST deducted by climate models with the application of high radiative forcing 20 – 25°C (Kershaw 1988). Also, soil temperatures reconstructed from the rainforest biome gave ~24 - 27°C for early Eocene and ~17 - 20°C for mid Eocene respectively were reconstructed using MBT'/CBT palaeothermometry for a warm terrestrial climate in the early Eocene and proved cooling at mid Eocene were in closed range to those of the MST (Pross *et al.* 2012). Marine temperature records in the high latitudes between 45° to 70° in both northern and southern hemisphere temperatures were found to be about 20°C prior to the EOT climatic transition and suddenly cooled to an average temperature of ~5°C based on proxy records of sea surface temperature from different locations (Liu *et al.* 2009).

The new data set reported here, has improved our current understanding of the EOT of Europe particularly from the continental section. In the upper Petrockstowe Basin, there was a decrease in the abundance of Gymnosperms like *Inaperturopollenites*, *Monocolpopollenites*, *Sequoaipollenites* and Angiosperms like *Tricolpate*, *Salixpollenites*, *Tetrapollenites*, *Pityospollenites* and *Ilexpollenites* across the EOT which are associated with a warm temperate climate which suggest a cooling event coincident with the drop in MBT'/CBTtemperatures. In the Bovey Basin a - 2‰ $\delta^{13}C_{TOC}$ shift coincided with changing lithofacies and a palynological change co-occurring with the disappearance of one of the major Eocene markers (*Pompeckjoidaepollenites*). The presence of species related to trees, shrubs and herbs of broad affinity, which tend to reflect palm pollen characteristics, suggests the climate as of then might be probably frost free. This palynological change and its accompanying $\delta^{13}C_{TOC}$ change therefore strongly suggests the presence of the Eocene – Oligocene boundary in both South John Acres Lane Quarry section, Bovey Basin and the upper Petrockstowe Basin. This is consistent with records documented by Chandler (1964), Selwood *et al* (1984) as evidence by similar climatic conditions in the Hampshire Basin (Collinson *et al.* 1981, Hooker *et al.* 2004, Hren *et al.* 2013).

Table 7.1: Terrestrial and marine Sites of the Eocene Oligocene Transition (EOT) locations in the mid - high latitudes

Geologic Age	Palaeolatitude	Location	Palaeotemperatures	ΔT	Reference
~ late Eocene early Oligocene	40°N	Petrockstowe & Bovey basins, South West, UK	25 -12°C; 21 to 18°C; max - min	13°C	Present Study
EOT ~34 - 33.7Ma	31°33'N, 88°02'W	St Stephen Quarry, Alabama, Gulf of Mexico, USA	SST >28°C (i.e.between 22±2.2°C and 33±2.2°C	11°C	Wade *et al*., 2012
EOT 33.5 - 34.0Ma	40N	Ebro Basin, Spain	~8°C and 14°C	6°C	Sheldon *et al*., 2012
EOT	75°29.356'N, 6°56.810'W	Norwegian Greenland Basin, Northern hemisphere, ODP Site 913B	Late Eocene MAAT ~13 - 15°C; Near E-O Boundary ~ 3 - 5°C	2°C	Schouten *et al*., 2008
33.5N E- O Lower Oligocene	75°29.356'N 6°56.810'E; 67°47.11'N 01°02.0'E 66°56.49'N 6°27.01'W	Norwegian Greenland Sea, Northern hemisphere	WMMT of 14°C±3°C; CMMT of 10 - 11°C±3C	3°C	Eldrett *et al*., 2009
34 - 33.5Ma	45 - 50°N	Hampshire Basin, UK	MAAT is 24°C before 34 Ma; 18°C early Oligocene, 4 - 6°C MAAT dropped using *V.Lentus* Clupmed isotope	6°C	Hren *et al*., 2013

7.5 Further work

The investigation of the Palaeogene sediments of the Petrockstowe and Bovey basins in SW England has identify areas for further enquiry that could be investigated. These are:

- High resolution analysis for palynology and MBT'/CBT possibly at a very short interval (~ 20 cm) would be recommended to constrain further the Eocene – Oligocene boundary in the Petrockstowe and Bovey basins. This is because the three samples indicating the cooling trend cannot be considered to be sufficiently robust to establish a cooling event history.
- Due to an absence of carbonates in the two basins, this study lacks an oxygen isotope record. This is a result of the high pH value of the environment. However, such a record could potentially be generated using the $\delta^{18}O$ of freshwater lake diatoms. They are silicates and therefore can be preserved in more acidic environments. For example in areas like Lake Pinarbasi, Turkey (Leng *et al.* 2001), a $\delta^{18}O_{diatom}$ curve proved the application of the $\delta^{18}O_{diatom}$ in palaeoclimatic reconstructions of terrestrial (lake, lacustrine) environments. Furthermore, a pilot

study using the Sodium Polytungstate ($3Na_2WO4_9WO_3.H_2O$) Separation (SPT) method for diatom extraction following (Morley *et al.* 2004) technique and subsequent SEM analyses (but not reported in this study) show a limited number of unidentified freshwater diatoms in sample MC52 at depth of about 391 m from the Petrockstowe core 1A, Petrockstowe Basin. Hence further research on this aspect is therefore strongly recommended.

- Extend organic geochemical study to look for palynological change using biomarkers such as long chain n-alkanes and n-alkanoic acids for example Alkenones $C_{37} – C_{39}$, Alkyl-alkenones $C_{36.}$

APPENDICES

Appendix 1

Table 4.3.1: Palynofacies results for Petrockstowe 1A core, Petrockstowe Basin, South West, UK

Sample ID	Slide No (BGS)	Depth (m)	Amorp (%)	Palyno (%)	Phy-Brwn (%)	Phy-Blk (%)	Trans (%)	Fungi (%)
MC3	MPA61578	23.5	10.2	4.0	74.3	3.1	7.7	0.6
MC12	MPA61579	65.8	21.3	32.5	0.6	5.0	36.9	3.8
MC13	MPA61580	75.5	37.3	42.2	3.7	6.7	9.8	0.3
MC18	MPA61581	109.4	28.9	23.7	7.0	6.1	30.7	3.6
MC19	MPA61582	111.3	24.0	58.9	2.6	1.8	12.8	0.0
MC20	MPA61583	116.0	21.4	58.7	11.1	1.6	7.1	0.0
MC27	MPA61584	202.3	18.5	73.2	1.5	3.0	3.9	0.0
MC35	MPA61585	257.3	23.9	66.0	1.3	1.6	6.6	0.6
MC42	MPA61586	311.2	10.2	76.4	0.6	0.3	9.3	3.2
MC48	MPA61587	354.8	9.9	79.8	0.7	1.1	8.5	0.0

Table 4.3.2: Palynofacies results for Petrockstowe 1B core, Petrockstowe Basin, South West, UK

Sample ID	Slide No (BGS)	Depth (m)	Amorp (%)	Palyno (%)	Phy-Brwn (%)	Phy-Blk (%)	Trans (%)	Fungi (%)
MC-54	MPA62269	405	0.7	15.3	3.3	63.0	10.0	7.7
MC-58	MPA62270	432	1.7	21.3	36.7	14.7	6.7	19.0
MC-60	MPA62271	523	0.0	25.0	31.7	10.0	20.0	13.3
MC-61	MPA62272	540	6.0	48.3	17.3	25.0	0.3	3.0
MC-63	PMA62273	569	5.7	83.0	1.3	10.0	0.0	0.0
MC-95	MPA62274	586	9.0	1.0	1.0	89.0	0.0	0.0
MC-64	MPA62275	586	4.0	3.0	34.7	58.0	0.0	0.3
MC-101	MPA62276	587	0.0	0.3	3.3	96.0	0.3	0.0
MC-102	MPA62277	588	2.0	6.0	24.3	61.0	6.3	0.3
MC-103	MPA62278	590	0.0	1.3	0.3	98.0	0.3	0.0
MC-104	MPA62279	591	1.0	1.0	6.3	91.0	0.3	0.0
MC-65	MPA62280	593	5.7	2.7	6.0	83.3	2.0	0.7
MC-96	MPA62281	596	3.7	4.3	42.0	41.7	6.3	2.0
MC-97	MPA62282	596	2.7	21.7	11.3	59.0	3.0	2.3
MC-66	MPA62283	598	4.0	3.0	12.3	79.3	1.0	0.3
MC-67	MPA62284	604	6.1	2.6	17.8	72.6	0.4	0.4
MC-68	MPA62285	605	7.0	5.3	13.3	73.3	0.7	0.3
MC-70	MPA62286	607	1.3	3.3	14.0	81.0	0.3	0.0
MC-73	MPA62287	611	1.3	36.7	27.7	22.7	5.7	6.0
MC-76	MPA62288	616	1.0	28.3	35.3	28.3	0.0	7.0

Table 3.3.3: Palynofacies results for the South John Acres Lane Quary section, Bovey Basin, Southwest, UK

Sample ID	Slide No (BGS)	Depth	Amorp (%)	Palyno (%)	Phy-Brwn (%)	Phy-Blk (%)	Trans (%)	Fungi (%)
SJAL065	MPA63260	47.4	8.3	85.7	0.0	0.7	4.0	1.3
SJAL067	MPA63259	45.7	15.3	72.0	1.0	1.0	9.0	1.7
SJAL069	MPA63258	43.7	3.3	91.7	0.0	2.0	2.3	0.7
SJAL062	MPA63257	40.1	18.7	73.3	0.3	2.0	5.3	0.3
SJAL060	MPA63256	38.9	17.7	71.7	1.0	2.3	7.0	0.3
SJAL056	MPA63255	38.1	28.0	53.7	1.0	5.7	11.7	0.0
SJAL053	MPA63254	35.8	32.3	51.6	2.8	1.4	10.9	1.1
SJAL048	MPA63253	34.4	25.4	3.2	54.2	0.0	16.2	1.1
SJAL046	MPA63252	31.9	15.0	76.3	0.0	0.7	8.0	0.0
SJAL045	MPA63251	31.5	16.0	70.0	0.7	0.3	13.0	0.0
SJAL044	MPA63250	31.3	18.7	77.3	0.0	0.0	3.7	0.3
SJAL042	MPA63249	30.6	0.0	0.0	0.0	0.0	0.0	0.0
SJAL040	MPA63248	29.7	7.0	81.0	0.0	0.0	12.0	0.0
SJAL039	MPA63247	29.2	39.7	34.0	1.3	1.3	23.0	0.7
SJAL038	MPA63246	28.9	17.0	43.3	0.7	6.7	18.7	13.7
SJAL037	MPA63245	28.8	22.0	67.3	0.0	1.3	8.7	0.7
SJAL036	MPA63244	25.7	0.0	0.0	0.0	0.0	0.0	0.0
SJAL034	MPA63243	23.5	25.7	14.3	0.4	1.6	58.0	0.0
SJAL032	MPA63242	22.7	29.3	64.7	0.3	2.7	3.0	0.0
SJAL031	MPA63241	20.5	36.8	11.7	0.0	14.2	37.2	0.0
SJAL029	MPA63240	18.7	49.0	2.3	0.0	48.0	0.3	0.3
SJAL028	MPA63239	17.6	23.7	73.7	0.0	0.7	2.0	0.0
SJAL027	MPA63238	16.7	50.9	3.8	0.0	3.5	41.2	0.7
SJAL026	MPA63237	15.8	24.2	1.0	0.0	57.8	17.0	0.0
SJAL024	MPA63236	14.6	8.3	0.7	0.0	91.0	0.0	0.0
SJAL023	MPA63235	13.9	0.0	0.0	0.0	0.0	0.0	0.0
SJAL022	MPA63234	13.4	18.7	81.3	0.0	0.0	0.0	0.0
SJAL021	MPA63233	12.8	20.4	58.1	0.0	7.9	13.6	0.0
SJAL020	MPA63232	11.8	26.0	24.7	0.0	37.3	12.0	0.0
SJAL019	MPA63231	10.2	32.7	42.0	0.0	8.3	17.0	0.0
SJAL018	MPA63230	9.3	17.7	69.3	0.0	0.3	9.3	3.3
SJAL017	MPA63229	8.8	25.0	74.7	0.0	0.0	0.3	0.0
SJAL016	MPA63228	8.6	42.2	26.2	0.0	0.0	27.3	4.3
SJAL015	MPA63227	8.2	35.4	8.4	0.0	11.1	16.4	28.8
SJAL014	MPA63226	7.7	0.0	0.0	0.0	0.0	0.0	0.0
SJAL013	MPA63225	6.7	42.7	6.5	0.0	8.2	42.3	0.4

Appendix 2

Table 4.3.5: Result of palynomorphs abundance/diversity count data in each sample/slide in Petrockstow core 1A, Petrockstowe Basin, South West UK.

Sample ID	Slide Number (BGS)	Depth (m)	*Inaperturopollenites*	*Monocolpopollenites*	*Laevigatisporites*	*Plicapollis Pseudoexcelsus*	*Tricolporopollenites*	*Arecipites*	*Sequoiapollenites*	*Salixpollenites*	*Tiliaepollenites*	*Cicatricosisporites*	*Tetrad*	*Pompeckjoidaepollenites*	*Fungi/Algae*	*Trilete*	*Bissaccate*	*Graminidites*	*Porocolpopollenites*	*Tricolpate*	*Unidentified*	*Total*
MC3	MPA61578	23.5	0											3		2				3	3	11
MC12	MPA61579	65.8	1	5	3						2			4	2	5	18			56	14	110
MC13	MPA61580	75.8	2	2	1		4	9		1	83			3			37				5	147
MC18	MPA61581	109.4		1	2		42	6			1			4	6	1	24				4	91
MC19	MPA61582	111.3	19	93	59	2	57	11						5		2	7		1		8	264
MC20	MPA61583	116.0	21	24	81		4	1	4			5		3		18	5				6	172
MC27	MPA61584	202.3	10	37	13		70	16	1		33	1	1	3	5		113	4			4	311
MC35	MPA61585	257.3	16	11	36		2	3							8	1	25				3	105
MC42	MPA61586	311.2	26	38	36		8	1				197		1	2		7				4	320
MC48	MPA61587	354.8																				
MC54	MPA62269	405.1		20	4		18															42

Table 4.3.6: Result of palynomorphs abundance/diversity express in percentage in Petrockstowe core 1A, Petrockstowe Basin, South West, UK.

Sample ID	Slide Number (BGS)	Depth (m)	*Inaperturopollenites*	*Monocolpopollenites*	*Laevigatisporites*	*Plicapollis*	*Tricolporopollenites*	*Arecipites*	*Sequoiapollenites*	*Salixpollenites*	*Tiliaepollenites*	*Cicatricosisporites*	*Tetrad*	*Pompeckjoidaepollenites*	*Fungi*	*Trilete*	*Bissaccate*	*Graminidites*	*Porocolpopollenites*	*Tricolpate*	*Unidentified*
MC3	MPA61578	23.5	0	0	0	0	0	0	0	0	0	0	0	27	0	18	0	0	0	27	27
MC12	MPA61579	65.8	1	5	3	0	0	0	0	0	2	0	0	4	2	5	16	0	0	51	13
MC13	MPA61580	75.8	1	1	1	0	3	6	0	1	56	0	0	2	0	0	25	0	0	0	3
MC18	MPA61581	109.4	0	1	2	0	46	7	0	0	1	0	0	4	7	1	26	0	0	0	4
MC19	MPA61582	111.3	7	35	22	1	22	4	0	0	0	0	0	2	0	1	3	0	0	0	3
MC20	MPA61583	116.0	12	14	47	0	2	1	2	0	0	3	0	2	0	10	3	0	0	0	3
MC27	MPA61584	202.3	3	12	4	0	23	5	0	0	11	0	0	1	2	0	36	1	0	0	1
MC35	MPA61585	257.3	15	10	34	0	2	3	0	0	0	0	0	0	8	1	24	0	0	0	3
MC42	MPA61586	311.2	8	12	11	0	3	0	0	0	0	62	0	0	1	0	2	0	0	0	1
MC48	MPA61587	354.8																			
MC54	MPA62269	405.1	0	48	10		43														

Table 4.3.7: Result of palynomorphs abundance/diversity count data in each sample in Petrockstowe core 1B, Petrockstowe Basin, Southwest, UK

Smaple ID	Slide Number (BGS)	Depth (m)	*Monolet*	*Monocolpopollenites*	*Minorpollis*	*Plicapollis*	*Tricolporopollenites*	*Tricolpopollenites*	*Salixpollenites*	*Tiliaepollenites*	*Tetraporopollenites*	*Tricolpate*	*Polypodiaceoisporites sp*	*Pityosporites*	*Inaperturopollenites*	*Cicatricosisporites*	*Laevigatisporites*	*Stereisporites*	*Cingulatisporites*	*Pompeckjoidaepollenites*	*Trilete*	*Bissaccate*	*Quacudites*	*Triporate*	*Graminidites*	*Fungi/Algae*	*Total*
MC58	MPA62270	431.6		42			65		1					2	9		10				3	1			2	14	149
MC60	MPA62271	523.0		19		6	45	1	5	3					14		5				5	7			1	8	119
MC61	MPA62272	540.1	22	15		11	19		2		4		89	1	37	3	46		9	2	23	2				1	286
MC63	MPA62273	569.1	11			2			1								3			1							18
MC95	MPA62274	585.5	5	1			1														12						19
MC64	MPA62275	586.4	1	1																	9						11
MC101	MPA62276	587.0																									0
MC102	MPA62277	588.3			1		11					1					9	1								1	24
MC103	MPA62278	590.1																									0
MC104	MPA62279	591.0																									0
MC65	MPA62280	593.1																									0
MC96	MPA62281	595.6																								11	11
MC97	MPA62282	595.9				1											1					1					3
MC66	MPA62283	598.0																									0
MC67	MPA62284	603.8																									0
MC68	MPA62285	605.0		2		1	1			1						1	3	2									11
MC70	MPA62286	606.6				1											1										2
MC73	MPA62287	610.5		9			19		1	1					1		2	1				1				12	47
MC76	MPA62288	616.0		11		5	13								2		3						1	1		12	48

Table 4.3.8: Result of palynomorphs abundance/diversity express in percentage in Petrockstowe core 1B, Petrockstowe Basin, South West, UK.

Smaple ID	Slide Number (BGS)	Depth (m)	*Monolet*	*Monocolpopollenites*	*Minorpollis*	*Plicapollis*	*Tricolporopollenites*	*Tricolpopollenites*	*Salixpollenites*	*Tiliaepollenites*	*Tetraporopollenites*	*Tricolpate*	*Polypodiaisporites sp*	*Pityosporites*	*Inaperturopollenites*	*Cicatricosisporites*	*Laevigatisporites*	*Stereisporites*	*Cingulatisporites*	*Pompeckjoidaepollenites*	*Trilets*	*Bissaccate*	*Quacudites*	*Vacuopollis fsp*	*Triporate*	*Graminidites*	*Fungi*	
MC58	MPA62270	431.6	0.0	28.2	0.0	0.0	43.6	0.0	0.7	0.0	0.0	0.0	0.0	1.3	6.0	0.0	6.7	0.0	0.0	0.0	2.0	0.7	0.0	0.0	0.0	1.3	9.4	
MC60	MPA62271	523.0	0.0	16.0	0.0	5.0	37.8	0.8	4.2	2.5	0.0	0.0	0.0	0.0	11.8	0.0	4.2	0.0	0.0	0.0	4.2	5.9	0.0	0.0	0.0	0.8	6.7	
MC61	MPA62272	540.1	0.0	4.9	0.0	3.6	6.2	0.0	0.7	0.0	1.3	0.0	29.0	0.3	12.1	1.0	15.0	0.0	2.9	0.7	14.3	0.7	0.0	7.2	0.0	0.0	0.3	
MC63	MPA62273	569.1	0.0	0.0	0.0	28.6	0.0	0.0	14.3	0.0	0.0	0.0	0.0	0.0	0.0	0.0	42.9	0.0	0.0	14.3	0.0	0.0	0.0	0.0	0.0	0.0	0.0	
MC95	MPA62274	585.5	0.0	50.0	0.0	0.0	50.0	0.0	0.0	0.0	0.0	0.0	0.0	0.0	0.0	0.0	0.0	0.0	0.0	0.0	0.0	0.0	0.0	0.0	0.0	0.0	0.0	
MC64	MPA62275	586.4	50.0	50.0	0.0	0.0	0.0	0.0	0.0	0.0	0.0	0.0	0.0	0.0	0.0	0.0	0.0	0.0	0.0	0.0	0.0	0.0	0.0	0.0	0.0	0.0	0.0	
MC101	MPA62276	587.0																										
MC102	MPA62277	588.3	0.0	0.0	4.2	0.0	45.8	0.0	0.0	0.0	0.0	4.2	0.0	0.0	0.0	0.0	37.5	4.2	0.0	0.0	0.0	0.0	0.0	0.0	0.0	0.0	4.2	
MC103	MPA62278	590.1																										
MC104	MPA62279	591.0																										
MC65	MPA62280	593.1																										
MC96	MPA62281	595.6	0.0	0.0	0.0	0.0	0.0	0.0	0.0	0.0	0.0	0.0	0.0	0.0	0.0	0.0	0.0	0.0	0.0	0.0	0.0	0.0	0.0	0.0	0.0	0.0	100.0	
MC97	MPA62282	595.9	0.0	0.0	0.0	33.3	0.0	0.0	0.0	0.0	0.0	0.0	0.0	0.0	0.0	0.0	33.3	0.0	0.0	0.0	0.0	33.3	0.0	0.0	0.0	0.0	0.0	
MC66	MPA62283	598.0																										
MC67	MPA62284	603.8																										
MC68	MPA62285	605.0	0.0	18.2	0.0	9.1	9.1	0.0	0.0	9.1	0.0	0.0	0.0	0.0	0.0	9.1	27.3	18.2	0.0	0.0	0.0	0.0	0.0	0.0	0.0	0.0	0.0	
MC70	MPA62286	606.6	0.0	0.0	0.0	50.0	0.0	0.0	0.0	0.0	0.0	0.0	0.0	0.0	0.0	0.0	50.0	0.0	0.0	0.0	0.0	0.0	0.0	0.0	0.0	0.0	0.0	
MC73	MPA62287	610.5	0.0	19.1	0.0	0.0	40.4	0.0	2.1	2.1	0.0	0.0	0.0	0.0	2.1	0.0	4.3	2.1	0.0	0.0	0.0	2.1	0.0	0.0	0.0	0.0	25.5	
MC76	MPA62288	616.0	0.0	22.9	0.0	10.4	27.1	0.0	0.0	0.0	0.0	0.0	0.0	0.0	4.2	0.0	6.3	0.0	0.0	0.0	0.0	0.0	2.1	0.0	2.1	0.0	25.0	

Table 4.3.9: Result of palynomorphs abundance/diversity count data in each sample in the South John Acres Lane Quarry, Bovey Basin, Southwest, UK.

Height (m)	Sample ID	Slide Number (BGS)	Monolet	Monocolpopollenites	Minorpollis	Plicapollis	Tricolporopollenites	Tricolpopollenites	Triporopollenites	Salixpollenites	Tiliaepollenites	Tricolpate	Porocolpopollenites	Cycadopites	Inaperturopollenites	Cicatricosisporites	Laevigatisporites	Stereisporites	Cingulatisporites	Pompeckjoidaepollenites	Trilets	Bissacate	Quaculites	Verrucatosporites	Areciptes	Sequoiapollenites	Graminidites	Pseudoplicapollis	Interpollis Microsupplingensis	Podocarpidites	Psophosphaera Pseudotsugoides	Leiotriletes	Reticuloidosporites dentatus	Tetradites	Fungi/Algae	Unidentified	Total
47.4	SJAL065	MPA63260		51	1	7	14			2	2				101	1	94	2							4	4					1				2	3	289
45.7	SJAL067	MPA63259	3	55		1	24				3			5	114		72	2	1	4					1	23								1	2	4	315
43.7	SJAL069	MPA63258	1	26			6			7				8	115		122				1				3	23										1	313
40.1	SJAL062	MPA63257		65		1	40			2	3				66		64			1	2				3	24										1	272
38.9	SJAL060	MPA63256	5	22	8	3	27			9	10			6	98		79			6		3				25									5	1	307
38.1	SJAL056	MPA63255		26	1	2	1				1			4	22	25	43			6			3		2	1										10	147
35.8	SJAL053	MPA63254		9		1	2				1			12	33	1	31			1				3		10										21	125
34.4	SJAL048	MPA63253				1									2		2																		3		8
31.9	SJAL046	MPA63252		11		3	1			1				7	28		106			3						46									2	3	211
31.5	SJAL045	MPA63251		41		20				3	1				28		69	1		2		5			2	1		1	2				1			10	187
31.3	SJAL044	MPA63250		36	1	2	5			7				3	41	17	133	5				1				10				4					2	5	272
30.6	SJAL042	MPA63249		15										9	30		11									24											89
29.7	SJAL040	MPA63248		50							1			26	73		85								2	47											284
29.2	SJAL039	MPA63247		14			8			3	2				29	1	37			2																1	97
28.9	SJAL038	MPA63246		9		1				1					63	31	25	1																	19	2	152
28.8	SJAL037	MPA63245		17	3	1	7			2					101	31	135			1		2													4		304
25.7	SJAL036	MPA63244																																			
23.5	SJAL034	MPA63243		9		3	3			2					11		10	1				5															44
22.7	SJAL032	MPA63242		46	6	11	1			4	1				67		22			7	1				6											1	173
20.5	SJAL031	MPA63241			3	2									7		4			2																	18
18.7	SJAL029	MPA63240				3									2																						5
17.6	SJAL028	MPA63239		45	3	3	51								93		51			4					2											1	253
16.7	SJAL027	MPA63238		1		1	2		1						3		2			4															1		15
15.8	SJAL026	MPA63237																																			
14.6	SJAL024	MPA63236																																			
13.9	SJAL023	MPA63235																																			
13.4	SJAL022	MPA63234		13		32	6								64		110			6							1										232
12.8	SJAL021	MPA63233		5	6					1					4		77	1		3	1					2											100
11.8	SJAL020	MPA63232		9						1	1		3		3		43			14																1	75
10.2	SJAL019	MPA63231		5			3			2	4				8		92	2							1											1	118
9.3	SJAL018	MPA63230				2	15				5	12	6		18		25			6					3		1								1	5	99
8.8	SJAL017	MPA63229				20	12	16			2				68	106	10			4	3				2											15	258
8.6	SJAL016	MPA63228		5		26	2				6				11					6															2	11	69
8.2	SJAL015	MPA63227				3	1								1		2																		14	1	22
7.7	SJAL014	MPA63226				9									4																					1	14
6.7	SJAL013	MPA63225																																			
6.0	SJAL012	MPA63224																																			
5.3	SJAL011	MPA63223																																			
3.8	SJAL008	MPA63222		1			5								2		7				1														7	4	27
3.2	SJAL006	MPA63221																																			
2.8	SJAL005	MPA63220		1											1																						2
2.3	SJAL004	MPA63219																																			
1.8	SJAL003	MPA63218													10		1				5															5	21
1.2	SJAL002	MPA63217																																			
0.1	SJAL001	MPA63216																		4																	

Table 4.4.0: Result of palynomorphs abundance/diversity express in percentage in the South John Acres Lane Quarry, Bovey Basin, Southwest, UK.

Height (m)	Sample ID	Slide Number (BGS)	*Monadet*	*Monocolpopollenites*	*Minorpollis*	*Plicapollis*	*Tricolporopollenites*	*Tricolpopollenites*	*Triporopollenites*	*Salixpollenites*	*Tiliaepollenites*	*Tricolpate*	*Porocolpopollenites*	*Cycadopites*	*Inaperturopollenites*	*Cicatricosisporites*	*Laevigatisporites*	*Stereisporites*	*Cingulatisporites*	*Pompeckjoidaepollenites*	*Triletes*	*Bisaccate*	*Quacudites*	*Verrucatosporites*	*Arecipites*	*Sequoiapollenites*	*Graminidites*	*Pseudoplicapollis*	*Interpollis Microsupplingensis*	*Podocarpidites*	*Psophosphaera Pseudotsugoides*	*Leiotriletes*	*Reticuloidosporites dentatus*	*Tetradites*	*Fungi*	Unidentified
47.4	SJAL065	MPA63260	0	18	0	2	5	0	0	1	1	0	0	0	35	0	33	1	0	0	0	0	0	0	1	1	0	0	0	0	0	0	0	0	1	1
45.7	SJAL067	MPA63259	1	17	0	0	8	0	0	0	1	0	0	2	36	0	23	1	0	1	0	0	0	0	0	7	0	0	0	0	0	0	0	0	1	1
43.7	SJAL069	MPA63258	0	8	0	0	2	0	0	2	0	0	0	3	37	0	39	0	0	0	0	0	0	0	1	7	0	0	0	0	0	0	0	0	0	0
40.1	SJAL062	MPA63257	0	24	0	0	15	0	0	1	1	0	0	0	24	0	24	0	0	0	1	0	0	0	1	9	0	0	0	0	0	0	0	0	0	0
38.9	SJAL060	MPA63256	2	7	3	1	9	0	0	3	3	0	0	2	32	0	26	0	0	2	0	1	0	0	0	8	0	0	0	0	0	0	0	0	2	0
38.1	SJAL056	MPA63255	0	18	1	1	1	0	0	0	1	0	0	3	15	17	29	0	0	4	0	0	2	0	1	1	0	0	0	0	0	0	0	0	0	7
35.8	SJAL053	MPA63254	0	7	0	1	2	0	0	0	1	0	0	10	26	1	25	0	0	1	0	0	0	2	0	8	0	0	0	0	0	0	0	0	0	17
34.4	SJAL048	MPA63253	0	0	0	13	0	0	0	0	0	0	0	0	25	0	25	0	0	0	0	0	0	0	0	0	0	0	0	0	0	0	0	0	38	0
31.9	SJAL046	MPA63252	0	5	0	1	0	0	0	0	0	0	0	3	13	0	50	0	0	1	0	0	0	0	0	22	0	0	0	0	0	0	0	0	1	1
31.5	SJAL045	MPA63251	0	22	0	11	0	0	0	2	1	0	0	0	15	0	37	1	0	1	0	3	0	0	1	1	0	1	1	0	0	0	1	0	0	5
31.3	SJAL044	MPA63250	0	13	0	1	2	0	0	3	0	0	0	1	15	6	49	2	0	0	0	0	0	0	0	4	0	0	0	1	0	0	0	0	1	2
30.6	SJAL042	MPA63249	0	17	0	0	0	0	0	0	0	0	0	10	34	0	12	0	0	0	0	0	0	0	0	27	0	0	0	0	0	0	0	0	0	0
29.7	SJAL040	MPA63248	0	18	0	0	0	0	0	0	0	0	0	9	26	0	30	0	0	0	0	0	0	0	1	17	0	0	0	0	0	0	0	0	0	0
29.2	SJAL039	MPA63247	0	14	0	0	8	0	0	3	2	0	0	0	30	1	38	0	0	2	0	0	0	0	0	0	0	0	0	0	0	0	0	0	0	1
28.9	SJAL038	MPA63246	0	6	0	1	0	0	0	1	0	0	0	0	41	20	16	1	0	0	0	0	0	0	0	0	0	0	0	0	0	0	0	0	13	1
28.8	SJAL037	MPA63245	0	6	1	0	2	0	0	1	0	0	0	0	33	10	44	0	0	0	0	1	0	0	0	0	0	0	0	0	0	0	0	0	1	0
25.7	SJAL036	MPA63244																																		
23.5	SJAL034	MPA63243	0	20	0	7	7	0	0	5	0	0	0	0	25	0	23	2	0	0	0	11	0	0	0	0	0	0	0	0	0	0	0	0	0	0
22.7	SJAL032	MPA63242	0	27	3	6	1	0	0	2	1	0	0	0	39	0	13	0	0	4	1	0	0	0	3	0	0	0	0	0	0	0	0	0	0	1
20.5	SJAL031	MPA63241	0	0	17	11	0	0	0	0	0	0	0	0	39	0	22	0	0	11	0	0	0	0	0	0	0	0	0	0	0	0	0	0	0	0
18.7	SJAL029	MPA63240	0	0	0	60	0	0	0	0	0	0	0	0	40	0	0	0	0	0	0	0	0	0	0	0	0	0	0	0	0	0	0	0	0	0
17.6	SJAL028	MPA63239	0	18	1	1	20	0	0	0	0	0	0	0	37	0	20	0	0	2	0	0	0	0	1	0	0	0	0	0	0	0	0	0	0	0
16.7	SJAL027	MPA63238	0	7	0	7	13	0	7	0	0	0	0	0	20	0	13	0	0	27	0	0	0	0	0	0	0	0	0	0	0	0	0	0	7	0
15.8	SJAL026	MPA63237																																		
14.6	SJAL024	MPA63236																																		
13.9	SJAL023	MPA63235																																		
13.4	SJAL022	MPA63234	0	6	0	14	3	0	0	0	0	0	0	0	28	0	47	0	0	3	0	0	0	0	0	0	0	0	0	0	0	0	0	0	0	0
12.8	SJAL021	MPA63233	0	5	6	0	0	0	0	1	0	0	0	0	4	0	77	1	0	3	1	0	0	0	0	2	0	0	0	0	0	0	0	0	0	0
11.8	SJAL020	MPA63232	0	12	0	0	0	0	0	1	1	0	4	0	4	0	57	0	0	19	0	0	0	0	0	0	0	0	0	0	0	0	0	0	0	1
10.2	SJAL019	MPA63231	0	4	0	0	3	0	0	2	3	0	0	0	7	0	78	2	0	0	0	0	0	0	1	0	0	0	0	0	0	0	0	0	0	1
9.3	SJAL018	MPA63230	0	0	0	2	15	0	0	0	5	1	6	0	18	0	25	0	0	6	0	0	0	0	3	0	1	0	0	0	0	0	0	0	1	5
8.8	SJAL017	MPA63229	0	0	0	8	5	6	0	0	1	0	0	0	26	41	4	0	0	2	1	0	0	0	1	0	0	0	0	0	0	0	0	0	0	6
8.6	SJAL016	MPA63228	0	7	0	38	3	0	0	0	9	0	0	0	16	0	0	0	0	9	0	0	0	0	0	0	0	0	0	0	0	0	0	0	3	16
8.2	SJAL015	MPA63227	0	0	0	14	5	0	0	0	0	0	0	0	5	0	9	0	0	0	0	0	0	0	0	0	0	0	0	0	0	0	0	0	64	5
7.7	SJAL014	MPA63226	0	0	0	64	0	0	0	0	0	0	0	0	29	0	0	0	0	0	0	0	0	0	0	0	0	0	0	0	0	0	0	0	0	7
6.7	SJAL013	MPA63225																																		
6.0	SJAL012	MPA63224																																		
5.3	SJAL011	MPA63223																																		
3.8	SJAL008	MPA63222	0	4	0	0	19	0	0	0	0	0	0	0	7	0	26	0	0	0	4	0	0	0	0	0	0	0	0	0	0	0	0	0	26	15
3.2	SJAL006	MPA63221																																		
2.8	SJAL005	MPA63220	0	50	0	0	0	0	0	0	0	0	0	0	50	0	0	0	0	0	0	0	0	0	0	0	0	0	0	0	0	0	0	0	0	0
2.3	SJAL004	MPA63219																																		
1.8	SJAL003	MPA63218	0	0	0	0	0	0	0	0	0	0	0	0	48	0	5	0	0	0	24	0	0	0	0	0	0	0	0	0	0	0	0	0	0	24
1.2	SJAL002	MPA63217																																		
0.1	SJAL001	MPA63216																																		

Appendix 3

One way Cluster analysis of S17 Bray Curtis similarity percentages for sample from South John Acres Lane Quarry, Bovey Basin

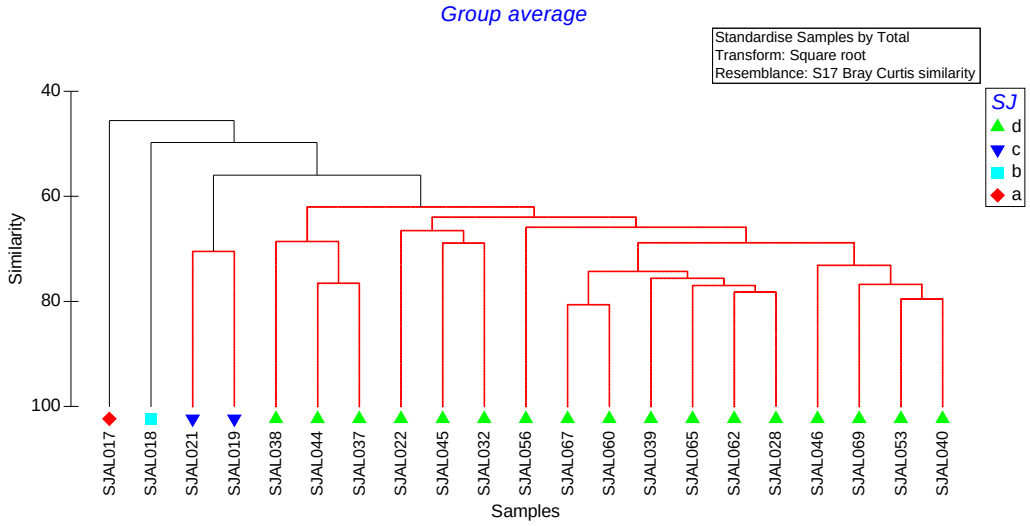

Appendix 4

One way Cluster analysis of S17 Bray Curtis similarity percentage for sample from Petrockstowe cores 1A & 1B, Petrockstowe Basin

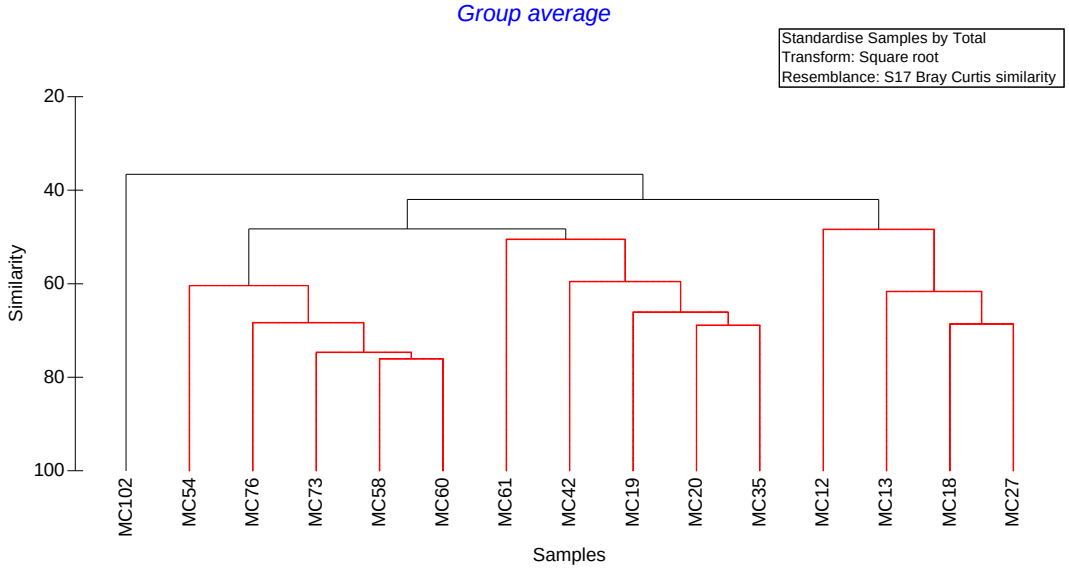

Appendix 5

Cluster analysis using SIMPER of sample from South John Acres Lane Quarry, Bovey Basin

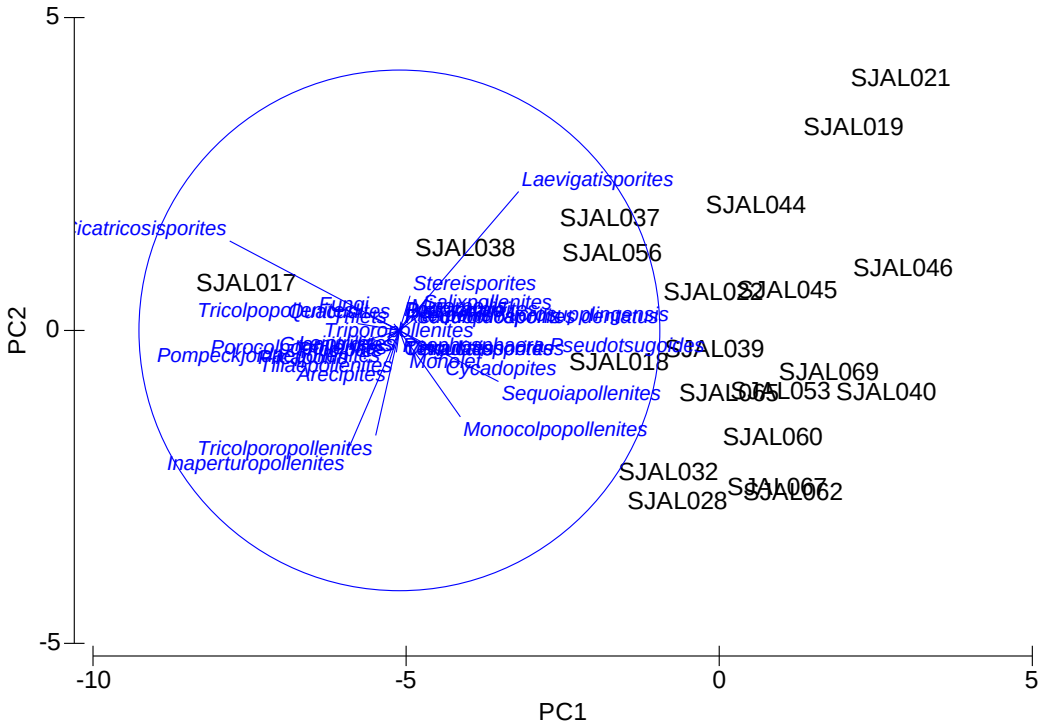

Appendix 6

Cluster analysis of samples from Petrockstowe cores 1A & 1B, Petrockstowe Basin

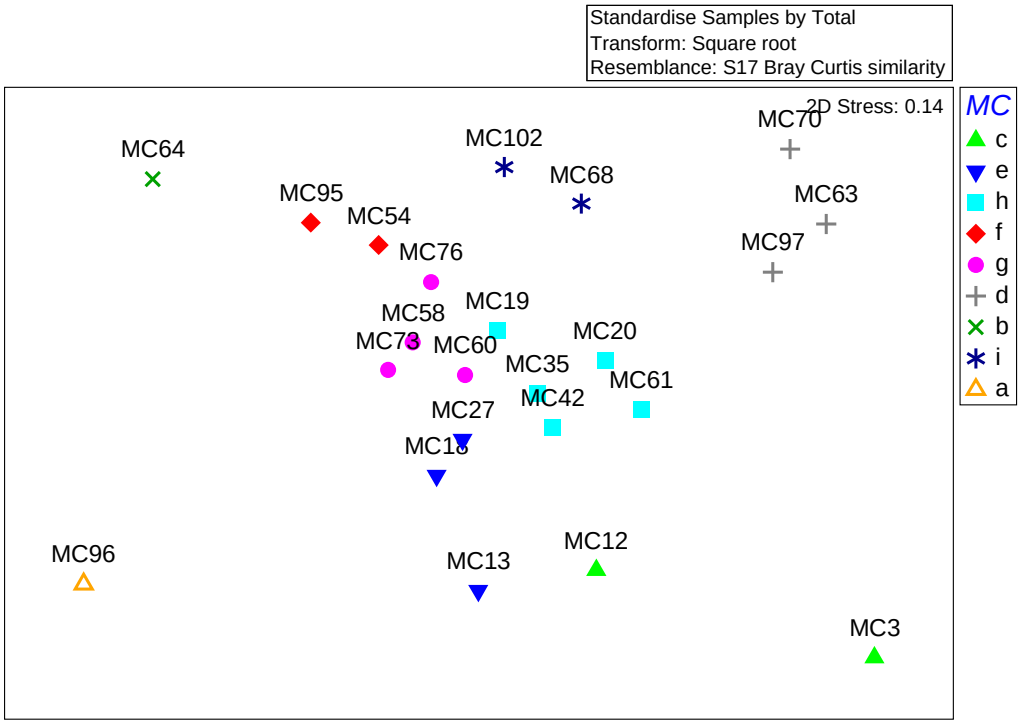

Appendix 7

Two way cluster analysis Bray-Curtis paired group using PAST for South John Acres Lane Quarry sample, Bovey Basin

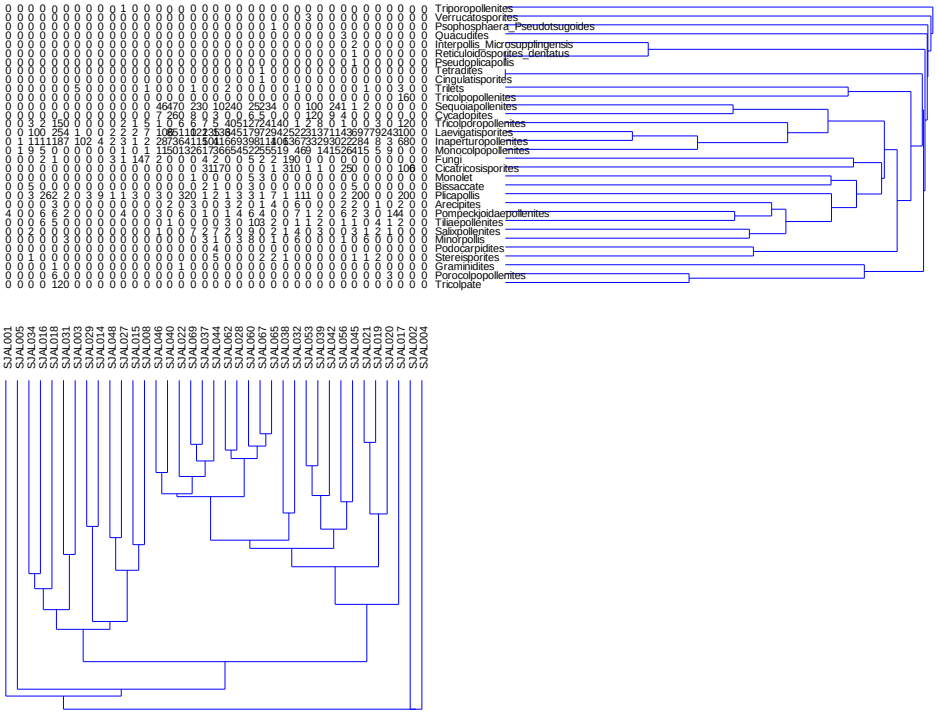

Appendix 8

Two way cluster analysis Bray-Curtis paired group using PAST for Petrockstowe core 1A, Petrockstowe Basin

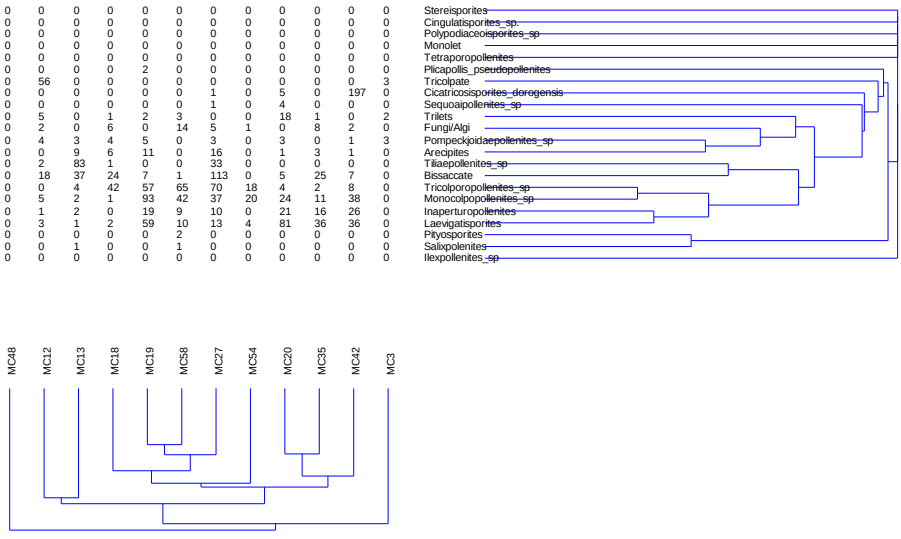

Appendix 9

Two way cluster analysis Bray-Curtis paired group using PAST for Petrockstowe core 1B, Petrockstowe Basin

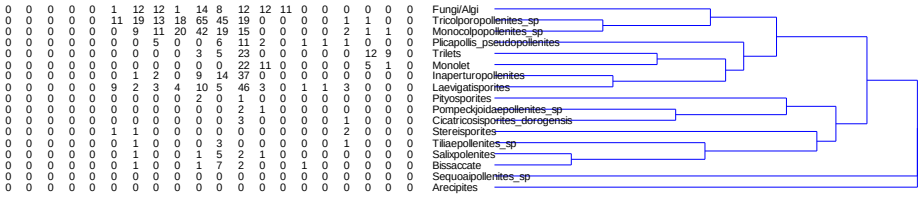

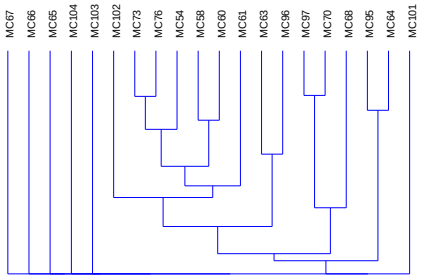

Appendix 10

Table 5.1: The δ13CTOC results for Petrockstowe core 1A produce from the analysis of TOC in sediment samples

Sample	Depth (m)	Depth (ft)	$\delta^{13}C_{TOC}$ (‰VPDB)	wt%C	Sample	Depth (m)	Depth (ft)	$\delta^{13}C_{TOC}$ (‰VPDB)	wt%C
MC1	7.3	24	-24.0	0.35	MC27	202.33	663	-26.5	2.69
MC2	10.82	36	-26.9	0.58	MC28	207.39	680	-26.3	0.09
MC3	23.53	77	-23.3	2.30	MC29	218.88	718	-26.1	0.43
MC4	25.70	84	-25.2	0.62	MC30	232.45	762	-26.0	0.92
MC5	39.68	130	-26.6	1.376	MC32	239.60	786	-26.7	1.15
MC6	43.65	143	-25.9	0.19	MC33	244.33	801	-25.6	0.13
MC7	45.29	148	-26.7	0.05	MC35	257.31	844	-24.9	20.62
MC8	46.82	153	-25.1	0.36	MC36	266.40	874	-27.2	0.42
MC9	50.94	167	-24.5	0.59	MC37	276.24	906	-26.2	0.09
MC10	58.22	191	-26.5	0.54	MC38	282.49	926	-25.8	3.18
MC11	65.62	215	-25.9	0.43	MC39	285.59	936	-26.2	6.27
MC12	65.84	216	-26.2	2.68	MC41	293.83	964	-27.4	0.43
MC13	75.50	247	-25.6	2.98	MC42	311.23	1021	-25.9	5.73
MC14	82.11	269	-26.6	0.04	MC43	315.80	1036	-27.5	4.51
MC15	88.45	290	-26.3	0.28	MC44	330.89	1085	-26.7	1.90
MC16	94.09	308	-27.1	0.83	MC45	331.29	1086	-26.2	7.49
MC17	100.24	328	-26.7	0.06	MC46	341.10	1119	-26.6	1.31
MC18	109.42	359	-26.8	1.68	MC47	346.56	1137	-26.6	1.74
MC19	111.40	365	-27.2	1.98	MC48	354.89	1164	-24.2	42.65
MC20	116.07	380	-26.5	5.21	MC49	361.49	1186	-26.2	6.11
MC21	121.68	399	-26.1	0.06	MC50	369.11	1211	-26.4	2.66
MC22	140.50	461	-26.1	0.12	MC51	379.78	1246	-25.8	0.92
MC23	155.51	510	-27.0	0.26	MC52	390.60	1281	-26.8	3.39
MC24	161.54	530	-26.3	0.13	MC53	398.77	1308	-26.2	18.54
MC25	174.13	571	-26.2	0.09	MC54	405.08	1329	-26.0	0.31
MC26	197.18	646	-25.7	0.44	MC55	412.82	1354	-27.0	0.33
					MC56	418.00	1371	-26.7	0.35

Table 5.2: The δ13CTOC results for Petrockstowe core 1B produce from the analysis of TOC in sediments

Sample	Depth (m)	Depth (ft)	$\delta^{13}C_{TOC}$ (‰VPDB)	wt%C	Sample	Depth (m)	Depth (ft)	$\delta^{13}C_{TOC}$ (‰VPDB)	wt%C
MC56	417.88	1371	-26.7	0.35	MC66	598.02	1962	-27.0	0.15
MC58	431.60	1416	-25.2	18.80	MC67	603.81	1981	-27.3	0.10
MC99	513.59	1685	-27.4	0.06	MC68	605.03	1985	-26.5	0.13
MC100	515.11	1690	-27.1	0.06	MC69	605.64	1987	-26.1	0.15
MC91	517.25	1697	-25.5	0.07	MC70	606.55	1990	-26.8	0.11
MC60	523.04	1716	-26.4	0.75	MC71	606.86	1991	-26.7	0.11
MC61	540.11	1772	-27.0	0.08	MC72	609.90	2001	-26.4	0.09
MC92	553.21	1815	-26.5	0.05	MC73	610.51	2003	-26.3	0.81
MC63	569.06	1867	-26.6	0.12	MC74	612.34	2009	-26.8	0.11
MC93	571.20	1874	-26.3	0.03	MC75	613.26	2012	-26.6	0.37
MC94	584.00	1916	-26.5	0.05	MC76	616.00	2021	-26.5	0.64
MC95	585.52	1921	-26.6	0.07	MC77	617.22	2025	-25.6	0.12
MC64	586.44	1924	-28.6	0.05	MC78	617.83	2027	-27.4	0.08
MC101	587.04	1926	-28.3	0.06	MC79	622.10	2041	-26.2	0.30
MC102	588.26	1930	-28.4	0.06	MC80	623.32	2045	-27.0	0.61
MC103	590.09	1936	-28.5	0.07	MC81	624.84	2050	-27.0	1.36
MC104	591.01	1939	-28.1	0.10	MC82	629.11	2064	-26.3	0.41
MC105	591.92	1942	-28.2	0.03	MC83	643.13	2110	-26.7	0.12
MC65	593.14	1946	-27.9	0.02	MC84	643.43	2111	-26.7	0.73
MC96	595.58	1954	-27.3	0.04	MC85	644.35	2114	-25.8	5.41
MC97	595.88	1955	-26.5	0.05	MC86	644.96	2116	-26.2	0.18
MC98	597.10	1959	-26.9	0.07	MC87	645.57	2118	-26.1	0.10

Table 5.3: The δ13CTOC results from South John acres Lane Quarry section, produce from the analysis of TOC in sediments

Sample	Depth (m)	$\delta^{13}C_{TOC}$ (‰VPDB)	wt%C	Sample	Depth (m)	$\delta^{13}C_{TOC}$ (‰VPDB)	wt%C
SJAL64	48.10	-26.0	36.6	SJAL32	22.70	-26.1	0.4
SJAL65	47.40	-27.1	7.4	SJAL31	20.50	-25.6	0.1
SJAL66	46.50	-26.4	51.2	SJAL30	19.10	-25.9	0.1
SJAL67	45.70	-26.5	9.2	SJAL29	18.70	-25.3	0.1
SJAL68	45.20	-26.4	33.7	SJAL28	17.60	-26.8	9.1
SJAL69	43.70	-26.3	2.7	SJAL27	16.70	-25.3	5.1
SJAL70	42.90	-27.2	36.6	SJAL26	15.80	-25.5	0.1
SJAL63	40.40	-25.8	51.9	SJAL25	15.20	-25.2	0.0
SJAL62	40.10	-27.2	15.1	SJAL24	14.60	-25.1	0.1
SJAL61	39.50	-27.8	57.0	SJAL23	13.90	-27.8	2.8
SJAL60	38.90	-27.1	3.1	SJAL22	13.40	-27.3	6.4
SJAL57	38.90	-23.1	60.1	SJAL21	12.80	-26.0	0.4
SJAL58	38.90	-23.2	55.9	SJAL20	11.80	-25.7	0.1
SJAL59	38.60	-22.5	61.8	SJAL19	10.20	-25.1	0.6
SJAL56	38.10	-26.7	12.0	SJAL18	9.30	-23.9	4.3
SJAL55	37.60	-26.2	37.3	SJAL17	8.80	-27.0	9.8
SJAL54	36.30	-26.2	48.5	SJAL16	8.60	-26.4	0.3
SJAL53	35.80	-25.9	3.1	SJAL15	8.20	-25.4	0.1
SJAL52	35.40	-26.6	17.1	SJAL14	7.70	-25.3	0.1
SJAL51	35.30	-26.7	5.6	SJAL13	6.70	-26.1	0.1
SJAL50	35.10	-26.1	29.6	SJAL12	6.00	-25.2	0.1
SJAL49	34.70	-25.8	2.4	SJAL11	5.30	-24.9	0.0
SJAL48	34.40	-26.3	0.1	SJAL10	5.00	-25.8	0.0
SJAL47	33.70	-26.0	37.4	SJAL09	4.20	-26.5	0.0
SJAL46	31.90	-25.1	2.7	SJAL08	3.80	-26.4	1.8
SJAL45	31.50	-26.1	13.2	SJAL07	3.40	-25.4	0.1
SJAL44	31.30	-25.8	3.7	SJAL06	3.20	-27.3	0.8
SJAL43	30.80	-26.3	32.8	SJAL05	2.80	-25.9	0.1
SJAL42	30.60	-25.2	4.1	SJAL04	2.30	-26.2	0.3
SJAL41	30.20	-25.2	45.2	SJAL03	1.75	-27.0	1.4
SJAL40	29.70	-25.8	1.9	SJAL02	1.20	-26.5	0.3
SJAL39	29.20	-26.4	10.9	SJAL 01	0.05	-26.1	0.2
SJAL38	28.90	-26.7	2.4				
SJAL37	28.80	-26.5	8.5				
SJAL36	25.70	-26.7	0.7				
SJAL35	23.80	-25.1	0.2				
SJAL34	23.50	-26.2	1.3				
SJAL33	23.50	-26.0	17.9				

Table 6.1a: Geochemical data for the Petrockstowe cores 1A & 1B, Petrockstowe Basin, Southwest, UK

		GDGTs (response)												
		Isoprenoidds GDGTs						Branched GDGTs						
Sample	ID	0	1	2	3	Cren	Cren'	Ia	Ib	Ic	IIa	IIb	IIc	IIIa
MC5	KT	3026270	404681	670701	625244	12268	0	4674864	423384		1567960	118494	75833	191816
MC12	6103ngi	2870220	487307	268714	232822	72354	0	25003235	128447	672009	7352322	142817	122265	871929
MC12	6104ngi	3045429	490404	180893	453681	0	0	24488536	338828	671712	8304521	86726	154498	1047342
MC16	6107ngi	873359	0	0	0	0	0	10501416	0	0	1527721	0	0	0
MC16	6108ngi	778464	0	0	0	342235	0	0	0	0	1409547	0	0	0
MC18	6101ngi	3987591	999230	1266037	578884	464343	0	3369431	1045821	354157	6283365	0	0	722858
MC18	6102ngi	4217635	1225611	1151382	701828	0	0	23254342	999122	213806	6136613	151964	59838	739902
MC20	KT	1959187	302371	375320	362396	0	0	19209795	576224		2714135	90876	97946	319626
MC22B	9120	0	0	0	0	0	0	247615						0
MC23	6097ngi					0	0	560591	2546	3041	11741			
MC23	6098ngi					0	0	15347	2691	4772	0			
MC26B	8970	14553208	589582	625067	459943	153185	0	68917245	1858168	475782	13505113	347878	172490	1374305
MC29	6099ngi	57837						8227494	454941	0	0			
MC29	6100ngi	2419						7799351	535533	4161	15075			
MC32	6095ngi	822420	194449	3406	3468	0	0	15144042	11257	2722	1038751			
MC32	6096ngi	723694	6828	10495	53119	6371	1124	15068755	6485	7810	0			3968
MC35	KT	25645245	3406078	8321311	3993188	0	0	25580546	1069495	0	8682545	290000	83793	1727994
MC38	6105ngi	3678920	523417	835587	303909	0	0	13698559	202729	100727	4081277			
MC38	6106ngi	3855859	453744	139280	260926	0	0	14248607	0	157153	4651009			644328
MC41B	9119		0	0	0	0	0		0	0	0	0	0	0
MC42	6109ngi	3089921	558518		273692	0	0	25775967	0	705306	3929237			
MC42	6110ngi	2931372	593413			0	0	24654578	675010	0	3396356			
MC48	KT	7956495	694493	926153	764771	0	0	3669421	195829	0	582706			466288
MC50B	8967	17512976	1215065	1427872	1428124	406654	0	33313751	2230406	623128	19389117	640674	197234	3174240

Table 6.1b: Geochemical data for the Petrockstowe cores 1A & 1B, Petrockstowe Basin, Southwest, UK

Sample	ID	TEX	GDGT index-1	GDGT index-2	TEX-H	TEX-L	H-L	[2]/[3]	MI	%GDGT-0	MBT'	CBT	MAT	pH	BIT
MC5	KT	0.7620	-0.4041	-0.1180	30.53	19.62	10.90	1.073	0.993	99.60	0.7229	1.0615	17.20	5.81	0.998
MC12	6103ngi	0.5072	-0.5658	-0.2948	18.43	8.71	9.73	1.154	0.932	97.54	0.7524	2.0766	12.36	3.81	0.998
MC12	6104ngi	0.5641	-0.7937	-0.2487	21.59	-6.68	28.27	0.399	1.000	100.00	0.7266	1.8868	12.64	4.18	1.000
MC16	6107ngi									100.00	0.8730				1.000
MC16	6108ngi								0.000	69.46	0.0000				0.805
MC18	6101ngi	0.6487	-0.3515	-0.1880	25.74	23.17	2.57	2.187	0.860	89.57	0.4050	0.9652	7.89	6.00	0.957
MC18	6102ngi	0.6019	-0.4272	-0.2205	23.52	18.07	5.45	1.641	1.000	100.00	0.7754	1.4071	16.87	5.13	1.000
MC20	KT	0.7093	-0.4427	-0.1492	28.40	17.02	11.38	1.036	1.000	100.00	0.8599	1.5167	18.87	4.91	1.000
MC22B	9120										1.0000				1.000
MC23	6097ngi										0.9797	2.3519			1.000
MC23	6098ngi										1.0000	0.7560			1.000
MC26B	8970	0.6479	-0.4280	-0.1885	25.71	18.01	7.70	1.359	0.916	98.96	0.8223	1.5724	17.38	4.80	0.998
MC29	6099ngi									100.00	1.0000	1.2573	24.68	5.42	1.000
MC29	6100ngi									100.00	0.9982	1.1641	25.15	5.61	1.000
MC32	6095ngi	0.0341	-1.7716	-1.4666	-61.72	-72.68	10.96	0.982	1.000	100.00	0.9354	3.1576	11.90	1.68	1.000
MC32	6096ngi	0.9046	-0.8269	-0.0435	35.62	-8.91	44.53	0.198	0.904	99.13	0.9990	3.0485			1.000
MC35	KT	0.7833	-0.2763	-0.1061	31.35	28.25	3.09	2.084	1.000	100.00	0.7119	1.4014	14.93	5.14	1.000
MC38	6105ngi	0.6852	-0.2989	-0.1642	27.37	26.73	0.65	2.749	1.000	100.00	0.7743	1.9430	13.80	4.07	1.000
MC38	6106ngi	0.4687	-0.7875	-0.3291	16.09	-6.26	22.35	0.534	1.000	100.00	0.7312				1.000
MC41B	9119														
MC42	6109ngi	0.3289		-0.4830	5.56			0.000	1.000	100.00	0.8708				1.000
MC42	6110ngi	0.0000							1.000	100.00	0.8818	1.6186	18.97	4.71	1.000
MC48	KT	0.7089	-0.4109	-0.1494	28.38	19.17	9.21	1.211	1.000	100.00	0.7865	1.3367	17.61	5.27	1.000
MC50B	8967	0.7015	-0.4550	-0.1539	28.07	16.19	11.88	1.000	0.909	97.73	0.6072	1.2638	12.47	5.41	0.993

Table 6.2a: Geochemical data for the South John Acres Lane Quarry section, Bovey Basin, Southwest, UK

		GDGTs (reponse)												
		Isoprenod GDGTs						Branched GDGTs						
Sample	ID	0	1	2	3	Cren	Cren'	Ia	Ib	Ic	IIa	IIb	IIc	IIIa
SJAL064B_b	9311gni	56348427	5228153	3774868	5127049	244445			18378514	5956586	92982665	4924431	599126	4924431
SJAL067B-b	9275gni	11464661	1715316	1384513	1477591	142941			8808003	9738717	35108655	914753	1273024	1952501
SJAL069b	6118ngi	2904233	1110812	173828	0	0	0	31491963	1333075	1415244	2190904	0	0	0
SJAL062B-b	9281gni	99397914	14275102		10687015	966119			30101249	17825603	77898577	7136481	7317040	14046548
SJAL060B	9121	552249	166235	216489	177490	0	0	39768137	2737409	3280783	2127834			
SJAL049B_a	9260gni	3257091	805927	629580	527162				1048058	1505131	5395913		324336	469135
SJAL049B-b	9261gni	3237978	710833	498821	462494				506131	1749416	5414316		305326	479727
SJAL046B-a	9248gni	8614356	2887518	2316543	1965792	370538		60544503	1673281	1380297	11565333	336241	411826	1278417
SJAL046B_b	9249gni	9325391	2906183	1725059	1988113	317693		62482610	1764586	1611260	10750591	631782	374321	1680889
SJAL042b	6124ngi	9422153	0	1565087	1276075	565803	0	35328142	1727511	0	0	0	0	0
SJAL042a	6123ngi	10546437	2017220	0	1100879	0	0	34496267	844154	0	0	0	0	672352
SJAL038a	6115ngi	1387090	179731	0	0	0	0	18079998	712168	2524281	729273	0	0	0
SJAL037B	8971	43178417	6526191	5063062	3629064	552637	0	719061446	21141218	14856194	96934761	4054449	1990185	15068733
SJAL032B_b	9247gni	163266	336882	135559	26430	32171		2725970	47902	80224	73578	64857	116415	95816
SJAL029B	8968	14469649	1791731	1344036	930341		0	1134804			793014			1878016
SJAL022B-a	9240gni	59801	31482	27375	27804	0	0	1284678	32441	0	156567	0	0	0
SJAL022B_b	9241gni	71968	22673	7945	17552	2049	0	1242595	19811	13007	128525	3938	2205	4151
SJAL017B	9117	4418768	2156314	2353025	2729517	207492	0	144897071	3314377	2034590	11408711	0	0	1156653
SJAL015B_a	9234gni	1667345	963159	246960	963159	451	0	505596	77686	39233	107918	37580	3348	21676
SJAL002B-b	9287gni	416837						736354	282205					

Table 6.2b: Geochemical data for south John Acres Lane Quarry section, Bovey Basin

Sample	ID	TEX	GDGT index-1	GDGT index-2	TEX-H	TEX-L	H-L	[2]/[3]	MI	%GDGT-0	MBT'	CBT	MAT	pH	BIT
SJAL064B_b	9311gni	0.6300	-0.5732	-0.2007	24.87	8.21	16.67	0.7363	0.9830	99.568	0.1905	0.6010	3.31	6.72	0.998
SJAL067B-b	9275gni	0.6253	-0.5193	-0.2039	24.65	11.85	12.81	0.9370	0.9697	98.769	0.3209	0.5576	7.60	6.80	0.996
SJAL069b	6118ngi	0.1353	-0.8687	-0.8687	-20.82	-11.73	-9.08		1.0000	100.000	0.9399	1.4026	21.99	5.14	1.000
SJAL062B-b	9281gni	0.4281		-0.3684	13.40			0.0000	0.9627	99.037	0.3106	0.3205	8.62	7.27	0.990
SJAL060B	9121	0.7033	-0.4129	-0.1529	28.14	19.03	9.11	1.2197	1.0000	100.000	0.9556	1.1848	23.72	5.57	1.000
SJAL049B_a	9260gni	0.5894	-0.4938	-0.2296	22.89	13.57	9.33	1.1943	1.0000	100.000	0.2920	0.7117	5.83	6.50	1.000
SJAL049B-b	9261gni	0.5749	-0.5253	-0.2404	22.16	11.44	10.72	1.0785	1.0000	100.000	0.2668	1.0293	3.24	5.87	1.000
SJAL046B-a	9248gni	0.5973	-0.4907	-0.2238	23.29	13.78	9.51	1.1784	0.9509	95.876	0.8239	1.5549	17.54	4.84	0.995
SJAL046B_b	9249gni	0.5610	-0.5840	-0.2511	21.43	7.48	13.95	0.8677	0.9542	96.705	0.8305	1.4852	18.14	4.97	0.996
SJAL042b	6124ngi	1.0000	-0.2590	0.0000	38.60	29.42	9.18	1.2265	0.8339	94.335	1.0000	1.3107	24.38	5.32	0.984
SJAL042a	6123ngi	0.3531		-0.4522	7.67			0.0000	1.0000	100.000	0.9813	1.6114	22.09	4.73	1.000
SJAL038a	6115ngi	0.0000							1.0000	100.000	0.9669	1.4218	22.72	5.10	1.000
SJAL037B	8971	0.5712	-0.4780	-0.2432	21.96	14.64	7.32	1.3951	0.9650	98.736	0.8648	1.5104	19.05	4.92	0.999
SJAL032B_b	9247gni	0.3247	-0.5659	-0.4885	5.19	8.70	-3.52	5.1291	0.9394	83.539	0.8906	1.3949	20.51	5.15	0.989
SJAL029B	8968	0.5593	-0.4808	-0.2523	21.34	14.45	6.89	1.4447	1.0000	100.000	0.2982				1.000
SJAL022B-a	9240gni	0.6367	-0.5005	-0.1961	25.19	13.12	12.07	0.9846	1.0000	100.000	0.8938	1.6476	19.17	4.65	1.000
SJAL022B_b	9241gni	0.5293	-0.7827	-0.2763	19.70	-5.93	25.63	0.4526	0.9592	97.232	0.9018	1.7614	18.78	4.43	0.999
SJAL017B	9117	0.7021	-0.4880	-0.1536	28.09	13.96	14.14	0.8621	0.9721	95.515	0.9228	1.6736	19.93	4.60	0.999
SJAL015B_a	9234gni	0.5568	-0.9445	-0.2543	21.21	-16.85	38.06	0.2564	0.9998	99.973	0.7850	0.7261	21.03	6.47	0.999
SJAL002B-b	9287gni									100.000	1.0000	0.4165	29.45	7.08	

REFERENCE

ABELS, H., LAURETANO, V., VAN YPEREN, A., HOPMAN, T., ZACHOS, J.C, LOURENS, L.J., GINGERICH, P.D., & BOWEN, G.J. 2015. Carbon isotope excursions in paleosol carbonate marking five early Eocene hyperthermals in the Bighorn Basin, Wyoming. *Carbon*, **11**, 1857–1885.

ABELS, H.A., CLYDE, W.C., GINGERICH, P.D., HILGEN, F.J., FRICKE, H.C., BOWEN, G.J. & LOURENS, L.J. 2012a. Terrestrial carbon isotope excursions and biotic change during Palaeogene hyperthermals. *Nature Geoscience*, **5**, 326–329.

ABE-OUCHI, A. & BLATTER, H. 1993. On the initiation of ice sheets. *Annals of Glaciology*, **18**, 203–203.

AGNINI, C., MACRÌ, P., BACKMAN, J., BRINKHUIS, H., FORNACIARI, E., GIUSBERTI, L., LUCIANI, V., RIO, D., SLUIJS, A. & SPERANZA. 2009. An early Eocene carbon cycle perturbation at 52.5 Ma in the Southern Alps: Chronology and biotic response. *Paleoceanography*, **24**, PA2209.

ALLEN, P.A. & ALLEN, J.R. 2013. *Basin Analysis: Principles and Application to Petroleum Play Assessment*. John Wiley & Sons.

ARTHUR, M. 1989. The Cenozoic evolution of the Lundy pull-apart basin into the Lundy rhomb horst. *Geological Magazine*, **126**, 187–198.

ASHLEY, G.M. 1975. Rhythmic sedimentation in glacial lake Hitchcock, Massachusetts-Connecticut.

AUBRY, M.P. 2000. Where should the Global Stratotype Section and Point (GSSP) for the Paleocene/Eocene boundary be located? *Bulletin de la Société géologique de France*, **171**, 461–476.

AZIZ, H.A., HILGEN, F.J., VAN LUIJK, G.M., SLUIJS, A., KRAUS, M.J., PARES, J.M. & GINGERICH, P.D. 2008. Astronomical climate control on paleosol stacking patterns in the upper Paleocene–lower Eocene Willwood Formation, Bighorn Basin, Wyoming. *Geology*, **36**, 531–534.

BALLANTYNE, A., GREENWOOD, D., DAMSTÉ, J.S., CSANK, A., EBERLE, J. & RYBCZYNSKI, N. 2010. Significantly warmer Arctic surface temperatures during the Pliocene indicated by multiple independent proxies. *Geology*, **38**, 603–606.

BATTEN, D. 1982. Palynofacies, palaeoenvironments and petroleum. *Journal of Micropalaeontology*, **1**, 107–114.

BATTEN, D.J. & STEAD, D.T. 2005. Palynofacies analysis and its stratigraphic application. *In*: *Applied Stratigraphy*. Springer, 203–226.

BAUERSACHS, T., ROCHELMEIER, J. & SCHWARK, L. 2015. Seasonal lake surface water temperature trends reflected by heterocyst glycolipid based molecular thermometers. *Biogeosciences Discussions*, **12**, 751–778.

BENDLE, J.A., WEIJERS, J.W.H., MASLIN, M.A., DAMSTE SINNINGHE, J.S., SCHOUTEN, S., HOPMANS, E.C., BOOT, C.S., & PANCOST, R.D. 2010. Major changes in glacial and Holocene terrestrial temperatures and sources of organic carbon recorded in the Amazon fan by tetraether lipids. *Geochemistry, Geophysics, Geosystems*, **11**, Q12007, doi: 10.1029/2010gc003308.

BERGER, W. 2007. Cenozoic cooling, Antarctic nutrient pump, and the evolution of whales. *Deep Sea Research Part II: Topical Studies in Oceanography*, **54**, 2399–2421.

BERGGREN, W.A. & PEARSON, P.N. 2005. A revised tropical to subtropical Paleogene planktonic foraminiferal zonation. *The Journal of Foraminiferal Research*, **35**, 279–298.

BERNER, R.A. 1981. A new geochemical classification of sedimentary environments. *Journal of Sedimentary Research*, **51**.

BIJL, P.K., SCHOUTEN, S., SLUIJS, A., REICHART, G.-J., ZACHOS, J.C. & BRINKHUIS, H. 2009. Early Palaeogene temperature evolution of the southwest Pacific Ocean. *Nature*, **461**, 776–779.

BIJL, P.K., HOUBEN, A.J., SCHOUTEN, S., BOHATY, S.M., SLUIJS, A., REICHART, G., DAMSTE SINNINGHE, J.S. & BRINKHUIS, H. 2010. Transient Middle Eocene atmospheric CO2 and temperature variations. *Science*, **330**, 819–821.

BIRCHFIELD, G., WEERTMAN, J. & LUNDE, A.T. 1982. A model study of the role of high-latitude topography in the climatic response to orbital insolation anomalies. *Journal of Atmospheric Sciences*, **39**, 71–87.

BLYTH, F.G.H. 1962. The structure of the north-eastern tract of the Dartmoor granite. *Quarterly Journal of the Geological Society*, **118**, 435.

BOHATY, S.M. & ZACHOS, J.C. 2003. Significant Southern Ocean warming event in the late middle Eocene. *Geology*, **31**, 1017–1020, doi: 10.1130/G19800.1.

BOHATY, S.M., ZACHOS, J.C., FLORINDO, F. & DELANEY, M.L. 2009. Coupled greenhouse warming and deep-sea acidification in the middle Eocene. *Paleoceanography*, **24**.

BOSTICK, N.H. 1971. Thermal alteration of clastic organic particles as an indicator of contact and burial metamorphism in sedimentary rocks. *Geoscience and Man*, **3**, 83–92.

BOULTER, M. & CRAIG, D. 1979. A middle Oligocene pollen and spore assemblage from the Bristol Channel. *Review of Palaeobotany and Palynology*, **28**, 259–272.

BOULTER, M. & MANUM, S. 1996. Oligocene and Miocene vegetation in high latitudes of the North Atlantic: palynological evidence from the Hovgård Ridge in the Greenland Sea (site 908).

BOULTER, M.C. 1980. Irish Tertiary Plant Fossils in a European Context. *Journal of Earth Sciences*, **3**, 1–11.

BOULTER, M.C. & RIDDICK, A. 1986. Classification and analysis of palynodebris from the Palaeocene sediments of the Forties Field. *Sedimentology*, **33**, 871–886, doi: 10.1111/j.1365-3091.1986.tb00988.x.

BOWEN, G.J. & ZACHOS, J.C. 2010. Rapid carbon sequestration at the termination of the Palaeocene-Eocene Thermal Maximum. *Nature Geoscience*.

BOWEN, G.J., KOCH, P.L., GINGERICH, P.D., NORRIS, R.D., BAINS, S. & CORFIELD, R.M. 2001. Refined isotope stratigraphy across the continental Paleocene-Eocene boundary on Polecat Bench in the northern Bighorn Basin. *Paleocene-Eocene stratigraphy and biotic change in the Bighorn and Clarks Fork basins, Wyoming. University of Michigan Papers on Paleontology*, **33**, 73–88.

BOWEN, G.J., KOCH, P.L., GINGERICH, P.D., NORRIS, R.D., BAINS, S. & CORFIELD, R.M. 2001. Refined isotope stratigraphy across the continental Paleocene-Eocene boundary on Polecat Bench in the northern Bighorn Basin. *Paleocene-Eocene stratigraphy and biotic change in the Bighorn and Clarks Fork basins, Wyoming. University of Michigan Papers on Paleontology*, **33**, 73–88.

BOWEN, G.J., CLYDE, W.C., KOCH, P.L., TING, S., ALROY, J., TSUBAMOTO, T. & WANG, Y. 2002. Mammalian dispersal at the Paleocene/Eocene boundary. *Science*, **295**, 2062–2065.

BOWEN, G.J., CLYDE, W.C., KOCH, P., TING, S., ALROY, J., TSUMBAMOTO, T., WANG, Y & WANG, Y. 2002. Mammalian Dispersal at the Paleocene/Eocene Boundary. *Science*, **295**, 2062–2065, doi: 10.1126/science.1068700.

BOWEN, G.J., BEERLING, D.J., KOCH, P.L., ZACHOS, J.C. & QUATTLEBAUM, T. 2004. A humid climate state during the Palaeocene/Eocene thermal maximum. *Nature*, **432**, 495–499.

BOWEN, G.J., BRALOWER, T.J., DELANEY, M.L., DICKENS, G.R., KELLY, D.C., KOCH, P.L., PUMP, L.R., MENG, J., SLOAN, L.C., THOMAS, E., WING, S.L., & ZACHOS, J.C. 2006. Eocene hyperthermal event offers insight into greenhouse warming. *Eos, Transactions American Geophysical Union*, **87**, 165.

BOWEN, G.J., MAIBAUER, B.J., KRAUS, M.J., URSULA, R., WESTERHOLD, T., STEIMKE, A., GINGERICH, P.D., WING, S.L., & CLYDE, W.C. 2014. Two massive, rapid releases of carbon during the onset of the Palaeocene-Eocene thermal maximum. *Nature Geoscience*.

BRIDGE, J.S., SMITH, N.D., TRENT, F., GABRIEL, S.L. & BERSTEIN, P. 1986. Sedimentology and morphology of a low-sinuosity river: Calamus River, Nebraska Sand Hills. *Sedimentology*, **33**, 851–870, doi: 10.1111/j.1365-3091.1986.tb00987.x.

BRIDGE, J.S., ALEXANDER, J., COLLIER, R.E.L., GAWTHORPE, R.L. & JARVIS, J. 1995. Ground-penetrating radar and coring used to study the large-scale structure of point-bar deposits in three dimensions. *Sedimentology*, **42**, 839–852, doi: 10.1111/j.1365-3091.1995.tb00413.x.

BRISTOW, C. 1968. The derivation of the Tertiary sediments in the Petrockstow Basin, North Devon, The Proceedings of the Ussher Society. 29–35.

BRISTOW, C. & HUGHES, D. 1971. A Tertiary thrust fault on the southern margin of the Bovey Basin. *Geological magazine*, **108**, 61–67.

BRISTOW, C. & ROBSON, J. 1994. Palaeogene basin development in Devon. *Transactions of the Institution of Mining and Metallurgy. Section B. Applied Earth Science*, **103**.

BRISTOW, C., PALMER, Q. & PIRRIE, D. 1992. Palaeogene basin development: new evidence from the southern Petrockstow Basin, Devon. *Proceedings-Ussher Society*, **8**, 19–19.

BROCHIER-ARMANET, C., BOUSSAU, B., GRIBALDO, S. & FORTERRE, P. 2008. Mesophilic Crenarchaeota: proposal for a third archaeal phylum, the Thaumarchaeota. *Nature Reviews Microbiology*, **6**, 245–252.

BROWN, C.A., RIDING, J.B. & WARNY, S. 2008. *Palynological Techniques*. Dallas, Tex., American Association of Stratigraphic Palynologists Foundation.

BRYANT, LAN D., KANTOROWICZ, J.D. & LOVE, C.F. 1988. The origin and recognition of laterally continuous carbonate-cemented horizons in the Upper Lias Sands of southern England. *Marine and Petroleum Geology*, **5**, 108–133, doi: 10.1016/0264-8172(88)90018-9.

BURGESS, J.D. 1974. Microscopic examination of kerogen (dispersed organic matter) in petroleum exploration. *Geological Society of America Special Papers*, **153**, 19–30.

BUZAS, M.A. 1979. The Measurement of Species Diversity.*Special Pubilcations of The Society of Economic Paleontologists and Mineralogists (SPEM), Foraminiferal Ecology and Paleontology (SC6)*

CASTAÑEDA, I.S. & SCHOUTEN, S. 2011. A review of molecular organic proxies for examining modern and ancient lacustrine environments. *Quaternary Science Reviews*, **30**, 2851–2891, doi: 10.1016/j.quascirev.2011.07.009.

CATLING, D.C. 1999. A chemical model for evaporites on early Mars: Possible sedimentary tracers of the early climate and implications for exploration. *Journal of Geophysical Research: Planets*, **104**, 16453–16469.

CATTELL, A. 1996. The connection between the Decoy and Bovey Basins. *Proceedings-Ussher Society*, **9**, 130–132.

CATUNEANU, O. 2006. *Principles of Sequence Stratigraphy*. Elsevier.

CERLING, T.E. & HARRIS, J.M. 1999. Carbon isotope fractionation between diet and bioapatite in ungulate mammals and implications for ecological and paleoecological studies. *Oecologia*, **120**, 347–363.

CHANDLER, M.E.J. 1957. *The Oligocene Flora of the Bovey Tracey Lake Basin, Devonshire*. British Museum (Natural History) Geology.

CHANDLER, M.E.J. 1964. *The Lower Tertiary Floras of Southern England*. order of the Trustees of the British Museum.

CHATEAUNEUF, J. 1972. Contribution à l'étude de l'Aquitanien. La coupe de Carry-le-Rouet (Bouches-du-Rhône, France). Ve Congrès du Néogène méditerranéen. Volume III, Étude palynologique. *Bulletin Bureau de Recherches Géologiques et Minières*, **4**, 59–65.

CHEW, A.E. 2009. Paleoecology of the early Eocene Willwood mammal fauna from the central Bighorn Basin, Wyoming. *Paleobiology*, **35**, 13–31.

CIAIS, P., SABINE, C., ET AL. 2013. Climate change 2013: the physical science basis. *Contribution of Working Group I to the Fifth Assessment Report of the Intergovernmental Panel on Climate Change, chapter Carbon and Other Biogeochemical Cycles. Cambridge University Press, Cambridge*.

CLARET, J., JARDINE, S. & ROBERT, P. 1981. La diversité des roches mères pétrolières: aspects géologiques et implications économiques à partir de quatre exemples. *Bulletin dês Centres Recherche Exploration-Production Elf-Aquitaine*, **5**, 383–417.

CLARKE, K. & WARWICK, R. 1994. An approach to statistical analysis and interpretation. *Change in Marine Communities*, **2**.

CLARKE, K.R. 1993. Non-parametric multivariate analyses of changes in community structure. *Australian Journal of Ecology*, **18**, 117–143, doi: 10.1111/j.1442-9993.1993.tb00438.x.

CLYDE, W.C., HAMZI, W., FINARELLI, J.A., WING, S.L., SCHANKLER, D. & CHEW, A. 2007. Basin-wide magnetostratigraphic framework for the Bighorn Basin, Wyoming. *Geological Society of America Bulletin*, **119**, 848–859.

COCCIONI, R., MONACO, P., MONECHI, S., NOCCHI, M. & PARISI, G. 1988. Biostratigraphy of the Eocene-Oligocene boundary at Massignano (Ancona, Italy). *The Eocene-Oligocene boundary in the Umbria-Marche Basin (Italy): Ancona, International Union of Geological Sciences Special Publication: Ancona, Italy, Fratelli Annibelli Publishers*, 59–74.

COLLINSON, J. 1996. Alluvial sediments. *Sedimentary environments: processes, facies and stratigraphy*, **3**, 37–82.

COLLINSON, J.D. 1969. The sedimentology of the Grindslow Shales and the Kinderscout Grit: a deltaic complex in the Namurian of northern England. *Journal of Sedimentary Research*, **39**.

COLLINSON, M. 1992. Vegetational and floristic changes around the Eocene/Oligocene boundary in western and central Europe. In Prothero, D. R., Berggren, W. A. (eds). *Eocene-Oligocene climatic and biotic evolution, Princeton University Press, Princeton, NJ,* **22**, 437–450.

COLLINSON, M. & CLEAL, C. 2001. Late middle Eocene-early Oligocene (Bartonian-Rupelian) and Miocene palaeobotany of Great Britain. *Geological Conservation Review Series*, **22**, 227–303.

COLLINSON, M., HOOKER, J. & GROCKE, D. 2003a. Cobham lignite bed and penecontemporaneous macrofloras of southern England: A record of vegetation and fire across the Paleocene-Eocene Thermal Maximum. *Special Papers-Geological Society of America*, 333–350.

COLLINSON, M.E., FOWLER, K. & BOULTER, M. 1981a. Floristic changes indicate a cooling climate in the Eocene of southern England. *Nature*, **291**, 315–317.

COLLINSON, M.E., STEART, D.C., HARRINGTON, G., HOOKER, J.J., SCOTT, A.C., ALLEN, L.O., GLASSPOOL, I.J., & GIBBSON, S.J. 2009. Palynological evidence of vegetation dynamics in response to palaeoenvironmental change across the onset of the Paleocene-Eocene Thermal Maximum at Cobham, Southern England. *Grana*, **48**, 38–66, doi: 10.1080/00173130802707980.

COMBAZ, A. 1964. Les palynofacies. *Revue de Micropaléontologie*, **7**, 205–218.

CORREIA, M. 1970. Diagenesis of sporopollenin and other comparable organic substances: application to hydrocarbon research. *In*: Symposium On Sporopollenin.

COXALL, H.K., WILSON, P.A., PÄLIKE, H., LEAR, C.H. & BACKMAN, J. 2005. Rapid stepwise onset of Antarctic glaciation and deeper calcite compensation in the Pacific Ocean. *Nature*, **433**, 53–57.

CRAMER, B.S. & KENT, D.V. 2005. Bolide summer: The Paleocene/Eocene thermal maximum as a response to an extraterrestrial trigger. *Palaeogeography, Palaeoclimatology, Palaeoecology*, **224**, 144–166.

CRAMER, B.S., WRIGHT, J.D., KENT, D.V. & AUBRY, M. 2003. Orbital climate forcing of δ13C excursions in the late Paleocene–early Eocene (chrons C24n–C25n). *Paleoceanography*, **18**.

CROUCH, E.M. & BRINKHUIS, H. 2005. Environmental change across the Paleocene–Eocene transition from eastern New Zealand: a marine palynological approach. *Marine Micropaleontology*, **56**, 138–160.

CROUCH, E.M., HEILMANN-CLAUSEN, C., BRINKHUIS, H., MORGANS, H.E.G., ROGERS, K.M., EGGER, H. & SCHMITZ, B. 2001. Global dinoflagellate event associated with the late Paleocene thermal maximum. *Geology*, **29**, 315–318.

CROWELL, J.C. 1974. Origin of Late Cenozoic Basins in Southern California. *Special Publication of the Society of Economic Paleontologists and Mineralogists (SEPM) Tectonics and Sedimentation (SP22).*

CUI, Y., KUMP, L.R., RIDGWELL, A.J., CHARLES, A.J., JUNIUM, C.K., DIEFENDORF, A.F., FREEMAN, K.H., URBAN, N.M., & HARDING, I.C. 2011. Slow release of fossil carbon during the Palaeocene-Eocene Thermal Maximum. *Nature Geoscience*, **4**, 481–485.

CURRAY, J. 1979. Tectonics of the Andaman Sea and Burma. *Am. Assoc. Pet. Geol. Mem.*, **29**, 189–198.

CURTIS, C. & SPEARS, D. 1968. The formation of sedimentary iron minerals. *Economic Geology*, **63**, 257–270.

DAMSTÉ, J.S.S., OSSEBAAR, J., ABBAS, B., SCHOUTEN, S. & VERSCHUREN, D. 2009. Fluxes and distribution of tetraether lipids in an equatorial African lake: Constraints on the application of the TEX< sub> 86 palaeothermometer and BIT index in lacustrine settings. *Geochimica Et Cosmochimica Acta*, **73**, 4232–4249.

DEAN, W.E., ARTHUR, M.A. & CLAYPOOL, G.E. 1986. Depletion of 13 C in Cretaceous marine organic matter: Source, diagenetic, or environmental sigal? *Marine Geology*, **70**, 119–157.

DEARMAN, W. 1963. Wrench-faulting in Cornwall and south Devon. *Proceedings of the Geologists' Association*, **74**, 265–287.

DECONTO, R.M. & POLLARD, D. 2003. Rapid Cenozoic glaciation of Antarctica induced by declining atmospheric CO 2. *Nature*, **421**, 245–249.

DECONTO, R.M., POLLARD, D., WILSON, P.A., PÄLIKE, H., LEAR, C.H. & PAGANI, M. 2008. Thresholds for Cenozoic bipolar glaciation. *Nature*, **455**, 652–656.

DECONTO, R.M., GALEOTTI, S., PAGANI, M., TRACY, D., SCHAEFER, K., ZHANG, T., POLLARD, D., & BEERLING, D. 2012. Past extreme warming events linked to massive carbon release from thawing permafrost. *Nature*, **484**, 87–91, doi: 10.1038/nature10929.

DE GEER, G. 1912. *A Geochronology of the Last 12000 Years.* Compte redu du XI Congres Geologique International (Stockholm 1910).

DE JONGE, C., STADNITSKAIA, A., HOPMANS, E.C., CHERKASHOV, G., FEDOTOV, A. & SINNINGHE DAMSTÉ, J.S. 2014. In situ produced branched glycerol dialkyl glycerol tetraethers in suspended particulate matter from the Yenisei River, Eastern Siberia. *Geochimica Et Cosmochimica Acta*, **125**, 476–491, doi: 10.1016/j.gca.2013.10.031.

DICKENS, G.R. 2011. Down the Rabbit Hole: Toward appropriate discussion of methane release from gas hydrate systems during the Paleocene-Eocene thermal maximum and other past hyperthermal events. *Climate of the Past*, **7**, 831–846.

DICKENS, G.R., O'NEIL, J.R., REA, D.K. & OWEN, R.M. 1995. Dissociation of oceanic methane hydrate as a cause of the carbon isotope excursion at the end of the Paleocene. *Paleoceanography*, **10**, 965–971.

DICKENS, G.R., CASTILLO, M.M. & WALKER, J.C.G. 1997. A blast of gas in the latest Paleocene: Simulating first-order effects of massive dissociation of oceanic methane hydrate. *Geology*, **25**, 259.

DIEFENDORF, A.F., MUELLER, K.E., WING, S.L., KOCH, P.L. & FREEMAN, K.H. 2010. Global patterns in leaf 13C discrimination and implications for studies of past and future climate. *Proceedings of the National Academy of Sciences*, **107**, 5738–5743.

DIESSEL, C.F. 1992. *Coal Formation and Sequence Stratigraphy*. Springer, Berling Heidelberg. pp. 461 - 514

DOMINGO, L., LÓPEZ-MARTÍNEZ, N., LENG, M.J. & GRIMES, S.T. 2009. The Paleocene–Eocene Thermal Maximum record in the organic matter of the Claret and Tendruy continental sections (South-central Pyrenees, Lleida, Spain). *Earth and Planetary Science Letters*, **281**, 226–237.

DONDERS, T.H., WEIJERS, J.W.H., MUNSTERMAN, D.K., KLOOSTERBOER-VAN HOEVE, M.L., BUCKLES, L.K., PANCOST, R.D., SCHOUTEN, S., SINNINGHE DAMSTE, J.S., & BRINKHUIS, H. 2009. Strong climate coupling of terrestrial and marine environments in the Miocene of northwest Europe. *Earth and Planetary Science Letters*, **281**, 215–225, doi: 10.1016/j.epsl.2009.02.034.

DUPUIS, C., AUBRY, M.P., STERBAUT, E., BERGGREN, W.A., OUDA, K., MAGGIONCALDA, R., CRAMER, B.S., KENT, D.V., SPEIJER, R.P., & HEILMANN-CLAUSEN, C. 2003. The Dababiya Quarry Section: Lithostratigraphy, clay mineralogy, geochemistry and paleontology. *Micropaleontology*, **49**, 41–59.

EDGAR, K.M., WILSON, P.A., SEXTON, P.F. & SUGANUMA, Y. 2007. No extreme bipolar glaciation during the main Eocene calcite compensation shift. *Nature*, **448**, 908–911, doi: 10.1038/nature06053.

EDWARDS, R. 1971. *The geology of the Bovey Basin*. (Doctoral dissertation, University of Exeter).

EDWARDS, R. 1976. Tertiary sediments and structure of the Bovey Basin, South Devon. *Proceedings of the Geologists' Association*, **87**, 1–26.

EKWENYE, O., NICHOLS, G., COLLINSON, M., NWAJIDE, C. & OBI, G. 2014. A paleogeographic model for the sandstone members of the Imo Shale, south-eastern Nigeria. *Journal of African Earth Sciences*, **96**, 190–211.

ELDRETT, J., GREENWOOD, D., POLLING, M., BRINKHUIS, H. & SLUIJS, A. 2014. A seasonality trigger for carbon injection at the Paleocene–Eocene Thermal Maximum. *Climate of the Past*, **10**, 759–769.

ELDRETT, J.S., GREENWOOD, D.R., HARDING, I.C. & HUBER, M. 2009. Increased seasonality through the Eocene to Oligocene transition in northern high latitudes. *Nature*, **459**, 969–973, doi: http://www.nature.com/nature/journal/v459/n7249/suppinfo/nature08069_S1.html.

EXON, N. 2000. Evolutionary and climatic consequences of opening the Tasmanian seaway: Results from Ocean drilling. *Geological Society of Australia Abstracts*, **59**, p – 146.

FARLEY, K. & ELTGROTH, S. 2003. An alternative age model for the Paleocene–Eocene thermal maximum using extraterrestrial< sup> 3 He. *Earth and Planetary Science Letters*, **208**, 135–148.

FASHAM, M.J.R. 1971. A gravity survey of the Bovey Tracy basin, Devon. *Geological Magazine*, **108**, 119–129, doi: 10.1017/S0016756800051141.

FAURE, K., HARRIS, C. & WILLIS, J.P. 1995. A profound meteoric water influence on Genesis in the Permian Waterberg coalfield, South Africa: evidence from stable isotopes. *Journal of Sedimentary Research*, **65**.

FENNING, P. & FRESHNEY, E. 1968. Preliminary results of a borehole at Petrockstow, north Devon. *Geological magazine*, **105**, 188–190.

FIGUEIRIDO, B., JANIS, C.M., PÉREZ-CLAROS, J.A., RENZI, M.D. & PALMQVIST, P. 2012. Cenozoic climate change influences mammalian evolutionary dynamics. *Proceedings of the National Academy of Sciences*, **109**, 722–727, doi: 10.1073/pnas.1110246108.

FOREMAN, B. 2014. Climate-driven generation of a fluvial sheet sand body at the Paleocene–Eocene boundary in north-west Wyoming (USA). *Basin Research*, **26**, 225–241.

FRESHNEY, E. 1970. Cyclical sedimentation in the Petrockstow Basin, in Proceedings of the USSHER Society, ed. Shelwood, E. B. 179–189.

FRESHNEY, E., BEER, K., WRIGHT, J.E. & BRITAIN, G.S. OF G. 1979. *Geology of the Country around Chulmleigh*. Institute of Geological Sciences, Natural Environment Research Council.

FRESHNEY, E.C., BEER, K.E. & WRIGHT, J.E. 1979a. *Geology of the Country around Chulmleigh*. Institute of Geological Sciences Natural H.

FRESHNEY, E.C., EDWARDS, R.A., ISAAC, K.P., WITTE, G., WILKINSON, G.C., BOULTER, M.C. & BAIN, J.A. 1982. A Tertiary basin at Dutson, near Launceston, Cornwall, England. *Proceedings of the Geologists' Association*, **93**, 395–402, doi: 10.1016/S0016-7878(82)80024-2.

FRICKE, H.C., CLYDE, W.C., O'NEIL, J.R. & GINGERICH, P.D. 1998. Evidence for rapid climate change in North America during the latest Paleocene thermal maximum: oxygen isotope compositions of biogenic phosphate from the Bighorn Basin (Wyoming). *Earth and Planetary Science Letters*, **160**, 193–208.

FRIEDRICH, O., NORRIS, R.D. & ERBACHER, J. 2012. Evolution of middle to Late Cretaceous oceans—A 55 my record of Earth's temperature and carbon cycle. *Geology*, **40**, 107–110.

GALAZZO, F.B., GIUSBERTI, L., LUCIANI, V. & THOMAS, E. 2013. Paleoenvironmental changes during the Middle Eocene Climatic Optimum (MECO) and its aftermath: The benthic foraminiferal record from the Alano section (NE Italy). *Palaeogeography, Palaeoclimatology, Palaeoecology*, **378**, 22–35.

GALEOTTI, S., KRISHNAN, S., PAGANI, M., LANCI, L., GAUDIO, A., ZACHOS, J.C., MONECHI, S., MORELLI, G., & LOURENS, L. 2010. Orbital chronology of Early Eocene hyperthermals from the Contessa Road section, central Italy. *Earth and Planetary Science Letters*, **290**, 192–200, doi: 10.1016/j.epsl.2009.12.021.

GAREL, S., SCHNYDER, J., JACOB, J., DUPIUS, C., BOUSSAFIR, M., LE MILBEAU, C., STORME, J., IAKOVLEVA, A.I., YANS, J., BAUDIN, F., FLEHOC, C., & QUESNEL, F. 2013. Paleohydrological and paleoenvironmental changes recorded in terrestrial sediments of the Paleocene–Eocene boundary (Normandy, France). *Palaeogeography, Palaeoclimatology, Palaeoecology*, **376**, 184–199.

GIBBS, S.J., BOWN, P.R., MURPHY, B.H., SLUIJS, A., EDGAR, K.M., PALIKE, H., BOLTON, C.T., & ZACHOS, J.C. 2012. Scaled biotic disruption during early Eocene global warming events. *Biogeosciences*, **9**, 4679–4688.

GINGERICH, P. 2001. Biostratigraphy of the continental Paleocene-Eocene boundary interval on Polecat Bench in the northern Bighorn Basin. *Paleocene-Eocene stratigraphy and biotic change in the Bighorn and Clarks Fork basins, Wyoming: University of Michigan Papers on Paleontology*, **33**, 37–71.

GINGERICH, P.D. 1980. *Early Cenozoic Paleontology and Stratigraphy of the Bighorn Basin, Wyoming: Commemorating of the 100th Anniversary of JL Wortman's Discovery of Fossil Mammals in the Bighorn Basin*. Museum of Paleontology, University of Michigan.

GINGERICH, P.D. 2006. Environment and evolution through the Paleocene-Eocene thermal maximum. *Trends in Ecology & Evolution*, **21**, 246–253, doi: 10.1016/j.tree.2006.03.006.

GORIN, G. 1975. Etude palynostratigraphique des sédiments paléogènes de la Grande Limagne (Massif central, France): avec applications de la statistique et de l'informatique.

GRADSTEIN, F.M., OGG, J.G. & SMITH, A.G. 2004. *A Geologic Time Scale 2004*. Cambridge University Press.

GREENWOOD, D.R. & WING, S.L. 1995. Eocene continental climates and latitudinal temperature gradients. *Geology*, **23**, 1044–1048.

GRESSLY, A. 1838. *Observations geologiques sur le Jura soleurois*. Neuchatel, Auf Kosten der Gesellschaft.

GRIMES, S.T., HOOKER, J.J., COLLINSON, M.E. & MATTEY, D.P. 2005. Summer temperatures of late Eocene to early Oligocene freshwaters. *Geology*, **33**, 189–192.

HABIB, D. 1982. Sedimentary supply origin of Cretaceous black shales. *Nature and Origin of Cretaceous Carbon-rich Facies. Academic Press, New York*, 113–127.

HAMMER, Ø., HARPER, D. & RYAN, P. 2001. PAST: Paleontological Statistics Software Package for Education and Data Analysis.[Computer program] Palaeontología Electrónica. *Disponible desde Internet en: http://palaeoelectronica. org/2001_1/past/issue1_01. htm (con acceso 23/05/2014).[Links]*.

HARRINGTON, G. 2001. Pollen assemblages and Paleocene–Eocene stratigraphy in the Bighorn and Clarks Fork Basins. *Paleocene–Eocene stratigraphy and biotic change in the Bighorn and Clarks Fork Basins, Wyoming: University of Michigan Papers on Paleontology*, **33**, 89–96.

HARRINGTON, G.J. & JARAMILLO, C.A. 2007. Paratropical floral extinction in the Late Palaeocene–Early Eocene. *Journal of the Geological Society*, **164**, 323–332.

HERFORT, L., SCHOUTEN, S., BOON, J.P., WOLTERING, M., BAAS, M., WEIJERS, J. & SINNINGHE DAMSTÉ, J.S. 2006. Characterization of transport and deposition of terrestrial organic matter in the southern North Sea using the BIT index. *Limnology and Oceanography*, **51**, 2196–2205.

HODGSON, E., GRIMES, S.T., PRICE, G.D., FITZPATRICK, M.E., HART, M.B. & LENG, M.J. 2011. Paleogene carbon isotope excursions in the Bunkers Hill borehole: Hampshire Basin, UK. *Proceedings of the Geologists' Association*, **122**, 460–471.

HOFMANN, C.C., MOHAMED, O. & EGGER, H. 2011. A new terrestrial palynoflora from the Palaeocene/Eocene boundary in the northwestern Tethyan realm (St. Pankraz, Austria). *Review of Palaeobotany and Palynology*.

HOLBROOK, J.M. 1996. Complex fluvial response to low gradients at maximum regression: A genetic link between smooth sequence-boundary morphology and architecture of overlying sheet sandstone. *Journal of Sedimentary Research*, **66**.

HOLLIS, C., HINES, B., LITTLER, K., VILLASANTE-MARCOS, V., KULHANEK, D.K., STRONG, C.P., ZACHOS, J.C., EGGINS, S.M., NORTHCOTE, L., & PHILIPS, A. 2015. Onset of the Paleocene–Eocene Thermal Maximum in the southern Pacific Ocean (DSDP Site 277, Campbell Plateau). *Climate of the Past Discussions*, **11**, 243–278.

HOLLIS, C.J., HANDLEY, L., CROUCH, E.M., MORGANS, H.E.G., BAKER, J.A., CREECH, J., COLLINS, K.S., GIBBS, S.J., HUBER, M., SCHOUTEN, S., ZACHOS, J.C., & PANCOST, R.D. 2009. Tropical sea temperatures in the high-latitude South Pacific during the Eocene. *Geology*, **37**, 99–102.

HOLLOWAY, S. & CHADWICK, R.A. 1986. The Sticklepath-Lustleigh fault zone: Tertiary sinistral reactivation of a Variscan dextral strike-slip fault. *Journal of the Geological Society*, **143**, 447–452, doi: 10.1144/gsjgs.143.3.0447.

HOOKER, J., GRIMES, S., MATTEY, D., COLLINSON, M. & SHELDON, N. 2009. Refined correlation of the UK Late Eocene–Early Oligocene Solent Group and timing of its climate history. *Geological Society of America Special Papers*, **452**, 179–195.

HOOKER, J.J., COLLINSON, M.E. & SILLE, N. 2004. Eocene-Oligocene mammalian faunal turnover in the Hampshire Basin, UK: calibration to the global time scale and the major cooling event. *Journal of the Geological Society*, **161**, 161.

HOPMANS, E.C., WEIJERS, J.W.H., SCHEFUß, E., HERFORT, L., SINNINGHE DAMSTÉ, J.S. & SCHOUTEN, S. 2004. A novel proxy for terrestrial organic matter in sediments based on branched and isoprenoid tetraether lipids. *Earth and Planetary Science Letters*, **224**, 107–116.

HREN, M.T., SHELDON, N.D., GRIMES, S.T., COLLINSON, M.E., HOOKER, J.J., BUGLER, M. & LOHMANN, K.C. 2013. Terrestrial cooling in Northern Europe during the Eocene–Oligocene transition. *Proceedings of the National Academy of Sciences*, **110**, 7562–7567, doi: 10.1073/pnas.1210930110.

HUBER, M. & CABALLERO, R. 2011. The early Eocene equable climate problem revisited. *Climate of the Past*, **7**, 603–633.

HUGUET, C., SCHIMMELMANN, A., THUNELL, R., LOURENS, L.J., SINNINGHE DAMSTÉ, J.S. & SCHOUTEN, S. 2007. A study of the TEX86 paleothermometer in the water column and sediments of the Santa Barbara Basin, California. *Paleoceanography*, **22**.

JANSONIUS, J. & HILLS, L. 1976. Genera File of Fossil Pollen and Spores. *University of Calgary, Canada*, **3286**.

JARAMILLO, C., OCHOA, D., CONTRERAS, L., PAGANI, M., CARVAJAL-ORTIZ, H., PRATT, L.M., KRISHNAN, S., CARDONA, A., ROMERO, M., QUIROZ, L., RODRIGUEZ, G., RUEDA, M.J., DE LA PARRA, F., MORON, S., GREEN, W., BAYONA, G., MONTES, C., QUINTERO, O., RAMIREZ, R., MORA, G., SCHOUTEN, S., BERMUDEZ, H., NAVARRETE, R., PARRA, F., ALVARAN, M., OSORNO, J., CROWLEY, J.L., VALENCIA, V., & VERVOORT, J. 2010. Effects of rapid global warming at the Paleocene-Eocene boundary on Neotropical vegetation. *Science*, **330**, 957–961.

JONES, T.P. 1994. Ultrastructural and chemical studies on Oligocene fossil wood from Bovey Tracey, Devon, UK. *Review of Palaeobotany and Palynology*, **81**, 279–288.

JOVANE, L., FLORINDO, F., COCCIONI, R., DINARE-TURELL, J., MARSILI, A., MONECHI, S., ROBERTS, A.P., & SPROVIERI, M. 2007. The middle Eocene climatic optimum event in the Contessa Highway section, Umbrian Apennines, Italy. *Geological Society of America Bulletin*, **119**, 413–427.

JUKES-BROWNE, A.J. 1909. The Depth and Succession of the Bovey Deposits (Devon). *Quarterly Journal of the Geological Society*, **65**, 162–165.

KATZ, M.E., CRAMER, B.S., MOUNTAIN, G.S., KATZ, S. & MILLER, K.G. 2001. Uncorking the bottle: What triggered the Paleocene/Eocene thermal maximum methane release? *Paleoceanography*, **16**, 549–562.

KENDER, S., STEPHENSON, M.H., RIDING, J.B., LENG, M.L., KNOX, R.W.O., PECK, V.L., KENDRICK, C.P., ELLIS, M.A., VANE, C.H., & JAMIESON, R. 2012. Marine and terrestrial environmental changes in NW Europe preceding carbon release at the Paleocene–Eocene transition. *Earth and Planetary Science Letters*, **353–354**, 108–120, doi: 10.1016/j.epsl.2012.08.011.

KENNETT, J. & SHACKLETON, N. 1976. Oxygen isotopic evidence for the development of the psychrosphere 38 Myr ago, Nature, 260, pp. 513-515.

KENNETT, J.P. 1977. Cenozoic evolution of Antarctic glaciation, the circum-Antarctic Ocean, and their impact on global paleoceanography. *Journal of geophysical research*, **82**, 3843–3860.

KENNETT, J.P. & STOTT, L. 1991. *Abrupt Deep-Sea Warming, Palaeoceanographic Changes and Benthic Extinctions at the End of the Palaeocene*.

KERSHAW, A. 1988. Australasia. *In*: *Vegetation History*. Springer, 237–306.

KEY, J. 1862. On the Bovey Deposit. *Quarterly Journal of the Geological Society*, **18**, 9–20.

KIM, J., SCHOUTEN, S., BUSCAIL, R., LUDWIG, W., BONNIN, J., SINNINGHE DAMSTÉ, J.S. & BOURRIN, F. 2006. Origin and distribution of terrestrial organic matter in the NW Mediterranean (Gulf of Lions): Exploring the newly developed BIT index. *Geochemistry, Geophysics, Geosystems*, **7**.

KIM, J.H., SCHOUTEN, S., HOPMANS, E.C., DONNER, B. & DAMSTE, J.S.S. 2008. Global sediment core-top calibration of the TEX86 paleothermometer in the ocean. *Geochimica Et Cosmochimica Acta*, **72**, 1154–1173, doi: 10.1016/i.gca.2007.12.010.

KIM, J.-H., VAN DER MEER, J., SCHOUTEN, S., HELMKE, P., WILLMOTT, V., SANGIORGI, F., KOC, N., HOPMANS, E.C., DAMSTE SINNINGHE, J.S. 2010. New indices and calibrations derived from the distribution of crenarchaeal isoprenoid tetraether lipids: Implications for past sea surface temperature reconstructions. *Geochimica Et Cosmochimica Acta*, **74**, 4639–4654, doi: 10.1016/j.gca.2010.05.027.

KIM, J.-H., ZELL, C., MOREIRA-TURCQ, P., PEREZ, M.A.P., ABRIL, G., MORTILLARO, J., WEIJERS, J.H.W.H., MEZIANE, T., & DAMSTE SINNINGHE, J.S. 2012. Tracing soil organic carbon in the lower Amazon River and its tributaries using GDGT distributions and bulk organic matter properties. *Geochimica Et Cosmochimica Acta*, **90**, 163–180, doi: 10.1016/j.gca.2012.05.014.

KOCH, P.L., ZACHOS, J.C. & GINGERICH, P.D. 1992. Correlation between isotope records in marine and continental carbon reservoirs near the Paleocene Eocene boundary. Nature Vol. 358; pp 319 - 322.

KOCH, P.L., CLYDE, W.C., HEPPLE, R.P., FOGEL, M.L., WING, S.L. & ZACHOS, J.C. 2003. Carbon and oxygen isotope records from paleosols spanning the Paleocene-Eocene boundary, Bighorn Basin, Wyoming. *SPECIAL PAPERS-GEOLOGICAL SOCIETY OF AMERICA*, 49–64.

KOMAR, N., ZEEBE, R.E. & DICKENS, G.R. 2013. Understanding long-term carbon cycle trends: The late Paleocene through the early Eocene. *Paleoceanography*, **28**, 650–662, doi: 10.1002/palo.20060.

KOTTHOFF, U., GREENWOOD, D., MCCARTHY, F., MÜLLER-NAVARRA, K., PRADER, S. & HESSELBO, S. 2014. Late Eocene to middle Miocene (33 to 13 million years ago) vegetation and climate development on the North American Atlantic Coastal Plain (IODP Expedition 313, Site M0027). *Climate of the Past*, **10**, 1523–1539.

KRAUS, M.J. & RIGGINS, S. 2007. Transient drying during the Paleocene–Eocene Thermal Maximum (PETM): analysis of paleosols in the Bighorn Basin, Wyoming. *Palaeogeography, Palaeoclimatology, Palaeoecology*, **245**, 444–461.

KRAUS, M.J., MCINERNEY, F.A., WING, S.L., SECORD, R., BACZYNSKI, A.A. & BLOCH, J.I. 2013. Paleohydrologic response to continental warming during the Paleocene–Eocene Thermal Maximum, Bighorn Basin, Wyoming. *Palaeogeography, Palaeoclimatology, Palaeoecology*, **370**, 196–208.

KRUTZSCH, W. 1959. *Mikropalaeontologische (sporenpalaeontologische) Untersuchungen in Der Braunkohle Des Geiseltales*. Berlin, Akademie Verlag.

KURTZ, A., KUMP, L., ARTHUR, M., ZACHOS, J. & PAYTAN, A. 2003. Early Cenozoic decoupling of the global carbon and sulfur cycles. *Paleoceanography*, **18**, 1090.

LAKE, S.D. & KARNER, G.D. 1987. Compressional Intra-Plate Deformations in the Alpine Foreland The structure and evolution of the Wessex Basin, southern England: an example of inversion tectonics. *Tectonophysics*, **137**, 347–378, doi: 10.1016/0040-1951(87)90328-3.

LANCI, L. & LOWRIE, W. 1997. Magnetostratigraphic evidence that 'tiny wiggles' in the oceanic magnetic anomaly record represent geomagnetic paleointensity variations. *Earth and Planetary Science Letters*, **148**, 581–592.

LAURETANO, V., LITTLER, K., POLLING, M., ZACHOS, J. & LOURENS, L. 2015. Frequency, magnitude and character of hyperthermal events at the onset of the Early Eocene Climatic Optimum. *Climate of the Past Discussions*, **11**.

LEAR, C.H., ELDERFIELD, H. & WILSON, P. 2000. Cenozoic deep-sea temperatures and global ice volumes from Mg/Ca in benthic foraminiferal calcite. *science*, **287**, 269–272.

LEAR, C.H., ROSENTHAL, Y., COXALL, H.K. & WILSON, P. 2004. Late Eocene to early Miocene ice sheet dynamics and the global carbon cycle. *Paleoceanography*, **19**, 1–11.

LEAR, C.H., BAILEY, T.R., PEARSON, P.N., COXALL, H.K. & ROSENTHAL, Y. 2008. Cooling and ice growth across the Eocene-Oligocene transition. *Geology*, **36**, 251.

LEIDER, A., HINRICHS, K.-U., MOLLENHAUER, G. & VERSTEEGH, G.J. 2010. Core-top calibration of the lipid-based and TEX 86 temperature proxies on the southern Italian shelf (SW Adriatic Sea, Gulf of Taranto). *Earth and Planetary Science Letters*, **300**, 112–124.

LENG, M., BARNKER, P., GREENWOOD, P., ROBERTS, N. & REED, J. 2001. Oxygen isotope analysis of diatom silica and authigenic calcite from Lake Pinarbasi, Turkey. *Journal of Paleolimnology*, **25**, 343–349.

LITTLER, K., RÖHL, U., WESTERHOLD, T. & ZACHOS, J.C. 2014. A high-resolution benthic stable-isotope record for the South Atlantic: Implications for orbital-scale changes in Late Paleocene–Early Eocene climate and carbon cycling. *Earth and Planetary Science Letters*, **401**, 18–30.

LIU, X.-L., ZHU, C., WAKEHAM, S.G. & HINRICHS, K.-U. 2014. In situ production of branched glycerol dialkyl glycerol tetraethers in anoxic marine water columns. *Marine Chemistry*, **166**, 1–8, doi: 10.1016/j.marchem.2014.08.008.

LIU, Z., PAGANI, M., ZINNIKER, D., DECONTO, R., HUBER, M., BRINKHUIS, H., SHAH, S.R., LECKIE, R.M., & PEARSON, A. 2009. Global cooling during the Eocene-Oligocene climate transition. *Science*, **323**, 1187–1190.

LOOPE, D.B., KETTLER, R.M., WEBER, K.A., HINRICHS, N.L. & BURGESS, D.T. 2012. Rinded iron-oxide concretions: hallmarks of altered siderite masses of both early and late diagenetic origin. *Sedimentology*, **59**, 1769–1781.

LOURENS, L.J., SLUIJS, A., KROON, D., ZACHOS, J.C., THOMAS, E., ROHL, U., BOWLES, J., & RAFFI, I. 2005. Astronomical pacing of late Palaeocene to early Eocene global warming events. *Nature*, **435**, 1083–1087, doi: 10.1038/nature03814.

LUDVIGSON, G.A., GONZÁLEZ, L.A., METZGER, R.A., WITZKE, B.J., BRENNER, R.L., MURILLO, A.P. & WHITE, T.S. 1998. Meteoric sphaerosiderite lines and their use for paleohydrology and paleoclimatology. *Geology*, **26**, 1039–1042.

LUNT, D.J., RIDGWELL, A., SLUIJS, A., ZACHOS, J., HUNTER, S. & HAYWOOD, A. 2011. A model for orbital pacing of methane hydrate destabilization during the Palaeogene. *Nature Geoscience*, **4**, 775–778.

LUTERBACHER, H., HARDENBOL, J. & SCHMITZ, B. 2000. Decision of the voting members of the International Subcommission on Paleogene Stratigraphy on the criterion for the recognition of the Paleocene/Eocene boundary. *Newsletter of the International Subcommission on Paleogene Stratigraphy*, **9**, 13.

MACHIN, J. 1971. Plant microfossils from Tertiary deposits of the Isle of Wight. *New Phytologist*, **70**, 851–872.

MACLENNAN, J. & JONES, S.M. 2006. Regional uplift, gas hydrate dissociation and the origins of the Paleocene–Eocene Thermal Maximum. *Earth and Planetary Science Letters*, **245**, 65–80.

MAGIONCALDA, R., DUPUIS, C., SMITH, T., STEURBAUT, E. & GINGERICH, P.D. 2004. Paleocene-Eocene carbon isotope excursion in organic carbon and pedogenic carbonate: Direct comparison in a continental stratigraphic section. *Geology*, **32**, 553–556.

MAI, D.H. 1976. Fossile Früchte und Samen aus dem Mitteleozän des Geiseltales. *Abh Zentr. geol. Inst.*, **26**, 93–149.

MARTÍN-CLOSAS, C., PERMANYER, A. & VILA, M.-J. 2005. Palynofacies distribution in a lacustrine basin. *Geobios*, **38**, 197–210.

MAW, G. 1864. On a supposed deposit of boulder-clay in north Devon. *Quarterly Journal of the Geological Society*, **20**, 445–451.

MCCARROLL, D. & LOADER, N.J. 2004. Stable isotopes in tree rings. *Quaternary Science Reviews*, **23**, 771–801.

MCINERNEY, F.A. & WING, S.L. 2011. The Paleocene-Eocene thermal maximum: a perturbation of carbon cycle, climate, and biosphere with implications for the future. *Annual Review of Earth and Planetary Sciences*, **39**, 489–516.

MENDONÇA FILHO, J., CHAGAS, R., MENEZES, T., MENDONÇA, J., DA SILVA, F. & SABADINI-SANTOS, E. 2010. Organic facies of the Oligocene lacustrine system in the Cenozoic Taubaté basin, Southern Brazil. *International Journal of Coal Geology*, **84**, 166–178.

MENDONÇA FILHO, J.G., DE OLIVEIRA, A.D., DA SILVA, F.S., DE OLIVEIRA MENDONÇA, J., RONDON, N.F., DA SILVA, T.F. & MENEZES, T.R. 2012. *Organic Facies: Palynofacies and Organic Geochemistry Approaches*. INTECH Open Access Publisher.

MENG, J. & MCKENNA, M.C. 1998. Faunal turnovers of Palaeogene mammals from the Mongolian Plateau. *Nature*, **394**, 364–367.

MÉNOT, G., BARD, E., ROSTEK, F., WEIJERS, J.W.H., HOPMANS, E.C., SCHOUTEN, S. & DAMSTÉ, J.S.S. 2006. Early Reactivation of European Rivers During the Last Deglaciation. *Science*, **313**, 1623–1625, doi: 10.1126/science.1130511.

MIALL, A.D. 1985. Architectural-element analysis: a new method of facies analysis applied to fluvial deposits. *Earth-Science Reviews*, **22**, 261–308.

MIALL, A.D. 1988. Architectural elements and bounding surfaces in fluvial deposits: anatomy of the Kayenta Formation (Lower Jurassic), southwest Colorado. *Sedimentary Geology*, **55**, 233–240, 247–262.

MIDDELBURG, J.J. 1991. Organic carbon, sulphur, and iron in recent semi-euxinic sediments of Kau Bay, Indonesia. *Geochimica et Cosmochimica Acta*, **55**, 815–828.

MIDDLETON, H.A. & NELSON, C.S. 1996. Origin and timing of siderite and calcite concretions in late Palaeogene non-to marginal-marine facies of the Te Kuiti Group, New Zealand. *Sedimentary Geology*, **103**, 93–115.

MILLER, K.G. 1992. Middle Eocene to Oligocene stable isotopes, climate, and deep-water history: The Terminal Eocene Event. *Eocene-Oligocene climatic and biotic evolution*, 160–177.

MILLER, K.G., FAIRBANKS, R.G. & MOUNTAIN, G.S. 1987. Tertiary oxygen isotope synthesis, sea level history, and continental margin erosion. *Paleoceanography*, **2**, 1–19.

MILLER, K.G., WRIGHT, J.D. & FAIRBANKS, R.G. 1991. Unlocking the ice house: Oligocene-Miocene oxygen isotopes, eustasy, and margin erosion. *Journal of Geophysical Research*, **96**, 6829–6848.

MORLEY, D.W., LENG, M.J., MACKAY, A.W., SLOANE, H.J., RIOUAL, P. & BATTARBEE, R.W. 2004. Cleaning of lake sediment samples for diatom oxygen isotope analysis. *Journal of Paleolimnology*, **31**, 391–401, doi: 10.1023/B:JOPL.0000021854.70714.6b.

MOSBRUGGER, V., UTESCHER, T. & DILCHER, D.L. 2005. Cenozoic continental climatic evolution of Central Europe. *Proceedings of the National Academy of Sciences of the United States of America*, **102**, 14964–14969.

MURPHY, B.H., FARLEY, K.A. & ZACHOS, J.C. 2010. An extraterrestrial 3He-based timescale for the Paleocene–Eocene thermal maximum (PETM) from Walvis Ridge, IODP Site 1266. *Geochimica et Cosmochimica Acta*, **74**, 5098–5108, doi: 10.1016/j.gca.2010.03.039.

MYERS, K. & MILTON, N. 1996. *Concepts and Principles of Sequence Stratigraphy*. Wiley Online Library.

NICOLO, M.J., DICKENS, G.R., HOLLIS, C.J. & ZACHOS, J.C. 2007. Multiple early Eocene hyperthermals: Their sedimentary expression on the New Zealand continental margin and in the deep sea. *Geology*, **35**, 699.

NOCCHI, M., MONECHI, S., ET AL. 1988. The extinction of the Hantkeninidae as a marker for recognizing the Eocene-Oligocene boundary: a proposal. *The Eocene–Oligocene Boundary in the Marche–Umbria Basin (Italy). International Union of Geological Sciences Commission on Stratigraphy*, 249–252.

NONG, G.T., NAJJAR, R.G., SEIDOV, D. & PETERSON, W.H. 2000. Simulation of ocean temperature change due to the opening of Drake Passage. *Geophysical Research Letters*, **27**, 2689–2692.

NORRIS, R., TURNER, S.K., HULL, P. & RIDGWELL, A. 2013. Marine ecosystem responses to Cenozoic global change. *Science*, **341**, 492–498.

NUNES, F. & NORRIS, R.D. 2006. Abrupt reversal in ocean overturning during the Palaeocene/Eocene warm period. *Nature*, **439**, 60–63.

OBOH-IKUENOBE, F.E., OBI, C.G. & JARAMILLO, C.A. 2005. Lithofacies, palynofacies, and sequence stratigraphy of Palaeogene strata in Southeastern Nigeria. *Journal of African Earth Sciences*, **41**, 79–101.

OWEN, L.A., RICHARDS, B., RHODES, E.J., CUNNINGHAM, W.D., WINDLEY, B.F., BADAMGARAY, J. & DORJNAMJAA, D. 1998. Relic permafrost structures in the Gobi of Mongolia: age and significance. *Journal of Quaternary Science*, **13**, 539–547.

PAGANI, M., ZACHOS, J.C., FREEMAN, K.H., TIPPLE, B. & BOHATY, S. 2005. Marked decline in atmospheric carbon dioxide concentrations during the Paleogene. *Science*, **309**, 600–603.

PAGANI, M., PEDENTCHOUK, N., HUBER, M., SLUIJS, A., SCHOUTEN, S., BRINKHUIS, H., DAMSTE SINNINGHE, J.S., DICKENS, G.R., EXPEDITION 302 SCIENTISTS, BACKMAN, J., CLEMENS, S., CRONIN, T., EYNAUD, F., GATTECCECA, J., JAKOBSSON, M., JORDAN, R., KAMINSKI, M., KING, J., KOC, N., MARTINEZ, N.C., McINROY, D., MOORE, Jr, T.C., O'REGON, M., ONODERA, J., PALIKE, H., REA, B., RIO, D., SAKAMOTO, T., SMITH, D.C., ST. JOHN, K.E.K., SUTO, I., SUZUKI, N., TAKAHASHI, K., WATANABE, M., & YAMAMOTO, M. 2006. Arctic hydrology during global warming at the Palaeocene/Eocene thermal maximum. *Nature*, **442**, 671–675.

PANCHUK, K., RIDGWELL, A. & KUMP, L. 2008. Sedimentary response to Paleocene-Eocene Thermal Maximum carbon release: A model-data comparison. *Geology*, **36**, 315–318.

PEARSON, P.N. & PALMER, M.R. 2000. Atmospheric carbon dioxide concentrations over the past 60 million years. *Nature*, **406**, 695–699.

PEARSON, P.N., VAN DONGEN, B.E., NICHOLAS, C.J., PANCOST, R.D., SCHOUTEN, S., SINGANO, J.M. & WADE, B.S. 2007. Stable warm tropical climate through the Eocene Epoch. *Geology*, **35**, 211–214.

PEARSON, P.N., MCMILLAN, I.K., WADE, B.S., JONES, T.D., COXALL, H.K., BOWN, P.R. & LEAR, C.H. 2008. Extinction and environmental change across the Eocene-Oligocene boundary in Tanzania. *Geology*, **36**, 179–182.

PEARSON, P.N., FOSTER, G.L. & WADE, B.S. 2009. Atmospheric carbon dioxide through the Eoceneâ€“Oligocene climate transition. *Nature*, **461**, 1110–1113.

PETERSE, F., KIM, J.-H., SCHOUTEN, S., KRISTENSEN, D.K., KOÇ, N. & SINNINGHE DAMSTÉ, J.S. 2009. Constraints on the application of the MBT/CBT palaeothermometer at high latitude environments (Svalbard, Norway). *Organic geochemistry*, **40**, 692–699.

PETERSE, F., PRINS, M.A., BEETS, C.J., TROELSTRA, S.R., ZHENG, H., GU, Z., SCHOUTEN, S., & SINNINGHE DAMSTÉ, J.S. 2011. Decoupled warming and monsoon precipitation in East Asia over the last deglaciation. *Earth and Planetary Science Letters*, **301**, 256–264.

PETERSE, F., SCHOUTEN, S., VAN DER MEER, J., VAN DER MEER, M.T.J. & DAMSTE, J.S.S. 2012a. Distribution of branched tetraether lipids in geothermally heated soils: Implications for the MBT/CBT temperature proxy (vol 40, pg 201, 2009). *Organic geochemistry*, **51**, 11–12, doi: 10.1016/j.orggeochem.2012.07.004.

PETERSE, F., VAN DER MEER, J., ET AL. 2012b. Revised calibration of the MBT–CBT paleotemperature proxy based on branched tetraether membrane lipids in surface soils. *Geochimica Et Cosmochimica Acta*, **96**, 215–229, doi: 10.1016/j.gca.2012.08.011.

POSTMA, G. 1997. The geology of fluvial deposits, sedimentary facies, basin analysis and petroleum geology: Andrew D. Miall. Springer-Verlag, Berlin, 1996, xvi+ 582 pp., DM 118.-(hardcover), ISBN 3-540-59186-9.

POWELL, A., DODGE, J. & LEWIS, J. 1990. 17. Late Neogene to Pleistocene Palynological Facies of The Peruvian Continental Margin Upwelling, LEG 1121.

PREMOLI SILVA, I. & GRAHAM JENKINS, D. 1993. Decision on the Eocene-Oligocene boundary stratotype. *Episodes-Newsmagazine of the International Union of Geological Sciences*, **16**, 379–382.

PREMOLI SILVA, I., ORLANDO, M., MONECHI, S., MADILE, M., NAPOLEONE, G. & RIPEPE, M. 1988. Calcareous plankton biostratigraphy and magnetostratigraphy at the Eocene/Oligocene transition in the Gubbio area. *The Eocene-Oligocene boundary in the Umbria-Marche Basin (Italy): Ancona, International Union of Geological Sciences Commission on Stratigraphy, International Subcommission on Paleogene Stratigraphy Report*, 137–161.

PROSS, J., CONTRERAS, L., BIJL, P.K., GREENWOOD, D.R., BOHATY, S.M., SCHOUTEN, S., BENDLE, J.A., ROHL, U., TAUXE, L., RAINE, I., HUCK, C.E., VAN DE FLIERDT, T., JAMIESON, S.S.R., STICKLEY, C.E., VAN DE SCHOOTBRUGGE, ESCUTIA, C., BRINKHUIS, H., & INTEGRATED OCEAN DRILLING PROGRAM EXPEDITION 318 SCIENTISTS. 2012. Persistent near-tropical warmth on the Antarctic continent during the early Eocene epoch. *Nature*, **488**, 73–77, doi: 10.1038/nature11300.

PROTHERO, D.R. & HEATON, T.H. 1996. Faunal stability during the early Oligocene climatic crash. *Palaeogeography, Palaeoclimatology, Palaeoecology*, **127**, 257–283.

PUNT, W., HOEN, P., BLACKMORE, S., NILSSON, S. & LE THOMAS, A. 2007. Glossary of pollen and spore terminology. *Review of Palaeobotany and Palynology*, **143**, 1–81.

PYE, K., DICKSON, J.A.D., SCHIAVON, N., COLEMAN, M.L. & COX, M. 1990. Formation of siderite-Mg-calcite-iron sulphide concretions in intertidal marsh and sandflat sediments, north Norfolk, England. *Sedimentology*, **37**, 325–343, doi: 10.1111/j.1365-3091.1990.tb00962.x.

QUINN, M.F. 2006. Lough Neagh: the site of a Cenozoic pull-apart basin. *Scottish Journal of Geology*, **42**, 101–112.

RAJAN, S., MACKENZIE, F.T. & GLENN, C.R. 1996. A thermodynamic model for water column precipitation of siderite in the Plio-Pleistocene Black Sea. *American Journal of Science*, **296**, 506–548.

RAVEN, J., CALDEIRA, K., ELDERFIELD, H., HOEGH-GULDBERG, O., LISS, P., RIEBESELL, U., SHEPHERD, J., TURLEY, C., & WATSON, A. 2005. Ocean acidification due to increasing atmospheric carbon dioxide, Policy Doc. 12/05, 60 pp., R. Soc., London.

READING, H.G. 1980. Characteristics and recognition of strike-slip fault systems. *Sedimentation in oblique-slip mobile zones*, **4**, 7–26.

READING, H.G. 1996. Sedimentary Environments: Processes, Facies and Stratigraphy. 688 p.

REA, D.K. & LYLE, M.W. 2005. Paleogene calcite compensation depth in the eastern subtropical Pacific: Answers and questions. *Paleoceanography*, **20**.

REID, C. & REID, E.M. 1911. The Lignite of Bovey Tracey. *Philosophical Transactions of the Royal Society of London. Series B, Containing Papers of a Biological Character*, **201**, 161–178.

RIDGWELL, A. & SCHMIDT, D.N. 2010. Past constraints on the vulnerability of marine calcifiers to massive carbon dioxide release. *Nature Geoscience*, **3**, 196–200, doi: 10.1038/ngeo755.

ROBERT, C. & KENNETT, J.P. 1997. Antarctic continental weathering changes during Eocene-Oligocene cryosphere expansion: Clay mineral and oxygen isotope evidence. *Geology*, **25**, 587–590.

ROCHE, É. & SCHULER, M. 1976. *Analyse Palynologique (pollen et Spores) de Divers Gisements Du Tongrien de Belgique: Interprétation Paléoécologique et Stratigraphique*. Ministère des Affaires Économiques, Administration des Mines, Service Géologique de Belgique.

RÖHL, U., WESTERHOLD, T., MONECHI, S., THOMAS, E., ZACHOS, J.C. & DONNER, B. 2005. The Third and Final Early Eocene Thermal Maximum: Characteristics, Timing and Mechanisms of the 'X'Event. *In*: GSA Annual Meeting.

RUFFELL, A. 2002. The northwestwards continuation of the Sticklepath Fault: Bristol Channel, SW Wales, St. Georges Channel and Ireland. *Geoscience in south-west England*, **10**, 131–141.

RULL, V. 2003. Contribution of quantitative ecological methods to the interpretation of stratigraphically homogeneous pre-quaternary sediments: A palynological example from the oligocene of Venezuela. *Palynology*, **27**, 75–98.

SAVIN, S.M. 1977. The history of the Earth's surface temperature during the past 100 million years. *Annual review of earth and planetary sciences*, **5**, 319–355.

SCHER, H.D., BOHATY, S.M., ZACHOS, J.C. & DELANEY, M.L. 2011. Two-stepping into the icehouse: East Antarctic weathering during progressive ice-sheet expansion at the Eocene–Oligocene transition. *Geology*, **39**, 383–386, doi: 10.1130/G31726.1.

SCHOUTEN, S., HOPMANS, E.C. & DAMSTE, J.S.S. 2004. The effect of maturity and depositional redox conditions on archaeal tetraether lipid palaeothermometry. *Organic Geochemistry*, **35**, 567–571.

SCHOUTEN, S., ELDRETT, J., GREENWOOD, D.R., HARDING, I., BAAS, M. & DAMSTÉ, J.S.S. 2008. Onset of long-term cooling of Greenland near the Eocene-

Oligocene boundary as revealed by branched tetraether lipids. *Geology*, **36**, 147–150.

SCHOUTEN, S., HOPMANS, E.C. & SINNINGHE DAMSTÉ, J.S. 2013. The organic geochemistry of glycerol dialkyl glycerol tetraether lipids: A review. *Organic geochemistry*, **54**, 19–61, doi: 10.1016/j.orggeochem.2012.09.006.

SCOTT, A. 1929. *Ball Clays*. Mem. Geol. Surv, Special Dep. Min. Res. GB. (31) HMSO, 1-78.

SEBAG, D., DISNAR, J.-R., GUILLET, B., DI GIOVANNI, C., VERRECCHIA, E.P. & DURAND, A. 2006. Monitoring organic matter dynamics in soil profiles by 'Rock-Eval pyrolysis': bulk characterization and quantification of degradation. *European Journal of Soil Science*, **57**, 344–355.

SELWOOD, E.B., EDWARDS, R., CHESTER, J., HAMBLIN, R., HENSON, M., RIDDOLLS, B. & WATERS, R. 1984. *Geology of the Country around Newton Abbot*. Natural Environment Research Council.

SHACKLETON, N. & KENNETT, J. 1975. Late Cenozoic oxygen and carbon isotopic changes at DSDP Site 284: Implications for glacial history of the Northern Hemisphere and Antarctica. *Initial reports of the deep sea drilling project*, **29**, 801–807.

SHEARMAN, D.J. 1967. On tertiary fault movements in North Devonshire. *Proceedings of the Geologists' Association*, **78**, 555–IN4, doi: 10.1016/S0016-7878(68)80003-3.

SHELDON, N.D. & RETALLACK, G.J. 2004. Regional paleoprecipitation records from the late Eocene and Oligocene of North America. *The Journal of Geology*, **112**, 487–494.

SHELDON, N.D., COSTA, E., CABRERA, L. & GARCÉS, M. 2012. Continental Climatic and Weathering Response to the Eocene-Oligocene Transition. *The Journal of Geology*, **120**, 227–236, doi: 10.1086/663984.

SINNINGHE DAMSTE, J.S., HOPMANS, E.C., PANCOST, R.D., SCHOUTEN, S. & GEENEVASEN, J.A.J. 2000. Newly discovered non-isoprenoid glycerol dialkyl glycerol tetraether lipids in sediments. *Chemical Communications*, 1683–1684.

SINNINGHE DAMSTÉ, J.S., OSSEBAAR, J., SCHOUTEN, S. & VERSCHUREN, D. 2012. Distribution of tetraether lipids in the 25-ka sedimentary record of Lake Challa: extracting reliable TEX< sub> 86 and MBT/CBT palaeotemperatures from an equatorial African lake. *Quaternary Science Reviews*, **50**, 43–54.

SLUIJS, A., BRINKHUIS, H., CROUCH, E.M., JOHN, C.M., HANDLEY, L., MUNSTERMAN, D., BOHATY, S.M., ZACHOS, J.C., REICHART, G., SCHOUTEN, S., PANCOST, R.D., SINNINGHE DAMSTÉ, J.S., WELTERS, N.L.D., LOTTER, A.F., & DCIKENS, G.R. 2008a. Eustatic variations during the Paleocene-Eocene greenhouse world. *Paleoceanography*, **23**.

SLUIJS, A., SCHOUTEN, S., PAGANI, M., WOLERING, M., BRINKHUIS, H., SINNINGHE DAMSTÉ, J.S., DICKENS, G.R., HUBER, M., REICHART, G., STEIN, R., MATTHIESSEN, J., LOURENS, L.J., PEDENTCHOUK, N., BACKMAN, J., MORAN, K., & THE EXPEDITION 302 SCIENTISTS. 2006. Subtropical Arctic Ocean temperatures during the Palaeocene/Eocene thermal maximum. *Nature*, **441**, 610–613, doi: http://www.nature.com/nature/journal/v441/n7093/suppinfo/nature04668_S1.html.

SLUIJS, A., BRINKHUIS, H., SCHOUTEN, S., BOHATY, S.M., JOHN, C.M., ZACHOS, J.C., RECIHART, G., SINNINGHE DAMSTÉ, J.S., CROUCH, E.M., & DICKENS, G.R. 2007a. Environmental precursors to rapid light carbon injection at the Palaeocene/Eocene boundary. *Nature*, **450**, 1218–1221.

SLUIJS, A., BOWEN, G., BRINKHUIS, H., LOURENS, L. & THOMAS, E. 2007b. The Palaeocene-Eocene Thermal Maximum super greenhouse: biotic and geochemical signatures, age models and mechanisms of global change. *Deep Time Perspectives on Climate Change: Marrying the Signal From Computer Models and Biological Proxies*, 323–347.

SLUIJS, A., SCHOUTEN, S., DONDERS, T.H., SCHOON, P.L., ROHL, U., REICHART, G., SANGIORGI, F., KIM, J., SINNINGHE DAMSTÉ, J.S., & BRINKHUIS, H. 2009. Warm and wet conditions in the Arctic region during Eocene Thermal Maximum 2. *Nature Geoscience*, **2**, 777–780.

SLUIJS, A., ZEEBE, R.E., BIJL, P.K. & BOHATY, S.M. 2013. A middle Eocene carbon cycle conundrum. *Nature Geoscience*, **6**, 429–434, doi: 10.1038/ngeo1807.

SMITH, F.A., WING, S.L. & FREEMAN, K.H. 2007. Magnitude of the carbon isotope excursion at the Paleocene–Eocene thermal maximum: the role of plant community change. *Earth and Planetary Science Letters*, **262**, 50–65.

SMITH, R.W., BIANCHI, T.S. & LI, X. 2012. A re-evaluation of the use of branched GDGTs as terrestrial biomarkers: Implications for the BIT Index. *Geochimica Et Cosmochimica Acta*, **80**, 14–29, doi: 10.1016/j.gca.2011.11.025.

SMITH, T. 2000. Mammals from the Paleocene—Eocene transition in Belgium (Tienen Formation, MP7): Palaeobiogeographical and biostratigraphical implications. *Gff*, **122**, 148–149.

SMITH, T., ROSE, K.D. & GINGERICH, P.D. 2006. Rapid Asia–Europe–North America geographic dispersal of earliest Eocene primate Teilhardina during the Paleocene–Eocene thermal maximum. *Proceedings of the National Academy of Sciences*, **103**, 11223–11227.

SPOFFORTH, D.J.A., AGNINI, C., PALIKE, H., RIO, D., FORNACIARI, E., GIUSBERTI, L., LUCIAN, V., LANCI, L., & MUTTONI, G. 2010. Organic carbon burial following the middle Eocene climatic optimum in the central western Tethys. *Paleoceanography*, **25**, PA3210, doi: 10.1029/2009PA001738.

STAP, L., SLUIJS, A., THOMAS, E. & LOURENS, L. 2009. Patterns and magnitude of deep sea carbonate dissolution during Eocene Thermal Maximum 2 and H2, Walvis Ridge, southeastern Atlantic Ocean. *Paleoceanography*, **24**.

STAP, L., LOURENS, L.J., THOMAS, E., SLUIJS, A., BOHATY, S. & ZACHOS, J.C. 2010. High-resolution deep-sea carbon and oxygen isotope records of Eocene Thermal Maximum 2 and H2. *Geology*, **38**, 607–610, doi: 10.1130/G30777.1.

STASSEN, P., STEURBAUT, E., MORSI, A.-M., SCHULTE, P. & SPEIJER, R. 2012. Biotic impact of Eocene thermal maximum 2 in a shelf setting (Dababiya, Egypt). *Austrian Journal of Earth Sciences*, **105**, 154–160.

STAUB, J.R. & COHEN, A.D. 1979. The Snuggedy Swamp of South Carolina: a back-barrier estuarine coal-forming environment. *Journal of Sedimentary Petrology*, **49**, 133.

STEURBAUT, E., MAGIONCALDA, R., DUPUIS, C., VAN SIMAEYS, S., ROCHE, E. & ROCHE, M. 2003. Palynology, paleoenvironments, and organic carbon isotope evolution in lagoonal Paleocene-Eocene boundary settings in North Belgium. *Special Papers-Geological Society of America*, 291–318.

STURM, M. & MATTER, A. 1978. *Turbidites and Varves in Lake Brienz (Switzerland): Deposition of Clastic Detritus by Density Currents*. Wiley Online Library.

SUN, D., TAN, W., PEI, Y., ZHOU, L., WANG, H., YANG, H. & XU, Y. 2011. Late quaternary environmental change of Yellow River Basin: an organic geochemical record in Bohai Sea (North China). *Organic geochemistry*, **42**, 575–585.

SVENSEN, H., PLANKE, S., MALTHE-SØRENSSEN, A., JAMTVEIT, B., MYKLEBUST, R., EIDEM, T.R. & REY, S.S. 2004. Release of methane from a volcanic basin as a mechanism for initial Eocene global warming. *Nature*, **429**, 542–545.

SWEET, A., BRAMAN, D. & LERBEKMO, J. 1999. Sequential palynological changes across the composite Cretaceous-Tertiary (KT) boundary claystone and contiguous strata, western Canada and Montana, USA. *Canadian Journal of Earth Sciences*, **36**, 743–768.

TAPPAN, H.N. 1980. *The Paleobiology of Plant Protists*. WH Freeman.

TEICHMÜLLER, M. & TEICHMÜLLER, R. 1968. Cainozoic and Mesozoic coal deposits of Germany. *In*: *Coal and Coal-Bearing Strata*. Oliver and Boyd Edinburgh, 347–379.

THOMAS, D.J., ZACHOS, J.C., BRALOWER, T.J., THOMAS, E. & BOHATY, S. 2002. Warming the fuel for the fire: Evidence for the thermal dissociation of methane hydrate during the Paleocene-Eocene thermal maximum. *Geology*, **30**, 1067–1070.

THOMAS, E. 1989. Development of Cenozoic deep-sea benthic foraminiferal faunas in Antarctic waters. *Geological Society, London, Special Publications*, **47**, 283–296.

THOMAS, E. 1998. Biogeography of the late Paleocene benthic foraminiferal extinction. Late Paleocene-Early Eocene Climatic and Biotic Events in the Marine and Terrestrial Records. M. P. Aubry, S. Lucas and W. A. Berggren. New York, Columbia University Press: 214-243.

THOMAS, E. 1999. An Introduction to 'Biotic Responses to Major Paleoceanographic Changes'. *In*: *Reconstructing Ocean History*. Springer US, 163–171.

THOMAS, E. & SHACKLETON, N.J. 1996. The Paleocene-Eocene benthic foraminiferal extinction and stable isotope anomalies. *Geological Society, London, Special Publications*, **101**, 401–441.

THOMAS, E. & ZACHOS, J.C. 2000. Was the late Paleocene thermal maximum a unique event? *Gff*, **122**, 169–170.

THOMSON, P.W. & PFLUG, H.D. 1953. Pollen und Sporen des Mitteleuropäischen Tertiärs. *Palaeontographica Abteilung B*, 1–138.

TIERCELIN, J. 2009. Natural resources in the lacustrine facies of the Cenozoic rift basins of East Africa. *Lacustrine Facies Analysis (Special Publication 13 of the IAS)*, **30**, 3.

TIERNEY, J.E. & RUSSELL, J.M. 2009. Distributions of branched GDGTs in a tropical lake system: Implications for lacustrine application of the MBT/CBT paleoproxy. *Organic geochemistry*, **40**, 1032–1036, doi: 10.1016/j.orggeochem.2009.04.014.

TIERNEY, J.E., SCHOUTEN, S., PITCHER, A., HOPMANS, E.C. & SINNINGHE DAMSTÉ, J.S. 2012. Core and intact polar glycerol dialkyl glycerol tetraethers (GDGTs) in Sand Pond, Warwick, Rhode Island (USA): Insights into the origin of lacustrine GDGTs. *Geochimica Et Cosmochimica Acta*, **77**, 561–581, doi: 10.1016/j.gca.2011.10.018.

TING, S., BOWEN, G.J., KOCH, P.L., CLYDE, W.C., WANG, Y. & MCKENNA, M.C. 2003. Biostratigraphic, chemostratigraphic, and magnetostratigraphic study across the Paleocene-Eocene boundary in the Hengyang Basin, Hunan, China. *Special Papers-Geological Society of America*, 521–536.

TIPPLE, B.J. & PAGANI, M. 2007. The early origins of terrestrial C4 photosynthesis. *Annu. Rev. Earth Planet. Sci.*, **35**, 435–461.

TOGGWEILER, J.R. & SAMUELS, B. 1998. On the Ocean's Large-Scale Circulation near the Limit of No Vertical Mixing. *Journal of Physical Oceanography*, **28**, 1832–1852, doi: 10.1175/1520-0485(1998)028<1832:OTOSLS>2.0.CO;2.

TRAVERSE, A. 1988. Paleopalynology: Dept. *Geosci. college of Earth-Mineral Sci. Pennsylvanian state Univ.: 600pp*.

TRIPATI, A. & ELDERFIELD, H. 2005. Deep-sea temperature and circulation changes at the Paleocene-Eocene thermal maximum. *Science*, **308**, 1894.

TRIPATI, A., BACKMAN, J., ELDERFIELD, H. & FERRETTI, P. 2005. Eocene bipolar glaciation associated with global carbon cycle changes. *Nature*, **436**, 341–346.

TSCHUDY, R.H. 1958. A modification of the Schulze digestion method of possible value in studying oxidized coals. *Grana*, **1**, 34–38.

TURNER, C. 1979. *Geology of the Country around Bude and Bradworthy*. Geological Survey of Great britain, memoir 309.

TYE, R.S. & COLEMAN, J.M. 1989. Depositional processes and stratigraphy of fluvially dominated lacustrine deltas; Mississippi delta plain. *Journal of Sedimentary Research*, **59**, 973–996.

TYSON, R., WILSON, R. & DOWNIE, C. 1979. A stratified water column environmental model for the type Kimmeridge Clay.

TYSON, R.V. 1993. Palynofacies analysis. *In*: *Applied Micropalaeontology*. Springer, 153–191.

TYSON, R.V. 1995. *Sedimentary Organic Matter: Organic Facies and Palynofacies*. Springer.

VAN ANDEL, T.H., HEATH, G.R. & MOORE, T.C. 1975. Cenozoic History and Paleoceanography of the Central Equatorial Pacific Ocean A Regional Synthesis of Deep Sea Drilling Project Data. *Geological Society of America Memoirs*, **143**, 1–223.

VAN WAGONER, J.C., MITCHUM, R., CAMPION, K. & RAHMANIAN, V. 1990. Siliciclastic sequence stratigraphy in well logs, cores, and outcrops: concepts for high-resolution correlation of time and facies.

VERSCHUREN, D., SINNINGHE DAMSTÉ, J.S., MORNAUT, J., KRISTEN, I., BLAAUW, F., HAUG, G.H., & CHALLACEA PROJECT MEMBERS. 2009. Half-precessional dynamics of monsoon rainfall near the East African Equator. *Nature*, **462**, 637–641.

VINCENT, A. 1971. Drilling techniques in ball clays. *Quarterly Journal of Engineering Geology and Hydrogeology*, **4**, 241–247.

VINCENT, A. 1974. Sedimentary environments of the Bovey Basin. *Unpublished M. Phil. Thesis, University of Surrey, England*.

VINCENT, A. 1983. The origin and occurrence of Devon Ball Clays. *Geological Society, London, Special Publications*, **11**, 39–45.

WADE, B.S., HOUBEN, A.J., QUIAJTAAL, W., SCHOUTEN, S., ROSENTHAL, Y., MILLER, K.G., KATZ, M.E., WRIGHT, J.D., & BRINKHUIS, H. 2012. Multiproxy record of abrupt sea-surface cooling across the Eocene-Oligocene transition in the Gulf of Mexico. *Geology*, **40**, 159–162.

WALKER, R., WALKER, R. & JAMES, N. 1992. Facies, facies model and modern stratigraphic concepts. *Facies model: response to sea level change. Geological Association of Canada*, 1–14.

WALSH, E.M., INGALLS, A.E. & KEIL, R.G. 2008. Sources and transport of terrestrial organic matter in Vancouver Island fjords and the Vancouver-Washington Margin: A multiproxy approach using d 13Corg, lignin phenols, and the ether lipid BIT index. *Limnology and Oceanography*, **53**, 1054.

WEIJERS, J.W., SCHEFUß, E., SCHOUTEN, S. & DAMSTÉ, J.S.S. 2007a. Coupled thermal and hydrological evolution of tropical Africa over the last deglaciation. *Science*, **315**, 1701–1704.

WEIJERS, J.W.H., SCHOUTEN, S., VAN DEN DONKER, J.C., HOPMANS, E.C. & SINNINGHE DAMSTÉ, J.S. 2007c. Environmental controls on bacterial tetraether membrane lipid distribution in soils. *Geochimica Et Cosmochimica Acta*, **71**, 703–713, doi: 10.1016/j.gca.2006.10.003.

WEIJERS, J.W.H., SCHOUTEN, S., SLUIJS, A., BRINKHUIS, H. & SINNINGHE DAMSTÉ, J.S. 2007b. Warm arctic continents during the Palaeocene-Eocene thermal maximum. *Earth and Planetary Science Letters*, **261**, 230–238.

WEIJERS, J.W.H., BERNHARDT, B., PETERSE, F., WERNE, J.P., DUNGAIT, J.A.J., SCHOUTEN, S. & DAMSTE, J.S.S. 2011. Absence of seasonal patterns in MBT-CBT indices in mid-latitude soils. *Geochimica Et Cosmochimica Acta*, **75**, 3179–3190, doi: 10.1016/j.gca.2011.03.015.

WILKINSON, G.C. 1979. *A Palynological Survey of Some Tertiary Sediments in the Western Part of the British Isles.* Ph.D., Council for National Academic Awards.

WILKINSON, G.C. & BOULTER, M.C. 1981. Oligocene pollen and spores from the western part of the British Isles. *Palaeontographica Abteilung B*, 27–83.

WILKINSON, G.C., BAZLEY, R. A. B. & BOULTER, M.C. 1980. The geology and palynology of the Oligocene Lough Neagh Clays, Northern Ireland. *Journal of the Geological Society*, **137**, 65–75, doi: 10.1144/gsjgs.137.1.0065.

WING, S.L. & HARRINGTON, G.J. 2001. Floral response to rapid warming in the earliest Eocene and implications for concurrent faunal change. *Paleobiology*, **27**, 539–563.

WING, S.L., ALROY, J. & HICKEY, L.J. 1995. Plant and mammal diversity in the Paleocene to early Eocene of the Bighorn Basin. *Palaeogeography, Palaeoclimatology, Palaeoecology*, **115**, 117–155.

WING, S.L., BAO, H. & KOCH, P.L. 2000. An early Eocene cool period? Evidence for continental cooling during the warmest part of the Cenozoic. *Warm climates in Earth history. Cambridge University Press, Cambridge*, 197–237.

WING, S.L., HARRINGTON, G.J., SMITH, F.A., BLOCH, J.I., BOYER, D.M. & FREEMAN, K.H. 2005. Transient floral change and rapid global warming at the Paleocene-Eocene boundary. *Science*, **310**, 993–996.

WITKOWSKI, J., BOHATY, S.M., MCCARTNEY, K. & HARWOOD, D.M. 2012. Enhanced siliceous plankton productivity in response to middle Eocene warming at Southern Ocean ODP Sites 748 and 749. *Palaeogeography, Palaeoclimatology, Palaeoecology*, **326–328**, 78–94, doi: 10.1016/j.palaeo.2012.02.006.

WRIGHT, J.D. & MILLER, K.G. 1996. Control of North Atlantic deep water circulation by the Greenland-Scotland Ridge. *Paleoceanography*, **11**, 157–170.

WRIGHT, J.D. & SCHALLER, M.F. 2013. Evidence for a rapid release of carbon at the Paleocene-Eocene thermal maximum. *Proceedings of the National Academy of Sciences*, **110**, 15908–15913.

WYNN, J.G., BIRD, M.I. & WONG, V.N.L. 2005. Rayleigh distillation and the depth profile of 13C/12C ratios of soil organic carbon from soils of disparate texture in Iron Range National Park, Far North Queensland, Australia. *Geochimica Et Cosmochimica Acta*, **69**, 1961–1973.

YANG, G., ZHANG, C.L., XIE, S., CHEN, Z., GAO, M., GE, Z. & YANG, Z. 2013. Microbial glycerol dialkyl glycerol tetraethers from river water and soil near the Three Gorges Dam on the Yangtze River. *Organic geochemistry*, **56**, 40–50.

ZACHOS, J., PAGANI, M., SLOAN, L., THOMAS, E. & BILLUPS, K. 2001. Trends, rhythms, and aberrations in global climate 65 Ma to present. *Science*, **292**, 686–693.

ZACHOS, J.C., QUINN, T.M. & SALAMY, K.A. 1996. High-resolution (104 years) deep-sea foraminiferal stable isotope records of the Eocene-Oligocene climate transition. *Paleoceanography*, **11**, 251–266.

ZACHOS, J.C., WARA, M.W., BOHATY, S., DELANEY, M.L., PETRIZZO, M.R., BRILL, A., BRALOWER, T.J., PREMOLI-SILVA, I. 2003. A transient rise in tropical sea surface temperature during the Paleocene-Eocene Thermal Maximum. *Science*, **302**, 1551–1554.

ZACHOS, J.C., RÖHL, U., ET AL. 2005. Rapid Acidification of the Ocean During the Paleocene-Eocene Thermal Maximum. *Science*, **308**, 1611–1615, doi: 10.1126/science.1109004.

ZACHOS, J.C., SCHOUTEN, S., BOHATY, S., QUATTLEBAUM, T., SLUIJS, A., BRINKHUIS, H., GIBBS, S.J., & BRALOWER, T.J. 2006. Extreme warming of mid-latitude coastal ocean during the Paleocene-Eocene Thermal Maximum: Inferences from TEX86 and isotope data. *Geology*, **34**, 737–740.

ZACHOS, J.C., DICKENS, G.R. & ZEEBE, R.E. 2008. An early Cenozoic perspective on greenhouse warming and carbon-cycle dynamics. *Nature*, **451**, 279–283.

ZACHOS, J.C., MCCARREN, H., MURPHY, B., RÖHL, U. & WESTERHOLD, T. 2010. Tempo and scale of late Paleocene and early Eocene carbon isotope cycles: Implications for the origin of hyperthermals. *Earth and Planetary Science Letters*.

ZANAZZI, A., KOHN, M.J., MACFADDEN, B.J. & TERRY, D.O. 2007. Large temperature drop across the Eocene–Oligocene transition in central North America. *Nature*, **445**, 639–642.

ZANAZZI, A., JUDD, E., FLETCHER, A., BRYANT, H. & KOHN, M.J. 2015. Eocene–Oligocene latitudinal climate gradients in North America inferred from stable isotope ratios in perissodactyl tooth enamel. *Palaeogeography, Palaeoclimatology, Palaeoecology*, **417**, 561–568, doi: 10.1016/j.palaeo.2014.10.024.

ZEEBE, R.E., ZACHOS, J.C. & DICKENS, G.R. 2009. Carbon dioxide forcing alone insufficient to explain Palaeocene–Eocene Thermal Maximum warming. *Nature Geoscience*, **2**, 576–580.

ZHANG, C.L., WANG, J., WEI, Y., ZHU, C., HUANG, L. & DONG, H. 2012. Production of branched tetraether lipids in the lower Pearl River and estuary: effects of extraction methods and impact on bGDGT proxies. *Front. Microbiol*, **2**, 10–3389.

ZHU, C., WEIJERS, J.W.H., WAGNER, T., PAN, J.-M., CHEN, J.-F. & PANCOST, R.D. 2011. Sources and distributions of tetraether lipids in surface sediments across a large river-dominated continental margin. *Organic geochemistry*, **42**, 376–386, doi: 10.1016/j.orggeochem.2011.02.002.

ZIEGLER, P. 1990. Geological Atlas of Western and Central Europe, Shell Internationale Petroleum Maatschappij BV/Geological Society of London.

ZINK, K.-G., VANDERGOES, M.J., MANGELSDORF, K., DIEFFENBACHER-KRALL, A.C. & SCHWARK, L. 2010. Application of bacterial glycerol dialkyl glycerol tetraethers (GDGTs) to develop modern and past temperature estimates from New Zealand lakes. *Organic geochemistry*, **41**, 1060–1066, doi: 10.1016/j.orggeochem.2010.03.004.